CHROMATIN STABILITY AND DYNAMICS: TARGETING AND RECRUITMENT OF CHROMATIN MODIFIERS

EDITED BY: Sara Farrona, Rafal Archacki, Juan Armando Casas-Mollano and Iva Mozgová

PUBLISHED IN: Frontiers in Plant Science

frontiers Research Topics

frontiers

ISSN 1664-8714
ISBN 978-2-88971-091-1
DOI 10.3389/978-2-88971-091-1

About Frontiers

Frontiers is more than just an open-access publisher of scholarly articles: it is a pioneering approach to the world of academia, radically improving the way scholarly research is managed. The grand vision of Frontiers is a world where all people have an equal opportunity to seek, share and generate knowledge. Frontiers provides immediate and permanent online open access to all its publications, but this alone is not enough to realize our grand goals.

Frontiers Journal Series

The Frontiers Journal Series is a multi-tier and interdisciplinary set of open-access, online journals, promising a paradigm shift from the current review, selection and dissemination processes in academic publishing. All Frontiers journals are driven by researchers for researchers; therefore, they constitute a service to the scholarly community. At the same time, the Frontiers Journal Series operates on a revolutionary invention, the tiered publishing system, initially addressing specific communities of scholars, and gradually climbing up to broader public understanding, thus serving the interests of the lay society, too.

Dedication to Quality

Each Frontiers article is a landmark of the highest quality, thanks to genuinely collaborative interactions between authors and review editors, who include some of the world's best academicians. Research must be certified by peers before entering a stream of knowledge that may eventually reach the public - and shape society; therefore, Frontiers only applies the most rigorous and unbiased reviews.
Frontiers revolutionizes research publishing by freely delivering the most outstanding research, evaluated with no bias from both the academic and social point of view. By applying the most advanced information technologies, Frontiers is catapulting scholarly publishing into a new generation.

What are Frontiers Research Topics?

Frontiers Research Topics are very popular trademarks of the Frontiers Journals Series: they are collections of at least ten articles, all centered on a particular subject. With their unique mix of varied contributions from Original Research to Review Articles, Frontiers Research Topics unify the most influential researchers, the latest key findings and historical advances in a hot research area! Find out more on how to host your own Frontiers Research Topic or contribute to one as an author by contacting the Frontiers Editorial Office: frontiersin.org/about/contact

CHROMATIN STABILITY AND DYNAMICS: TARGETING AND RECRUITMENT OF CHROMATIN MODIFIERS

Topic Editors:
Sara Farrona, National University of Ireland Galway, Ireland
Rafal Archacki, University of Warsaw, Poland
Juan Armando Casas-Mollano, University of Minnesota, United States
Iva Mozgová, Academy of Sciences of the Czech Republic (ASCR), Czechia

Citation: Farrona, S., Archacki, R., Casas-Mollano, J. A., Mozgová, I., eds. (2021). Chromatin Stability and Dynamics: Targeting and Recruitment of Chromatin Modifiers. Lausanne: Frontiers Media SA. doi: 10.3389/978-2-88971-091-1

Table of Contents

frontiers in Plant Science

EDITORIAL
published: 31 May 2021
doi: 10.3389/fpls.2021.678702

Editorial: Chromatin Stability and Dynamics: Targeting and Recruitment of Chromatin Modifiers

Sara Farrona[1]*, *Iva Mozgová*[2], *Rafal Archacki*[3,4] and *Juan Armando Casas-Mollano*[5]

[1] Plant and Agricultural Biosciences Centre-Ryan Institute, National University of Ireland Galway, Galway, Ireland, [2] Biology Centre, Czech Academy of Sciences, Ceske Budejovice, Czech Republic, [3] Laboratory of Systems Biology, Faculty of Biology, University of Warsaw, Warsaw, Poland, [4] Institute of Biochemistry and Biophysics PAS, Warsaw, Poland, [5] BioTechnology Institute, University of Minnesota Twin Cities, St. Paul, United States

Keywords: chromatin dynamics, histone modifications, chromatin remodeling complexes, transcriptional regulation, plant development and responses

Editorial on the Research Topic

Chromatin Stability and Dynamics: Targeting and Recruitment of Chromatin Modifiers

OPEN ACCESS

Edited by:
Jean Molinier, UPR2357 Institut de biologie moléculaire des plantes (IBMP), France

Reviewed by:
Gilles Vachon, UMR5168 Laboratoire de Physiologie Cellulaire Vegetale (LPCV), France

***Correspondence:**
Sara Farrona
sara.farrona@nuigalway.ie

Specialty section:
This article was submitted to Plant Cell Biology, a section of the journal Frontiers in Plant Science

Received: *10 March 2021*
Accepted: *19 March 2021*
Published: *31 May 2021*

Citation:
Farrona S, Mozgová I, Archacki R and Casas-Mollano JA (2021) Editorial: Chromatin Stability and Dynamics: Targeting and Recruitment of Chromatin Modifiers. Front. Plant Sci. 12:678702. doi: 10.3389/fpls.2021.678702

Chromatin organizes nuclear genome in the restricted space of the nucleus and contributes to all nuclear processes which occur in the absence of internal membranes. Chromatin structure is highly dynamic allowing the unconstrained but controlled reprogramming of nuclear processes, including gene expression, in response to internal and external cues. This is particularly important in plants that, as sessile organisms, constantly need to modify their development and growth (Santos et al., 2020).

The articles published through this Research Topic present new data or discuss current knowledge related to our understanding of chromatin dynamics and its relevance for the regulation of plant growth and environmental responses. Furthermore, novel techniques to deepen our understanding and visualization of chromatin dynamics are also presented.

HISTONE MODIFICATIONS

As key structural components of the chromatin, histones are the main target of regulatory complexes and are subjected to an array of posttranslational modifications. One of the best studied histone modifications is methylation, from which histone H3 lysine 9 methylation has been shown to be associated to the silencing of genomic parasites and repetitive sequences in plants and most eukaryotes (Xu and Jiang). Recent progress in decoding the functions of histone H3 lysine 9 di-methylation (H3K9me2) in the model plant *Arabidopsis thaliana* (Arabidopsis) are discussed by Xu and Jiang. In their review, Xu and Jiang, give an overview of the methyltransferases involved in the methylation of H3K9 and how this modification is properly deposited at its target genomic regions. Current knowledge on the readers and functional outcomes of H3K9 methylation are also highlighted (Xu and Jiang). In an original research article, Demidov et al. shed light on the functions of the phosphorylation of the centromere-specific histone 3 (CENH3), a variant that replaces the canonical histone H3 in centromeric regions. Using a modification-specific antibody, Demidov et al. showed that Arabidopsis CENH3 is phosphorylated at serine 65 (CENH3 pS65) *in vivo*. CENH3 pS65 may have a role in reproductive development as suggested by its enrichment in floral buds and the defects in reproductive tissues, and plant growth and development, caused by perturbations in this

modification. The authors also provide evidence that the kinase Aurora3 may be involved in the phosphorylation of CENH3 S65 (Demidov et al.).

TECHNICAL ADVANCES

In vivo visualization of specific loci within chromatin is pivotal for understanding chromatin dynamics in plant nucleus in response to external or internal cues. Addressing the question of whether rapid ion-based signaling and changes in membrane potential can result in changes in chromatin dynamics, Matzke et al. have developed tools that allow *in-vivo* monitoring of concomitant changes in pH and chromatin dynamics at individual genomic loci in Arabidopsis. To monitor changes in pH elicited upon root treatment by extracellular ATP (eATP), the system employs the pH sensor protein SEpHluorinA227D targeted to different cellular membranes (including plasma membrane or inner nuclear membrane) or to specific chromatin loci tagged by Tet or Lac operator (Tet/Lac-O) sequences. This is combined with Tet/Lac-O-targeted fluorescent proteins that allow monitoring chromatin dynamics at these loci. Using the system, the authors show that addition of eATP can lead to reduction of pH at sites of chromatin-bound proteins, which correlates with changes in dynamics of chromatin-bound proteins (Matzke et al.). In a different article of this Research Topic, the groups of Holger Puchta and Andreas Houben use MS2 or PP7 aptamers, short RNA oligos that can be recognized by RNA-binding proteins fused to a reporter, that are incorporated into sgRNA to amplify the GFP signal for *in vivo* labeling of plant telomeric sequences using the CRISPR/deactivated Cas9 (dCas9) system. The system improved the detection possibilities and signal/noise ratio of telomeres in transiently transformed *Nicotiana benthamiana* (Khosravi et al.). Unfortunately, it proved not functional in stably transformed plants, including *N. benthamiana*, Arabidopsis or *Daucus carota* (carrot), perhaps, as the authors speculate, due to the interference of stable CRISPR/dCas9 RNP binding to telomeres with plant growth and development (Khosravi et al.). Nevertheless, the use of aptamers within sgRNA is a promising strategy for signal amplification and sensitivity during *in vivo* imaging of plant chromatin.

CHROMATIN-RELATED COMPLEXES

Protein-protein interactions of nuclear components to form different type of multimeric complexes play a key role in the regulation of chromatin dynamics. Grasser has reviewed our current knowledge of one of these complexes, the heterodimeric histone chaperone FACT that is well-conserved among eukaryotic organisms and controls nucleosome assembly/disassembly linked to some of the most important DNA-related processes (Formosa and Winston, 2020). In this review article, the role of Arabidopsis FACT in the regulation of transcription, particularly during elongation, is discussed (Grasser). In addition, the impact of FACT on plant developmental switches through the regulation of the expression of key developmental genes, such as *FLOWERING LOCUS C* (*FLC*), master repressor of flowering, and *DELAY OF GERMINATION 1* (*DOG1*), key repressor of germination, is highlighted. However, how this histone chaperone complex is recruited to the chromatin or what poses specific genes to be more dependent on FACT-mediated regulation are still open questions that will require further investigation (Grasser). The laboratories of José A. Jarrillo and Manuel Piñeiro have contributed to our understanding of the activities of the NuA4 complex in plant chromatin remodeling. In this Research Topic they provide an overview of the Arabidopsis putative NuA4 complex during flowering and also describe the essential role of this complex in other cellular processes (e.g., stress and hormone responses) (Espinosa-Cores et al.). Furthermore, the complex scenario of the interactions of NuA4 with accessory proteins to form different complex variants in other organisms is profusely covered and used to make an elegant comparison of the situation in Arabidopsis (Espinosa-Cores et al.).

METABOLISM AND CHROMATIN

Chromatin-based mechanisms are involved in transcriptional regulation of virtually all major developmental and growth processes, including key metabolic pathways. The research article by Meng et al. reports that in maize, ZmCHB101 is necessary for proper physiological responses and gene expression changes upon nitrate treatment. ZmCHB101 is a close homolog to Arabidopsis SWI3D, one of the subunits of the SWI/SNF remodeling complex (Meng et al.). The authors identified two *ZmCHB101* target genes involved in nitrate transport, and observed that nucleosome occupancy and selected histone modifications at these loci were affected in ZmCHB101 RNAi lines. Interestingly, the presence of nitrate seems to negatively affect ZmCHB101 binding to these targets, which in turn may facilitate the binding of another nitrate-associated regulator, ZmNLP3.1 (Meng et al.). How the occurrence of nitrate in the cell is exactly translated into observed downstream effects is an intriguing question that needs further investigation. The connection of metabolism with epigenetics is reviewed in this Research Topic by Leung and Gaudin. The review discusses current knowledge about how metabolites modulate chromatin-modifying machineries. Specially, it focuses on acetylation and methylation and the key substrates for these modifications, acetyl-coenzyme A and S-adenosylmethionine, which provide most of the current experimental data. However, as the authors emphasize, DNA and histones (but also non-histone proteins, RNAs and various metabolites) have been shown to be subjected to a myriad of different chemical modifications (Leung and Gaudin). Collectively, they may form a crucial link between the metabolic status of the cell, largely dependent on environmental conditions, and the epigenetic information with its output on gene expression. Plants, with their lifestyle and ability to produce vast amounts of secondary metabolites are especially interesting organisms to study these phenomena.

CONCLUSION

The diverse scope of themes covered by the articles in this Research Topic finely reflects the dynamic nature of the plant chromatin research field. Some of the most recent advances in this area presented during the 2019 European Workshop on Plant Chromatin (EWPC) have been collected and summarized in a review article in this Research Topic (Moreno-Romero et al.). We envisage that these and future advances in the chromatin and epigenetic field will become essential for understanding the fundaments of chromatin dynamics and, very importantly, to bridge the gap between this knowledge and its implementation for the epigenetic control of plant traits.

AUTHOR CONTRIBUTIONS

All authors listed have made a substantial, direct and intellectual contribution to the work, and approved it for publication.

ACKNOWLEDGMENTS

We thank the Frontiers editorial staff for assistance in putting together this Research Topic. This manuscript was supported by different grants: IM acknowledges the start-up support from the Czech Academy of Sciences; RA acknowledges the National Science Centre Poland Grant No. 2017/26/E/NZ2/00899; SF acknowledges the NUI Galway Research Grant for Returning Academic Careers QA151. IM, RA, and SF are members of COST-Action CA16212 INDEPTH.

REFERENCES

Formosa, T., and Winston, F. (2020). The role of FACT in managing chromatin: disruption, assembly, or repair? *Nucleic Acids Res.* 48, 11929–11941. doi: 10.1093/nar/gka a912

Santos, A. P., Gaudin, V., Mozgová, I., Ponvianne, F., Schubert, D., Tek, A. L., et al. (2020). Tidying-up the plant nuclear space: domains, functions, and dynamics. *J. Exp. Bot.* 71, 5160–5178. doi: 10.1093/jxb/era a282

Conflict of Interest: The authors declare that the research was conducted in the absence of any commercial or financial relationships that could be construed as a potential conflict of interest.

frontiers in Plant Science

ORIGINAL RESEARCH
published: 25 July 2019
doi: 10.3389/fpls.2019.00928

Deregulated Phosphorylation of CENH3 at Ser65 Affects the Development of Floral Meristems in *Arabidopsis thaliana*

Dmitri Demidov[1], Stefan Heckmann[1], Oda Weiss[1], Twan Rutten[1], Eva Dvořák Tomaštíková[2,3], Markus Kuhlmann[1], Patrick Scholl[1,4], Celia Maria Municio[1], Inna Lermontova[1] and Andreas Houben[1]*

[1] Leibniz Institute of Plant Genetics and Crop Plant Research, Gatersleben, Germany, [2] Centre of Plant Structural and Functional Genomics, Institute of Experimental Botany Academy of Sciences, Olomouc, Czechia, [3] Department of Plant Biology, Uppsala BioCenter and Linnean Center for Plant Biology, Swedish University of Agricultural Sciences, Uppsala, Sweden, [4] Independent Researcher, Plankstadt, Germany

Several histone variants are posttranslationally phosphorylated. Little is known about phosphorylation of the centromere-specific histone 3 (CENH3) variant in plants. We show that CENH3 of *Arabidopsis thaliana* is phosphorylated *in vitro* by Aurora3, predominantly at serine 65. Interaction of Aurora3 and CENH3 was found by immunoprecipitation (IP) in *A. thaliana* and by bimolecular fluorescence complementation. Western blotting with an anti-CENH3 pS65 antibody showed that CENH3 pS65 is more abundant in flower buds than elsewhere in the plant. Substitution of serine 65 by either alanine or aspartic acid resulted in a range of phenotypic abnormalities, especially in reproductive tissues. We conclude that Aurora3 phosphorylates CENH3 at S65 and that this post-translational modification is required for the proper development of the floral meristem.

Keywords: CENH3, phosphorylation, Aurora kinase, floral meristem, *Arabidopsis*

OPEN ACCESS

Edited by:
Juan Armando Casas-Mollano, University of Minnesota, United States

Reviewed by:
Sachihiro Matsunaga, Tokyo University of Science, Japan
Kai Wang, Fujian Agriculture and Forestry University, China

****Correspondence:***
Dmitri Demidov
demidov@ipk-gatersleben.de

Specialty section:
This article was submitted to Plant Cell Biology, a section of the journal Frontiers in Plant Science

Received: *02 May 2019*
Accepted: *02 July 2019*
Published: *25 July 2019*

Citation:
Demidov D, Heckmann S, Weiss O, Rutten T, Dvořák Tomaštíková E, Kuhlmann M, Scholl P, Municio CM, Lermontova I and Houben A (2019) Deregulated Phosphorylation of CENH3 at Ser65 Affects the Development of Floral Meristems in Arabidopsis thaliana. Front. Plant Sci. 10:928. doi: 10.3389/fpls.2019.00928

INTRODUCTION

Histone3 (H3) is the best studied histone variant, regarding its post-translational modifications (PTMs). In the centromeric region of most eukaryotic chromosomes, H3 is replaced by CENH3, originally referred to as CENPA in human (Earnshaw and Rothfield, 1985), or as HTR12 in *Arabidopsis thaliana* (Talbert et al., 2002). The incorporation of CENH3 into centromeric nucleosomes initiates the formation of the kinetochore, a protein complex which enables the microtubules to attach to the centromere (Earnshaw et al., 2013). CENH3 features a well conserved histone fold domain and a highly variable N-terminus. Non-plant CENH3s experience a variety of PTMs. For example, the trimethylation of glycine 1, along with the phosphorylation of serine 16, and serine 18 has been observed in cultured human cells (Bailey et al., 2013; Takada et al., 2017). Of yeast CENH3, the arginine residue 37 can be methylated, serine at position 9, 10, 14, 16, 17, 22, 33, 40, 105, and 154 are phosphorylated, and lysine 49 is acetylated (Samel et al., 2012; Boeckmann et al., 2013; Hoffmann et al., 2018; Mishra et al., 2019). The human CENPA serine 7 is phosphorylated during mitosis by the cell cycle-dependent Aurora kinase (Zeitlin et al., 2001; Kunitoku et al., 2003), an enzyme which can also phosphorylate histone H3 at serine 10 and 28 (Hsu et al., 2000; Kurihara et al., 2006), and the H1 serine residue 27 (Hergeth et al., 2011).

Phosphorylation of CENH3 is likely required for kinetochore function and normal chromosome segregation (Boeckmann et al., 2013; Goutte-Gattat et al., 2013). Phosphorylation of CENH3 at S68 by the cyclin-dependent kinase 1 prevents interaction with the chaperone HJURP which is required for loading of CENH3 to centromeric nucleosomes (Yu et al., 2015; Wang et al., 2017). The only documented PTM involving a plant CENH3 is phosphorylation of the maize CENH3 pS50, which has been interpreted as a spindle assembly checkpoint (Zhang et al., 2005). The protein kinase responsible for this phosphorylation has not yet been identified.

Plant Aurora kinases have been classified in two major subgroups, referred to as α and β type Aurora (Demidov et al., 2005; Kawabe et al., 2005; Kato et al., 2011). The *A. thaliana* genome encodes two α (AtAurora1 and 2) and one β (Aurora3) type Aurora kinases. These kinases are concentrated at the centromeres, and in the phragmoplast at the end of the mitotic cell division. Alignment of plant Auroras with the animal Aurora A and B types (Adams et al., 2001) revealed characteristics of both animal enzyme classes as well as plant-specific features (Demidov et al., 2005). Aurora3 phosphorylates the serine residues 10 and 28 of *A. thaliana* H3 (Kurihara et al., 2006).

Here, we aimed to elucidate whether *A. thaliana* CENH3 is phosphorylated by Aurora3. We show that CENH3 is a substrate of Aurora3 and that serine 65 of CENH3 is phosphorylated preferentially in meristematic tissues such as flower buds and flowers. Additionally, we demonstrate that CENH3 pS65 is important for the proper development of reproductive tissues and how the disturbance of CENH3 phosphorylation can in addition impair the growth and development of the whole plant.

MATERIALS AND METHODS

Plant Growth and Transformation

Ecotype Columbia-0 and heterozygous *cenh3-1/CENH3* (Ravi and Chan, 2010) *A. thaliana* plants were transformed using the floral dip method (Clough and Bent, 1998). T1 transformants were selected on Murashige and Skoog solid medium containing the relevant antibiotic(s) and were grown under either a 16 h or an 8 h photoperiod with a day/night temperature regime of 20°C/18°C. *Nicotiana benthamiana* and *Nicotiana tabacum* plants were grown under a 12 h photoperiod at a constant temperature of 26°C.

DNA Extraction and Genotyping

Genomic DNA was extracted according to Edwards et al. (1991). Selection for the *cenh3-1* allele was achieved using a dCAPS marker: the template was amplified using the primer air cenh3-1_mut_for/_rev and the amplicon digested with *Eco*RV. The amplicon of the 215 bp mutant allele is resistant to digestion, while the Wt allele splits into a 191 bp, and a 24 bp fragments. To distinguish between the endogenous CENH3 copy and the two CENH3 transgenes carrying S65A or S65D, an initial PCR based on the primer pair cenh3-1_mut_for/_mut2429r was performed: the amplicon was then used as a template for a second PCR/dCAPS assay as described above. Primer sequences are given in **Supplementary Table S1**.

Cloning of Transformation Constructs

To generate CENH3 genomic fragments carrying either S65A or S65D, a genomic fragment of CENH3 with its native 1500 bp-long promotor, inserted in the plasmid pCAMBIA1300 was excised by *Hin*dIII/*Bam*HI digestion, and then cloned into pBlueScript II KS (Stratagene). The S65A and S65D mutations were generated in the cloned copy using a Phusion® site-directed mutagenesis kit (Finnzymes[1]) according to supplier's protocol; the required 5′-phosphorylated primers were S65_A_for, S65_D_for and S65_A+D_gDNA_rev. The *CENH3* S65A and S65D sequences were excised by *Hin*dIII/*Bam*HI digestion and re-inserted. To generate the *CENH3* S65A and S65D fusions to EYFP, the *p35S:CENH3YFP* expression cassette (Lermontova et al., 2006) was processed using a Phusion® site-directed mutagenesis kit (Finnzymes): the required primers were S65_A_for, S65_D_for and S65_A+D_cDNA_rev. The expression cassettes (*p35S, CENH3YFP*-S65, -A65 or -D65 and *NOS* terminator) were restricted with *Sfi*I and inserted into the pLH7000 vector[2]. All constructs were verified by sequencing. Primer sequences are given in **Supplementary Table S1**.

Heterologous Expression in *E. coli*

Full length *CENH3* and Aurora3 cDNAs were amplified using a RevertAid H minus first strand cDNA synthesis kit (Thermo Fisher Scientific[3]), and inserted, after removal of the stop codon, into pENTR-D TOPO (Thermo Fisher Scientific, see text footnote 4). The *CENH3* open reading frame sequence was amplified using the primer pair CENH3_expr_for/_rev with Phusion High-Fidelity DNA Polymerase (Fermentas), and the amplicon inserted into a Champion™ pET101 Directional TOPO® Expression plasmid (Invitrogen). The sequence of the *CENH3* variant carrying the S65A substitution was obtained amplifying the wild-type plasmid with a mutated primer with a Phusion® site-directed mutagenesis kit (Finnzymes) using the primer S65_A_for. The constructs were transformed into *E. coli* BL21 (GE Healthcare Life Sciences[4]). The fragment of Aurora3 obtained by PCR based on the primer pair Aurora3G-LP/-RP was inserted into pDest15 (Invitrogen) to create a GST fusion tag and then transformed into *E. coli* C43 (Lucigen[5]). An active Aurora3 kinase was synthesized in *E. coli* as described by Swain et al. (2008). The synthesis of recombinant protein was induced by addition of 1 mM IPTG to the *E. coli* culture during the exponential growth phase. CENH3 and CENH3 S65A 6xHIS-fusions were purified by passing through a Ni-NTA agarose column (Qiagen[6]) under denaturing conditions, and dialyzed against urea (Tomaštíková et al., 2015). Recombinant proteins were tested by Coomassie staining of Tris–glycine (Laemmli,

[1]www.finnzymes.com
[2]www.dna-cloning.com
[3]https://www.thermofisher.com
[4]https://www.gelifesciences.com
[5]www.lucigen.com
[6]https://www.qiagen.com

1970) or Tris–tricine (Schagger and von Jagow, 1987) PAAGE. Primer sequences are given in **Supplementary Table S1**.

In vitro Kinase Assay

The *in vitro* protein kinase assays of recombinant Aurora3 and the CENH3 variants were performed as described by Karimi-Ashtiyani and Houben (2013). *In vitro* protein kinase assays of recombinant Aurora3 on CENH3 peptides were performed as described by Demidov et al. (2009). The required CENH3 peptides were synthesized by JPT Peptide Technologies GmbH[7]. Each *in vitro* kinase reaction was based on 2 μg peptide.

Bimolecular Fluorescence Complementation (BiFC) Constructs and the Detection of Fluorescence

An Aurora3 pENTR-D TOPO construct was generated using the Gateway system (Invitrogen, see text footnote 4) within the binary BiFC plant transformation vectors pSpyce-35S and pSpyne-35S (Walter et al., 2004). Leaves of 2–4 week old either *N. benthamiana* or *N. tabacum* plants were infiltrated on their abaxial side with the *Agrobacterium tumefaciens* strain C58C1 carrying the pCH32 helper plasmid. The p19 protein of tomato bushy stunt virus was used to suppress gene silencing (Walter et al., 2004). Co-infiltration was performed with equal titers of *A. tumefaciens* containing either a BiFC construct or the p19 silencing plasmid. The fluorescent protein fusion constructs used as controls for the localization of Aurora3 and CENH3 were previously described (Demidov et al., 2005; Lermontova et al., 2006). The preparation of tissue for confocal fluorescence microscopy followed the methods described by Keçeli et al. (2017). YFP was detected by a LSM780 laser scanning microscope (Carl Zeiss, Jena, Germany) using a 488 nm laser line for excitation in combination with a 505–550 nm band pass for detection (Lermontova et al., 2013). Specificity of the YFP signal was confirmed by photospectrometric analysis of the fluorescence signal by means of the META detector.

Analysis of Total Plant Protein

Plant tissue (200–300 mg) was powdered in liquid nitrogen and suspended in 0.5 mL 56 mM Na2CO3, 56 mM DTT, 2% w/v SDS, 12% w/v sucrose, and 2 mM EDTA. After holding for 10 min at 70°C, the cell debris was removed by centrifugation. A 30 μg aliquot of each total protein sample was analyzed by 10% PAGE containing acetic acid-urea (Spiker, 1980) or 10% Tris–tricine PAGE (Schagger and von Jagow, 1987) and either stained in Coomassie Blue or electro-transferred onto Immobilon TM PVDF membranes (Millipore[8]). The membranes were challenged with either anti-*A. thaliana* CENH3 (Abcam[9]) or a polyclonal anti-CENH3 pS65 antibody (antibodies were working only for Western blotting but not for indirect immunostaining) produced by Pineda Antibody Service (Berlin, Germany). The latter was raised against a synthetic phosphorylated pS65 residue (± 10 AA) peptide and was purified from serum using immobilized peptides (1, with pS65 residue and 2, with S65 residue). The specificity of the antibody was validated using an ELISA. The membranes were held for 12 h at 4°C in PBS containing 5% w/v low-fat milk powder and a 1:1,000 dilution of polyclonal rabbit anti-CENH3 or anti-CENH3 pS65 and monoclonal mouse H3 (Abcam, see text footnote 10). Bound antibodies were detected by incubation with anti-rabbit or anti-mouse antibodies conjugated to peroxidase (Sigma[10]) in a dilution 1:5,000 and visualized using an enhanced chemiluminescence assay (Pierce, see text footnote 4).

λ Phosphatase Treatment

Aliquots of ∼100 μg protein were incubated for 1 h at 30°C in 100 μL of a pH 7.5 buffer containing 50 mM HEPES, 100 mM NaCl, 2mM DTT, 1 mM MnCl2, 0.01% v/v Brij-35 in the presence of 100 U alkaline phosphatase (Sigma), and 4,000 U λ phosphatase (NEB[11]).

Immunoprecipitation (IP)

The protein preparations required for IP were extracted from 10-day old transgenic seedlings harboring the pCENH3:CENH3:YFP construct in *cenh3-1* mutant plants after crosslinking with dithiobis succinimidyl propionate (DSP) for 30 min and 4°C according to the supplier's (Thermo Fisher Scientific™ Pierce™) protocol. A 10 g sample of plant material was powdered in liquid nitrogen, and then extracted in 50 mL 200 mM Tris–HCl (pH7.5), 1.5 M NaCl, and 0.5% v/v Tween20. After 20 min centrifugation at 4°C and 15000 *g*, the supernatant was diluted with dH_2O 1:10 and incubated with 12 μL GFP-Trap resin (ChromoTek GmbH[12]) for 4 h at 4°C. The GFP-Trap agarose was rinsed in 1×PBS and eluted according to the supplier's protocol. A 15 μL aliquot of each protein sample was electrophoretically separated and transferred to a membrane which was then probed with an anti-AtAurora antibody (Demidov et al., 2005). An extract of wild type (Wt) seedling was used as negative control.

Indirect Immunofluorescence

Immunostaining was performed as described by Manzanero et al. (2000). Rabbit antibodies raised against Nicotiana CENPC (Nagaki et al., 2009) and a mouse antibody raised against GFP (Clontech[13]) were diluted 1:400 in PBS. The binding of the primary antibody was detected by using as a 1:200 diluted secondary antibody of either rhodamine-conjugated anti-rabbit IgG (Dianova[14]) or FITC-conjugated anti-mouse IgG (Dianova).

Preparation of Pollen Mother Cells for Meiotic Analysis

Flower buds were fixed and pollen mother cells prepared for microscopy following Sánchez-Morán et al. (2001) with minor modifications. The buds were fixed in Carnoy's solution (absolute

[7]https://www.jpt.com

[8]www.merckmillipore.com

[9]www.abcam.com

[10]https://www.sigmaaldrich.com

[11]https://www.neb.com

[12]www.chromotek.com

[13]https://www.clontech.com

[14]http://www.dianova.de

ethanol:chloroform:glacial acetic acid, 6:3:1), rinsed first in 3:1 ethanol:glacial acetic acid, and then in citrate buffer (pH 4.5) at room temperature. They were then softened by digestion in 0.3% w/v pectolyase, 0.3% w/v cytohelicase, and 0.3% w/v cellulase (Sigma) in citrate buffer for 2 h at 37°C. The enzyme mixture was replaced by an ice-cold citrate buffer to stop the reaction. Single buds were transferred onto a clean microscope slide in a drop of citrate buffer and macerated with a fine needle. A 10 μL aliquot of 60% (v/v) glacial acetic acid was added to each slide, which was then dried by laying on a hotplate (42°C) for 1 min, after which again 10 μL 60% (v/v) acetic acid was added, followed by 200 μL of cold 3:1 ethanol:glacial acetic acid. Finally, the slides were air-dried.

Scanning Electron and Light Microscopy

The preparation of tissue sections for scanning electron and light microscopy followed the methods described by Tikhenko et al. (2015).

Alexander Staining

Flowers and flower buds were immersed in 10% ethanol overnight at 10°C, and the anthers were stained following Alexander (1969) for 15 min at room temperature. Estimates of pollen grain numbers per anther were based on the inspection of six anthers per plant.

Accession Numbers

The following line was used: *cenh3-1/CENH3* (At1g01370, Ravi and Chan, 2010).

RESULTS

CENH3 Interacts With AtAurora Kinase *in vivo*

The *in vivo* interaction between *Arabidopsis* Aurora and CENH3 was investigated using immunoprecipitation (IP) and bimolecular fluorescence complementation (BiFC). The former experiment was based on soluble protein isolated from DSP cross-linked *A. thaliana* seedlings stably expressing CENH3YFP (Lermontova et al., 2006). Western blot analysis of the precipitates eluted from anti-GFP agarose (**Figures 1A,B**) revealed that a ∼34 kDa product which interacted with Aurora was more abundant in CENH3YFP expressing plants than in the wild type (Wt) controls (**Figure 1B**). The 65–70 kDa product observed could have been either a dimerized form of Aurora and/or a complex formed with other proteins and stabilized by crosslinking. The corresponding negative control with YFP only does not show signals in the elution fraction (**Supplementary Figure S1**). In the validating BiFC experiment, YFP-specific signals were detected within the nucleoplasm of infiltrated *N. benthamiana* cells (**Figures 1C,D**). A number of pSpyNeAurora3/pSpyCeCENH3 spot-like BiFC signals were observed in the nucleus of infiltrated leaves (**Figure 1C**, arrowed). The distribution of the BiFC signal differed from that of Aurora3GFP, which was concentrated in the nucleoplasm and around the cell periphery (**Supplementary Figure S2A**), but was comparable with the distribution of CENH3YFP (**Supplementary Figure S2B**). Similarly, distinct CENH3YFP fluorescence signals were generated when nuclei isolated from *N. tabacum* cells transiently expressing CENH3YFP were labeled with antibodies against both YFP and CENPC (**Supplementary Figure S2K**). None of the negative controls produced a fluorescence signal (**Supplementary Figures S2C–J**). These results suggest that CENH3 interacts with Aurora3 *in planta*.

Aurora3 Phosphorylates CENH3 *in vitro* at the Serine 65 Residue

To assess whether Aurora3 can phosphorylate CENH3 *in vitro*, recombinant Aurora3 and CENH3 were produced in *E. coli*. Presenting recombinant CENH3 (**Supplementary Figure S3A**) as the substrate for recombinant active Aurora3 (**Supplementary Figure S3B**) resulted in the production of kinase activity-dependent Western blot signals (**Figure 2A**), thus indicating phosphorylation of CENH3. The phosphorylation sites were identified by scanning CENH3 for the putative Aurora kinase phosphorylation motifs (R/K)1-3X(S/T) based on the information available for non-plant Aurora kinases (Dephoure et al., 2008; Gully et al., 2012). The resulting eleven putative target sites (**Supplementary Figure S3D**), each embedded within an 11–20 residue oligopeptide (**Supplementary Figure S3E**), were then tested as a potential substrate of Aurora3. Screening of preselected peptides by the *in vitro* kinase assay showed the strongest phosphorylation signal when the serine 65 residue was present (**Figure 2B**). This residue locates at the border between the N- terminus and the histone fold domain (**Figure 2C**). The Aurora3-dependent phosphorylation of the S65 residue was confirmed by showing that an S65A variant of CENH3 (**Supplementary Figure S3C**), which cannot undergo phosphorylation at this position, was phosphorylated with twofold lower efficiency than Wt CENH3 (**Supplementary Figures S4A,B**).

CENH3 Phosphorylation at Serine 65 Is Abundant in Reproductive Tissue

To analyze the presence and abundance of the CENH3 pS65 *in planta*, polyclonal antibodies were raised against the AtCENH3 peptide phosphorylated at serine 65 (hereafter CENH3 pS65). On Western blot performed, the strongest anti-CENH3 pS65 signal was detected in extracts of flower buds and the weakest in mature leaves (**Figure 3**). Western blotting with the same protein samples after phosphatase treatment showed only a weak immune signal, thereby demonstrating that the antibodies are specific to the phosphorylated form of AtCENH3, and retained only residual antigenicity to the non-phosphorylated form (**Figure 3**). A parallel Western blot using anti-CENH3 revealed a rather different distribution of signals (**Supplementary Figure S4C**). Here, strongest signals were found in proteins isolated from a rapidly growing cell suspension, and there was no quantitative difference in intensity between λ phosphatase-treated and non-treated samples. Although the quantity of CENH3 of the cell suspension extract was greater than that

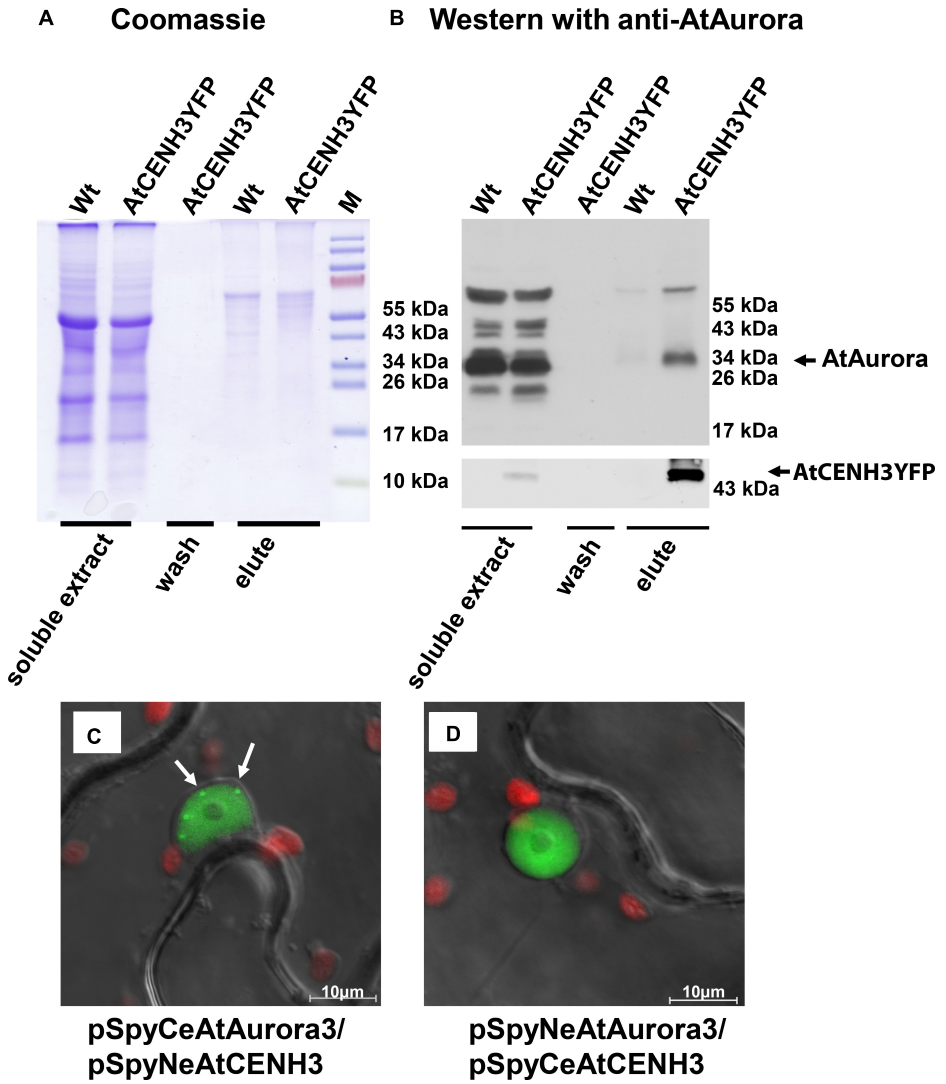

FIGURE 1 | *Arabidopsis thaliana* CENH3 interacts with Aurora3 kinase. **(A,B)** Western blot analysis using immuno-precipitated samples of *A. thaliana CENH3YFP* transformants and Wt plants. **(A)** Proteins separated by gel electrophoresis and visualized by Coomassie Blue staining. **(B)** Western blot probed with an anti-AtAurora, or anti-YFP (bottom part) antibodies. The negative control consisted of proteins extracted from Wt plants. **(C,D)** *In vivo* interaction of Aurora3 with CENH3 in the nucleoplasm as shown by BiFC in *N. benthamiana* leaves infiltrated with *A. tumefaciens* harboring the constructs **(C)** pSpyCeAurora3/pSpyNeCENH3 and **(D)** pSpyNeAurora3/pSpyCeCENH3. Some centromeres in **(C)** are arrowed. Red fluorescence corresponds to the autofluorescence of chlorophyll in the plastids.

present of the flower bud extract (**Supplementary Figure S4C**), the quantity of phosphorylated CENH3 was greater in the flower buds (**Figure 3**), suggesting a possible physiological function of CENH3 phosphorylation during the development of reproductive tissue.

CENH3 Phosphorylation at Serine 65 Is Involved in Development of Vegetative and Especially Reproductive Tissues

To study in more detail the role of CENH3 pS65, we generated cDNA or genomic CENH3 constructs containing S65A, and S65D mutations. To visualize the sub-cellular localization of S65 phosphorylated CENH3, YFP fusion constructs containing CENH3 cDNA either with the S65A or the S65D mutation under the 35S promoter were transformed into wild-type *A. thaliana* plants. *In vivo* fluorescence analysis of plants expressing the CENH3 S65A or the S65D variant revealed a concentration of YFP signal at the centromeres, which was not distinguishable from the distribution seen in control plants – CENH3YFP (**Supplementary Figures S5A–C**). To understand the functional role of S65 phosphorylated CENH3, heterozygote *cenh3-1* knock-out mutant plants were transformed with S65A, or S65D mutated CENH3 genomic constructs under the endogenous promoter. We assumed that the S65A mutation would prevent phosphorylation of CENH3 at this residue whereas the S65D mutation imitates the steric configuration and negative charge of phosphorylated S65 (Eot-Houllier et al., 2018). Both variants

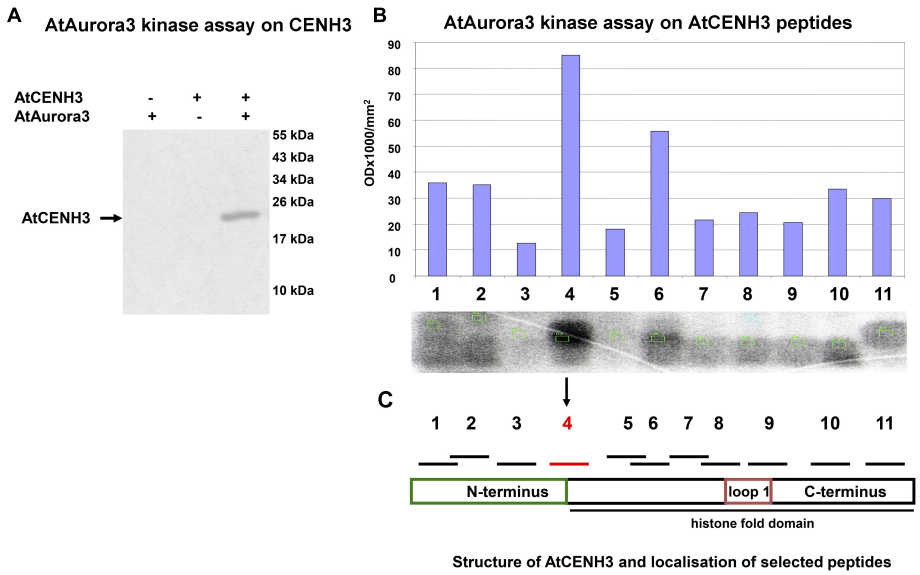

FIGURE 2 | Aurora3 phosphorylates CENH3 *in vitro*. **(A)** A kinase assay using recombinant CENH3 as substrate. Kinase reactions either without substrate or with no added enzyme were used as negative controls (–). **(B)** *In vitro* kinase screening of CENH3 phosphorylation sites based on 11 synthetic peptides containing putative Aurora kinase recognition motifs as substrate. **(C)** Schematic localization of selected peptides on CENH3.

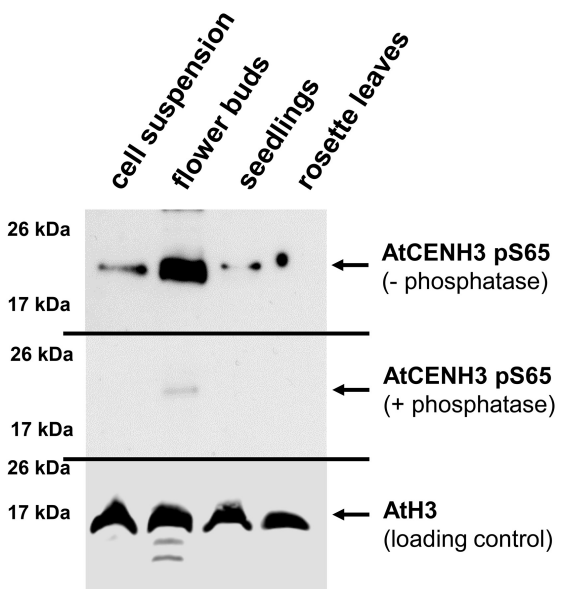

FIGURE 3 | CENH3 is phosphorylated at serine 65 in tissues with a high frequency of cell divisions. Western blot analysis, based on an anti-CENH3 pS65 antibody, shows variation between samples isolated from different *A. thaliana* tissues. Upper panel, non-treated samples; central panel: samples treated with phosphatase; lower panel, loading control (anti-histone H3). Total CENH3 amount and Coomassie staining for the same samples are shown in **Supplementary Figure S4C**.

were able to rescue the lethality associated with homozygosity for the *cenh3-1* mutation. A Western blot analysis based on an antibody recognizing CENH3 pS65 confirmed that neither of the two complemented lines experienced phosphorylation at position 65 (**Supplementary Figures S6A–C**). Phenotype analysis of the generated lines revealed no visible alteration in the growth of seedling roots (**Supplementary Figure S11**). A moderate difference in the vegetative growth rate at early growing stages (**Supplementary Figures S7, S10**) especially between 10 and 50 days after seeding (DAS), (compared to either the *cenh3-1* mutants transformed with CENH3 S65S or with Wt) was observed for 92% of the S65D-complemented and 93% of the S65A-complemented plants (**Figure 4A** and **Supplementary Table S3**). About 8% of the S65D-complemented and 7% of the S65A-complemented plants showed a stronger reduction in the growth rate and impaired development of floral meristems and reproductive organs (**Figure 4A** and **Supplementary Figure S8**). The affected plants formed no anthers or petals, although their pistil appeared to be normal (**Figure 4A** and **Supplementary Figures S9A,B**). In general, *cenh3-1* mutants complemented by S65A or S65D showed the same number (**Supplementary Table S3**) but a reduced biomass of leaves (**Supplementary Figure S10**) and were later flowering than Wt and S65S complemented lines (**Supplementary Figure S7** and **Supplementary Table S2**). It should be noted that in older plants (∼63 DAS), *cenh3-1* complemented mutants (S65A or S65D) showed an increased number of lateral stems compared to Wt, and S65S complemented lines (**Supplementary Figure S7** and **Supplementary Table S3**). Around 30% of the S65D-complemented and 38% of the S65A-complemented plants were largely sterile and only their most distal siliques set a reduced number of seeds compared to Wt or *cenh3-1* mutants transformed with CENH3 S65S (**Figures 4A,B**). Even the sum of developed and aborted seeds is lower in *cenh3-1* complemented mutant plants (S65A or S65D) than in Wt and

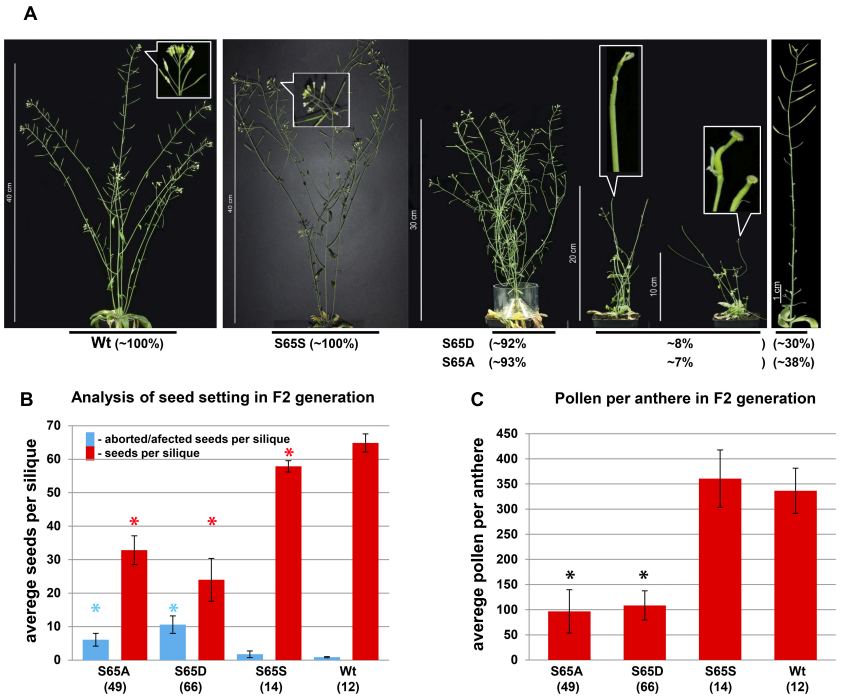

FIGURE 4 | Replacement of serine 65 of CENH3 results in an abnormal plant growth and flower development. **(A)** Complementation of the *cenh3-1* mutant with transgenes encoding either the CENH3 variants: Wt, S65D and S65A under native promotor, results in various phenotypical abnormalities especially involving reproductive structures (plants at 60 DAS). For each construct, 12 to 78 independent transgenic lines were obtained. **(B)** The CENH3 S65A and S65D transgenes do not rescue the *cenh3-1* mutant with respect to seed set as fully as does transgenic Wt CENH3. The average number of seeds per silique was determined based on seven siliques per plant. The numbers shown in parentheses refer to the number of independent lines used for analysis. Error bars correspond to standard deviation. **(C)** The complementation of *cenh3-1* by CENH3 S65A or S65D does not fully restore male fertility. The number of pollen per anther was determined based on fifteen anthers per plant. The average numbers shown in parentheses refer to the number of independent lines used for analysis. Error bars correspond to standard deviation. Columns indicated with asterisks were significantly different in comparison with Wt. The data were analyzed by one-way ANOVA-test (*$p < 0.05$). The calculations were performed with the statistical program SigmaPlot v12 (Systat Software, Inc.).

S65S complemented lines. In addition, the number of viable pollen grains in anthers of *cenh3-1* complemented mutants (S65A or S65D) was reduced compared to Wt and S65S complemented plants (**Figure 4C** and **Supplementary Figure S12**). Further, the male meiosis (130 pollen mother cells) of S65 mutant plants did not show any obvious abnormality compared to Wt ($n = 250$), nor was there any evidence for aneuploids or polyploids among their progeny. Western blot analysis with anti-CENH3 antibodies of protein extracts from complemented and Wt plants showed despite clear growth differences (20 DAS), a similar abundance of CENH3 in all plants (**Figures 5A,B**). *In silico* expression analysis of Aurora3 and CENH3 in different tissues revealed the highest expression levels of both genes in floral and shoot apical meristems (**Supplementary Figures S13A,B**).

DISCUSSION

AtAurora3 Interacts With CENH3 *in vivo* and Phosphorylates It *in vitro*

We have shown that Aurora3, likely an *A. thaliana* ortholog of human Aurora B, interacts with AtCENH3 *in vivo* and phosphorylates it *in vitro*. In human cells, both Aurora A and B interact and phosphorylate CENH3 (Kunitoku et al., 2003; Slattery et al., 2008), but the interaction is stronger with Aurora B (Yu et al., 2015). In *A. thaliana*, Aurora3 is associated with the centromeres during mitosis (Demidov et al., 2005). Here IP revealed *Arabidopsis* Aurora kinase binding with AtCENH3 in extracts of growing seedlings after crosslinking with DSP, which retained *in vivo* protein-protein interactions in the presence of 1.5 M NaCl in the extraction buffer. A high salt concentration is needed to release CENH3 from nucleosomes. Additionally, BiFC demonstrated the interaction between Aurora3 and AtCENH3 *in vivo*, specifically at the centromeres after infiltration in tobacco leaves. This finding is in accordance with the observation that heterologous CENH3 may localize to the centromeres in addition to the endogenous variant of CENH3 (see review by Lermontova and Schubert, 2013). *In vitro* phosphorylation of CENH3 by Aurora kinase has been demonstrated in a range of organisms (Kunitoku et al., 2003; Slattery et al., 2008). Since the CENH3 N-terminal sequence is highly variable (even between closely related species), the determination of phosphorylation sites used by Aurora3 in *A. thaliana* was not feasible based on sequence homology. Nevertheless, the Aurora recognition motif, which was experimentally determined closely resembled that used by Aurora A and Aurora B

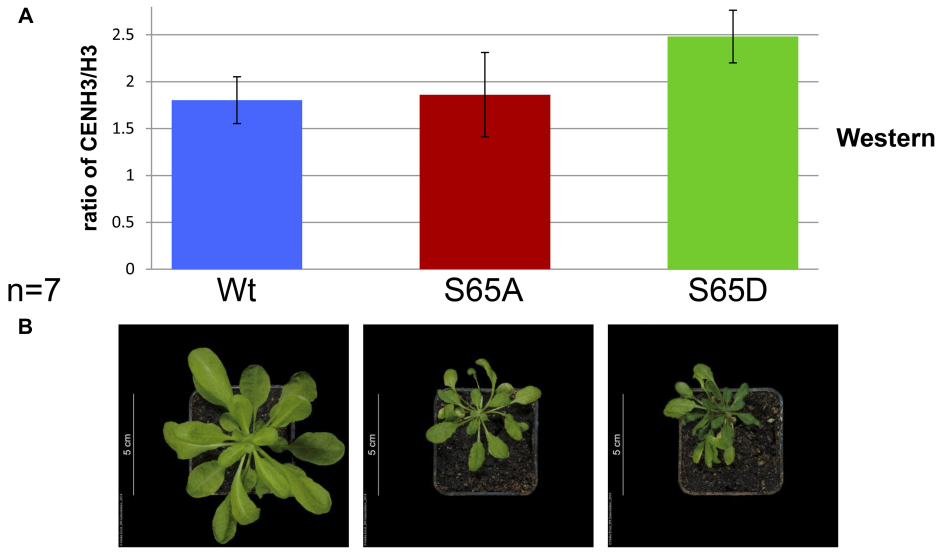

FIGURE 5 | The phenotype of *cenh3-1* mutants harboring *CENH3* S65A or S65D does not correlate with the ratio of CENH3: H3. **(A)** The average ratio of CENH3 to H3 (based on a Western blot using LI-COR Image Studio 3.1 analytic software) in Wt and *cenh3-1* plants harboring *CENH3* S65A or S65D. The experiment was performed in seven biological replicates with protein extracted from 7 × 5 independent transgenic F2 plants and 7 × 5 Wt plants. Error bars correspond to standard deviation. **(B)** Shows typical phenotype of plants (20 DAS) analyzed in **(A)**.

(Dephoure et al., 2008; Gully et al., 2012). Nine of the 11 peptides carrying Aurora recognition sites were weakly phosphorylated, suggesting that multiple CENH3 phosphorylation sites are targeted in *A. thaliana*. These data were confirmed by the kinase assay using recombinant CENH3 as substrate. Additionally, phosphorylation of CENH3 by Aurora3 *in vitro* also demonstrates the interaction of both proteins. Substitution of serine 65 reduced but did not fully abolish CENH3 phosphorylation (**Supplementary Figures S4A,B**) indicating the existence of multiple putative AtAurora3 phosphorylation sites. The sequence context of CENH3 S65 was found in most, but not all Brassicaceae genomes (Maheshwari et al., 2015). However, at position threonine 65 occurs more often than serine (**Supplementary Figure S14A**). In some cases, even a non-phosphorylatable alanine residue is present, irrespective of whether the species encodes one or multiple CENH3 variants (**Supplementary Figure S14B**). Other conserved blocks within the N-terminal region of plant CENH3s also harbor Aurora recognition motifs, though at a lower frequency. Possibly, conserved sequence blocks could be favored recognition motifs for enzymes involved in post-translational CENH3 modifications. The CENH3 N-terminus can also be phosphorylated by other kinases, for example, by the cyclin-dependent kinase 1 (Yu et al., 2015). The cell cycle-dependent phosphorylation of maize CENH3 at S50 (Zhang et al., 2005) is likely not mediated by Aurora kinase because of the lack of a recognition motif for this enzyme in the vicinity of this site.

The use of a CENH3 pS65-specific antibody confirmed the identity of the phosphorylation sites identified *in vitro* and *in vivo* since binding was abolished after the protein sample had been phosphatase-treated. In agreement with Heckmann et al. (2011), who showed that the intensity of CENH3 expression is related to the extent of cell division occurring in a certain tissue, the present analysis indicated that the abundance of CENH3 was particularly high in actively dividing cells, e.g., in suspension cultures. However, phosphorylation of CENH3 at S65 was particularly high in protein extracts from flower buds. Phosphorylation of CENH3 S65 is not restricted to generative tissue since it also occurred in seedlings and in suspension cultures; and it does not strictly correlate with cell division, because its occurrence was relatively low in actively dividing suspension cultures. Assuming a tissue type-dependent regulation of CENH3 phosphorylation would be consistent with the tissue type-dependent organization and regulation of centromeres (Kagawa et al., 2014; Ishii et al., 2015).

Phosphorylation of CENH3 S65 by Aurora3 Is Required for Proper Development of Floral Meristems

In order to uncover the physiological role of S65 phosphorylation *in vivo*, *cenh3-1* mutant plants were transformed with CENH3 gene variants displaying either S65A or S65D. Since the expression of Aurora3 and CENH3 depends on the cell cycle (Demidov et al., 2005; Heckmann et al., 2011; Lermontova et al., 2011a) and both are invovled in cell cycle control (Schumacher et al., 1998; Howman et al., 2000), we assume that the phosphorylation of serine 65 is cell cycle dependent in some meristematic tissues. This assumption is in line with the observation that in 30-days-old *cenh3-1* mutants complemented by S65A or S65D the average size of epidermal cells, is smaller than that of Wt or of S65S complemented lines (**Supplementary Figure S15A**). In 50-days-old plants, this difference is abolished

(**Supplementary Figure S15B**), and the size of leaf epidermal cells and plant age seem to be correlated (Kalve et al., 2014). Some of the S65A- and S65D-complemented *cenh3-1* mutant plants displayed defective differentiation of the apical meristem and developed shoots without male reproductive structures (**Figure 4A** and **Supplementary Figures S8**, **S9**). We assume that in *cenh3-1* complemented mutants (S65A or S65D), defects in the early floral meristem development lead to slower cell growth, and reduced biomass. This effect disappeared during later stages (**Supplementary Figure S7** and **Supplementary Table S2**). After 63 DAS, plants remain smaller compared to the controls (Wt and S65S). CENH3 transgenics (S65A and S65D) showed an increased number of lateral stems (**Supplementary Table S3**). We speculate that, over time, the blocking of shoot meristem development in S65 mutants is released. Partial compensation of such blocking is visibly by an increase in the number of lateral stems. However, they are smaller than in control plants because they already lost the time for normal growth during the life cycle. Therefore, CENH3 transformants (S65A and S65D) generally remain slightly smaller in size compared to controls (WT and S65S).

Because Aurora3 and CENH3 are strongly expressed in the floral meristem, phosphorylation mutations of CENH3 might contribute to the observed morphological changes of male generative organs. Most likely, the dynamic CENH3 phosphorylation of serine 65 is involved in the regulation of floral meristem development, as implied by the high abundance of pS65 in flower buds (**Figure 3**), and by the phenotypic effect of S65 substitutions which resembled those seen in plants expressing CENH3 variants with a modified N-terminus (Ravi et al., 2011) or just the CENH3 histone fold domain (Lermontova et al., 2011b).

Interestingly, overexpression of AtAurora1 in tobacco similarly results in an altered stamen morphology, in a reduced growth rate and in enlarged axillary meristems (Demidov et al., 2014). Down-regulation of *Arabidopsis* Aurora1 and Aurora3 results in reduced biomass, slow development, reduced pollen fertility and seed setting (Demidov et al., 2014). This phenotype is reminiscent, but not completely identical to, that of the S65A- and S65D-complemented *cenh3-1* mutants.

Two reasons why no phenotypic differences between the S65A- and the S65D-complemented *cenh3-1* mutants were found can be envisaged. Either the S65D complementation does not functionally compensate for S65 phosphorylation, in spite of its steric similarity to pS65. Alternatively, S65 undergoes highly dynamic phosphorylation and dephosphorylation, and both substitutions (S65A and S65D) impair the functionality of CENH3 and therefore result in the observed phenotype. Comparable results were observed for tissue-cultured human CENH3 mutants (Zeitlin et al., 2001). Substitution of CENH3 Ser7 by Ala or Glu (Glu like Asp imitates pSer) equally leads to an increase of the Flemming body lifetime and midbody length in comparison with the control. The authors explained this observation by a possible change in the CENH3 N-termini structure or due to the disruption of the phosphorylation/dephosphorylation dynamics of Ala7 and Glu7 mutated CENH3.

For a better understanding of the mechanisms involved in CENH3 S65 phosphorylation and its physiological significance in the development of meristems, additional experiments will be needed. For example, it would be of interest to analyze the expression of the key meristem development regulators in S65A- and S65D-complemented *cenh3-1* mutants.

The overall conclusion is that Aurora3 phosphorylates CENH3 at S65 and that this post-translational modification is required for the proper development of the floral meristem.

DATA AVAILABILITY

All datasets generated for this study are included in the manuscript and/or the **Supplementary Files**.

AUTHOR CONTRIBUTIONS

DD, SH, TR, MK, and AH designed the study. DD, IL, SH, OW, TR, EDT, MK, PS, and CM conducted the experiments. DD, TR, MK, and AH analyzed the data. DD, IL, and AH drafted the manuscript.

FUNDING

This research was made possible by grants from the German Research Foundation (SFB) 648 "Molecular mechanisms of information processing in plants" and by the BMBF 031B0192A "HaploTools." EDT was supported by the Nationl Programme of Sustainability I (LO1204) and The European Regional Development Fund project "Plants as a tool for sustainable global development" (no. CZ.02.1.01/0.0/0.0/16_019/0000827 to E.D.T.).

ACKNOWLEDGMENTS

We thank Karla Meier (IPK, Gatersleben) for technical assistance, Karin Lipfert for help with figure artwork, Ingo Schubert for critical reading of the manuscript and helpful suggestions, Kijo Nagaki (Okayama University, Japan) for providing CENPC-specific antibodies, Klaus Harter (Department of Plant Physiology, University of Tuebingen, Germany) for BIFC constructs, and the late Simon Chan (UC Davis, United States) for the cloned *A. thaliana* CENH3 genomic fragment and for seeds of the *A. thaliana cenh3-1* heterozygote.

SUPPLEMENTARY MATERIAL

The Supplementary Material for this article can be found online at: https://www.frontiersin.org/articles/10.3389/fpls.2019.00928/full#supplementary-material

REFERENCES

Adams, R. R., Carmena, M., and Earnshaw, W. C. (2001). Chromosomal passengers and the (aurora) ABCs of mitosis. *Trends Cell Biol.* 11, 49–54. doi: 10.1016/s0962-8924(00)01880-8

Alexander, M. P. (1969). Differential staining of aborted and nonaborted pollen. *Stain Technol.* 44, 117–122. doi: 10.3109/10520296909063335

Bailey, A. O., Panchenko, T., Sathyan, K. M., Petkowski, J. J., Pai, P. J., Bai, D. L., et al. (2013). Posttranslational modification of CENP-A influences the conformation of centromeric chromatin. *Proc. Natl. Acad. Sci. U.S.A.* 110, 11827–11832. doi: 10.1073/pnas.1300325110

Boeckmann, L., Takahashi, Y., Au, W. C., Mishra, P. K., Choy, J. S., Dawson, A. R., et al. (2013). Phosphorylation of centromeric histone H3 variant regulates chromosome segregation in *Saccharomyces cerevisiae*. *Mol. Biol. Cell* 24, 2034–2044. doi: 10.1091/mbc.E12-12-0893

Clough, S. J., and Bent, A. F. (1998). Floral dip: a simplified method for *Agrobacterium*-mediated transformation of *Arabidopsis thaliana*. *Plant J.* 16, 735–743. doi: 10.1046/j.1365-313x.1998.00343.x

Demidov, D., Hesse, S., Tewes, A., Rutten, T., Fuchs, J., Ashtiyani, R. K., et al. (2009). Aurora1 phosphorylation activity on histone H3 and its cross-talk with other post-translational histone modifications in Arabidopsis. *Plant J.* 59, 221–230. doi: 10.1111/j.1365-313X.2009.03861.x

Demidov, D., Lermontova, I., Weiss, O., Fuchs, J., Rutten, T., Kumke, K., et al. (2014). Altered expression of Aurora kinases in *Arabidopsis* results in aneu- and polyploidization. *Plant J.* 80, 449–461. doi: 10.1111/tpj.12647

Demidov, D., Van Damme, D., Geelen, D., Blattner, F. R., and Houben, A. (2005). Identification and dynamics of two classes of Aurora-like kinases in *Arabidopsis* and other plants. *Plant Cell* 17, 836–848. doi: 10.1105/tpc.104.029710

Dephoure, N., Zhou, C., Villen, J., Beausoleil, S. A., Bakalarski, C. E., Elledge, S. J., et al. (2008). A quantitative atlas of mitotic phosphorylation. *Proc. Natl. Acad. Sci. U. S. A.* 105, 10762–10767. doi: 10.1073/pnas.0805139105

Earnshaw, W. C., Allshire, R. C., Black, B. E., Bloom, K., Brinkley, B. R., Brown, W., et al. (2013). Esperanto for histones: CENP-A, not $CenH_3$, is the centromeric histone H_3 variant. *Chromosome Res.* 21, 101–106. doi: 10.1007/s10577-013-9347-y

Earnshaw, W. C., and Rothfield, N. (1985). Identification of a family of human centromere proteins using autoimmune sera from patients with scleroderma. *Chromosoma* 91, 313–321. doi: 10.1007/bf00328227

Edwards, K., Johnstone, C., and Thompson, C. (1991). A simple and rapid method for the preparation of plant genomic DNA for PCR analysis. *Nucleic Acids Res.* 19, 1349–1349. doi: 10.1093/nar/19.6.1349

Eot-Houllier, G., Magnaghi-Jaulin, L., Fulcrand, G., Moyroud, F. X., Monier, S., and Jaulin, C. (2018). Aurora A-dependent CENP-A phosphorylation at inner centromeres protects bioriented chromosomes against cohesion fatigue. *Nat. Commun.* 9:1888.

Goutte-Gattat, D., Shuaib, M., Ouararhni, K., Gautier, T., Skoufias, D. A., Hamiche, A., et al. (2013). Phosphorylation of the CENP-A amino-terminus in mitotic centromeric chromatin is required for kinetochore function. *Proc. Natl. Acad. Sci. U.S.A.* 110, 8579–8584. doi: 10.1073/pnas.1302955110

Gully, C. P., Velazquez-Torres, G., Shin, J. H., Fuentes-Mattei, E., Wang, E., Carlock, C., et al. (2012). Aurora B kinase phosphorylates and instigates degradation of p53. *Proc. Natl. Acad. Sci. U.S.A.* 109, E1513–E1522. doi: 10.1073/pnas.1110287109

Heckmann, S., Lermontova, I., Berckmans, B., De Veylder, L., Baumlein, H., and Schubert, I. (2011). The E2F transcription factor family regulates CENH3 expression in *Arabidopsis thaliana*. *Plant J.* 68, 646–656. doi: 10.1111/j.1365-313X.2011.04715.x

Hergeth, S. P., Dundr, M., Tropberger, P., Zee, B. M., Garcia, B. A., Daujat, S., et al. (2011). Isoform-specific phosphorylation of human linker histone H1.4 in mitosis by the kinase Aurora B. *J. Cell Sci.* 124(Pt 10), 1623–1628. doi: 10.1242/jcs.084947

Hoffmann, G., Samel-Pommerencke, A., Weber, J., Cuomo, A., Bonaldi, T., and Ehrenhofer-Murray, A. E. (2018). A role for CENP-A/Cse4 phosphorylation on serine 33 in deposition at the centromere. *Fems Yeast Res.* 18:fox094. doi: 10.1093/femsyr/fox094

Howman, E. V., Fowler, K. J., Newson, A. J., Redward, S., MacDonald, A. C., Kalitsis, P., et al. (2000). Early disruption of centromeric chromatin organization in centromere protein A (Cenpa) null mice. *Proc. Natl. Acad. Sci. U.S. A.* 97, 1148–1153. doi: 10.1073/pnas.97.3.1148

Hsu, J. Y., Sun, Z. W., Li, X., Reuben, M., Tatchell, K., Bishop, D. K., et al. (2000). Mitotic phosphorylation of histone H3 is governed by Ipl1/aurora kinase and Glc7/PP1 phosphatase in budding yeast and nematodes. *Cell* 102, 279–291. doi: 10.1016/s0092-8674(00)00034-9

Ishii, T., Karimi-Ashtiyani, R., Banaei-Moghaddam, A. M., Schubert, V., Fuchs, J., and Houben, A. (2015). The differential loading of two barley CENH3 variants into distinct centromeric substructures is cell type- and development-specific. *Chromosome Res.* 23, 277–284. doi: 10.1007/s10577-015-9466-8

Kagawa, N., Hori, T., Hoki, Y., Hosoya, O., Tsutsui, K., Saga, Y., et al. (2014). The CENP-O complex requirement varies among different cell types. *Chromosome Res.* 22, 293–303. doi: 10.1007/s10577-014-9404-1

Kalve, S., Fotschki, J., Beeckman, T., Vissenberg, K., and Beemster, G. T. S. (2014). Three-dimensional patterns of cell division and expansion throughout the development of *Arabidopsis thaliana* leaves. *J. Exp. Bot.* 65, 6385–6397. doi: 10.1093/jxb/eru358

Karimi-Ashtiyani, R., and Houben, A. (2013). In vitro phosphorylation of histone h3 at threonine 3 by *Arabidopsis* haspin is strongly influenced by posttranslational modifications of adjacent amino acids. *Mol. Plant* 6, 574–576. doi: 10.1093/mp/sss149

Kato, S., Imoto, Y., Ohnuma, M., Matsunaga, T. M., Kuroiwa, H., Kawano, S., et al. (2011). Aurora kinase of the red alga *cyanidioschyzon merolae* is related to both mitochondrial division and mitotic spindle formation. *Cytologia* 76, 455–462. doi: 10.1508/cytologia.76.455

Kawabe, A., Matsunaga, S., Nakagawa, K., Kurihara, D., Yoneda, A., Hasezawa, S., et al. (2005). Characterization of plant Aurora kinases during mitosis. *Plant Mol. Biol.* 58, 1–13. doi: 10.1007/s11103-005-3454-x

Keçeli, B. N., De Storme, N., and Geelen, D. (2017). *In Vivo* ploidy determination of *Arabidopsis thaliana* male and female gametophytes. *Methods Mol. Biol.* 1669, 77–85. doi: 10.1007/978-1-4939-7286-9_7

Kunitoku, N., Sasayama, T., Marumoto, T., Zhang, D., Honda, S., Kobayashi, O., et al. (2003). CENP-A phosphorylation by Aurora-A in prophase is required for enrichment of Aurora-B at inner centromeres and for kinetochore function. *Dev. Cell* 5, 853–864. doi: 10.1016/s1534-5807(03)00364-2

Kurihara, D., Matsunaga, S., Kawabe, A., Fujimoto, S., Noda, M., Uchiyama, S., et al. (2006). Aurora kinase is required for chromosome segregation in tobacco BY-2 cells. *Plant J.* 48, 572–580. doi: 10.1111/j.1365-313x.2006.02893.x

Laemmli, U. K. (1970). Cleavage of structural proteins during the assembly of the head of bacteriophage T4. *Nature* 227, 680–685. doi: 10.1038/227680a0

Lermontova, I., Koroleva, O., Rutten, T., Fuchs, J., Schubert, V., Moraes, I., et al. (2011a). Knockdown of CENH3 in Arabidopsis reduces mitotic divisions and causes sterility by disturbed meiotic chromosome segregation. *Plant J.* 68, 40–50. doi: 10.1111/j.1365-313X.2011.04664.x

Lermontova, I., Kuhlmann, M., Friedel, S., Rutten, T., Heckmann, S., Sandmann, M., et al. (2013). *Arabidopsis* KINETOCHORE NULL2 is an upstream component for centromeric histone H_3 variant $cenH_3$ deposition at centromeres. *Plant Cell* 25, 3389–3404. doi: 10.1105/tpc.113.114736

Lermontova, I., Rutten, T., and Schubert, I. (2011b). Deposition, turnover, and release of CENH3 at Arabidopsis centromeres. *Chromosoma* 120, 633–640. doi: 10.1007/s00412-011-0338-5

Lermontova, I., and Schubert, I. (2013). "CENH3 for Establishing and Maintaining Centromeres„" in *Plant Centromere Biology*. eds J. Jiming and J. A. Birchler (Hoboken,: Wiley-Blackwell), 67–82. doi: 10.1002/9781118525715.ch6

Lermontova, I., Schubert, V., Fuchs, J., Klatte, S., Macas, J., and Schubert, I. (2006). Loading of *Arabidopsis centromeric* histone CENH3 occurs mainly during G2 and requires the presence of the histone fold domain. *Plant Cell* 18, 2443–2451. doi: 10.1105/tpc.106.043174

Maheshwari, S., Tan, E. H., West, A., Franklin, F. C., Comai, L., and Chan, S. W. (2015). Naturally occurring differences in CENH3 affect chromosome segregation in zygotic mitosis of hybrids. *PLoS Genet.* 11:e1004970. doi: 10.1371/journal.pgen.1004970

Manzanero, S., Arana, P., Puertas, M. J., and Houben, A. (2000). The chromosomal distribution of phosphorylated histone H3 differs between plants and animals at meiosis. *Chromosoma* 109, 308–317. doi: 10.1007/s004120000087

Mishra, P. K., Olafsson, G., Boeckmann, L., Westlake, T. J., Jowhar, Z. M., Dittman, L. E., et al. (2019). Cell cycle-dependent association of polo kinase Cdc5 with

CENP-A contributes to faithful chromosome segregation in budding yeast. *Mol. Biol. Cell* 30, 1020–1036. doi: 10.1091/mbc.e18-09-0584

Nagaki, K., Kashihara, K., and Murata, M. (2009). Characterization of the two centromeric proteins CENP-C and MIS12 in *Nicotiana* species. *Chromosome Res.* 17, 719–726. doi: 10.1007/s10577-009-9064-8

Ravi, M., and Chan, S. W. (2010). Haploid plants produced by centromere-mediated genome elimination. *Nature* 464, 615–618. doi: 10.1038/nature08842

Ravi, M., Shibata, F., Ramahi, J. S., Nagaki, K., Chen, C., Murata, M., et al. (2011). Meiosis-specific loading of the centromere-specific histone CENH3 in *Arabidopsis thaliana*. *PLoS Genet.* 7:e1002121. doi: 10.1371/journal.pgen.1002121

Samel, A., Cuomo, A., Bonaldi, T., and Ehrenhofer-Murray, A. E. (2012). Methylation of CenH3 arginine 37 regulates kinetochore integrity and chromosome segregation. *Proc. Natl. Acad. Sci. U.S.A.* 109, 9029–9034. doi: 10.1073/pnas.1120968109

Sánchez-Morán, E., Benavente, E., and Orellana, J. (2001). Analysis of karyotypic stability of homoeologous-pairing (ph) mutants in allopolyploid wheats. *Chromosoma* 110, 371–377. doi: 10.1007/s004120100156

Schagger, H., and von Jagow, G. (1987). Tricine-sodium dodecyl sulfate-polyacrylamide gel electrophoresis for the separation of proteins in the range from 1 to 100 kDa. *Anal. Biochem.* 166, 368–379. doi: 10.1016/0003-2697(87)90587-2

Schumacher, J. M., Golden, A., and Donovan, P. J. (1998). AIR-2: an Aurora/Ipl1-related protein kinase associated with chromosomes and midbody microtubules is required for polar body extrusion and cytokinesis in *Caenorhabditis elegans* embryos. *J. Cell Biol.* 143, 1635–1646. doi: 10.1083/jcb.143.6.1635

Slattery, S. D., Moore, R. V., Brinkley, B. R., and Hall, R. M. (2008). Aurora-C and Aurora-B share phosphorylation and regulation of CENP-A and Borealin during mitosis. *Cell Cycle* 7, 787–795. doi: 10.4161/cc.7.6.5563

Spiker, S. (1980). A modification of the acetic acid-urea system for use in microslab polyacrylamide-gel electrophoresis. *Anal. Biochem.* 108, 263–265. doi: 10.1016/0003-2697(80)90579-5

Swain, J. E., Ding, J., Wu, J., and Smith, G. D. (2008). Regulation of spindle and chromatin dynamics during early and late stages of oocyte maturation by *Aurora* kinases. *Mol. Hum. Reprod.* 14, 291–299. doi: 10.1093/molehr/gan015

Takada, M., Zhang, W., Suzuki, A., Kuroda, T. S., Yu, Z., Inuzuka, H., et al. (2017). FBW7 Loss promotes chromosomal instability and tumorigenesis via cyclin E1/CDK2-mediated phosphorylation of CENP-A. *Cancer Res.* 77, 4881–4893. doi: 10.1158/0008-5472.can-17-1240

Talbert, P. B., Masuelli, R., Tyagi, A. P., Comai, L., and Henikoff, S. (2002). Centromeric localization and adaptive evolution of an *Arabidopsis histone* H3 variant. *Plant Cell* 14, 1053–1066. doi: 10.1105/tpc.010425

Tikhenko, N., Rutten, T., Tsvetkova, N., Voylokov, A., and Borner, A. (2015). Hybrid dwarfness in crosses between wheat (*Triticum aestivum* L.) and rye (*Secale cereale* L.): a new look at an old phenomenon. *Plant Biol.* 17, 320–326. doi: 10.1111/plb.12237

Tomaštíková, E., Demidov, D., Jeřábková, H., Binarová, P., Houben, A., Doležel, J., et al. (2015). TPX2 Protein of *Arabidopsis* activates aurora kinase 1, but not aurora kinase 3 in vitro. *Plant Mol. Biol. Rep.* 33, 1988–1995. doi: 10.1007/s11105-015-0890-x

Walter, M., Chaban, C., Schutze, K., Batistic, O., Weckermann, K., Nake, C., et al. (2004). Visualization of protein interactions in living plant cells using bimolecular fluorescence complementation. *Plant J.* 40, 428–438.

Wang, K., Yu, Z., Liu, Y., and Li, G. (2017). Ser68 phosphorylation ensures accurate cell-cycle-dependent CENP-A deposition at centromeres. *Dev. Cell* 40, 5–6. doi: 10.1016/j.devcel.2016.12.015

Yu, Z., Zhou, X., Wang, W., Deng, W., Fang, J., Hu, H., et al. (2015). Dynamic phosphorylation of CENP-A at Ser68 orchestrates its cell-cycle-dependent deposition at centromeres. *Dev. Cell* 32, 68–81. doi: 10.1016/j.devcel.2014.11.030

Zeitlin, S. G., Shelby, R. D., and Sullivan, K. F. (2001). CENP-A is phosphorylated by Aurora B kinase and plays an unexpected role in completion of cytokinesis. *J. Cell Biol.* 155, 1147–1157.

Zhang, X., Li, X., Marshall, J. B., Zhong, C. X., and Dawe, R. K. (2005). Phosphoserines on maize CENTROMERIC HISTONE H3 and histone H3 demarcate the centromere and pericentromere during chromosome segregation. *Plant Cell* 17, 572–583. doi: 10.1105/tpc.104.028522

Conflict of Interest Statement: The authors declare that the research was conducted in the absence of any commercial or financial relationships that could be construed as a potential conflict of interest.

frontiers in Plant Science

ORIGINAL RESEARCH
published: 17 October 2019
doi: 10.3389/fpls.2019.01267

Evidence That Ion-Based Signaling Initiating at the Cell Surface Can Potentially Influence Chromatin Dynamics and Chromatin-Bound Proteins in the Nucleus

Antonius J.M. Matzke, Wen-Dar Lin and Marjori Matzke**

Institute of Plant and Microbial Biology, Academia Sinica, Taipei, Taiwan

OPEN ACCESS

Edited by:
Iva Mozgova,
Academy of Sciences of the Czech Republic, Czechia

Reviewed by:
Kiwamu Tanaka,
Washington State University, United States
Frédéric Pontvianne,
UMR5096 Laboratoire Génome et développement des plantes, France
Célia Baroux,
University of Zurich, Switzerland

***Correspondence:**
Antonius J.M. Matzke
antoniusmatzke@gate.sinica.edu.tw
Marjori Matzke
marjorimatzke@gate.sinica.edu.tw

Specialty section:
This article was submitted to Plant Cell Biology, a section of the journal Frontiers in Plant Science

Received: *01 April 2019*
Accepted: *11 September 2019*
Published: *17 October 2019*

Citation:
Matzke AJM, Lin W-D and Matzke M (2019) Evidence That Ion-Based Signaling Initiating at the Cell Surface Can Potentially Influence Chromatin Dynamics and Chromatin-Bound Proteins in the Nucleus. Front. Plant Sci. 10:1267. doi: 10.3389/fpls.2019.01267

We have developed tools and performed pilot experiments to test the hypothesis that an intracellular ion-based signaling pathway, provoked by an extracellular stimulus acting at the cell surface, can influence interphase chromosome dynamics and chromatin-bound proteins in the nucleus. The experimental system employs chromosome-specific fluorescent tags and the genome-encoded fluorescent pH sensor SEpHluorinA227D, which has been targeted to various intracellular membranes and soluble compartments in root cells of *Arabidopsis thaliana*. We are using this system and three-dimensional live cell imaging to visualize whether fluorescent-tagged interphase chromosome sites undergo changes in constrained motion concurrently with reductions in membrane-associated pH elicited by extracellular ATP, which is known to trigger a cascade of events in plant cells including changes in calcium ion concentrations, pH, and membrane potential. To examine possible effects of the proposed ion-based signaling pathway directly at the chromatin level, we generated a pH-sensitive fluorescent DNA-binding protein that allows pH changes to be monitored at specific genomic sites. Results obtained using these tools support the existence of a rapid, ion-based signaling pathway that initiates at the cell surface and reaches the nucleus to induce alterations in interphase chromatin mobility and the surrounding pH of chromatin-bound proteins. Such a pathway could conceivably act under natural circumstances to allow external stimuli to swiftly influence gene expression by affecting interphase chromosome movement and the structures and/or activities of chromatin-associated proteins.

Keywords: genetically encoded voltage indicator, confocal imaging, chromatin dynamics, fluorescence chromosome tagging, ion-based signaling, pH, SEpHluorin

INTRODUCTION

The development, viability and environmental responsiveness of unicellular and multicellular organisms depends on the integration of diverse molecular, chemical and mechanical signaling pathways that ultimately exert an effect on gene expression. In addition to these classical signaling pathways, electrical signaling is increasingly recognized as an essential and rapid means to transmit information within and between cells and throughout whole organisms (Levin and Stevenson, 2012;

Mousavi et al., 2013; Cohen and Venkatachalam, 2014; Choi et al., 2016; Hedrich et al., 2016; Gilroy et al., 2018). On the cellular level, the electrical component at the plasma membrane (PM) comprises both the trans-membrane potential, which is generated primarily by proton gradients in plants (Duby and Boutry, 2009), and the surface potential, which represents the electrical potential over a small distance from the plane of the membrane. Surface potentials are normally sufficiently negative to enrich for cations at the membrane surface (Kinraide et al., 1998; Cohen and Venkatachalam, 2014). Plant endomembranes also contain electrogenic proton pumps, which together with counter ion fluxes establish cell-internal pH gradients that are important for responses of plants to a variety of developmental and environmental cues (Sze and Chanroj, 2018).

We are interested in testing the hypothesis that extracellular stimuli can influence gene expression *via* a rapid electrical/ion-based pathway acting from the cell surface to the nucleus through interconnected intracellular membrane systems (Matzke and Matzke, 1991; Matzke et al., 2010b). Electrical conveyance of information throughout the cell by means of intracellular membranes has been envisaged as a "cytoplasmic nervous system" (Sepheri-Rad et al., 2018) and proposed to feature the endoplasmic reticulum (ER), which is closely associated with the PM through membrane contact sites (Wang et al., 2017) and physically continuous with the outer nuclear membrane (ONM) (Matzke and Matzke, 1991; Sepheri-Rad et al., 2018). Electrical signals could trigger multiple events at membranes including opening of voltage-gated ion channels; changes in surface potentials by release of membrane-bound ions; and alterations in the structures and/or activities of integral membrane proteins, as well as membrane-associated proteins and other polyelectrolytes such as DNA (Matzke and Matzke, 1991; Bezanilla, 2008).

Investigating electrical/ion-based pathways and their effects on the nuclear genome in living cells requires non-invasive techniques for assessing changes in trans-membrane electrical potentials and concentrations of soluble and membrane-associated ions, as well as a means to detect effects at the genomic DNA level. Ideally, these techniques should allow changes to be monitored simultaneously at multiple membrane systems and at chromatin within individual cells, as well as across populations of cells in intact organisms. Genome-encoded fluorescent sensors of membrane voltage and of various ions, such as H^+ and Ca^{+2}, together with methods for fluorescent-tagging of interphase chromosomes and three-dimensional (3D) live cell imaging technology represent useful tools for such studies.

Genome-encoded voltage indicators (GEVIs) have been developed and used in animal systems for the detection of coordinated changes in PM potential in different subpopulations of neuronal cells (Knöpfel, 2012). Different GEVIs are based on either changes in Förster resonance energy transfer (FRET) or fluorescence intensity (Matzke and Matzke, 2013; Knöpfel et al., 2015). FRET-based GEVIs rely on two differently colored fluorescent proteins, which shift in proximity in response to changes in trans-membrane potential, thus positioning the two proteins to favor the occurrence of FRET. By contrast, fluorescence intensity-based GEVIs comprise only a single fluorescent protein that shows alterations in fluorescence intensity following changes in membrane voltage. Although the former can be used to quantify shifts in membrane potential, currently available intensity-based GEVIs provide a qualitative assessment of membrane voltage changes (Cohen and Venkatachalam, 2014; Hilleary et al., 2018).

GEVIs are beginning to be adapted for use in plant systems. We have tested both FRET- and intensity-based GEVIs in root cells of stably transformed *Arabidopsis* seedlings. In our experiments, several genome-encoded FRET-based GEVIs, under the control of either the *RPS5A* promoter or the constitutive UBI-10 promoter were not expressed strongly enough to detect changes in PM voltage (Matzke and Matzke, 2013). However, a transiently expressed FRET-based GEVI was used successfully to study membrane trafficking involving a SNARE protein in cells of the root elongation zone (Grefen et al., 2015).

We also tested the fluorescence intensity-based GEVI ArcLight, which is a voltage-sensing derivative of the fluorescent pH-sensing protein SEpHluorin (Miesenböck, 2012; Han et al., 2014). The voltage sensitivity of ArcLight was achieved by adding the voltage-sensing domain of *Ciona intestinalis* voltage-sensing phosphatase (Ci-VSD) to SEpHluorin, and changing amino acid 227 from alanine to aspartic acid (A227D) (Han et al., 2014). Arclight has been used in metazoan systems to study changes in PM voltage, which is largely determined in animal cells by the trans-membrane distributions of Na^+ and K^+ ions. In plant cells, however, where H^+ ions are the major contributor to the membrane potential, the pH sensitivity of the SEpHluorin-moiety of ArcLight appears to override its voltage sensitivity (Matzke and Matzke, 2015). The predominance of pH sensing was revealed by the identical responses of ArcLight and SEpHluorinA227D (ArcLight without the Ci-VSD; referred to hereafter as SEpHluorinD) in root cells following application of extracellular ATP (eATP) (Matzke and Matzke, 2015). In animals and plants, eATP functions as an external signaling molecule that triggers a cascade of responses including changes in cytosolic calcium, which are coincident with changes in cytosolic pH (Felle, 2001; Behera et al., 2018), as well as changes in membrane conductance (Tanaka et al., 2010; Cao et al., 2014) and gene expression (Jewell et al., 2019). Therefore, even though ArcLight does not appear to be suitable for directly detecting changes in membrane voltage in plant systems, it can be used as an intensity-based fluorescent sensor of qualitative shifts in pH, which can occur as a downstream consequence of changes in membrane potential. Able to act as either a signal or a messenger in plant cells, pH has important roles in mediating responses to multiple environmental cues and influencing gene expression (Felle, 2001).

Among the techniques available for observing DNA in living cells, fluorescent labeling of specific chromatin sites using bacterial Tet and Lac operator-repressor systems has proven useful in a number of studies on chromatin dynamics in yeast, *Drosophila* and plants (Weiss et al., 2018). This method is based on binding of a fusion protein comprising a bacterial repressor protein (RP) and a fluorescent protein (FP) to the cognate operator repeats introduced as a tandem array into the host genome by transformation procedures. The tagged genomic sites can be visualized as bright fluorescent dots under a fluorescence microscope. We combined

the Tet and Lac systems for two-color fluorescence labeling of chromosome sites in *Arabidopsis* and demonstrated considerable variability of 3D interphase chromatin arrangement in root cells (Matzke et al., 2003; Matzke et al., 2005; Matzke et al., 2008; Matzke et al., 2010a). Use of the Lac system to study chromatin dynamics in yeast and *Drosophila* indicated that interphase chromatin is not static but undergoes significant, constrained diffusive motion ("jiggling") within the nucleus, such that a given chromatin segment oscillates within a restricted nuclear subregion with a typical radius of 0.5 to 0.7 μm (Marshall et al., 1997; Soutoglou and Misteli, 2007; McNally, 2009; Bronshtein et al., 2016). Similar observations using the Lac system were made in plants (Kato and Lam, 2003; Rosin et al., 2008). Local diffusional motion of chromatin has been suggested to be important for gene regulation, possibly because it permits a locus to enter nuclear environments favorable for optimal expression (Soutoglou and Misteli, 2007).

Using the tools described above, we are testing the aforementioned hypothesis of an electrical/ion-based signaling pathway operating from the PM to the nucleus to elicit changes at the genome level. In a partial test of the hypothesis, we previously used membrane-targeted SEpHluorinD to demonstrate that eATP provokes virtually instantaneous and synchronous reductions in pH at the PM and the inner nuclear membrane (INM) of root cells (Matzke and Matzke, 2015). This finding is consistent with rapid inter-membrane communication that affects proton activities at both membrane surfaces. Here we describe improved tools and further tests of the hypothesis to investigate possible direct effects of the proposed electrical/ion-based signaling pathway on the genome. Results from pilot studies presented here suggest that eATP can trigger changes in interphase chromatin mobility and the surrounding pH at specific genomic sites concomitantly with eATP-induced changes in pH at the PM and INM.

MATERIALS AND METHODS

Constructs and Plant Material

The building blocks of the constructs and the final constructs used in this study are shown in supplementary **Data Sheet 1**. SEpHluorinD was targeted to the PM using a CBL1 motif and to the INM and ONM using SUN2 and WPP motifs, respectively (Matzke and Matzke, 2015). Depending on whether the SUN2 motif is positioned at the N- or C-terminus, SEpHluorinD can be on the nucleoplasmic face of the INM or within the perinuclear space (compartment between INM and ONM). We found that the latter variant gives a cleaner signal (**Data Sheet 2** in supplement) and therefore this version of SUN2-SEpHluorinD was used to produce the results presented in this paper.

Because fluorescence of SEpHluorin is highest around pH 7.5 and extinguished at pH 5.5 (Miesenböck, 2012), it is suitable for qualitative assessments of shifts in pH within this range. A decrease in pH results in a reduction of the fluorescence intensity of SEpHluorin with a maximum visible change of approximately 2 pH units (Miesenböck, 2012). SEpHluorinD tethered to different membranes using specific targeting motifs as described above provides an indication of proton activity at the membrane surface. The rationale for the estimated reductions in pH reported in this paper following eATP treatment is shown in supplementary **Data Sheet 3.**

The chromosomal positions of the T-DNA insertions containing either *lac* or *tet* operator repeats and a gene encoding the cognate repressor protein (RP)-fluorescence protein (FP) fusion proteins (TetR-YFP and either LacR-dsRed2 or EGFP) are depicted in supplementary **Data Sheet 4**. The genes encoding the fusion proteins, which are under the transcriptional control of the 35S promoter, have become silenced over time (Matzke et al., 2010a). Therefore, for the present study, a second T-DNA encoding the desired RP-FP fusion protein under the transcriptional control of the *RPS5A* promoter (At3g11940) (Weijers et al., 2001), was introduced (**Data Sheet 1** in supplement). Because lines 16:101, 16:112 and 5:106 display the strongest and most reliable fluorescent dots, possibly owing to large, complex insertions of the operator repeats (Matzke et al., 2008), they have been used to generate the results shown in this report.

The Arabidopsis (*Arabidopsis thaliana*) transgenic lines used in this study are in the Col-0 ecotype (Matzke et al., 2005). Transgenic lines for which data are reported here did not show obvious developmental defects when cultivated under standard conditions (see below), and after data collection at the seedling stage, could be planted in soil for further growth and seed set. Seeds of the 16 operator repeat-containing Arabidopsis lines are available from the Arabidopsis Biological Resource Center (Ohio University, USA) in selected double insertions under the stock numbers CS72296-CS72301 and in single insertions under stock numbers CS72302-CS72317.

Fixation of Plant Seedlings

Seedlings were fixed for 5 min in ice-cold methanol and 30 s in ice-cold acetone. The seedlings were immediately dried between paper towels and then transferred to distilled water until mounting on a slide in imaging buffer for confocal microscopy (Kato and Lam, 2003).

Confocal Microscopy and Acquisition of Data to Analyze Fluorescent Intensity Changes of Membranes and Alleles, and Chromatin Dynamics

Confocal microscopy (using a Leica TCS LSI confocal microscope equipped with a 63× oil immersion objective) was used to acquire 3D time-lapse data. We routinely image the area of the transition zone because the nuclei in this region are mostly round and non-mobile, features that improve the ability to study chromatin dynamics over time and after eATP addition.

Growth and Mounting of Seedlings for Confocal Microscopy and Addition of eATP During Acquisition

Arabidopsis seedlings were grown vertically in square petri dishes containing solid Murashige and Skoog (MS) medium in an incubator at 22°C to 25°C under a 16-h light/8-h dark cycle. When the roots were approximately 2.5 cm in length, the seedlings were mounted in a sterile hood on 25 × 75 × 1.0 mm microscope slides (SUPERFROST PLUS, Thermo Scientific Art. No. J1800AMNZ) in 63-μl imaging solution [5-mM potassium chloride, 10-mM

MES hydrate, 10-mM calcium chloride, adjusted to pH 5.8 with Tris(hydroxymethyl)aminoethane) (Loro et al., 2012)]. The root was then covered with a 24 × 40-mm microscope cover glass Nr.1 (Marienfeld laboratory glassware Ref. 0101192) in which a perforation of approximately 1.5 mm in diameter (centered 3 cm away from the right edge of the slide) had been drilled under water with a diamond coated 1.5-mm drill (Kralj et al., 2011). The root tip was positioned approximately 5 mm from the perforation and the cover slip was sealed at the edges with rubber cement (Fixogum Art.-Nr. 2901 10 000, Marabu, Germany). The microscope slide was placed into the slide holder of a Leica TCS LSI confocal microscope equipped with a 63× oil immersion objective (**Data Sheet 5** in supplement).

After adding a drop of TypeF Immersion liquid (Leica Cat. Nr. 11 513 859) on the coverslip approximately one centimeter above the root tip, the objective was lowered until it touched the immersion liquid. Under visual inspection through the oculars, the root was observed and followed until the transition zone of the root tip was centered in the viewing field. Live mode imaging was used to adjust intensity and gain settings of the lasers 488 nm for the green channel and 532 nm for the red channel. For eATP experiments, acquisition was set to 31 min with acquisition of 21 pictures in 1 µm distances every minute first for the green channel and second for the red channel.

For eATP addition, 7 µl of a freshly made ATP solution (100-mM adenosine 5′-triphosphate disodium salt hydrate, Sigma A2383 in imaging solution adjusted to pH 5.8 with Tris(hydroxymethyl)aminomethane, Merck 1.08382) was pipetted with a Gilson P20 into Teflon tubing mounted through a blue pipette tip on a holder on the microscope stage and positioned right over the perforation in the cover slip (**Data Sheet 5** in supplement). We found that the best distance of root tip to the perforation in the cover slip is approximately 5 mm. The leaves of the seedling were then covered with a Parafilm "globe" (produced by stretching the Parafilm in a small area with a thumb) to prevent desiccation during the acquisition period. Imaging was started and during the thirteenth red channel acquisition, the 7-µl 100-mM ATP solution was pipetted into the perforation of the cover slip. The 100 mM ATP added at the perforation site on the coverslip is likely to become diluted to a lower concentration during diffusion to the root tip (distance ca. 0.5 cm) in the thin layer of imaging buffer. After the acquisition period the seedling was removed from the slide and put on an MS agar plate for recovery overnight. Seedlings remain viable and can be planted in soil for seed harvest.

Confocal Data Analysis

The time-lapse data obtained from the experiments described above and presented in **Figures 1**–**5** and Supplementary **Data Sheet 6** were analyzed in Imaris 64 bit software version 7.7.0 (www.bitplane.com). The data were analyzed as described below to determine: fluorescence intensities of INM membrane tagged with SUN2-SEpHluorinD and fluorescence-tagged genomic sites; 3D distances between fluorescent dots/alleles for chromatin dynamics; 3D distances from each allele to the INM; and measurements of nuclear volume.

Fluorescence Intensities

Nuclei were isolated using the Crop 3D function resulting in "single nuclei 3D time lapse" Imaris files. These files were used to read the intensity values displayed of detected dots (or "spots"; term used by Imaris software), which represented either fluorescent nuclei with a diameter of approximately 10 µm or fluorescent tagged genomic locations with a diameter of approximately 1 to 2.28 µm (ellipsoid 2-4,56 µm). Intensity values of "spots" were listed in Excel files (**Table 1** in supplement) and graphically displayed in **Figures 2**, **3**, **4** and **5**. Fluorescent intensities were normalized with the start set at 1. Fluorescence intensity data from 10 nuclei were compiled into one graph and supplemented with standard deviation bars. Graphs from individual nuclei before normalization are shown in supplementary **Data Sheet 8**.

Estimation of ΔpH

Changes in pH (ΔpH) at all cellular locations and genomic sites was estimated based on the magnitude of reduction of SEpHluorin fluorescence within its known pH range of fluorescence (Miesenböck, 2012) as described in supplementary **Data Sheet 3**. Estimated values of ΔpH were added to graphs of individual nuclei in supplementary **Data Sheet 8**.

Patterns in Reductions of Fluorescence Intensity

Graphs showing changes in pH over time at the INM (**Figure 2**), and at three genomic loci (**Figures 2**, **3**, **4** and **5)** show potentially three types of fluorescence change that can occur during the data collection period and affect the pattern of the trace: 1) bleaching, which manifests as a continuous and irreversible decline in fluorescence [most obvious in buffer control (**Figure 3**) and pH-insensitive fluorescent proteins (**Figures 2**, **4**, and **5**)]; 2) dislocation turbulence, which is sometimes observed as sharp spike upon eATP addition through the perforation in the cover slip at time-point 13 (for examples, see supplementary **Data Sheet 8**, nucleus 2 in **Figure 2**, bottom; and **Videos 1** and **2**, time-point 13); and 3) reductions in fluorescence owing to a pH change at the locus under study. The last change is observed as a drop in fluorescence occurring over approximately 2 to 7 min, followed usually by at least partial recovery (most visible in blue boxed nuclei in parts labeled "**Figure 3C**" and "**Figure 5C**" in **Data Sheet 8**, in supplement).

Analysis of Chromatin Dynamics

Starting from the "single nuclei 3D time lapse" Imaris files; see above), each time point was isolated using the Crop time function (producing "single nuclei 3D" Imaris files). These files were used to determine the 3D distances between the two dots/alleles of fluorescent tagged genomic locations. After Imaris detection of fluorescent dots/alleles, the dots were separated using the "split" function of Imaris and the distance between them computed using the "compute distances between spots" function. Distance values displayed were entered into Excel files (**Table 2** in supplement). For chromatin dynamic analysis, allelic distances were pasted into an Excel chromatin dynamics analyses file obtained from the Ton Bisseling lab (Laboratory of Molecular Biology, Wageningen University) and modified by Ulf Naumann (Gregor Mendel Institute, Vienna, Austria). The modified Excel file, formatted for data from 10 nuclei and eleven time points (numbers can be adjusted

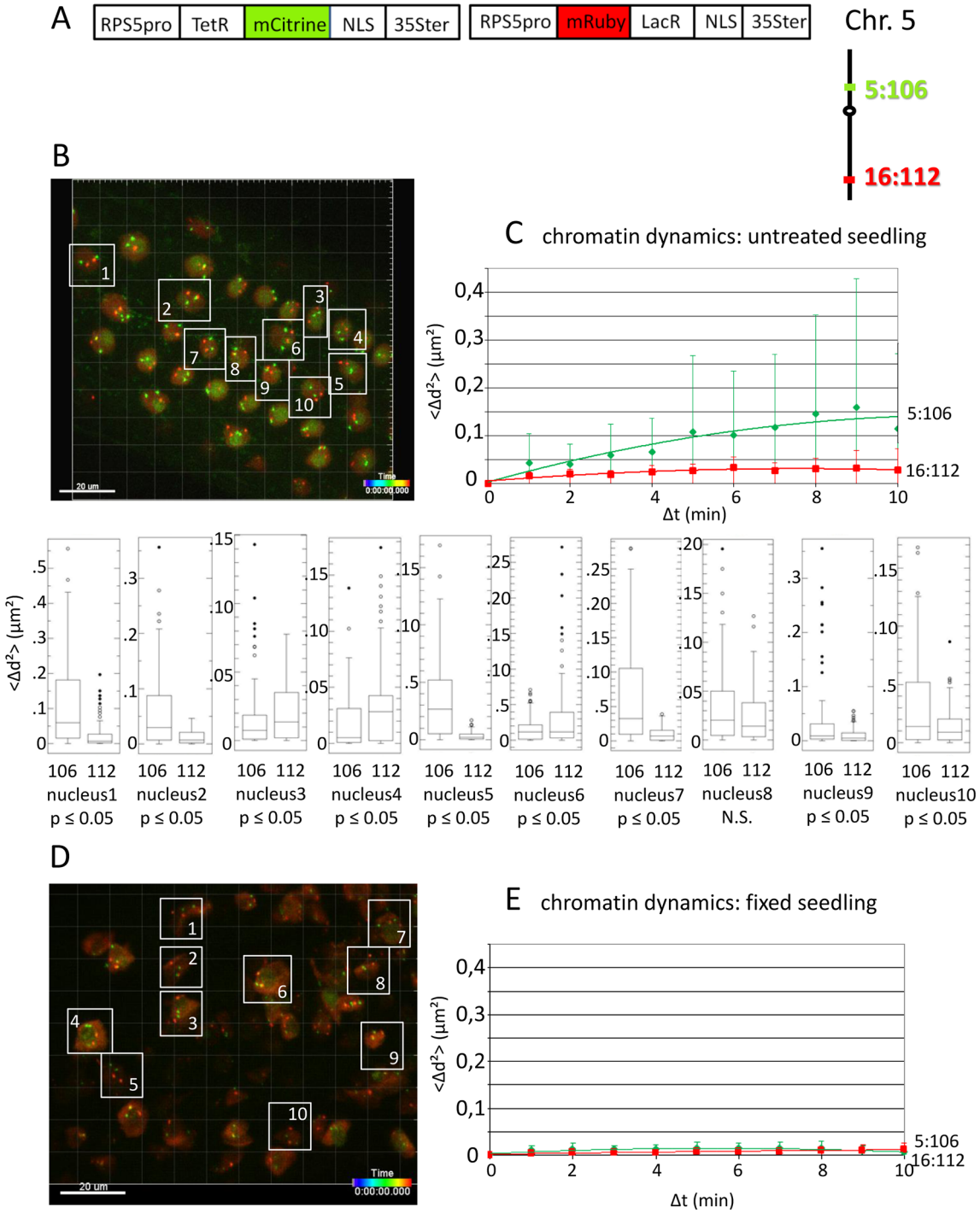

FIGURE 1 | Continued

as needed) is available in the Supplementary material as "chromatin dynamics analyses file" (**Table 15** in supplement) which contains 20 sheets (10 nuclei, before and after eATP) plus an "average" sheet. In the chromatin dynamics analysis file, changes in allelic distance (d) during the 1-min time intervals were used to calculate the mean squared distance change in d(t) as $<\Delta d^2> = < [d(t)-d(t+\Delta t)]^2>$ and a plot of cumulative traveling distances $<\Delta d^2(\mu m^2)>$ (cumulated (squared) distance travel since t0) against elapsed time intervals, Δt (delta t = elapsed time since t0), is generated (see **Figures 1–3** and supplementary **Data Sheet 6**). The generated curve was replaced by order2 polynomial trendlines using the Excel chart function to visualize plateauing of the values. The height of the plateau of the trendlines reflects the size of the confinement region. The radius of confinement in µm is the square root of that value. Higher plateau

FIGURE 1 | Analysis of chromatin dynamics in untreated plants. **(A)** The construct encoded two nuclear-localized fusion proteins: TetR-mCitrine and mRuby-LacR (**Data Sheet 1**, combination **Figure 1,** in supplement**)**. Both genes are under the transcriptional control of the *RPS5A* promoter (RPS5pro) and the 35S terminator (35Ster). NLS, nuclear localization signal. Right: TetR-mCitrine and mRuby-LacR fusion proteins bind, respectively, to *tetO* repeats at locus 5:106 and *lacO* repeats at locus 16:112. The two loci are integrated on the top and bottom arms of chromosome 5, respectively (green, locus 5:106; red, locus 16:112). **(B)** Left: Confocal image (maximum projection; enlargement in **Data Sheet 9** in supplement) at time point t1 of fluorescent-tagged loci 5:106 and 16:112 in nuclei of cells in the root transition zone. Two red and two green dots are visible in most nuclei. Nuclei boxed in white were used to measure distances between the two red alleles and the two green alleles in the same nucleus. For confocal microscopy, *Arabidopsis* seedlings harboring these fluorescent-tagged loci were mounted on a slide in imaging buffer. One 3D data set, allowing measurement of allelic distances in Imaris, was acquired from both the red and green channels every minute (21 planes) over a time period of 10 min (**Video 3**). A total of 10 data records (one for each nucleus), each containing eleven time points, was analyzed (**Table 2**, **sheets 1–2**, in supplement). **(C)** Chromatin dynamics in living cells was determined by plotting the cumulative overall mean squared change in distance between the two alleles $<\Delta d^2>(\mu m^2)$ against elapsed time intervals Δt. The plateau height of the trendline reflects the size of the confinement region. Higher plateau values indicate increased chromatin movement (Qian et al., 1991). The graph shows a scatterplot of the $<\Delta d^2>$ values (cumulated (squared) distance travel since t0) for 10 nuclei over a period of 10 min (Δt = elapsed time since t0) and is overlaid with order two polynomial trendlines and standard deviation bars are shown. The $\Delta d^2(\mu m^2)$ rises to 0.14 for locus 5:106 and 0.03 for locus 16:112 during the 10-min data acquisition period in this experiment. These $\Delta d^2(\mu m^2)$ values correspond to radiuses of confinement of 0.4 µm and 0.17 µm, respectively, in nuclei with an approximate diameter of 10 µm, which is in line with previous results (Marshall et al., 1997; Kato and Lam, 2003). Single nuclei box plot analyses and calculation of *p* values using the Δd^2 values revealed nine nuclei with significantly different changes in chromatin mobility ($p \leq 0.05$) between locus 5:106 and locus 16:112 (**Table 3**). N.S., not significant. **(D)** Same procedure as in part **C** using fixed seedlings as a negative control for "jiggling" of alleles. Left: nuclei boxed in white used for measurements (**Table 2**, **sheets 3–4** in supplement). **(E)** Chromatin dynamics (fixed seedling): $<\Delta d^2>(\mu m^2)$ of fixed seedlings against elapsed time intervals (**Table 4**, in supplement). Motion in living cells (part **C**) is greater than in fixed cells, indicating that the movement is not due to measurement error.

values indicate a larger region of confinement, meaning motion ("jiggling") is less constrained (Marshall et al., 1997; Berg, 2016).

Statistical Analyses

For average chromatin dynamics data (**Figures 1C** and **D**, **Figure 2C** and **Figure3C** and Supplementary **Data Sheet 6C**), standard deviations were calculated in Excel using the STDEV.S function with the Δd^2 averages from all 10 nuclei at all 10 time points in a given experiment and shown in the figures (**Tables 3–7**, column C, lines 27–38**,** in supplement). Box plot analyses of Δd^2 values for individual nuclei and calculations of *p* values were performed using the "Data Entry: Student's t-test" (http://www.physics.csbsju.edu/stats/t-test_bulk_form.html). The Δd^2 values for individual nuclei were also compared using one-sided KS tests, which confirmed the statistical significance determined by the t-test (**Table 11**_KS_Fig1C, **Table 12**_KS_Fig2C, **Table 13**_KS_Fig3C, **Table 14**_KS_**Data Sheet 6C**, in the supplement; each sheet of these files corresponds to a single nucleus). The *t*-test *p* values are two-sided; a significant *t*-test *p* value means the first set is greater than the second one or vice versa. The KS test used is one-sided; it gives a significant *p* value only when the first set is greater than the second one.

For fluorescence intensity experiments (**Figures 2D** and **E**, **Figure 3D** and **E**, **Figure 4C**, and **Figure 5C**), standard deviations of the average fluorescence intensity values of 10 nuclei (boxed in white in the confocal images shown) at each time point were calculated using the STDEV.S function of Excel and added as error bars. To calculate *p* values, the "t test" function of Excel was used to compare normalized fluorescence intensity data (i.e. differences in the drop in fluorescence intensity—high point to low point—during time points indicated in the figures) from pH-sensitive versus pH-insensitive fluorescent proteins or buffer control (**Table 10**, **Data Sheet 7** in supplement). The *p* values were added to the figure legends.

3D Distances From Each Allele to the INM

The distance between each allele and the INM was measured in Imaris. By using the surface function and choosing the automated creation option, we created the INM surface. The distance between spots and the created INM surface were then computed using the "distance between spots and surfaces" function in Imaris and the resulting values returned by Imaris were pasted into Excel for the graphical display (**Data Sheet 7** and **Table 8**, in supplement**)**.

Nuclear Volume Measurements

Nuclear volume measurements were performed in Imaris by using the "surface" function and choosing the automated creation option. Nuclear volumes could then be read in the statistics tap of the created surfaces under the "detailed" tap choosing "volumes." In the list of all volumes displayed (in μm^3), the highest value highlighted the nucleus in yellow; if other surfaces were also highlighted in yellow—which could sometimes occur later in the time course—the time point was excluded from the Excel file. Consequently, in supplementary **Data Sheet 7** there are missing data points of volume measurements toward the end of the experiment (**Table 9** in supplement**).**

RESULTS

Changes in Fluorescence Intensity of Membrane-Associated and Soluble SEpHluorinD in Root Cells in Response to eATP

Tool Improvement

Constructs used in this study are shown in supplementary **Data Sheet 1**. Improvements made since a previous study (Matzke and Matzke, 2015) in the construct collection include using the *RPS5A* promoter (At3g11940) (Weijers et al., 2001) instead of the UBI-10 promoter (At4g05320) (Grefen et al., 2010) to drive expression of SEpHluorinD and other fluorescent proteins, and targeting SEpHluorinD to additional cellular compartments, including the cytoplasm, nucleoplasm and INM facing the nucleoplasm. Of these, the clearest localization of SEpHluorin was observed at the cytoplasmic face of the PM, the INM facing the perinuclear space, and the nucleoplasm. Hence, these locations were used in the present study. Correct membrane localization and responses of SEpHluorinD in the PM and INM to 2 mM eATP application in root cells has been documented previously (Matzke and Matzke, 2015) and has been confirmed and expanded in this study, which

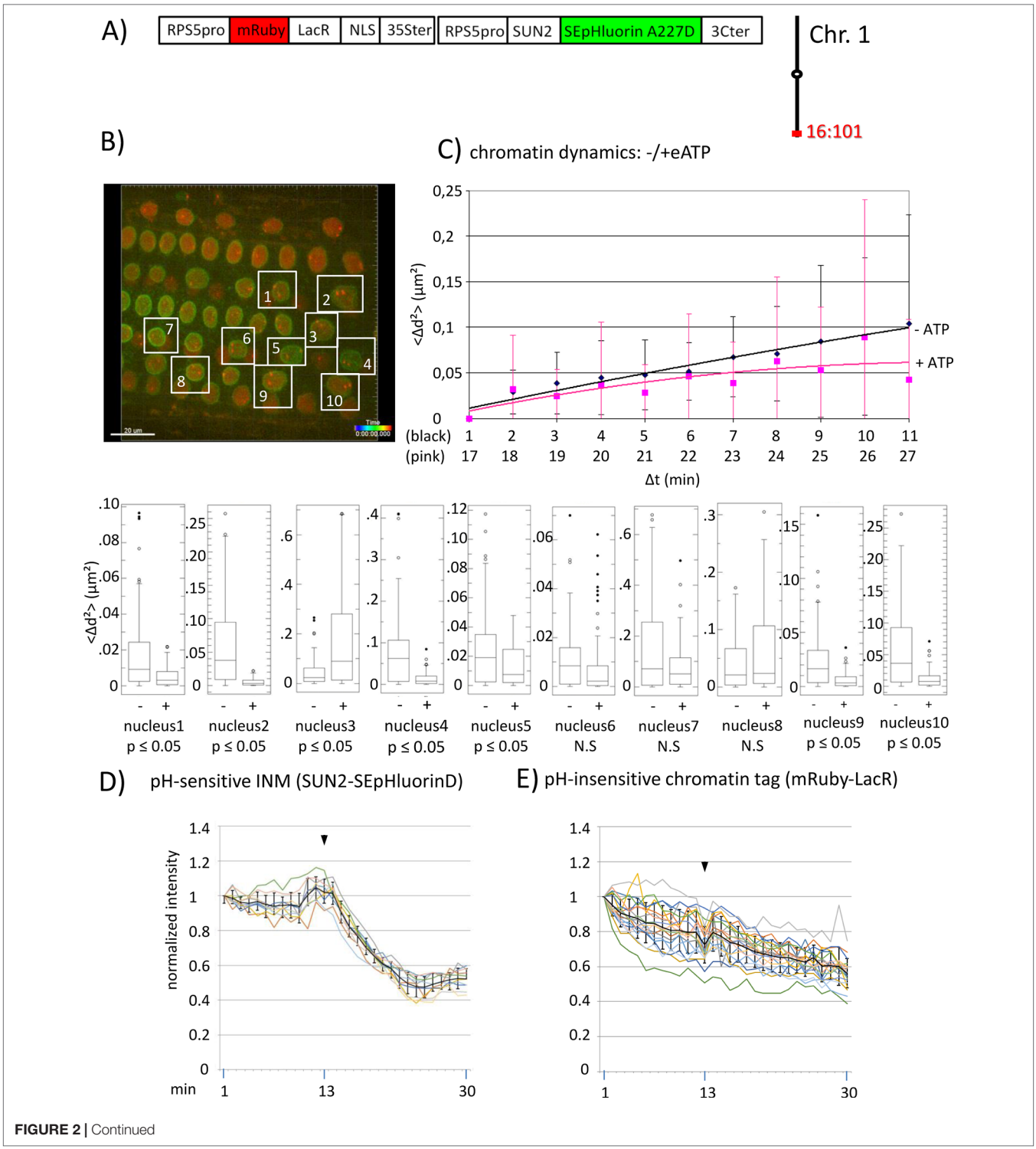

FIGURE 2 | Continued

also tested 100-mM ATP (**Data Sheet 2** in supplement). The *RPS5A* promoter gives relatively reliable expression in the root tip region, particularly in the transition zone, which was the region examined in this work. The transition zone is important for perceiving environmental signals and hormone crosstalk (Kong et al., 2018) and was regarded by Charles Darwin as the "brain" of the root (Baluška et al., 2009).

Experimental Support for the Hypothesis Using New Constructs

Experiments using SEpHluorinD targeted to the PM, the INM facing the perinuclear space, and the nucleoplasm indicated that eATP induces immediate and contemporaneous decreases in pH (i.e. the fluorescence of SEpHluorinD diminishes) at all cellular locations tested (PM, cytoplasm, ONM, INM and nucleoplasm)

FIGURE 2 | Chromatin dynamics and fluorescence intensity changes at the INM following addition of eATP. **(A)** The construct encoded nuclear-localized mRuby-LacR fusion protein (pH-insensitive) and, in opposite orientation, SUN2-SEpHluorin227D, which is pH-sensitive and localized to the perinuclear face of the INM *via* the SUN2 targeting signal. Both genes are under the transcriptional control of the RPS5pro; the first contains the 35ter and the second contains the 3C terminator (3Cter). For readability, the module encoding RPS5pro-SUN2-SEpHluorin-3C is in the orientation shown but it is actually in the opposite orientation (**Data Sheet 1**, combination **Figure 2**, in supplement). (**Data Sheet 1**, combination **Figure 2**, in supplement). Right: the mRuby-LacR fusion protein binds to *lacO* repeats integrated at locus 16:101 on the bottom arm of chromosome 1. **(B)** Confocal image (maximum projection; enlargement in supplementary **Data Sheet 9**) at time point t1 of fluorescent-tagged locus 16:101 in nuclei of cells in the root transition zone. Two red dots are visible in most nuclei. Nuclei boxed in white were used to measure distances between the two red alleles and fluorescent intensity analysis (parts **D** and **E**). **(C)** Chromatin dynamics: *Arabidopsis* seedlings harboring the above construct were mounted on a slide in imaging buffer for confocal microscopy. A 3D data set allowing measurement of allelic distances in Imaris was acquired every minute (21 planes) over a time period of 30 min during which eATP was added at 13 to 14 min during red channel acquisition. A total of 10 data records (10 nuclei), each containing 30 time points, was collected (**Table 2**, **sheet 5** in supplement). Chromatin dynamics was determined as described in the legend to **Figure 1**. The graph shows a scatterplot of the $<\Delta d^2>$ values [cumulative (squared) distance travel since t0 and after eATP addition since t17], and standard deviation bars (**Table 5** in supplement) for 10 nuclei over a period of 30 min (Δt = elapsed time since t0, and after eATP addition since t17) and is overlaid with order 2 polynomial trendlines, which indicate "jiggling" before (black) and after (pink) eATP addition. To detect differences in mobility of locus 16:101 before and after eATP treatment, the analysis was restarted following the addition of eATP (following cessation of dislocation turbulence), hence producing two lines. Time points 12-16 were excluded from the analysis owing to data acquired during dislocation turbulence caused by addition of eATP. Single nuclei box plot analyses and calculation of p values using the Δd^2 values revealed seven nuclei with significantly different changes in mobility ($p \leq 0.05$) of locus 16:101 following eATP treament. N.S., not significant; **(D)** Normalized fluorescence intensity values of all 10 white-boxed nuclei shown in part **B** are overlaid in one graph together with calculated average values, to which standard deviation error bars were added (normalized and non-normalized numbers can be viewed, respectively, in **sheets 1** of **Tables 1** and **10** in supplement). Arrowheads indicate addition of eATP at time point 13. Using these normalized data, the calculated difference in the magnitude of the drop in fluorescence intensity in SUN2-SEpHluorinD versus bleaching of mRuby-LacR between time points 14-25 in response to eATP is statistically significant ($p \leq 0.05$). In supplementary **Data Sheet 8**, part **Figure 2D**, ΔpH values are shown under each nucleus1-10 [maximum ΔpH 0.9 (nucleus 7), minimum ΔpH 0.3 (nucleus 2); average (n = 10) 0.6]. Fluorescence intensity at INM is read in spot objects (spot size approximately 10 µm) capturing punctual fluorescence. **(E)** Response of the pH-insensitive mRuby-LacR chromatin tag following eATP treatment: normalized intensities of all 10 nuclei overlaid in one graph (numbers before normalization can be viewed in supplementary **Table 1**, **sheet 2**). Fluorescence intensities of individual nuclei are shown in supplementary **Data Sheet 8**, part **Figure 2E**.

(**Data Sheet 2** in supplement, and **Figure 2D**). Following the initial sharp decreases in pH, the further timing of the pH reductions was similar in all locations, with the lowest level occurring around 2 min after eATP application followed by a gradual reapproach to the baseline over the next 15 min. The maximum decrease in pH was estimated from the changes in SEpHluorinD fluorescence intensity to be approximately 0.9 pH unit (**Data Sheet 3** in supplement). Treatment with both 2 mM and 100 mM eATP elicited similar responses, indicating that ATP acts over a broad concentration range in this system. For unknown reasons, the baseline was exceeded during the recovery phase after application of 100 mM ATP in some cases (**Data Sheet 2** in supplement).

Analysis of Chromatin Dynamics

Tool Improvement

To study 3D interphase chromosome arrangement in *Arabidopsis* roots, we previously used a collection of 16 distinct transgenic lines, each of which harbors a unique genomic site fluorescently tagged with either the Lac system or the Tet system (Matzke et al., 2005; **Data Sheet 4** in supplement). Although the *lac* or *tet* operator (*lacO or tetO*) repeats are stably integrated at these different genomic sites, the genes encoding the repressor protein-fluorescent protein (RP-FP) fusion proteins (*TetR-EYFP* and either *LacR-dsRed2* or *EGFP* under the control of the 35S promoter), which are on the same T-DNA construct as the operator repeats (**Data Sheet 4** in supplement), have become silenced over time. Therefore, to adapt these lines for studying chromatin dynamics in the experiments reported here, the desired RP-FP fusion proteins were supplied in trans from a second T-DNA that was introduced into the operator-repeat containing lines by super-transformation using a different selection marker (**Data Sheet 1**). In addition to gene silencing, a further problem with the original lines was the presence of EYFP (Tet system) and EGFP or dsRed2 (Lac system) in the RP-FP fusion proteins. These FPs contain intact dimerization domains, which can lead to unwanted protein-mediated chromosome pairing of repetitive operator arrays (Mirkin et al., 2013). Therefore, to avoid aberrant protein-mediated pairing of tagged genomic sites during studies of chromatin dynamics, monomeric mCitrine was used in the new Tet-R construct instead of EYFP, and monomeric mRuby was used in the new Lac-R constructs instead of EGFP and dsRed2 (Supplementary **Data Sheet 1**, combination **Figure 1**, in supplement).

To demonstrate the feasibility of using the improved fluorescence tagging system to simultaneously study the dynamics of unlinked and distinctly colored genomic sites, we used an Arabidopsis line harboring the homozygous loci 5:106 and 16:112, which contain *tetO* and *lacO* repeats integrated on the top and bottom arms of chromosome 5, respectively. The repeats bind Tet-repressor (TetR)-mCitrine and mRuby-Lac-repressor (LacR) fusion proteins that are encoded on a second T-DNA, resulting in strong, differently colored fluorescent signals at the two tagged chromatin sites (**Figures 1A**, **B**). Data from a pilot experiment of chromatin dynamics in the root tip region of untreated seedlings are shown in **Figure 1C**. The graph is based on the analyses of the cumulative 3D distance changes between the alleles in 10 nuclei during 10 min; the $\Delta d^2(\mu m^2)$ values obtained for each nucleus were averaged and displayed in the graph. When calculated as an order 2 polynomial trendline, the results suggested that in 10 sampled nuclei in adjacent cells, locus 5:106 (green) was on average more dynamic than locus 16:112 (red). Standard deviations of the plotted average values of Δd^2 were relatively high. However, an examination of individual nuclei revealed inter-nucleus variability. Nine (90%) of 10 nuclei displayed a statistically significant difference ($p < 0.05$) in mobility between locus 16:112 and locus 5:106, and of these, six (60%) followed the average trend of higher mobility at locus 5:106 (**Figure 1C**).

These findings suggest that distinct loci in the same nucleus may frequently exhibit variations in the degree of chromatin mobility ("jiggling"; **Video 3** in supplement). By contrast, fixed, nonviable seedlings show little movement (**Figures 1D**, **E**).

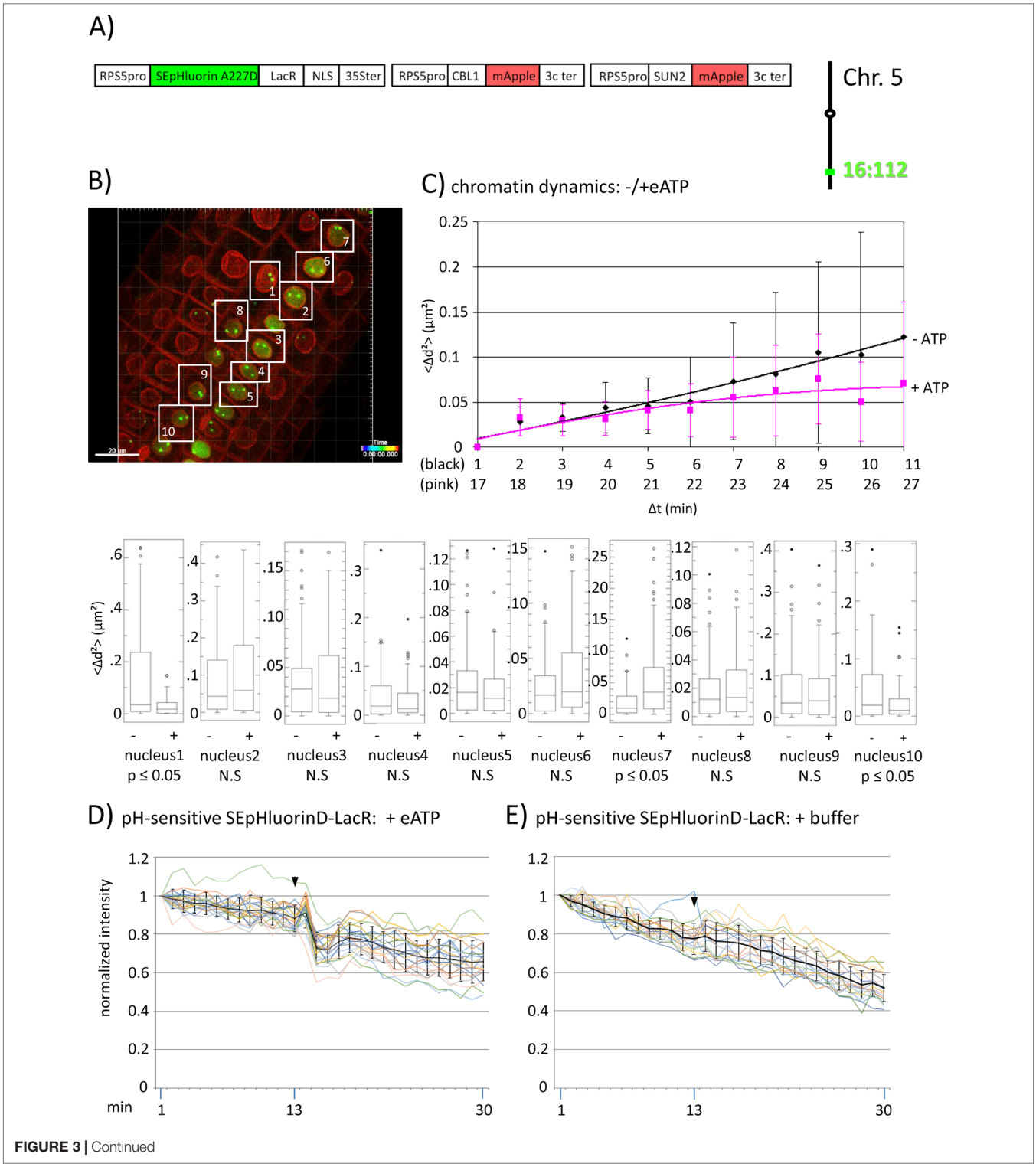

FIGURE 3 | Continued

Experimental Support for the Hypothesis

1. Chromatin Dynamics Following Addition of eATP

We also investigated chromatin dynamics before and after addition of eATP during data acquisition. For this analysis, we used a line harboring locus 16:101, which contains homozygous *lacO* repeats on the bottom arm of chromosome 1, and a second T-DNA that encodes INM-localized pH-sensitive SEpHluorinD and an mRuby-LacR fusion protein, which is insensitive to pH (**Data Sheet 1**; combination **Figure 2**, in supplement). By observing the fluorescence intensity changes of INM-localized SEpHluorinD, we can verify that eATP treatment has an effect on pH at the nuclear rim and at the same time, monitor dynamics of the

FIGURE 3 | Fluorescence intensity changes of a pH-sensitive fluorescent DNA-binding protein following addition of eATP. **(A)** The construct encoded nuclear-localized SEpHluorinD-LacR fusion protein as a pH-sensitive fluorescent DNA-binding protein, and SUN2-mApple and CBL1-mApple as INM and PM visual markers. All three genes are under the transcriptional control of the RPS5 promoter; the first contains the 35ter and the last two contain the 3C terminator (3Cter) for readability, the module encoding RPS5pro-LacR is in the orientation shown but it is actually in the opposite orientation (**Data Sheet 1**, combination **Figure 3**, in supplement). Right: The SEpHluorinD-LacR fusion protein binds to *lacO* repeats integrated at locus 16:112 on the bottom arm of chromosome 5. **(B)** Confocal image (maximum projection; enlargement in **Data Sheet 9** in supplement) at time point t1 of homozygous fluorescent-tagged locus 16:112 in nuclei of cells in the root transition zone. Two green dots are visible in most nuclei. Nuclei used for chromatin dynamics analyses (part **C**) and fluorescence intensity analysis (parts **D** and **E**) are boxed in white. **(C)** Chromatin dynamics: Mounting, confocal microscopy, eATP treatment, data acquisition and data analysis of *Arabidopsis* seedlings harboring the above construct were carried out as described in the legend to **Figure 2**. Chromatin dynamics was determined as described in the legend to **Figure 1**. The graph shows a scatterplot of the average Δd^2 ($<\Delta d^2>$) values [cumulative (squared) distance travel since t0 and after eATP addition since t17], and standard deviation bars (**Table 2**, **sheet 6** in supplement) for 10 nuclei over a period of 30 min (Δt = elapsed time since t0) and is overlaid with order 2 polynomial trendlines, which indicate "jiggling" before (black) and after (pink) eATP addition**.** Time points 12-16 were excluded from the analysis owing to unreliable data acquired during dislocation turbulence caused by addition of eATP. To detect differences in the mobility of locus 16:112 before and after eATP treatment, the analysis was restarted following the addition of eATP, hence producing two lines. Bottom: Single nuclei box plot analyses and calculation of *p* values using the Δd^2 values revealed three nuclei with significantly different changes ($p \leq 0.05$) in the mobility of locus 16:112 following eATP treatment. N.S., not significant. **(D)** pH-sensitive SEpHluorin-LacR chromatin tag: normalized fluorescence intensity profiles of the two 16:112 alleles in the 10 white-boxed nuclei (numbered in white in part **B)** are overlaid in one graph together with the calculated average values, to which standard deviation bars were added. eATP addition is indicated with a black arrowhead at frames 13-14**.** Fluorescence intensities of individual nuclei are shown in supplementary **Data Sheet 8**, part **3D**, in which the boxed areas in the fluorescent intensity graphs highlight the region of interest. ΔpH values are shown under each nucleus1-10 for both alleles [maximum ΔpH 0.4 (nucleus 9); minimum ΔpH 0.1 (nuclei 4 and 5); average (n = 20) 0.2]. Normalized and non-normalized data are shown, respectively, in **Data Sheets 3** of **Tables 10** and **1**. Using the normalized data, the calculated difference in the magnitude of the drop in fluorescence intensity in SEpHluorinD-LacR plus eATP versus bleaching in the buffer control between the time points 14-16 points is statistically significant ($p \leq 0.05$). **(E)** pH-sensitive SEpHluorinD-LacR chromatin tag: Buffer control without eATP (original data can be viewed in supplementary **Table 1**, **sheet 4**). The spikes in fluorescence reflect dislocation turbulence, which occurs upon addition of eATP or buffer. The fluorescence intensity at the genomic location is read in spots objects (1-2.8 μm) capturing punctual fluorescence of the tagged regions.

lacO sites colored with mRuby-LacR protein in multiple nuclei (**Figures 2A** and **B**). An order 2 polynomial trendline of average Δd2 values for 10 nuclei at each time point suggested generally reduced chromatin dynamics (pink line) of locus 16:101 after eATP treatment compared to before eATP exposure (black line) during the 30 min of data acquisition [i.e. $\Delta d^2(\mu m^2)$ plateaus at approximately 0.10 before ATP treatment and approximately 0.07 after ATP addition] (**Figure 2C**). Examination of individual nuclei again revealed inter-nucleus variability. Seven of ten (70%) of the sampled nuclei displayed statistically significant ($p < 0.05$) changes in chromatin mobility, and of these, six exhibited reduced mobility of locus 16:101 after eATP treatment, and are thus consistent with the trend seen in the averaged results (**Figure 2C**).

A concomitant drop in fluorescence intensity followed by partial leveling off of INM-localized SEpHluorinD upon application of eATP demonstrated that this stimulus was effective in inducing a pH change at the nuclear periphery (**Figure 2D**). As expected, the pH-insensitive mRuby-LacR chromatin tag did not exhibit a drop in fluorescence intensity following eATP treatment, only a continuous and irreversible decline (**Figure 2E**) similar to that seen with the buffer-only control (**Figure 3**). (Patterns of reductions in fluorescence are described in the *Materials and Methods* section.) These results supported the idea that the drop in fluorescence intensity observed with INM-localized SEpHluorinD depends on the pH sensitivity of this protein.

A significantly different change in mobility following eATP addition was also observed in a certain percentage of nuclei at other loci tested 'locus 16:112 (**Figure 3C**; **Table 6**); and locus 5:106 (**Data Sheet 6C** in supplement and **Table 7**)'. Collectively, the findings on three loci support a correlation in at least some nuclei between concurrent changes in chromatin dynamics and nuclear pH.

2. Can eATP-Induced pH Changes Be Sensed by Chromatin Proteins?

The experiments described above demonstrate coordinated and transient changes in pH in close proximity to the PM and INM and in the nucleoplasm subsequent to application of eATP (**Data Sheet 2** in supplement). Moreover, the pH changes elicited by eATP could be temporally correlated with changes in chromatin motion in the nucleus (**Figure 2**). An interesting follow-up question is whether these pH changes are felt directly by chromatin-associated proteins, which would be important for pH-dependent regulation of chromatin structure and gene expression. Alternatively, chromatin constituents may be insulated from surrounding changes in pH and fail to respond to eATP.

To investigate this question, we assembled a construct encoding a SEpHluorinD-LacR fusion protein together with PM and INM-targeted mApple, which served in this experiment as red visual markers for these two membrane systems (**Figures 3A**, **B**; **Data Sheet 1**, combination **Figure 3**, in supplement). Through the LacR domain, the RF-FP fusion protein can bind to the *lacO* repeats integrated into the genome and through the SEpHluorinD moiety, the RP-FP fusion protein can respond to pH changes as revealed by alterations in fluorescence intensity. If eATP-induced changes in nuclear pH affect chromatin directly, then eATP should elicit fluorescence changes in chromatin-bound SEpHluorinD. The construct was used to super-transform a line harboring locus 16:112, which contains homozygous *lacO* repeat arrays on the bottom arm of chromosome 5 (**Figure 3A**, right). In a pilot experiment using this line, eATP treatment elicited not only a statistically significant ($p < 0.05$) change in chromatin dynamics in 30% of sampled nuclei (**Figure 3C**), but also a relatively rapid reduction (occurring over a period of approximately 3 min in individual nuclei) followed by a partial leveling off in the fluorescence intensity of SEpHluorin-LacR at both 16:112 alleles. These findings indicate a drop in pH directly at the corresponding genomic sites. This pattern was particularly visible in nuclei 1, 2, 3, 6, 7, 8, 9 and 10 (blue boxed, **Data Sheet 8**, parts "**Figure 3D** and **Figure 3E**" in supplement). Addition of buffer did not induce a comparable response (**Figure 2E**, **Figure 4A** and **B**, and **Figure 5C**, right), consistent with the observed decrease in fluorescence being dependent on eATP. A similar lack of response was observed with pH-insensitive RP-FP

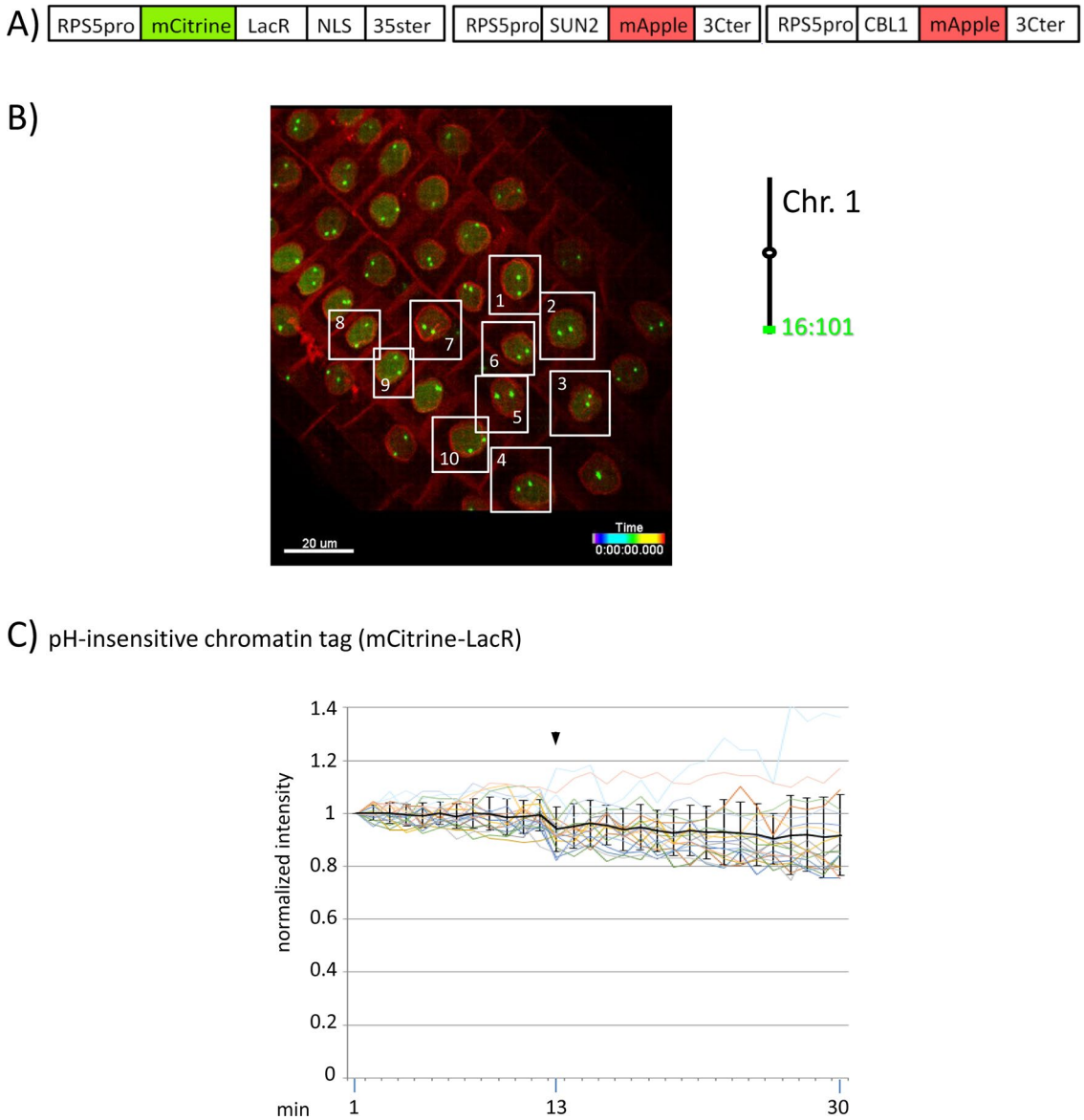

FIGURE 4 | Fluorescence intensity of a pH-insensitive fluorescent DNA-binding protein (mCitrine-LacR) following addition of eATP. **(A)** The construct encoded nuclear-localized mCitrine-LacR fusion protein as a pH-insensitive fluorescent DNA-binding protein, and SUN2-mApple and CBL1-mApple as INM and PM visual markers. All three genes are under the transcriptional control of the RPS5 promoter; the first contains the 35ter and the last two contain the 3C terminator (3Cter). For readability, the module encoding RPS5pro-mCitrine-LacR is in the orientation shown but it is actually in the opposite orientation (**Data Sheet 1**, combination **Figure 3**, in supplement). (**Data Sheet 1**, combination **Figure 4**, in supplement). **(B)** Confocal image (maximum projection; enlargement in **Data Sheet 9** in supplement) at time point t1 of homozygous fluorescent-tagged locus 16:101 in nuclei of cells in the root transition zone. Two green dots are visible in most nuclei. Nuclei used for fluorescence intensity analysis (part **C**) are boxed in white. Right: The mCitrine-LacR fusion protein binds to *lacO* repeats integrated at locus 16:101 on the bottom arm of chromosome 1. **(C)** pH-insensitive chromatin tag (mCitrine-LacR): Fluorescence intensity profiles of normalized intensities of all 10 white-boxed nuclei (in part **B**) are overlaid in one graph together with the calculated average values, to which standard deviation bars were added. Fluorescence intensities of individual nuclei can be viewed in supplementary **Data Sheet 8**, part **Figure 4C**. Addition of eATP is indicated with black arrowheads at frames 13-14. Normalized and non-normalized numbers are shown, respectively, in **sheets 5** of **Tables 10** and **1**, in supplement. Using the normalized data, the calculated difference in the magnitude of the drop in fluorescence intensity of SEpHluorinD-LacR (**Figure 3D**) versus bleaching of mCitrine-LacR (this figure) between the time points 14-16 points in response to eATP is statistically significant ($p \leq 0.05$). Fluorescence intensity at genomic location is read in spot objects (1-2.8 µm) capturing punctual fluorescence.

fusion proteins mRuby-LacR and mCitrine-LacR following eATP treatment (**Figures 2E, 4,** and **5C, right**; see individual nuclei in corresponding parts of **Data Sheet 8** in supplement). These findings demonstrate that the behavior of SEpHLuorinD-LacR in this experiment is dependent on its pH sensitivity. From the magnitude of the decrease in SEpHluorinD fluorescence, the maximum reduction in pH at locus 16:112 was estimated to be approximately 0,4 pH units (**Data Sheet 3** in supplement).

To substantiate the observed effects of eATP on the pH at a specific genomic site, a modified experiment was performed

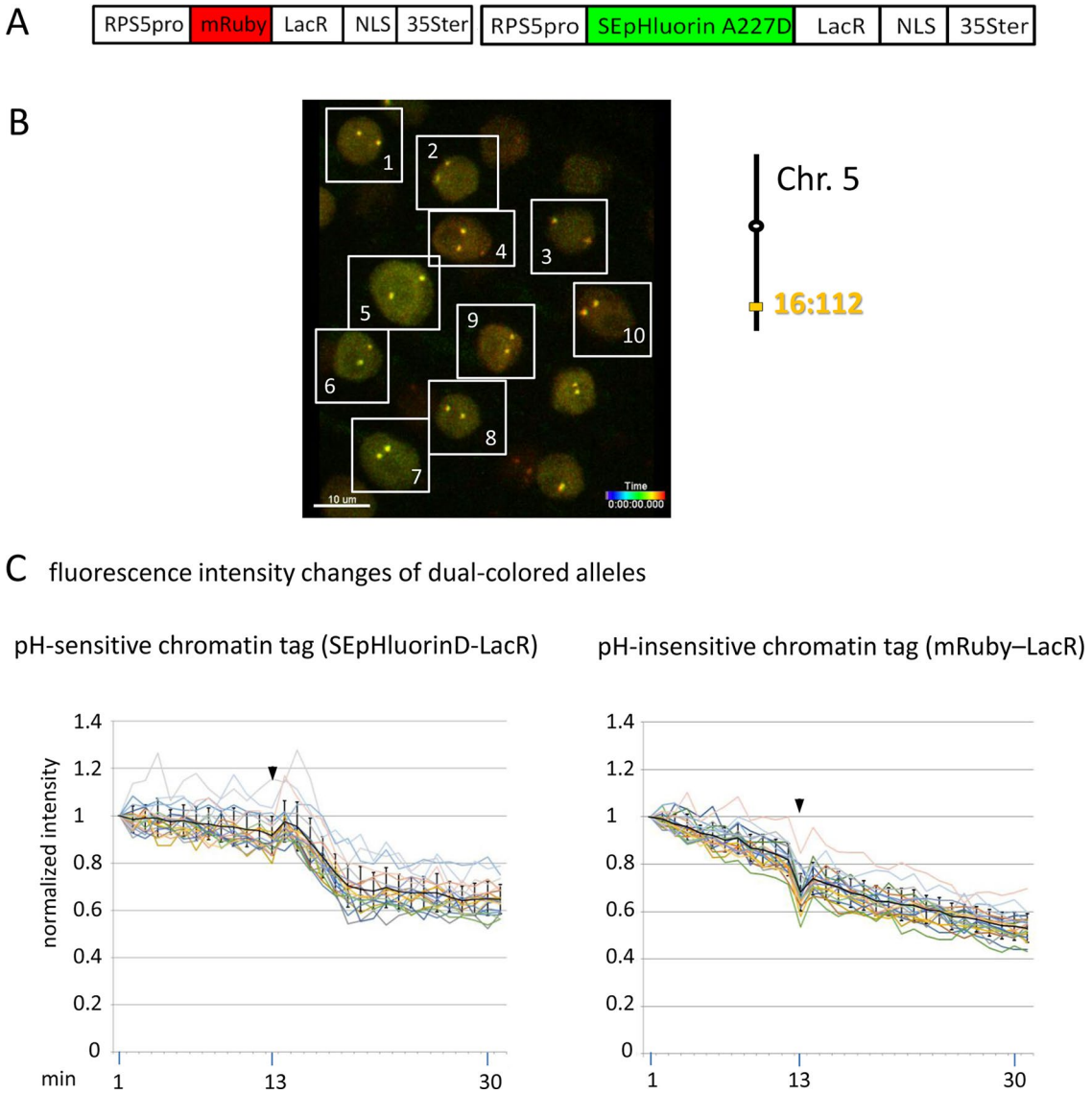

FIGURE 5 | Comparison of fluorescence intensity changes of pH-sensitive and pH-insensitive fluorescent DNA-binding proteins following addition of eATP. **(A)** The construct used in this experiment encoded a nuclear-localized SEpHluorinD-LacR fusion protein as a pH-sensitive fluorescent DNA-binding protein, and mRuby-LacR as a pH-insensitive DNA-binding protein. Both genes are under the transcriptional control of the RPS5 promoter and the 35ter (**Data Sheet 1**, combination **Figure 5**, in supplement). Right: The SEpHluorinD-LacR fusion protein and the mRuby-LacR fusion protein both bind to the tandem *lacO* repeats integrated at locus 16:112 on the bottom arm of chromosome 5. **(B)** Confocal image (maximum projection; enlargement in **Data Sheet 9** in supplement) of double fluorescent-tagged locus 16:112 at time point t1 in nuclei of cells in the root transition zone. Two yellow dots are visible in most nuclei. Nuclei used for fluorescence intensity analysis (part **C**) are boxed in white. **(C)** Fluorescence intensity changes of dual-colored alleles. Response of pH-sensitive tag SEpHluorinD-LacR (left) and pH-insensitive mRuby-LacR (right) to eATP addition (black arrowheads, frames 13-14)**.** Fluorescence intensity profiles of normalized intensities of all 10 nuclei recorded in the green and red channels in the same experiment are overlaid in two separate graphs together with the calculated average values, to which standard deviation bars were added (**Table 10**, **Data Sheet 6**, in supplement)**.** Normalized and non-normalized data can be viewed respectively, in **Data Sheets 6** of **Tables 10** and **1**. Using the normalized data, the calculated difference in the magnitude of the drop in fluorescence intensity of SEpHluorinD-LacR versus mRuby-LacR between the time points 14 to 21 in response to eATP is statistically significant ($p \leq 0.05$). The spike in fluorescence of the mRuby pH-insensitive tag reflects dislocation turbulence following eATP application. Fluorescence intensities of individual nuclei are shown in supplementary **Data Sheet 8**, part **Figure 5C**. ΔpH values are shown under each nucleus1-10 for both alleles [maximum ΔpH 0.5 (nucleus 5, one allele); minimum ΔpH 0.2 (nuclei 1, 2, 4, 6,9, one allele, nucleus 10 both alleles); average ΔpH 0.3 (n = 20)]. Fluorescence intensity at genomic location is read in spot objects (1–2.8 μm) capturing punctual fluorescence.

using pH-sensitive and pH-insensitive chromatin tags bound at the same locus. For this, a construct was assembled that encoded two RP-FP fusion proteins: SEpHluorinD-LacR and mRuby-LacR (**Data Sheet 1**, combination **Figure 5**, in supplement), which represent, respectively, pH-sensitive and pH-insensitive proteins that bind to *lacO* repeats (**Figure 5A**). After introducing this construct into a line harboring homozygous locus 16:112, two yellow fluorescent dots arising from co-localization of the

red and green RP-FP fusion proteins at both 16:112 alleles were observed in root tip nuclei (**Figure 5B**). Reproducing the results in **Figure 3D**, treatment with eATP in a pilot experiment resulted in a relatively rapid decrease (approximately 7 min) followed by a partial leveling off in the fluorescence of the SEpHluorinD-LacR in all nuclei observed (**Figure 5C, left**). The decrease in fluorescence intensity following eATP addition was observed at each allele of locus 16:112, consistent with a coordinate drop in pH directly at both alleles of this locus. At the same time, no comparable drop in fluorescence intensity of the mRuby-LacR tag at either of the two alleles of locus 16:112 was observed, only a continuous decline in fluorescence consistent with bleaching (**Figure 5C, right**). The results suggest that the relatively rapid response of SEpHluorinD-LacR to eATP is not a general reaction of RP-FP fusion proteins but depends on the pH sensitivity of SEpHluorinD. The collective findings support the hypothesis that an extracellular stimulus that triggers changes in nuclear pH can also incite concurrent changes in the surrounding pH of chromatin-associated proteins.

DISCUSSION

We have developed and used improved tools to obtain support for the existence of a rapid, ion-based signaling pathway that initiates at the cell surface and reaches chromatin in the nucleus to impact interphase chromosome dynamics and chromatin-bound proteins. Although experimentally induced by eATP in our system, such an ion-based pathway could possibly operate in natural settings to allow external signaling molecules and environmental stimuli to quickly adjust gene expression by changing the structures and/or activities of chromatin proteins. Moreover, interconnected electrical/ionic-based signaling pathways could exert an overall patterning effect on cellular constituents at the subcellular, cellular and supra-cellular levels by altering the spatial and temporal distribution of ions sequestered at the charged surfaces of membranes and in membrane-bound compartments.

It is not clear how pH changes at the PM, which are induced by an extracellular signal that presumably does not enter the cell, are transmitted to the nuclear membranes and nucleoplasm to influence the properties of chromatin. When considering the series of events involved in the observed pH changes, it is important to separate the pH changes themselves, which generally take approximately 2 to 7 min to reach a maximum in our experiments, from the immediate and simultaneous initiation of these changes at the PM and INM following eATP exposure. The genomic sites tagged with a pH-sensitive DNA-binding protein also exhibited decreased SEpHluorinD fluorescence following similar kinetics. Since the pH changes at all three locations are highly synchronized, one speculation is that an electrical signal is rapidly conveyed from the PM to the nucleus through internal membranes. This electrical signal could trigger the opening or closing of H^+ channels in the INM and subsequent release of protons from the perinuclear space and/or INM surfaces, resulting in pH-dependent changes in the properties and behavior of chromatin. Although the bulk pH of the cytoplasm, nucleoplasm and ER in plant cells has been estimated using a pH-sensitive fluorescent protein to range from 7.0 to 7.4 (Shen et al., 2013), localized membrane surface pH and other micro-domains of pH within a cell can differ from bulk pH in ways that are physiologically relevant (Maouyo et al., 2000; Felle, 2001). If a particular locus is situated peripherally in the nucleus, it could fall under the influence of a variable INM surface pH. Alternatively, protons, which are highly mobile in plant cells (Felle, 2001), could diffuse rapidly away from the INM after release from the perinuclear space and enter the nucleoplasm to affect not only peripheral but also more centrally located chromatin sites. The pH of the perinuclear space *per se* has not been determined, but existence of H^+ pumps in NMs of at least some cell types (Santos et al., 2016) suggests the possibility of regulated transport of protons from the perinuclear compartment into and out of the nucleoplasm.

Influence of pH Changes on Chromatin

Changes in pH can conceivably bring about alterations in chromatin mobility and function in different ways. For example, chromatin "jiggling," which appears to be evolutionarily conserved among eukaryotes, is largely attributed to the activity of ATP-dependent chromatin remodeling complexes that continually open and close condensed chromatin fibers to regulate access of the transcriptional machinery to genomic DNA (Soutoglou and Misteli, 2007; McNally, 2009). The activities of chromatin remodelers and other transcriptional proteins are likely to be sensitive to differences in the local pH. Consistent with this supposition, our results demonstrate that a fluorescent DNA-binding protein can directly perceive changes in the surrounding pH and undergo alterations that affect fluorescence intensity (Campbell and Choy, 2001). Chromatin mobility and function could also be influenced indirectly through pH-induced alterations of nucleoskeletal elements. The integrity and stability of the actin-containing nuclear matrix, which helps to organize chromatin and facilitate chromatin remodeling and transcription, are known to be sensitive to changes in pH values (Libertini and Small, 1984; Wang et al., 1989).

Inter-Nucleus Variability

The considerable variability in our data appears to reflect natural heterogeneity that is increasingly recognized as an inherent feature among individual cells of a given population (Argueso et al., 2019; Nicholson, 2019). Although average values can suggest overall trends in the data, they can mask real and potentially important differences at the single cell/nucleus level (Argueso et al., 2019; Nicholson, 2019). Indeed, examination of our data on the level of single nuclei revealed that all nuclei within a given group of cells did not respond identically to eATP treatment. In the experiments examining chromatin dynamics, examples of reduced, increased and unchanged motion can be observed in nuclei of neighboring cells. Similarly, pH-sensitive chromatin bound proteins did not respond identically to eATP in all sampled nuclei of a given root. The observed heterogeneity may depend on a number of factors, including fluctuations in the physiological status of individual nuclei during the period of data acquisition, and varying locations of different chromatin sites in 3D nuclear space. An additional source of variation may arise from the exact position in the root and identity of the cells

sampled. Although we aimed to study cells in microscopically visible layers of the transition zone, this region does not have clearly defined borders to the adjoining elongation zone or meristematic region. Heterogeneity in individual cells of a population could conceivably enable plants to adapt more effectively to a constantly changing environment by providing alternative physiological states that offer a range of advantageous properties.

Reproducibility of Results

Although the experiments have been carried out using different transgenic plant lines expressing various fluorescent proteins, the findings display a high degree of internal consistency. For example, in experiments examining fluorescence intensity changes of pH-insensitive fluorescent proteins, two different pH-insensitive fluorescent chromatin-binding proteins (mRuby-LacR and mCitrine-LacR) bound to two different loci (locus 16:101 and locus 16:112) showed similar responses following eATP addition in three different experiments (**Figures 2E**, **4C**, and **5C right**). In addition, two different pH-sensitive fluorescent fusion proteins (SEpHluorinD fused to either LacR or SUN2) exhibited similar behavior following eATP addition in three different experiments (**Figures 2D**, **3D left**, and **5C left**). Finally, in experiments to assess changes in chromatin dynamics, three different fluorescent chromatin-binding proteins (pH-sensitive SEpHluorinD-LacR and TetR-SEpHluorinD) and a pH-insensitive fluorescent chromatin-binding protein (mRuby-LacR) that bound, respectively, to three different loci (locus 5:106, locus 16:101 and locus 16:112) displayed altered chromatin dynamics following eATP treatment in three different experiments (**Figures 2C** and **3C**, and **Data Sheet 6C**, in supplement**).** These consistent trends among experiments reinforce the reproducibility of our results.

Limitations of Experimental System

The set of tools described here can be used in closely monitored experiments to obtain dependable results on 3D interphase chromosome mobility and pH at specific genomic loci and other cellular locations. That said, further improvements and developments of tools and imaging technology will be required in the future to overcome several limitations of the current experimental system (Lobet, 2017). For example, despite the use of the more reliable *RPS5A* promoter in the improved constructs, the expression level of the RP-FP fusion proteins in root cells is still not completely stable and fluorescent signals from chromatin-tagged sites are often weak and non-uniform within a single seedling and among sibling seedlings. Therefore, before performing confocal microscopy, it remains necessary to screen seedlings under a stereo-fluorescence microscope to identify those with the strongest signals in the root tip. Even in plants originally exhibiting strong fluorescent signals from a tagged locus, this phenotype is often not inherited in progeny, probably due to frequent silencing of genes encoding RP-FP fusion proteins (Matzke et al., 2010a). Hence, the most intense signals are usually observed in primary transformants. Further improvements in constructs (for example, finding and using promoters less susceptible to silencing) will facilitate more uniform expression in primary transformants and consistent heritability of strong expression in subsequent generations. These advances will allow the establishment of stable transgenic lines that can be used repeatedly for experiments.

Treatment of seedlings mounted on slides with eATP is tricky and it is difficult to avoid introducing a degree of uncertainty into the experiments. Although the method described here (adding the ATP solution to the seedling root through a perforation in the cover slip) can be done relatively quickly, it is not possible with this technique to determine the actual concentration of available ATP present at the root tip. However, as our results indicate, eATP works over a wide concentration range in this system (**Data Sheet 2** in supplement), so some variation in eATP concentration around the root tip can be tolerated. Addition of eATP (or buffer) using this method also leads to transient "dislocation turbulence" (up and/or down displacement of the root) (Supplementary **Videos 1** and **2**). The use of a microfluidic chip (Grossmann et al., 2018) might alleviate these problems in future studies.

Our system is versatile and potentially allows many other treatments to be examined such as electrical pulses, different hormones, temperature shifts, mutations in signal transduction components, and various ionophores and ion channel blockers. To study the proposed pathway in other cell types, different tissue-specific promoters can be used to drive expression of RP-FP fusion proteins and SEpHluorinD derivatives. Additional targeting signals can be used to direct SEpHluorinD to other cellular locations (e.g., the ER, organelles, outer surface of PM). The eventual development of brighter and more photo-stable FPs that have unique excitation and emission spectra in combination with more sensitive microscopes will be useful for simultaneous visualization and data acquisition from multiple fluorescent sensors within the cell.

Future Perspective

Although these experiments can only be considered initial tests of the hypothesis, the overall findings generally support the existence of a highly efficient and interconnected electrical/ion-based signaling pathway extending from the PM to the nucleus, possibly through intervening membrane systems, which can influence chromatin behavior. The experiments reported here relied on fluorescent proteins that are sensitive to pH and not directly to membrane voltage. Although pH changes can be a downstream consequence of voltage changes, a more definitive test of the proposed pathway awaits the development of GEVIs that reliably respond to shifts in voltage at multiple membrane systems in plant cells. Developing such tools is an important goal for the future (Matzke and Matzke, 2015; Basu and Haswell, 2017). In support of the existence and evolutionarily conservation of this hypothetical pathway, a recent study using an ER-localized ArcLight derivative

in human cells indicated that electrical signals at the PM can affect the voltage of internal membranes (Sepheri-Rad et al., 2018).

DATA AVAILABILITY STATEMENT

All datasets generated for this study are included in the manuscript/**Supplementary Files**.

AUTHOR CONTRIBUTIONS

AM and MM were involved in all aspects of this work. W-DL contributed to statistical evaluation of the data.

FUNDING

Funding for this project was provided by Academia Sinica (AS) and the Institute of Plant and Microbial Biology at AS.

ACKNOWLEDGMENTS

We thank Map Chen (Major Instruments, Taiwan) for advice on using the Micam camera and confocal microscope.

SUPPLEMENTARY MATERIAL

The Supplementary Material for this article can be found online at: https://www.frontiersin.org/articles/10.3389/fpls.2019.01267/full#supplementary-material

SUPPLEMENTARY VIDEO 1 | Dislocation turbulence_Figure3C_front view.avi: locus 16:112 (green), 30 minutes (in Video reduced to 6 secs: 5 acquisition points /sec, +ATP at time point 13 during red channel acquisition), PM and INM colored in red (CBL1-mApple and SUN2-mApple respectively)

SUPPLEMENTARY VIDEO 2 | Dislocation turbulence_ side view of Video1

SUPPLEMENTARY VIDEO 3 | Chromatin ‚jiggling' Figure1B_right.avi : locus 5:106 (green), locus 16:112 (red), 10 minutes (in Video reduced to 2 secs: 5 acquisition points/sec)

REFERENCES

Argueso, C.T., Assmann, S. M., Birnbaum, K. D., Chen, S., Dinneny, J. R., Doherty C. J. et al. (2019). Directions for research and training in plant omics: Big Questions and Big Data. *Plant Direct* 3 (4), e00133. doi: 10.1002/pld3.133

Baluška, F., Mancuso, S., Volkmann, D., and Barlow, P. W. (2009). The "root-brain" hypothesis of Charles and Francis Darwin: Revival after more than 125 years. *Plant Signal. Behav.* 4, 16:1121–16:1127. doi: 10.4161/psb.4.12.10574

Basu, D., and Haswell, E. S. (2017). Plant mechanosensitive ion channels: an ocean of possibilities. *Curr. Opin. Plant Biol.* 40, 43–48. doi: 10.1016/j.pbi.2017.07.002

Behera, S., Zhaolong, X., Luoni, L., Bonza, M. C., Doccula, F. G., De Michelis, M. I., et al. (2018). Cellular Ca2+ signals generate defined pH signatures in plants. *Plant Cell* 30, 2704–2719. doi: 10.1105/tpc.18.00655

Berg, H. C. (2016). *Random Walks in Biology*. Expanded Edition, Princeton, New Jersey: Princeton University Press.

Bronshtein, I., Kanter, I., Kepten, E., Lindner, M., Berezin, S., Shav-Tal, Y., et al. (2016). Exploring chromatin organization mechanisms through its dynamic properties. *Nucleus* 7, 27–33. doi: 10.1080/19491034.2016.1139272

Bezanilla, F. (2008). How membrane proteins sense voltage. *Nat. Rev. Mol. Cell Biol.* 9, 323–332. doi: 10.1038/nrm2376

Campbell, T. N., and Choy, F. Y. M. (2001). The effect of pH on green fluorescent protein: a brief review. *Mol. Biol. Today* 2, 1–4.

Cao, Y., Tanaka, K., Nguyen, C. T., and Stacey, G. (2014). Extracellular ATP is a central signaling molecule in plant stress responses. *Curr. Opin. Plant Biol.* 20, 82–87. doi: 10.1016/j.pbi.2014.04.009

Choi, W. G., Hilleary, R., Swanson, S. J., Kim, S. H., and Gilroy, S. (2016). Rapid, long-distance electrical and calcium signaling in plants. *Annu. Rev. Plant Biol.* 67, 287–307. doi: 10.1146/annurev-arplant-043015-112130

Cohen, A. E., and Venkatachalam, V. (2014). Bringing bioelectricity to light. *Annu. Rev. Biophys.* 43, 211–232. doi: 10.1146/annurev-biophys-051013-022717

Duby, G., and Boutry, M. (2009). The plant plasma membrane proton pump ATPase: a highly regulated P-type ATPase with multiple physiological roles. *Pflügers Arch. – Eur. J. Physiol.* 457, 645–655. doi: 10.1007/s00424-008-0457-x

Felle, H. H. (2001). pH: signal and messenger in plant. *Plant Biol.* 3, 577–591. doi: 10.1055/s-2001-19372

Gilroy, S., Trebacz, K., and Salvador-Recatalà, V. (2018). Editorial: inter-cellular electrical signals in plant adaptation and communication. *Front. Plant Sci.* 15, 9, 643. doi: 10.3389/fpls.2018.00643

Grefen, C., Donald, N., Hashimoto, K., Kudla, J., Schumacher, K., and Blatt, M. R. (2010). A ubiquitin-10 promoter-based vector set for fluorescent protein tagging facilitates temporal stability and native protein distribution in transient and stable expression studies. *Plant J.* 64, 355–365. doi: 10.1111/j.1365-313X.2010.04322.x

Grefen, C., Karnik, R., Larson, E., Lefoulon, C., Wang, Y., Waghmare, S., et al. (2015). A vesicle-trafficking protein commandeers Kv channel voltage sensors for voltage-dependent secretion. *Nat. Plants* 1, 15108. doi: 10.1038/nplants.2015.166

Grossmann, G., Krebs, K., Maizel, A., Stahl, Y., Vermeer, J. E. M., and Ott, T. (2018). Green light for quantitative live-cell imaging in plants. *J. Cell Sci.* 131, jcs209270. doi: 10.1242/jcs.209270

Han, Z., Jin, L., Chen, F., Loturco, J. J., Cohen, L. B., Bondar, A., et al. (2014). Mechanistic studies of the genetically encoded fluorescent protein voltage probe ArcLight. *PLoS One* 9, e113873. doi: 10.1371/journal.pone.0113873

Hedrich, R., Salvador-Recatalà, V., and Dreyer, I. (2016). Electrical wiring and long-distance plant communication. *Trends Plant Sci.* 21, 376–387. doi: 10.1016/j.tplants.2016.01.016

Hilleary, R., Choi, W. G., Kim, S. H., Lim, S. D., and Gilroy, S. (2018). Sense and sensibility: the use of fluorescent protein-based genetically encoded biosensors in plants. *Curr. Opin. Plant Biol.* 46, 32–38. doi: 10.1016/j.pbi.2018.07.004

Jewell, J. B., Sowders, J. M., He, R., Willis, M. A., Gang, D. R., and Tanaka, K. (2019). Extracellular ATP shapes a defense-related transcriptome both independently and along with other defense signaling pathways. *Plant Physiol.* 179, 1144–1158. doi: 10.1104/pp.18.01301

Kato, N., and Lam, E. (2003). Chromatin of endoreduplicated pavement cells has greater range of movement than that of diploid guard cells in *Arabidopsis thaliana*. *J. Cell Sci.* 116, 2195–2201. doi: 10.1242/jcs.00437

Kinraide, T. B., Yermiyahu, U., and Rytwo, G. (1998). Computation of surface electrical potentials of plant cell membranes. Correspondence to published zeta potentials from diverse plant sources. *Plant Physiol.* 118, 505–512. doi: 10.1104/pp.118.2.505

Knöpfel, T. (2012). Genetically-encoded optical indicators for the analysis of neuronal circuits. *Nat. Rev. Neurosci.* 13, 687–700. doi: 10.1038/nrn3293

Knöpfel, T., Gallero-Salas, Y., and Song, C. (2015). Genetically encoded voltage indicators for large scale cortical imaging come of age. *Curr. Opin. Chem. Biol.* 27, 75–83. doi: 10.1016/j.cbpa.2015.06.006

Kong, X., Liu, G., Liu, J., and Ding, Z. (2018). The root transition zone: a hot spot for signal crosstalk. *Trends Plant Sci.* 23, 403–409. doi: 10.1016/j.tplants.2018.02.004

Kralj, J. M., Hochbaum, D. R., Douglass, A. D., and Cohen, A. E. (2011). Electrical spiking in *Escherichia coli* probed with a fluorescent voltage-indicating protein. *Science* 333, 345–348. doi: 10.1126/science.1204763

Levin, M., and Stevenson, C. G. (2012). Regulation of cell behavior and tissue patterning by bioelectrical signals: challenges and opportunities for biomedical engineering. *Annu. Rev. Biomed. Eng.* 14, 295–323. doi: 10.1146/annurev-bioeng-071811-150114

Libertini, L. J., and Small, E. W. (1984). Effects of pH on the stability of chromatin core particles. *Nucleic Acids Res.* 12, 4351–4359. doi: 10.1093/nar/12.10.4351

Lobet, G. (2017). Image analysis in plant sciences: publish then perish. *Trends Plant Sci.* 22, 559–566. doi: 10.1016/j.tplants.2017.05.002

Loro, G., Drago, I., Pozzan, T., Schiavo, F. L., Zottini, M., and Costa, A. (2012). Targeting of Cameleons to various subcellular compartments reveals a strict cytoplasmic/mitochondrial Ca2+ handling relationship in plant cells. *Plant J.* 71, 1–13. doi: 10.1111/j.1365-313X.2012.04968.x

Maouyo, D., Chu, S., and Montrose, M. H. (2000). pH heterogeneity at intracellular and extracellular plasma membrane sites in HT29-C1 cell monolayers. *Am. J. Physiol. Cell Physiol.* 278, C973–C981. doi: 10.1152/ajpcell.2000.278.5.C973

Marshall, W. F., Straight, A., Marko, J. F., Swedlow, J., Dernburg, A., Belmont, A., et al. (1997). Interphase chromosomes undergo constrained diffusional motion in living cells. *Curr. Biol.* 7, 930–939. doi: 10.1016/S0960-9822(06)00412-X

Matzke, A. J. M., and Matzke, M. A. (1991). The electrical properties of the nuclear envelope, and their possible role in the regulation of eukaryotic gene expression. *Bioelectrochem. Bioenerg.* 25, 357–370. doi: 10.1016/0302-4598(91)80002-K

Matzke, A. J. M., van der Winden, J., and Matzke, M. (2003). Tetracycline operator/repressor system to visualize fluorescence-tagged T-DNAs in interphase nuclei of Arabidopsis. *Plant Mol. Biol. Rep.* 21, 9–19. doi: 10.1007/BF02773392

Matzke, A. J. M., Huettel, B., van der Winden, J., and Matzke, M. (2005). Use of two-color fluorescence-tagged transgenes to study interphase chromosomes in living plants. *Plant Physiol.* 139, 1586–1596. doi: 10.1104/pp.105.071068

Matzke, A. J. M., Huettel, B., van der Winden, J., and Matzke, M. (2008). "The Nucleus," in *Fluorescent transgenes to study interphase chromosomes in living plants*, vol. 1. Ed. R. Hancock (Totowa, New Jersey: Humana Press), 241–226. doi: 10.1007/978-1-59745-406-3_16

Matzke, A. J. M., Watanabe, K., van der Winden, J., Naumann, U., and Matzke, M. (2010a). High frequency, cell type-specific visualization of fluorescent-tagged genomic sites in interphase and mitotic cells of living *Arabidopsis* plants. *Plant Methods* 6, 2. doi: 10.1186/1746-4811-6-2

Matzke, A. J. M., Weiger, T. M., and Matzke, M. (2010b). Ion channels at the nucleus: electrophysiology meets the genome. *Mol. Plant* 3, 642–652. doi: 10.1093/mp/ssq013

Matzke, A. J. M., and Matzke, M. (2013). Membrane "potential-omics": toward voltage imaging at the cell population level in roots of living plants. *Front. Plant Sci.* 4, 311. doi: 10.3389/fpls.2013.00311

Matzke, A. J. M., and Matzke, M. (2015). Expression and testing in plants of ArcLight, a genetically-encoded voltage indicator used in neuroscience research. *BMC Plant Biol.* 15, 245. doi: 10.1186/s12870-015-0633-z

Mousavi, S. A. R., Chauvin, A., Pascaud, F., Kellenberger, S., and Farmer, E. E. (2013). GLUTAMATE RECEPTOR-LIKE genes mediate leaf-to-leaf wound signaling. *Nature* 500, 422–426. doi: 10.1038/nature12478

McNally, J. G. (2009). Transcription, chromatin condensation, and gene migration. *J. Cell Biol.* 185, 7–9. doi: 10.1083/jcb.200903056

Miesenböck, G. (2012). Synapto-pHluorins: genetically encoded reporters of synaptic transmission. *Cold Spring Harb. Protoc.* 2012, 213–217. doi: 10.1101/pdb.ip067827

Mirkin, E. V., Chang, F. S., and Kleckner, N. (2013). Protein-mediated chromosome pairing of repetitive arrays. *J. Mol. Biol.* 426, 550–557. doi: 10.1016/j.jmb.2013.11.001

Nicholson, D. J. (2019). Is the cell really a machine? *J. Theor. Biol.* 477, 108–126. doi: 10.1016/j.jtbi

Qian, H., Sheetz, M. P., and Elson, E. L. (1991). Single particle tracking. Analysis of diffusion and flow in two-dimensional systems. *Biophys. J.* 60, 910–921. doi: 10.1016/S0006-3495(91)82125-7

Rosin, F. M., Watanabe, N., Cacas, J. L., Kato, N., Arroyo, J. M., Fang, Y., et al. (2008). Genome-wide transposon tagging reveals location-dependent effects on transcription and chromatin organization in Arabidopsis. *Plant J.* 55, 514–525. doi: 10.1111/j.1365-313X.2008.03517.x

Santos, J. M., Martínez-Zaguilán, R., Facanha, A. R., Hussain, F., and Sennoune, S. R. (2016). Vacuolar H+-ATPase in the nuclear membranes regulates nucleocytosolic proton gradients. *Am. J. Physiol. Cell Physiol.* 311, C547–C558. doi: 10.1152/ajpcell.00019.2016

Sepheri-Rad, M., Cohen, L. B., Braubach, O., and Baker, B. J. (2018). Monitoring voltage fluctuations of intracellular membranes. *Sci. Rep.* 8, 6911. doi: 10.1038/s41598-018-25083-7

Shen, J., Zeng, Y., Zhuang, X., Sun, L., Yao, X., Pimpl, P., et al. (2013). Organelle pH in the *Arabidopsis* endomembrane system. *Mol. Plant.* 6, 1419–1437. doi: 10.1093/mp/sst079

Soutoglou, E., and Misteli, T. (2007). Mobility and immobility of chromatin in transcription and genome stability. *Curr. Opin. Genet. Dev.* 17, 435–442. doi: 10.1016/j.gde.2007.08.004

Sze, H., and Chanroj, S. (2018). Plant endomembrane dynamics: studies of K+/H+ antiporters provide insights on the effects of pH and ion homeostasis. *Plant Physiol.* 177, 875–895. doi: 10.1104/pp.18.00142

Tanaka, K., Gilroy, S., Jones, A. M., and Stacey, G. (2010). Extracellular ATP signaling in plants. *Trends Cell Biol.* 20, 602–608. doi: 10.1016/j.tcb.2010.07.005

Wang, P., Hawes, C., and Hussey, P. J. (2017). Plant endoplasmic reticulum-plasma membrane contact sites. *Trends Plant Sci.* 22, 289–297. doi: 10.1016/j.tplants.2016.11.008

Wang, F., Sampogna, R. V., and Ware, B. R. (1989). pH dependence of actin self-assembly. *Biophys. J.* 55, 293–298. doi: 10.1016/S0006-3495(89)82804-8

Weijers, D., Franke-van Dijk, M., Vencken, R. J., Quint, A., Hooykaas, P., and Offringa, R. (2001). An *Arabidopsis* Minute-like phenotype caused by a semi-dominant mutation in a *RIBOSOMAL PROTEIN S5* gene. *Development* 128, 4289–4299.

Weiss, L. E., Naor, T., and Shechtman, Y. (2018). Observing DNA in live cells. *Biochem. Soc. Trans.* 46, 729–740. doi: 10.1042/BST20170301

Conflict of Interest: The authors declare that the research was conducted in the absence of any commercial or financial relationships that could be construed as a potential conflict of interest.

frontiers in Plant Science

PERSPECTIVE
published: 07 February 2020
doi: 10.3389/fpls.2019.01795

Looking At the Past and Heading to the Future: Meeting Summary of the 6th European Workshop on Plant Chromatin 2019 in Cologne, Germany

*Jordi Moreno-Romero[1], Aline V. Probst[2], Inês Trindade[3], Kalyanikrishna[4], Julia Engelhorn[5,6] and Sara Farrona[7]**

[1] Centre for Research in Agricultural Genomics (CRAG), CSIC-IRTA-UAB-UB, Campus UAB, Bellaterra, Barcelona, Spain, [2] GReD, Université Clermont Auvergne, CNRS, INSERM, BP 38, Clermont–Ferrand, France, [3] Institute for Biochemistry and Biology, University of Potsdam, Potsdam, Germany, [4] Institute for Biology, Freie Universität Berlin, Berlin, Germany, [5] Institute for Molecular Physiology, Heinrich-Heine-Unverisität, Düsseldorf, Germany, [6] Max Planck Institute for Plant Breeding Research, Cologne, Germany, [7] Plant and AgriBiosciences Centre, Ryan Institute, NUI Galway, Ireland

OPEN ACCESS

Edited by:
Bo Liu,
University of California, Davis, United States

Reviewed by:
Li Pu,
Chinese Academy of Agricultural Sciences, China
Giorgio Perrella,
ENEA–Centro Ricerche Trisaia, Italy

***Correspondence:**
Sara Farrona
sara.farrona@nuigalway.ie

Specialty section:
This article was submitted to Plant Cell Biology, a section of the journal Frontiers in Plant Science

Received: *24 October 2019*
Accepted: *23 December 2019*
Published: *07 February 2020*

Citation:
Moreno-Romero J, Probst AV, Trindade I, Kalyanikrishna, Engelhorn J and Farrona S (2020) Looking At the Past and Heading to the Future: Meeting Summary of the 6th European Workshop on Plant Chromatin 2019 in Cologne, Germany. Front. Plant Sci. 10:1795. doi: 10.3389/fpls.2019.01795

In June 2019, more than a hundred plant researchers met in Cologne, Germany, for the 6th European Workshop on Plant Chromatin (EWPC). This conference brought together a highly dynamic community of researchers with the common aim to understand how chromatin organization controls gene expression, development, and plant responses to the environment. New evidence showing how epigenetic states are set, perpetuated, and inherited were presented, and novel data related to the three-dimensional organization of chromatin within the nucleus were discussed. At the level of the nucleosome, its composition by different histone variants and their specialized histone deposition complexes were addressed as well as the mechanisms involved in histone post-translational modifications and their role in gene expression. The keynote lecture on plant DNA methylation by Julie Law (SALK Institute) and the tribute session to Lars Hennig, honoring the memory of one of the founders of the EWPC who contributed to promote the plant chromatin and epigenetic field in Europe, added a very special note to this gathering. In this perspective article we summarize some of the most outstanding data and advances on plant chromatin research presented at this workshop.

Keywords: EWPC2019, chromatin, epigenetics, transcription, nucleus

INTRODUCTION

Last year, the Max Planck Institute for Plant Breeding Research in Cologne hosted the 6th European Workshop on Plant Chromatin (EWPC). A total of 110 researchers met to present the most recent focuses, advances, and challenges in the plant chromatin and epigenetics field during this 2-day workshop that comprised more than 25 standard talks and a similar number of short PechaKucha-style talks. Many other topics were talked over during the poster sessions in which the participants had the opportunity to discuss new discoveries and concepts in plant chromatin science in a thriving atmosphere.

Several talks emphasized the complexity of chromatin organization within the three-dimensional space of the nucleus and presented cutting-edge techniques developed to provide a deeper and higher-resolution view of chromatin structure (**Figure 1**). As in previous EWPCs, histone variants and histone marks were an important theme for many research laboratories. Considerable progress has been made in recent years to understand their links to transcriptional regulation. Also, of note have been the advances in our understanding of the proteins and complexes that are involved in the deposition of histone variants and marks, which, additionally, may act as readers of these chromatin features.

Current challenges that have arisen from issues such as food security and climate change have added a new dimension to the study of epigenetic regulation of plant traits and epigenetic inheritance of transcriptional stages. For that reason, the link between chromatin dynamics, gene expression, and plant developmental adaptation to the environment was also substantially addressed in the meeting. To advance in this field, analyses of chromatin architecture changes at different developmental stages and the tissue- or cell-specific level that have been technically challenging were presented.

Julie Law from the Salk Institute (La Jolla, USA) was invited to present the keynote lecture, which highlighted some of the most important past and present contributions to the DNA methylation field from her laboratory. Julie gave an overview of the crucial roles played by DNA methylation in gene regulation and transposon silencing. In addition, she reported that a family of four putative chromatin remodeling factors, CLASSY (CLSY) 1–4, associate with the RNA-directed DNA methylation (RdDM) pathway components Pol-IV and SAWADEE HOMEODOMAIN HOMOLOG 1 (SHH1) (Law et al., 2011). Further recent studies showed that CLSY proteins function individually as locus-specific regulators of RdDM and in global regulation of DNA methylation patterns in Arabidopsis

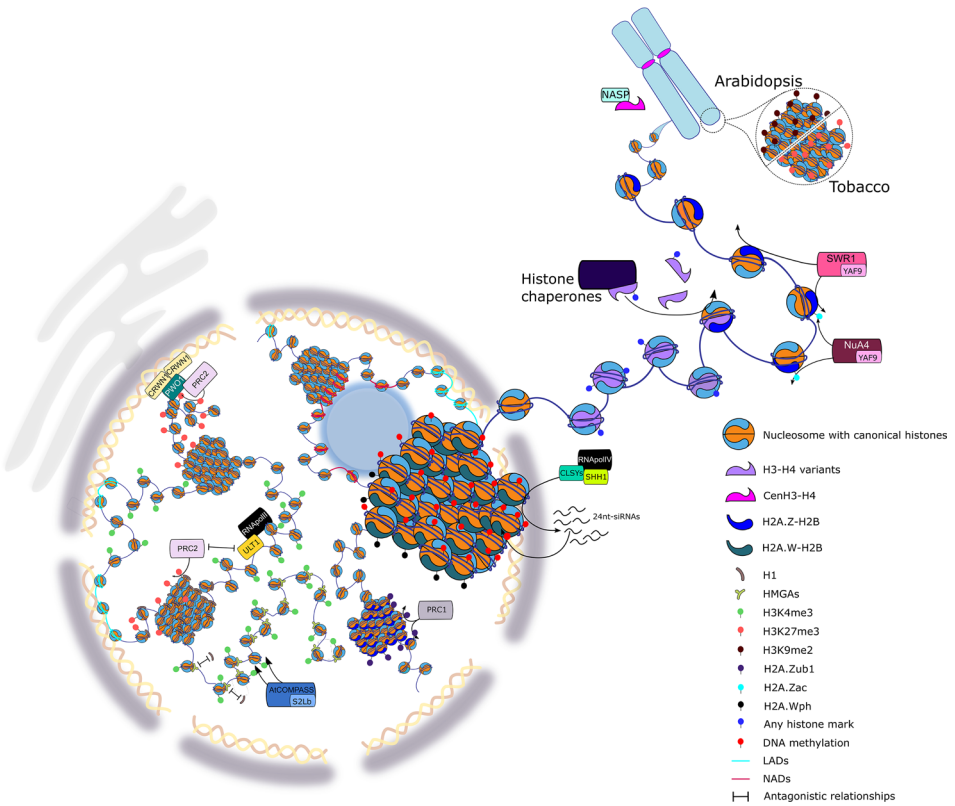

FIGURE 1 | Highlights of the European Plant Chromatin Workshop 2019. Chromatin organization is a central player in controlling gene expression and concomitantly regulating plant development and plant responses to the environment. The scheme illustrates some of the aspects of plant chromatin organization presented at the EWPC ranging from local chromatin changes touching the bricks of the nucleosome to higher-order chromatin organization. At the level of the nucleosome, modifications of the DNA molecule and histone proteins were discussed, such as the regulation of DNA methylation involving the CLASSY (CLSY) proteins, the incorporation of specific variants of histones H1, H3, and H2A through dedicated histone chaperone complexes, and the dynamics of non-histone DNA-binding proteins, such as HIGH MOBILITY GROUP A (HMGA). Post-translational modifications of histones are set by specific complexes exemplified here by COMPLEX PROTEINS ASSOCIATED WITH SET1 (COMPASS), involved in H3K4me3, Nucleosome Acetyltransferase of Histone H4 (NuA4), in H2A.Z acetylation, and Polycomb Repressive Complex 1 (PRC1), in H2A.Z monoubiquitination. The role of chromatin remodelers in the deposition of histones is also depicted through H2A.Z-mediated deposition by the SWI/SNF-Related protein 1 (SWR1) complex. Modification of H2A.W by phosphorylation and its association to the heterochromatin was observed. The interplay between repressive modifications set by PRC2 and the antagonizing activity of ULTRAPETALA1 (ULT1) allows for a dynamic transcriptional regulation. Finally, the formation of specific chromatin domains in the nucleus, such as telomeres, nucleolus/lamina associated domains (NADs/LADs), or the association of chromatin domains *via* PWWP INTERACTOR OF POLYCOMB (PWO1) to CRWN1, a plant lamina component, were presented.

(Zhou et al., 2018). The next phase of the Law's laboratory work aims to identify the roles of CLSY proteins in controlling DNA methylation patterns in a tissue-specific manner.

The EWPC was also the perfect venue for honoring the memory of Professor Lars Hennig who has recently passed away (Mozgová et al., 2018a). Together with Claudia Köhler and Valérie Gaudin, he established the EWPC in 2009 as one of the main gathering platforms for the plant epigenetic research community in Europe, bringing his enthusiasm and passion on plant science to these workshop series. During this tribute session, Lars' colleagues and alumni shared with the audience his impact and vision on the chromatin and epigenetics field.

This perspective article summarizes the main topics discussed during the EWPC 2019 and provides insight into the future paths that the plant epigenetic community will follow in the next years. We thank all the laboratories, which have contributed to the EWPC with recently published or unpublished data, and we apologize to the researchers whose work could not be cited due to space limitations.

SESSION 1: A VIEW ON CHROMATIN, TECHNIQUES, AND NUCLEAR STRUCTURE

The key bearer of genetic information in eukaryotic cells is chromatin, which is non-randomly distributed inside the nucleus and shows an extraordinary degree of compaction and spatial organization. Nuclear organization is achieved by many factors, including histone proteins, modifiers and readers, as well as structural components of the nuclear periphery and nuclear bodies, which together dynamically control the nuclear architecture and may form nuclear domains (Sexton and Cavalli, 2015). The first session of the EWPC meeting dealt with the role of these factors in chromatin and nuclear organization.

The core histones have been structurally conserved through evolution and have evolved to accomplish two conflicting and yet vital tasks: on one hand, the long DNA molecules have to be packaged within the limits of the eukaryotic nucleus, preventing knots and tangles and protecting the genome from physical damage; on the other hand, the information that is encoded in the DNA needs to be accessed at appropriate times (Rosa and Shaw, 2013). The linker DNA between nucleosomes is bound by linker histones H1 (Rutowicz et al., 2015; Kotliński et al., 2017) whose role is much less understood than core histones. A recent study presented by Célia Baroux (Zurich, Switzerland) provided a multi-scale functional analysis of Arabidopsis linker histones. The work, done in collaboration with the laboratories from Andrzej Jerzmanowski (Warsaw, Poland) and Fredy Barneche (Paris, France), showed that H1-deficient plants are viable but exhibit phenotypes in seed dormancy, flowering time, as well as lateral root and stomata formation. In addition to a role in heterochromatin compaction, H1 seems to regulate nucleosome distribution over gene bodies. Yet, the authors showed that H1-mediated chromatin organization may act downstream of transcriptional control for a large number of loci in Arabidopsis. In addition, a new connection was found between H1 and H3K27me3. The findings suggest that H1 may act as a chromatin organizer favoring the maintenance of this epigenetic mark as well as others (Rutowicz et al., 2019).

Frédéric Pontvianne (Perpignan, France) focused on the nucleolus, the largest nuclear body, which is well known as the site of ribosomal RNA (rRNA) gene transcription, rRNA processing, and ribosome biogenesis (Boisvert et al., 2007). In a previous study, Frédéric and co-workers identified chromatin regions associated with the nucleolus, termed Nucleolus Associated Domains (NADs). NADs are primarily genomic regions with heterochromatic signatures and include transposable elements (TEs), sub-telomeric regions, and mostly inactive protein-coding genes (Pontvianne et al., 2016). Recent data now suggest that the rRNA gene copy number impacts the organization of NADs, and this suggests a role of nucleolus organizer regions (NORs) in establishing domains of inactive chromatin associated with the nucleolus (Picart-Picolo et al., 2019).

Similar to the nucleolus, the nuclear periphery is another compartment within the nucleus that plays a crucial role in chromatin organization and nuclear architecture. Kalyanikrishna (Berlin, Germany) presented data showing a putative link between Polycomb Group (PcG)-mediated repression and the nuclear periphery in Arabidopsis. PWWP INTERACTOR OF POLYCOMB (PWO1) is a PWWP-domain containing protein able to interact with any of the three possible POLYCOMB REPRESSIVE COMPLEX 2 (PRC2) histone methyltransferases in Y2H, and PWO1-CURLY LEAF (CLF) interaction was confirmed in planta (Hohenstatt et al., 2018; Mikulski et al, 2019). Among the putative interactors of PWO1, CROWDED NUCLEI1 (CRWN1) has been identified (Mikulski et al, 2019). CRWN1 is a coiled coil analog of lamin proteins, whose absence alters nuclear morphology (Wang et al., 2013), and a set of H3K27me3 targets were upregulated in *crwn1 crwn2* double mutants in Arabidopsis. The interaction between PWO1 and CRWN1 suggests a role of the nuclear periphery in PRC2-mediated gene regulation in Arabidopsis (Mikulski et al., 2019). The Schubert laboratory continues to work on characterizing putative interactors involved in this pathway.

The post-translational modifications of telomere histones in plants have been investigated by Katerina Adamusova (Brno, Czech Republic). Among the canonical and non-canonical telomeres in plants, the authors found two kinds of epigenetic patterns regardless of the differences in telomere length and telomeric sequences used. One of them corresponds to the Arabidopsis-like pattern, where telomere histones are marked predominantly with H3K9me2. The other one is the tobacco-like pattern marked predominantly with H3K27me3 (Adamusová et al., 2019).

Hua Jiang (Gatersleben, Germany) discussed the role of AT-hook proteins in the regulation of gene expression by mediating the H3K9me2 heterochromatic mark at the nuclear matrix-associated regions (MARs). They identified AT-Hook Like 10 (AHL10), a member of the AT-hook family in Arabidopsis, and the SET domain containing SU(VAR)3-9 homolog (SUVH9) as interacting partners of ADMETOS (ADM), which functions in

establishing the postzygotic hybridization barrier in Arabidopsis. Significantly increased expression of *ADM* and *AHL10* in Arabidopsis triploid seeds results in H3K9me2 hypermethylation in MARs. Furthermore, AHL10-mediated H3K9me2 hypermethylation at MARs is independent of DNA methylation (Jiang et al., 2017). Apart from AHL10, the authors found that the overexpression line of another *AHL* also has increased H3K9me2 levels at TEs in sporophytic tissues, indicating a similar role for other members of this family.

SESSION 2: CHROMATIN, INHERITANCE, AND GENERATION CHANGES

Recent advances in our understanding of inter-generational inheritance of epigenetic and chromatin marks have revealed a variety of plant peculiarities, rendering this topic an exciting field of study with impact on our fundamental understanding of inheritance, phenotypic plasticity, population dynamics, and evolution (Köhler and Springer, 2017; Miryeganeh and Saze, 2019). Nevertheless, many open questions remain concerning what epigenetic information is inherited, the mechanisms of inheritance, and the processes involved in eventual reprogramming to prevent inheritance. To shed light on these questions, an enhanced understanding of gene regulation in gametophytes is vital. Sara Simonini (Zurich, Switzerland) focused her presentation on gene regulation in the female gametophyte and during early seed development by analyzing interaction partners and direct targets of the PRC2 methyltransferase MEDEA (MEA). Previous works have implicated MEA in the repression of seed development before fertilization and in endosperm cellularization (Chaudhury et al., 1997; Grossniklaus et al., 1998; Köhler et al., 2003a). The new unpublished data indicate that MEA interacts with histone deacetylases (HDACs), and that plants depleted in *HDACs* display similar abnormal phenotypes as *mea* mutants, suggesting an interplay between histone methylation and acetylation during early seed development.

The double fertilization process of plants generates an additional complication in the understanding of trans-generational inheritance and maternal and paternal contributions to the next generation. Thus, being able to distinguish events taking place in the endosperm from other plant tissues will be crucial to understand the peculiarities of this triploid tissue. An exciting technical advance in this direction was presented by Vikash Kumar Yadav (Uppsala, Sweden). He performed modified high-throughput chromatin conformation (mHi-C) on purified endosperm nuclei isolated by the INTACT method (Moreno-Romero et al., 2017), thus enabling Hi-C analysis on a limited number of nuclei. With this technique, he was able to observe elevated chromatin interaction levels in endosperm tissue compared to leaf tissue and discover that self-looping genes are on average expressed at a higher level compared to non-self-looping genes.

Heinrich Bente (Vienna, Austria) focused his presentation on yet another aspect of epigenetic inheritance, the phenomenon of paramutation, characterized by interallelic communication between epialleles at a single locus that results in stable and heritable silencing. Employing an epigenetically regulated resistance marker for hygromycin in Arabidopsis, Heinrich and his co-workers found that paramutation becomes apparent in F2 progeny of tetraploid hybrids but not in diploid ones. Small RNA profiles differ between the two epialleles, as do DNA methylation and chromatin marks. The fact that the paramutation is not observed at low temperatures, where also small RNA production is reduced (Baev et al., 2014), supports the assumption that small RNAs may be involved in paramutations.

Before epigenetic marks such as DNA methylation can be inherited between generations, they need to be maintained during cell divisions in the parents. Especially for asymmetric CHH methylation, maintenance is coupled to RdDM (Law and Jacobsen, 2010). Gergely Molnar (Tulin, Austria) reported the characterization of *freak show* (*fks*), a novel missense mutant of the RNA Polymerase V-specific subunit NRPE5A (Ream et al., 2009). The mutation displayed loss of transposon silencing due to generally reduced CG DNA methylation as well as hypermethylation at other loci, together leading to abnormal phenotypes, including flowering time defects and homeotic transformations. The findings seem to contrast canonical RNA Pol-V function in RdDM only, which mainly affects CHG and CHH methylation, and suggest a connection between an RdDM component and CG methylation maintenance.

SESSION 3: MAKING VARIATIONS OF CHROMATIN—INCORPORATING BRICKS OF DIFFERENT COLORS

To modulate nucleosome properties, including DNA accessibility and interactions between nucleosomes or even chromatin fibers, different histone variants can be incorporated. Recent years have seen accumulating evidence for the functional importance of these different histone variants for processes ranging from gene expression control and reprogramming to DNA repair processes in mammals and plants (Jiang and Berger, 2016; Buschbeck and Hake, 2017; Dabin and Polo, 2017).

Intriguing examples for these roles, reported by Anna Schmücke (Vienna, Austria), are the plant-specific histone variants H2A.W.6, H2A.W.7, and H2A.W.12, highly enriched in heterochromatin and involved in chromatin fiber–fiber interactions (Yelagandula et al., 2014). These histone variants are distinguished by a highly conserved KSPKK motif in their C-terminal tail. In response to DNA damage in heterochromatin, one of the three H2A.W variants, namely H2A.W.7, is phosphorylated at its SQE motif, and this phosphorylation is required for an appropriate DNA damage response (DDR) (Lorković et al., 2017). New evidence now indicates that only H2A.W.6, and not H2A.W.7, is phosphorylated in the conserved KSPKK motif in a cell cycle-dependent manner in Arabidopsis. Through a synthetic approach in fission yeast, she demonstrated that the phosphorylation of the KSPKK motif in addition to the phosphorylated SQE motif impairs a proper DNA damage

response. This exemplifies a highly complex relationship between histone variants, their post-translational modification status, and their biological function. Another interesting H2A variant is H2A.Z, which has been associated both with transcriptional activation and repression depending on its position within a gene (Coleman-Derr and Zilberman, 2012; Sura et al., 2017). Wiam Merini (Seville, Spain) presented recent data resolving part of the mystery of this dual role of H2A.Z in transcription. She showed that, similar to canonical H2A, H2A.Z can be mono-ubiquitinated by PRC1 and that this post-translational modification plays an important role in transcriptional repression independent of PRC2 activity (Gómez-Zambrano et al., 2019). Indeed, complementation with a ubiquitination-resistant H2A.Z protein failed to rescue expression of upregulated genes in *h2a.z* mutant plants revealing the importance of H2A.Z ubiquitination. In contrast, H2A.Z ubiquitination seems to be dispensable to the rescue expression of the genes downregulated in *h2a.z* mutant plants; these genes may simply require H2A.Z incorporation. Alternatively, other post-translational modifications may play a role; in yeast, H2A.Z is acetylated by the NuA4 complex (Lu et al., 2009). Indeed, the confirmation that H2A.Z acetylation occurs in plants was provided by José A. Jarillo (Madrid, Spain). He studied the plant homologues of YEAST ALL1-FUSED GENE FROM CHROMOSOME 9 (YAF9) proteins, which are common components of the SWR1 complex involved in H2A.Z deposition and the NuA4 complex. In the absence of YAF9 proteins, H2A.Z acetylation is reduced at the *FLC* chromatin, and *FLC* expression is repressed, while H2A.Z incorporation as such is unaffected at this locus (Crevillén et al., 2019).

Given the emerging roles of the different histone variants in gene expression control and DNA repair reported at this conference, it becomes clear that histone deposition needs to be tightly controlled in time and space, and histone chaperones play an important role in this process. As an example, loss of H3 histone chaperones, such as HISTONE REGULATOR A (HIRA) (Nie et al., 2014; Duc et al., 2015) and the Arabidopsis ALPHA THALASSEMIA-MENTAL REDARDATION X-LINKED (ATRX) homologue (Duc et al., 2017), which function in complementary pathways of histone H3.3 deposition, results in altered gene expression. Aline V. Probst (GReD, France) discussed work from her laboratory, showing that ATRX loss-of-function affects H3.3 deposition at genes characterized both by elevated H3.3 occupancy and high expression levels, whereas *hira* mutants show reduced nucleosomal occupancy both at genes and in heterochromatin translating into reactivation of transposable elements. While some H3 histone chaperones are highly conserved, species-specific chaperones deposit the centromeric histone CenH3 (Müller and Almouzni, 2014). So far, the factor responsible for escort and deposition of plant CenH3 has remained enigmatic. Inna Lermontova (Gatersleben, Germany) reported on the collaborative effort to search for histone CenH3 interactors and the identification of the plant homologue of NUCLEAR AUTOANTIGENIC SPERM PROTEIN (NASP) as a CenH3 binding protein. Previously shown to bind histone H3 monomers or H3-H4 dimers (Maksimov et al., 2016), the nuclear NASP protein interacts both with the N-terminal tail as well as with the histone fold domain of CenH3 and reduced *NASP* expression negatively affects CenH3 levels, suggesting that NASP functions as a CenH3 escort protein (Le Goff et al., 2019).

SESSION 4: A TRIBUTE TO LARS HENNIG

Professor Lars Hennig passed away last year, leaving a gap in the fields of chromatin biology and plant development (Mozgová et al., 2018a). Session 4 of the meeting gave a homage remembering him, not only as a valuable colleague, friend, and mentor, but also by highlighting his scientific contributions and how his work will impact future research.

Among many other topics, one of Lars' main interests were histone variants and chaperones. He contributed to the identification of MULTICOPY SUPRESSOR OF IRA 1 (MSI1) as one subunit of the CHROMATIN ASSEMBLY FACTOR 1 (CAF-1) chaperone complex (Hennig et al., 2003). Lars further showed that transgenerational aggravation of the CAF-1 mutant phenotype was related to a global change in DNA methylation (Mozgová et al., 2018b). Following this curiosity on DNA methylation levels during development, Minerva Trejo-Arellano (Uppsala, Sweden), a former PhD student of Lars, reported on changes of DNA methylation during dark-induced leaf senescence (**Figure 2A**). She showed that senescent leaves had expanded chromocenters, which is indicative of heterochromatin de-condensation. These chromatin changes were accompanied by a concerted downregulation of genes involved in epigenetically mediated silencing pathways and a deregulation of transposable elements. Surprisingly, no genome-wide changes in DNA methylation were detected, only localized differentially methylated regions (DMRs), especially in the CHH context (Trejo-Arellano et al., 2019). Among the epigenetic changes that occur during developmental transitions, Lars soon focused his attention on Polycomb activity. He contributed to the identification of MSI1 as part of the PRC2 (Köhler et al., 2003b) and explored its role in embryo-to-seedling transitions, a work developed by Iva Mozgová (České Budějovice, Czech Republic) during her postdoc in Lars' group. She found that the characteristic embryonic phenotype of the double mutant of *clf* and *swinger* (*clf swn*) (Chanvivattana et al., 2004; Mozgová et al., 2017), which is affected in two of the three possible methyltransferases of PRC2, depends on the presence of sucrose. This finding fits with the idea that, during this developmental transition, plant nutrition shifts from heterotrophic to autotrophic growth. Following this research line, Iva presented a progressive degradation of chloroplasts and an increase in Reactive Oxygen Species (ROS) in *clf swn* and, accordingly, the mitigation of the phenotype under reduced light intensities. Therefore, these data suggest an unexplored role of PRC2 in mediating the establishment and/or maintenance of photoautotrophic growth in Arabidopsis.

To further understand the multiple functions of PcG proteins, Lars' laboratory found a direct interaction between MSI1 and

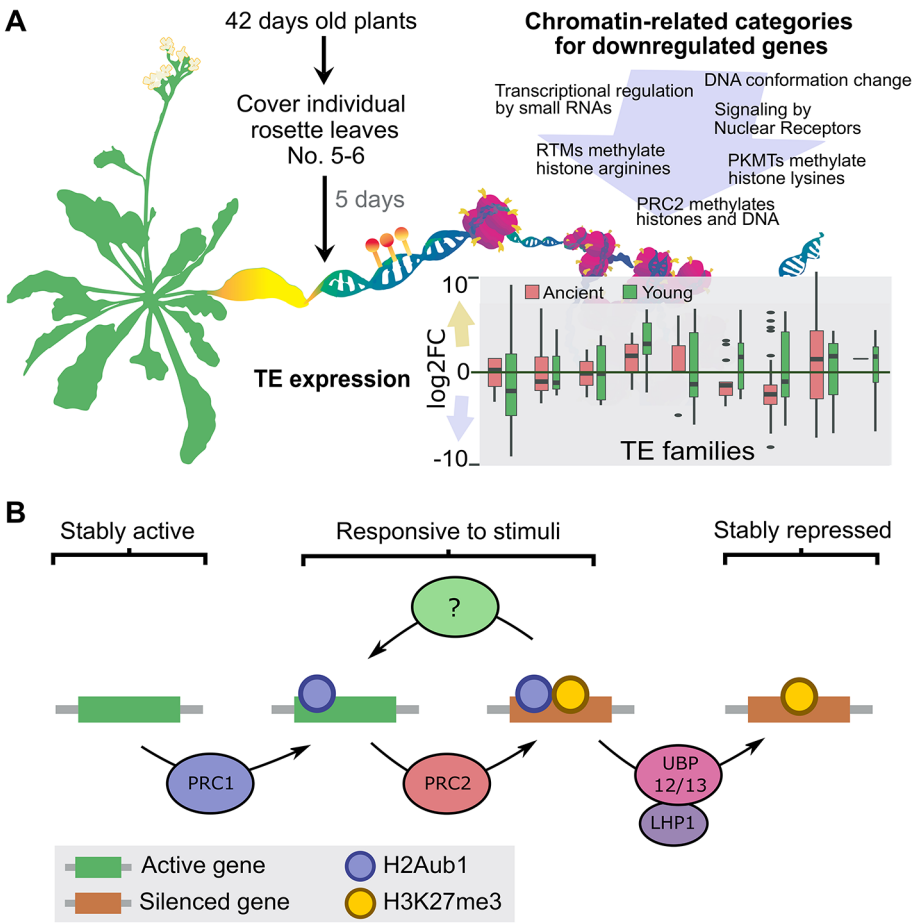

FIGURE 2 | Overview of recent contributions from former Lars' PhD students. **(A)** Dark-induced senescence causes localized changes in DNA methylation in Arabidopsis. Senescence was induced by covering individual Arabidopsis leaves. The yellowing of the covered-senescent leaves was accompanied by changes in the expression of transposable elements that depending on the TE family can be unaltered, up- or downregulated. Moreover, GO and pathway categories related with the maintenance of chromatin structure were enriched among the downregulated genes (for the complete analysis see Trejo-Arellano et al., 2019). Overall, the global DNA methylation landscape of the senescent leaves remained remarkably stable with only few localized DNA methylation changes detected, particularly in the CHH context **(B)** Working model for the UBP12/13-mediated gene repression. PRC2 causes silencing *via* deposition of H3K27me3, which in the majority of the cases is dependent on PRC1. However, by a mechanisms that remain to be resolved the product of PRC1 activity, H2Aub1, also creates an unstable state in which genes can be rapidly reactivated in response to a stimulus. Stable repression requires removal of H2Aub1 by LHP1-interacting UBP12/13. Figure courtesy of **(A)** M. Trejo, designed of Paulina Velasco, and **(B)** L. Kralemann.

LIKE HETEROCHROMATIN PROTEIN1 (LHP1) (Derkacheva et al., 2013). Studying LHP1 protein interactors, UBIQUITIN SPECIFIC PROTEASES (UBP) 12 and 13 were found, and it was demonstrated that UBP12 mediates the deubiquitination of H2A (Derkacheva et al., 2016). However, it has been shown that H2A ubiquitination (H2Aub) by PRC1 is largely independent of PRC2 activity (Zhou et al., 2017). To further understand the link between H2Aub and H3K27me3, Lars' former PhD student Lejon Kralemann (Uppsala, Sweden) presented a genome-wide analysis of these marks in mutants deficient for UBP12 and 13. The data suggest that H2Aub removal is required for preventing the loss of H3K27me3. In that model, LHP1 recruits UBP12/13 to deubiquitinate H2Aub and to stabilize H3K27me3-mediated repression (**Figure 2B**). Miyuki Nakamura (Uppsala, Sweden), a postdoc in Lars' former group, reported another role of LHP1 through its interaction with DEK proteins (Derkacheva et al., 2013), which are linked to chromatin and associated with DNA topoisomerase 1α (TOP1α) (Waidmann et al., 2014). Miyuki presented that DEKs genetically interact with LHP1 by enhancing the early flowering of the *lhp1* mutant, which is similar to what occurs in the *top1α lhp1* mutant (Liu et al., 2014). She proposed that LHP1 interaction with DEKs and TOP1α is important for PcG target gene regulation. These works exemplify the direction where Lars' research has lead the PcG field: finding new players of PcG activity and identifying mechanisms for target-specific PcG recruitment. In that direction, Justin Goodrich (Edinburgh, United Kingdom), through a second invited lecture, presented new data about *ANTAGONIST OF LHP1* (*ALP1*), which was identified in a suppressor screening of the *clf* mutant (Liang et al., 2015). The

interaction of ALP1 with PRC2 depends on ALP2, which interacts directly both with ALP1 and with MSI1, a core subunit of PRC2. To explain PcG antagonist function, Justin proposed that ALP1/ALP2 could compete for the core PRC2 complexes with other PcG "accessory proteins". Interestingly, ALP proteins are likely inactive Harbinger-type transposases that are already demonstrated for ALP1 (Liang et al., 2015). As Harbinger transposases are encoded as part of the sequence of the 'cut-and-paste' *Harbinger* transposon superfamily (Kapitonov and Jurka, 2004), this is an example of how transposon domestication could provide novel genes for the hosts, in particular as components of PRC2.

SESSION 5: AN OPEN VIEW ON CHROMATIN

Session 5 focused on different mechanisms that are involved in inducing a more relaxed and open chromatin structure, which usually correlates with an active transcription. For instance, Julia Engelhorn (Cologne, Germany) presented a very elegant approach in which Fluorescence Activated Cell Sorting (FACS) was combined with the Assay for Transposase-Accessible Chromatin with high-throughput sequencing (ATAC-seq), which allowed for the creation of maps with higher resolution than with DNase-seq from low cell numbers. Lines expressing the *pDORNRÖSCHEN-LIKE::GFP* in the *apetala1 cauliflower* mutant background were used (Wellmer et al., 2006), which allows for cell sorting of identical and highly synchronized Lateral Organ Founder Cells (LOFCs) (Frerichs et al., 2016). LOFCs-associated changes in chromatin accessibility were positively associated with transcriptional changes. In addition, highly accessible chromatin to the transposase corresponded well with previously described enhancer and conserved transcription factor (TF)-binding elements in promoters. These results also demonstrated that this approach can be further applied for genome-wide identification of novel transcriptional enhancers in plant specific cells (Frerichs et al., 2019).

Genome-wide approaches were also used to identify light-induced chromatin dynamics that occur at a very specific developmental switch, such as photomorphogenesis, which corresponds to the first perception of light after germination (Casal, 2013; Wu, 2014; Seluzicki et al., 2017). DE-ETIOLATED1 (DET1) is an atypical and conserved DAMAGED DNA BINDING PROTEIN 1 (DDB1)-CULLIN4 Associated Factor (DCAF) involved in the transcriptional reprogramming that occurs during photomorphogenesis (Chory et al., 1989; Pepper et al., 1994; Schroeder et al., 2002; Ma et al., 2003). Sandra Fonseca (Madrid, Spain) showed that DET1 and light control genome-wide levels and distribution of H2B ubiquitination (H2Bub) indirectly through degradation of a deubiquitination trimeric module (DUBm). One of the components of DUBm is UBP22, which acts as a major H2B deubiquitinase in the plant. Thus, DET1-mediated proteolytic degradation of DUBm is essential for chromatin reprogramming during photomorphogenesis (Nassrallah et al., 2018).

High Mobility Group A (HMGA) proteins have also been proposed to create a more permissive chromatin structure competing with linker histone H1 (Catez and Hock, 2010; Ozturk et al., 2014). Simon Amiard's (Clermont Ferrand, France) presentation focused on GH1-HMGA1 and GH1-HMGA2 proteins, which comprise a conserved central globular domain (GH1) as well as AT-hook domains (Kotliński et al., 2017). Both GH1-HMGA1 and GH1-HMGA2-GFP fusion proteins are present in interphase and mitotic nuclei but are excluded from chromocenters and centromeres, and protein–protein interaction studies indicate possible GH1-HMGA1 homodimerization and heterodimerization with GH1-HMGA2. Mutants affected in the *GH1-HMGA1* gene were impaired in development, with an overall size reduction due to smaller roots and leaves and a decrease in stem length, while *gh1-hmga2* mutants were phenotypically normal. *gh1-hmga1* mutants also showed shorter telomeres as a result of telomere instability (Charbonnel et al., 2018), and a transcriptome analysis of *gh1-hmga1* mutants suggested a contribution of GH1-HMGA1 proteins to gene expression control.

Another epigenetic hallmark of active chromatin is H3K4me3. In yeast, SET DOMAIN GROUP 1 (SET1) adds this mark as part of COMPlex of proteins ASsociated with SET1 (COMPASS). Another subunit of this complex, Swd2, is needed for the recruitment of COMPASS to specific chromatin domains enriched in H2Bub (Sun and Allis, 2002; Kim et al., 2009). In Arabidopsis, a more complex scenario may exist since H3K4me3 can be placed by different histone methyltransferases (Baumbusch et al., 2001; Thorstensen et al., 2011; Zhang and Ma, 2012), and the function of At-COMPASS-like complexes have not been fully characterized yet (Fromm and Avramova, 2014; Xiao et al., 2016). Clara Bourbosse (Paris, France) reported recent results that showed that SET DOMAIN GROUP 2 (SDG2)/ARABIDOPSIS TRITHORAX 3 (ATX3), which has a main role in the deposition of H3K4me3 in Arabidopsis (Berr et al., 2010; Guo et al., 2010), binds to SWD2-like b (S2Lb), which interacts with core subunits of AtCOMPASS in a high-molecular weight complex. In addition, S2Lb, together with SDG2, is required for deposition of H3K4me3 and directly targets highly expressed genes. However, mutations in *S2Lb* affect the steady state levels of only a few of its target genes. Therefore, as part of AtCOMPASS, S2Lb may be required for appropriate transcriptional dynamics but is not essential for gene expression. Interestingly, S2Lb recruitment and H3K4me3 deposition at target genes are independent of H2Bub, indicating that AtCOMPASS-S2Lb activity does not require H2Bub in contrast to yeast. Whether there is a crosstalk between this histone mark and other methyltransferases is still an open question (Fiorucci et al., 2019).

SESSION 6: FRIENDS AND FOES — CHROMATIN INTERACTORS AND TRANSCRIPTION REGULATION

Whether it is by changing large-scale chromatin conformation, nucleosome composition, and occupancy or histone post-translational modifications, chromatin regulation can impact plant

development in a variety of ways, as highlighted in the previous sessions. This complexity becomes more evident when, despite being highly conserved among the plant species, the function of chromatin regulators, as well as their target genes, also depends on the context in which they act (Hennig et al., 2005; Merini et al., 2017). The last session of the meeting focused on the interplay between different chromatin regulators and accessory factors as well as their role in transcription regulation and impact on plant development.

Chromatin-based regulation allows us to quickly and reversibly switch genes on and off through the concerted action of antagonistic regulators. One example was presented by Cristel Carles (Grenoble, France) with her latest work on ULTRAPETALA1 (ULT1). It was known that ULT1 antagonizes the activity of PRC2 and regulates levels of H3K27me3 at genes involved in flowering and meristem determination (Carles and Fletcher, 2009). The new work showed that ULT1 genome-wide targets strongly overlap with those of the H3K27me3 methyltransferase CLF but not with the genes targeted by the demethylase RELATIVE OF EARLY FLOWERING 6 (REF6). ULT1 interacts with RNA Pol II (RNAPII) and several chromatin remodelers, suggesting that it might be involved in their recruitment, preventing binding of PcG proteins at specific loci.

TFs have also been shown to play a role in recruiting chromatin-associated regulators to control different aspects of plant development (Vachon et al., 2018). Pawel Mikulski (Norwich, United Kingdom) presented his work on VP1/ABI3-LIKE 1 (VAL1), a transcriptional repressor that promotes histone deacetylation at the *FLC* locus and is required for PRC2 nucleation in cold-induced vernalization (Questa et al., 2016). VAL1 was found to interact with subunits of the PRC1 (Yang et al., 2013; Questa et al., 2016), PRC2 (Chen et al., 2018), and LHP1 (Yuan et al., 2016), but no differences were observed in H2Aub in the mutants. Interestingly, the authors found that VAL1 influences nucleosome mobility around the region of the PRC2 nucleation site, suggesting it may act through the recruitment of chromatin remodelers. Other ways to achieve specificity include the formation of alternative chromatin-associated complexes or the interaction of core components with specific accessory proteins (Förderer et al., 2016). One example of the former was presented by Hernan Lopez-Marin (Cologne, Germany) with the identification of SUPER DETERMINANT 1 (SDE1), a new regulator of axillary meristem initiation in tomato. The *sde1* mutation was mapped to a gene closely related to the PRC1 core components BMI1 and RING1 but which lacks the RING-finger domain required for depositing H2Aub (Buchwald et al., 2006). SDE1 interacts with LHP1, another component of the PRC1, suggesting it may be part of a new PcG complex involved in regulating axillary meristem initiation in tomato. Additionally, Sara Farrona (NUI, Galway) presented work from her laboratory on the identification of UBP5 as a new interactor of PWO1 and PRC2 subunits. As discussed in the first session of the meeting, PWO1 is itself an interactor of PRC2 methyltransferases and is involved in recruiting CLF to foci associated with the nuclear lamina (Hohenstatt et al., 2018; Mikulski et al., 2019). *ubp5* mutants show a pleiotropic phenotype and de-repression of several meristem identity genes, known targets of PRC2, suggesting that UBP5 acts together with PcG proteins to regulate plant development.

Chromatin environments are also crucial for correct gene expression since they can modulate RNA polymerase II (RNAPII) and TF accessibility to target DNA. An interesting example was presented by Sebastian Marquardt (Copenhagen, Denmark), who showed that the histone chaperone complex FACT is required for the repression of cryptic intragenic Transcriptional Start Sites (TSSs) during RNAPII-mediated transcription. In their repressed state, these TSSs are enriched in H3K4me1, a hallmark for RNAPII elongation, while, in the *fact* mutants, they show increased levels of H3K4me3, similar to promoter TSSs, indicating a role for FACT in the regulation of transcript isoform diversity (Nielsen et al., 2019). Moreover, a computational approach presented by Dmitry Lapin (Cologne, Germany) helped to define chromatin features predicting dependency of gene expression on the immunity regulator Enhanced Disease Susceptibility 1 (EDS1) in Arabidopsis. Machine-learning methods were used to test whether this dependency can be inferred from binding of TFs and occupancy of histone modifications from public ChIP-seq data. A neural network model provided the highest accuracy (up to 85%). Under non-stress conditions, EDS1-dependent loci have low H3K36me3 and RNAPII levels. Authors proposed that initial chromatin status contributes to the specificity of gene expression regulation in immunity. On the other hand, taking advantage of epigenetic hybrids (epiHybrids) from crosses with *decrease in dna methylation1* (*ddm1*)-derived epigenetic recombinant inbred lines (epiRILs), Ioanna Kakoulidou (Munich, Germany) showed that chromatin states can also impact subsequent generations. Previous work from the laboratory had shown that epiHybrids exhibit strong heterosis in several developmental traits, which correlates to DMRs in the parental lines (Lauss et al., 2018). Recently, the authors have used a high throughput phenotyping system to analyze 382 epiHybrids, and they were able to confirm that epigenetic divergence in the parents is sufficient to cause heterosis in the progeny. Future methylome, transcriptome, and small RNA-seq analyses of these epiHybrids are expected to contribute to a better understanding of how the parental epigenetic states affect the progeny.

CONCLUSIONS AND PERSPECTIVES

In summary, the EWPC2019 encouraged discussion about the most recent advances in epigenetics, chromatin-related mechanisms, and nuclear architecture in relation to the regulation of transcription and its impact on plants traits. Particularly, how the nuclear space is organized and how specific histones and structures within the nucleus, such as the nucleolus and the nuclear periphery, relate to specific chromatin domains was thoroughly discussed in various talks. However, we are still far from understanding the complexity that is shrouded

by the nuclear envelope. The extent of interplay between DNA methylation, various histone modifications, histone variants, and regulatory RNAs taking place during epigenetic inheritance processes remains to be elucidated. Likewise, much remains to be understood on the importance of core histone variants and their chaperones in chromatin structure through the control of nucleosome assembly and occupancy or the role of linker histones and other dynamic DNA-binding proteins. While histone modifications have so far rarely been considered in a variant-specific manner, combinations of histone variants with their particular marks constitute an additional layer of complexity to fine-tune chromatin regulation that is now just emerging and that will most certainly require further studies. While different presentations exposed the complexity of chromatin-based regulatory mechanisms in plants, it became clear that we need to investigate how chromatin-associated proteins are regulated in different tissues, developmental stages, and under specific environmental conditions, in order to fully understand their role in transcriptional regulation. Novel technical advances making use of CRISPR/Cas9 based strategies or new developments in 3C techniques together with a deeper characterization of multi-subunit complexes and their functions will help to better our understanding of the organization of plant genomes and nuclear protein networks in the near future. Simultaneously, studying the interplay between different regulators with the help of emerging technologies, such as the development of imaging and image-processing solutions that take into account the challenges of plant systems (Dumur et al., 2019) and other cell-specific techniques, will certainly yield important new findings. Finally, while most work presented at the meeting used Arabidopsis as a model system, the fundamental mechanisms identified might in the future be applied to crop species by, for example, exploiting natural epigenetic diversity in plant breeding or induced epigenetic variation involved in stress priming and memory (Springer and Schmitz, 2017; Mozgová et al, 2019; Forestan et al., 2019). We expect to see some of these questions addressed in the future and exciting new data on chromatin regulation in model and crop plants to be presented in forthcoming EWPCs.

The memory of Lars Hennig imbued specifically one of the meeting sessions but was also present in many other talks, demonstrating that the contributions of this excellent scientist and mentor will last over time. His work had a tremendous impact on the understanding of chromatin regulation and plant development, particularly concerning our knowledge of the PcG pathway, and will perpetuate through the ongoing contributions of many of his alumni who are still actively investigating these questions.

AUTHOR CONTRIBUTIONS

SF and AP created **Figure 1**. JM-R edited **Figure 2**. Each author (JM-R, K, JE, IT, AP, and SF) wrote one session. JM-R, AP, and SF wrote introduction and conclusions. All authors contributed to edit text and figures. IT edited references. SF coordinated the manuscript.

FUNDING

JM-R is supported by funding from the European Union's Horizon 2020 research and innovation program under the Marie Skłodowska-Curie grant agreement No 797473, financial support from the Spanish Ministry of Economy and Competitiveness through the "Severo Ochoa Program for Centres of Excellence in R&D" 2016-2019 (SEV-2015-0533), and by the CERCA Programme/Generalitat de Catalunya. AP, K, and SF acknowledge networking support from the COST Action CA16212 "Impact of nuclear domains on gene expression and plant traits (INDEPTH)." The EWPC was supported by grants from The German Research Foundation (TU126/14-1) and The Company of Biologists (EA1772). The organizers also acknowledge the generous contributions from industrial sponsors Zeiss Microscopy GmbH (Germany), Diagenode SA (Belgium), and Dispendix GmbH (Germany).

ACKNOWLEDGMENTS

We would like to thank all the authors that share with us their contribution. Finally, special thanks to Franziska Turck who organized the EWPC2019 and also contributed to this report.

REFERENCES

Adamusová, K., Khosravi, S., Fujimoto, S., Houben, A., Matsunaga, S., Fajkus, J., et al. (2019). Two combinatorial patterns of telomere histone marks in plants with canonical and non-canonical telomere repeats. *Plant J.* doi: 10.1111/tpj.14653

Baev, V., Milev, I., Naydenov, M., Vachev, T., Apostolova, E., Mehterov, N., et al. (2014). Insight into small RNA abundance and expression in high- and low-temperature stress response using deep sequencing in Arabidopsis. *Plant Physiol. Bioch.* 84, 105–114. doi: 10.1016/j.plaphy.2014.09.007

Baumbusch, L. O., Thorstensen, T., Krauss, V., Fischer, A., Naumann, K., Assalkhou, R., et al. (2001). The Arabidopsis thaliana genome contains at least 29 active genes encoding SET domain proteins that can be assigned to four evolutionarily conserved classes. *Nucleic Acids Res.* 29 (21), 4319–4333. doi: 10.1093/nar/29.21.4319

Berr, A., McCallum, E. J., Ménard, R., Meyer, D., Fuchs, J., Dong, A., et al. (2010). *Arabidopsis SET DOMAIN GROUP2* is required for H3K4 trimethylation and is crucial for both sporophyte and gametophyte development. *Plant Cell* 22 (10), 3232–3248. doi: 10.1105/tpc.110.079962

Boisvert, F.-M., van Koningsbruggen, S., Navascués, J., and Lamond, A. I. (2007). The multifunctional nucleolus. *Nat. Rev. Mol. Cell Bio.* 8 (7), 574–585. doi: 10.1038/nrm2184

Buchwald, G., van der Stoop, P., Weichenrieder, O., Perrakis, A., van Lohuizen, M., and Sixma, T. K. (2006). Structure and E3-ligase activity of the Ring-Ring complex of Polycomb proteins Bmi1 and Ring1b. *EMBO J.* 25 (11), 2465–2474. doi: 10.1038/sj.emboj.7601144

Buschbeck, M., and Hake, S. B. (2017). Variants of core histones and their roles in cell fate decisions, development and cancer. *Nat. Rev. Mol. Cell Biol.* 18 (5), 299–314. doi: 10.1038/nrm.2016.166

Carles, C. C., and Fletcher, J. C. (2009). The SAND domain protein ULTRAPETALA1 acts as a trithorax group factor to regulate cell fate in plants. *Gene Dev.* 23, 2723–2728. doi: 10.1101/gad.1812609

Casal, J. J. (2013). Photoreceptor signaling networks in plant responses to shade. *Annu. Rev. Plant Biol.* 64 (1), 403–427. doi: 10.1146/annurev-arplant-050312-120221

Catez, F., and Hock, R. (2010). Binding and interplay of HMG proteins on chromatin: lessons from live cell imaging. *Biochim. Biophys. Acta* 1799 (1–2), 15–27. doi: 10.1016/j.bbagrm.2009.11.001

Chanvivattana, Y., Bishopp, A., Schubert, D., Stock, C., Moon, Y. H., Sung, Z. R., et al. (2004). Interaction of Polycomb-group proteins controlling flowering in Arabidopsis. *Development* 131 (21), 5263–5276. doi: 10.1242/dev.01400

Charbonnel, C., Rymarenko, O., Da Ines, O., Benyahya, F., White, C. I., Butter, F., et al. (2018). The linker histone GH1-HMGA1 is involved in telomere stability and DNA damage repair. *Plant Physiol.* 177 (1), 311–327. doi: 10.1104/pp.17.01789

Chaudhury, A. M., Ming, L., Miller, C., Craig, S., Dennis, E. S., and Peacock, W. J. (1997). Fertilization-independent seed development in Arabidopsis thaliana. *Proc. Natl. Acad. Sci. U. S. A.* 94 (8), 4223–4228. doi: 10.1073/pnas.94.8.4223

Chen, N., Veerappan, V., Abdelmageed, H., Kang, M., and Allen, R. D. (2018). HSI2/VAL1 Silences AGL15 to regulate the developmental transition from seed maturation to vegetative growth in arabidopsis. *Plant Cell* 30, 600–619. doi: 10.1105/tpc.17.00655

Chory, J., Peto, C., Feinbaum, R., Pratt, L., and Ausubel, F. (1989). Arabidopsis thaliana mutant that develops as a light-grown plant in the absence of light. *Cell* 58 (5), 991–999. doi: 10.1016/0092-8674(89)90950-1000

Coleman-Derr, D., and Zilberman, D. (2012). Deposition of histone variant H2A.Z within gene bodies regulates responsive genes. *PloS Genet.* 8 (10), e1002988. doi: 10.1371/journal.pgen.1002988

Crevillén, P., Gómez-Zambrano, A., López, J. A., Vázquez, J., Piñeiro, M., and Jarillo, J. A. (2019). Arabidopsis YAF9 histone readers modulate flowering time through NuA4-complex-dependent H4 and H2A.Z histone acetylation at FLC chromatin. *New Phytol.* 222 (4), 1893–1908. doi: 10.1111/nph.15737

Dabin, J., and Polo, S. E. (2017). Choreography of parental histones in damaged chromatin. *Nucleus* 8 (3), 255–260. doi: 10.1080/19491034.2017.1292192

Derkacheva, M., Steinbach, Y., Wildhaber, T., Mozgová, I., Mahrez, W., Nanni, P., et al. (2013). Arabidopsis MSI1 connects LHP1 to PRC2 complexes. *EMBO J.* 32 (14), 2073–2085. doi: 10.1038/emboj.2013.145

Derkacheva, M., Liu, S., Figueiredo, D. D., Gentry, M., Mozgova, I., Nanni, P., et al. (2016). H2A deubiquitinases UBP12/13 are part of the Arabidopsis polycomb group protein system. *Nat. Plants* 2, 16126. doi: 10.1038/nplants.2016.126

Duc, C., Benoit, M., Le Goff, S., Simon, L., Poulet, A., Cotterell, S., et al. (2015). The histone chaperone complex HIR maintains nucleosome occupancy and counterbalances impaired histone deposition in CAF-1 complex mutants. *Plant J.* 81 (5), 707–722. doi: 10.1111/tpj.12758

Duc, C., Benoit, M., Détourné, G., Simon, L., Poulet, A., Jung, M., et al. (2017). Arabidopsis ATRX modulates H3.3 occupancy and fine-tunes gene expression. *Plant Cell* 29, 1773–1793. doi: 10.1105/tpc.16.00877

Dumur, T., Duncan, S., Graumann, K., Desset, S., Randall, R. S., Scheid, O. M., et al. (2019). Probing the 3D architecture of the plant nucleus with microscopy approaches: challenges and solutions. *Nucleus* 10 (1), 181–212. doi: 10.1080/19491034.2019.1644592

Förderer, A., Zhou, Y., and Turck, F. (2016). The age of multiplexity: recruitment and interactions of Polycomb complexes in plants. *Curr. Opin. Plant Biol.* 29, 169–178. doi: 10.1016/j.pbi.2015.11.010

Fiorucci, A.-S., Bourbousse, C., Concia, L., Rougée, M., Deton-Cabanillas, A.-F., Zabulon, G., et al. (2019). Arabidopsis S2Lb links AtCOMPASS-like and SDG2 activity in H3K4me3 independently from histone H2B monoubiquitination. *Genome Biol.* 20 (1), 100. doi: 10.1186/s13059-019-1705-4

Forestan, C., Farinati, S., Zambelli, F., Pavesi, G., Rossi, V., and Varotto, S. (2019). Epigenetic signatures of stress adaptation and flowering regulation in response to extended drought and recovery in Zea mays. *Plant Cell Environ.* 43 (1), 55–75. doi: 10.1111/pce.13660

Frerichs, A., Thoma, R., Abdallah, A. T., Frommolt, P., Werr, W., and Chandler, J. W. (2016). The founder-cell transcriptome in the Arabidopsis apetala1 cauliflower inflorescence meristem. *BMC Genomics* 17 (1), 855. doi: 10.1186/s12864-016-3189-x

Frerichs, A., Engelhorn, J., Altmüller, J., Gutierrez-Marcos, J., and Werr, W. (2019). Specific chromatin changes mark lateral organ founder cells in the Arabidopsis inflorescence meristem. *J. Exp. Bot.* 70 (15), 3867–3879. doi: 10.1093/jxb/erz181

Fromm, M., and Avramova, Z. (2014). ATX1/AtCOMPASS and the H3K4me3 marks: how do they activate Arabidopsis genes? *Curr. Opin. Plant Biol.* 21, 75–82. doi: 10.1016/j.pbi.2014.07.004

Gómez-Zambrano, Á., Merini, W., and Calonje, M. (2019). The repressive role of Arabidopsis H2A.Z in transcriptional regulation depends on AtBMI1 activity. *Nat. Commun.* 10 (1), 2828. doi: 10.1038/s41467-019-10773-1

Grossniklaus, U., Vielle-Calzada, J.-P., Hoeppner, M. A., and Gagliano, W. B. (1998). Maternal Control of Embryogenesis by MEDEA, a Polycomb Group Gene in Arabidopsis. *Science* 280 (5362), 446–450. doi: 10.1126/science.280.5362.446

Guo, L., Yu, Y., Law, J. A., and Zhang, X. (2010). SET DOMAIN GROUP2 is the major histone H3 lysine 4 trimethyltransferase in Arabidopsis. *Proc. Natl. Acad. Sci. U. S. A.* 107 (43), 18557–18562. doi: 10.1073/pnas.1010478107

Hennig, L., Taranto, P., Walser, M., Schönrock, N., and Gruissem, W. (2003). Arabidopsis MSI1 is required for epigenetic maintenance of reproductive development. *Development* 130 (12), 2555–2565. doi: 10.1242/dev.00470

Hennig, L., Bouveret, R., and Gruissem, W. (2005). MSI1-like proteins: An escort service for chromatin assembly and remodeling complexes. *Trends Cell Biol.* 15 (6), 295–302. doi: 10.1016/j.tcb.2005.04.004

Hohenstatt, M. L., Mikulski, P., Komarynets, O., Klose, C., Kycia, I., Jeltsch, A., et al. (2018). PWWP-DOMAIN INTERACTOR OF POLYCOMBS1 interacts with polycomb-group proteins and histones and regulates arabidopsis flowering and development. *Plant Cell* 30 (1), 117–133. doi: 10.1105/tpc.17.00117

Jiang, D., and Berger, F. (2016). Histone variants in plant transcriptional regulation. *BBA-Gene. Regul. Mech.* 1860 (1), 123–130. doi: 10.1016/j.bbagrm.2016.07.002

Jiang, H., Moreno-Romero, J., Santos-González, J., De Jaeger, G., Gevaert., K., Van De Slijke, E., et al. (2017). Ectopic application of the repressive histone modification H3K9me2 establishes post-zygotic reproductive isolation in Arabidopsis thaliana. *Gene Dev.* 31 (12), 1272–1287. doi: 10.1101/gad.299347.117

Köhler, C., and Springer, N. (2017). Plant epigenomics-deciphering the mechanisms of epigenetic inheritance and plasticity in plants. *Genome Biol.* 18, 132. doi: 10.1186/s13059-017-1260-9

Köhler, C., Hennig, L., Spillane, C., Pien, S., Gruissem, W., and Grossniklaus, U. (2003a). The Polycomb-group protein MEDEA regulates seed development by controlling expression of the MADS-box gene PHERES1. *Gene Dev.* 17, 1540–1553. doi: 10.1101/gad.257403

Köhler, C., Hennig, L., Bouveret, R., Gheyselinck, J., Grossniklaus, U., and Gruissem, W. (2003b). Arabidopsis MSI1 is a component of the MEA/FIE Polycomb group complex and required for seed development. *EMBO J.* 22 (18), 4804–4814. doi: 10.1093/emboj/cdg444

Kapitonov, V. V., and Jurka, J. (2004). Harbinger transposons and ancient HARBI1 Gene Derived from a Transposase. *DNA Cell Biol.* 23 (5), 311–324. doi: 10.1089/104454904323090949

Kim, J., Guermah, M., McGinty, R. K., Lee, J. S., Tang, Z., Milne, T. A., et al. (2009). RAD6-mediated transcription-coupled H2B ubiquitylation directly stimulates H3K4 methylation in human cells. *Cell* 137 (3), 459–471. doi: 10.1016/j.cell.2009.02.027

Kotliński, M., Knizewski, L., Muszewska, A., Rutowicz, K., Lirski, M., Schmidt, A., et al. (2017). Phylogeny-based systematization of arabidopsis proteins with histone H1 globular domain. *Plant Physiol.* 174 (1), 27–34. doi: 10.1104/pp.16.00214

Lauss, K., Wardenaar, R., Oka, R., van Hulten, M. H. A., Guryev, V., Keurentjes, K. J. B., et al. (2018). Parental DNA methylation states are associated with heterosis in epigenetic hybrids. *Plant Physiol.* 176, 1627–1645. doi: 10.1104/pp.17.01054

Law, J. A., and Jacobsen, S. E. (2010). Establishing, maintaining and modifying DNA methylation patterns in plants and animals. *Nat. Rev. Genet.* 11, 204–220. doi: 10.1038/nrg2719

Law, J. A., Vashisht, A. A., Wohlschlegel, J. A., and Jacobsen, S. E. (2011). SHH1, a homeodomain protein required for DNA methylation, as well as RDR2, RDM4, and chromatin remodeling factors, associate with RNA polymerase IV. *PloS Genet.* 7 (7), e1002195. doi: 10.1371/journal.pgen.1002195

Le Goff, S., Keçeli, B. N., Jeřábková, H., Heckmann, S., Rutten, T., Cotterell, S., et al. (2019). The H3 histone chaperone NASP^{SIM3} escorts CenH3 in *Arabidopsis*. *Plant J.* tpj, 14518. doi: 10.1111/tpj.14518

Liang, S. C., Hartwig, B., Perera, P., Mora-García, S., de Leau, E., Thornton, H., et al. (2015). Kicking against the PRCs – a domesticated transposase antagonises silencing mediated by polycomb group proteins and is an accessory component of polycomb repressive complex 2. *PloS Genet-* 11 (12), 1–26. doi: 10.1371/journal.pgen.1005660

Liu, X., Gao, L., Dinh, T. T., Shi, T., Li, D., Wang, R., et al. (2014). DNA topoisomerase I affects polycomb group protein-mediated epigenetic regulation and plant development by altering nucleosome distribution in Arabidopsis. *Plant Cell* 26 (7), 2803–2817. doi: 10.1105/tpc.114.124941

Lorković, Z. J., Park, C., Goiser, M., Jiang, D., Kurzbauer, M. T., Schlögelhofer, P., et al. (2017). Compartmentalization of DNA damage response between heterochromatin and euchromatin is mediated by distinct H2A histone variants. *Curr. Biol.* 27 (8), 1192–1199. doi: 10.1016/j.cub.2017.03.002

Lu, P. Y. T., Lévesque, N., and Kobor, M. S. (2009). NuA4 and SWR1-C: two chromatin-modifying complexes with overlapping functions and components. *Biochem. Cell Biol.* 87 (5), 799–815. doi: 10.1139/O09-062

Müller, S., and Almouzni, G. (2014). A network of players in H3 histone variant deposition and maintenance at centromeres. *BBA - Gene Regul. Mech.* 1839 (3), 241–250. doi: 10.1016/j.bbagrm.2013.11.008

Ma, L., Zhao, H., and Deng, X. W. (2003). Analysis of the mutational effects of the COP/DET/FUS loci on genome expression profiles reveals their overlapping yet not identical roles in regulating Arabidopsis seedling development. *Development* 130 (5), 969–981. doi: 10.1242/dev.00281

Maksimov, V., Nakamura, M., Wildhaber, T., Nanni, P., Ramström, M., Bergquist, J., et al. (2016). The H3 chaperone function of NASP is conserved in Arabidopsis. *Plant J.* 88 (3), 425–436. doi: 10.1111/tpj.13263

Merini, W., Romero-Campero, F. J., Gomez-Zambrano, A., Zhou, Y., Turck, F., and Calonje, M. (2017). The arabidopsis polycomb repressive complex 1 (PRC1) components AtBMI1A, B, and C impact gene networks throughout all stages of plant development. *Plant Physiol.* 173 (1), 627–641. doi: 10.1104/pp.16.01259

Mikulski, P., Hohenstatt, M. L., Farrona, S., Smaczniak, C., Stahl, Y., Kalyanikrishna,, et al. (2019). The chromatin-associated protein PWO1 interacts with plant nuclear lamin-like components to regulate nuclear size. *Plant Cell* 31 (5), 1141–1154. doi: 10.1105/tpc.18.00663

Miryeganeh, M., and Saze, H. (2019). Epigenetic inheritance and plant evolution. *Popul. Ecol.* 62 (1), 17–27. doi: 10.1002/1438-390X.12018

Moreno-Romero, J., Santos-González, J., Hennig, L., and Köhler, C. (2017). Applying the INTACT method to purify endosperm nuclei and to generate parental-specific epigenome profiles. *Nat. Protoc.* 12 (2), 238–254. doi: 10.1038/nprot.2016.167

Mozgová, I., Muñoz-Viana, R., and Hennig, L. (2017). PRC2 represses hormone-induced somatic embryogenesis in vegetative tissue of Arabidopsis thaliana. *PloS Genet.* 13 (1), e1006562. doi: 10.1371/journal.pgen.1006562

Mozgová, I., Alexandre, C., Steinbach, Y., Derkacheva, M., Schäfer, E., and Gruissem, W. (2018a). A tribute to lars hennig (1970–2018). *J. Exp. Bot.* 69 (21), 4989–4990. doi: 10.1093/jxb/ery337

Mozgová, I., Wildhaber, T., Trejo-Arellano, M. S., Fajkus, J., Roszak, P., Köhler, C., et al. (2018b). Transgenerational phenotype aggravation in CAF-1 mutants reveals parent-of-origin specific epigenetic inheritance. *New Phytol.* 220 (3), 908–921. doi: 10.1111/nph.15082

Mozgová, I., Mikulski, P., Pecinka, A., and Farrona, S. (2019). "Epigenetic mechanisms of abiotic stress response and memory in plants," in *Epigenetics in plants of agronomic importance: fundamentals and applications*. Eds. Alvarez-Venegas,, De-la-Peña, and Casas-Mollano, (Cham: Springer). doi: 10.1007/978-3-030-14760-0_1

Nassrallah, A., Rougée, M., Bourbousse, C., Drevensek, S., Fonseca, S., Iniesto, E., et al. (2018). DET1-mediated degradation of a SAGA-like deubiquitination module controls H2Bub homeostasis. *eLife* 7, e37892. doi: 10.7554/eLife.37892

Nie, X., Wang, H., Li, J., Holec, S., and Berger, F. (2014). The HIRA complex that deposits the histone H3.3 is conserved in Arabidopsis and facilitates transcriptional dynamics. *Biol. Open* 3 (9), 794–802. doi: 10.1242/bio.20148680

Nielsen, M., Ard, R., Leng, X., Ivanov, M., Kindgren, P., Pelechano, V., et al. (2019). Transcription-driven chromatin repression of Intragenic transcription start sites. *PloS Genet.* 15 (2), 1–33. doi: 10.1371/journal.pgen.1007969

Ozturk, N., Singh, I., Mehta, A., Braun, T., and Barreto, G. (2014). HMGA proteins as modulators of chromatin structure during transcriptional activation. *Front. Cell Dev.l Biol.* 2, 5. doi: 10.3389/fcell.2014.00005

Pepper, A., Delaney, T., Washburn, T., Poole, D., and Chory, J. (1994). DET1, a negative regulator of light-mediated development and gene expression in arabidopsis, encodes a novel nuclear-localized protein. *Cell* 78 (1), 109–116. doi: 10.1016/0092-8674(94)90577-0

Picart-Picolo, A., Picault, N., and Pontvianne, F. (2019). Ribosomal RNA genes shape chromatin domains associating with the nucleolus. *Nucleus* 10 (1), 67–72. doi: 10.1080/19491034.2019.1591106

Pontvianne, F., Carpentier, M. C., Durut, N., Pavlištová, V., Jaške, K., Schořová, Š., et al. (2016). Identification of nucleolus-associated chromatin domains reveals a role for the nucleolus in 3D organization of the A. thaliana Genome. *Cell Rep.* 16 (6), 1574–1587. doi: 10.1016/J.CELREP.2016.07.016

Questa, J. I., Song, J., Geraldo, N., An, H., and Dean, C. (2016). Transcriptional repressor VAL1 triggers silencing of FLC during vernalization. *Science* 1 (6298), 1–5. doi: 10.1126/science.aaf7354

Ream, T. S., Haag, J. R., Wierzbicki, A. T., Nicora, C. D., Norbeck, A. D., Zhu, J. K., et al. (2009). Subunit compositions of the RNA-silencing enzymes Pol IV and Pol V reveal their origins as specialized forms of RNA Polymerase II. *Mol. Cell* 33 (2), 192–203. doi: 10.1016/j.molcel.2008.12.015

Rosa, S., and Shaw, P. (2013). Insights into chromatin structure and dynamics in plants. *Biology* 2 (4), 1378–1410. doi: 10.3390/biology2041378

Rutowicz, K., Puzio, M., Halibart-Puzio, J., Lirski, M., Kotliński, M., Kroteń, M. A., et al. (2015). A specialized histone H1 variant is required for adaptive responses to complex abiotic stress and related DNA methylation in Arabidopsis. *Plant Physiol.* 169, 2080–2101. doi: 10.1104/pp.15.00493

Rutowicz, K., Lirski, M., Mermaz, B., Teano, G., Schubert, J., Mestiri, I., et al. (2019). Linker histones are fine-scale chromatin architects modulating developmental decisions in Arabidopsis. *Genome Biol.* 20 (1), 157. doi: 10.1186/s13059-019-1767-3

Schroeder, D. F., Gahrtz, M., Maxwell, B. B., Cook, R. K., Kan, J. M., Alonso, J. M., et al. (2002). De-Etiolated 1 and damaged DNA binding protein 1 interact to regulate arabidopsis photomorphogenesis. *Curr. Biol.* 12 (17), 1462–1472. doi: 10.1016/S0960-9822(02)01106-5

Seluzicki, A., Burko, Y., and Chory, J. (2017). Dancing in the dark: darkness as a signal in plants. *Plant Cell Environ.* 40 (11), 2487–2501. doi: 10.1111/pce.12900

Sexton, T., and Cavalli, G. (2015). The Role of Chromosome Domains in Shaping the Functional Genome. *Cell* 160 (6), 1049–1059. doi: 10.1016/j.cell.2015.02.040

Springer, N. M., and Schmitz, R. J. (2017). Exploiting induced and natural epigenetic variation for crop improvement. *Nat. Rev. Genet.* 18, 563–575. doi: 10.1038/nrg.2017.45

Sun, Z.-W., and Allis, C. D. (2002). Ubiquitination of histone H2B regulates H3 methylation and gene silencing in yeast. *Nature* 418 (6893), 104–108. doi: 10.1038/nature00883

Sura, W., Kabza, M., Karlowski, W. M., Bieluszewski, T., Kus-Slowinska, M., Pawełoszek, L., et al. (2017). Dual role of the histone variant H2A.Z in transcriptional regulation of stress-response genes. *Plant Cell* 29 (4), 791–807. doi: 10.1105/tpc.16.00573

Thorstensen, T., Grini, P. E., and Aalen, R. B. (2011). SET domain proteins in plant development. *BBA- Gene Regu. Mech. Elsevier* 1809 (8), 407–420. doi: 10.1016/J.BBAGRM.2011.05.008

Trejo-Arellano, M. S., Mehdi, S., de Jonge, J., Tomastíková, E. D., Köhler, C., and Hennig, L. (2019). Dark-induced senescence causes localized changes in DNA methylation. *Plant Physiol.* doi: 10.1104/pp.19.01154

Vachon, G., Engelhorn, J., and Carles, C. C. (2018). Interactions between transcription factors and chromatin regulators in the control of flower development. *J. Exp. Bot.* 69 (10), 2461–2471. doi: 10.1093/jxb/ery079

Waidmann, S., Kusenda, B., Mayerhofer, J., Mechtler, K., and Jonak, C. (2014). A DEK domain-containing protein modulates chromatin structure and function in Arabidopsis. *Plant Cell* 26 (11), 4328–4344. doi: 10.1105/tpc.114.129254

Wang, H., Dittmer, T. A., and Richards, E. J. (2013). Arabidopsis CROWDED NUCLEI (CRWN) proteins are required for nuclear size control and

heterochromatin organization. *BMC Plant Biol.* 13, 200. doi: 10.1186/1471-2229-13-200

Wellmer, F., Alves-Ferreira, M., Dubois, A., Riechmann, J. L., and Meyerowitz, E. M. (2006). Genome-wide analysis of gene expression during early arabidopsis flower development. *PloS Genet.* 2 (7), e117. doi: 10.1371/journal.pgen.0020117

Wu, S.-H. (2014). Gene expression regulation in photomorphogenesis from the perspective of the central dogma. *Annu. Rev. Plant Biol.* 65 (1), 311–333. doi: 10.1146/annurev-arplant-050213-040337

Xiao, J., Lee, U.-S., and Wagner, D. (2016). Tug of war: adding and removing histone lysine methylation in Arabidopsis. *Curre. Opin. Plant Biol.* 34, 41–53. doi: 10.1016/J.PBI.2016.08.002

Yang, C., Bratzel, F., Hohmann, N., Koch, M., Turck, F., and Calonje, M. (2013). VAL- and AtBMI1-Mediated H2Aub initiate the switch from embryonic to postgerminative growth in Arabidopsis. *Curr. Biol.* 23 (24), 1324–1329. doi: 10.1016/j.cub.2013.05.050

Yelagandula, R., Stroud, H., Holec, S., Zhou, K., Feng, S., Zhong, X., et al. (2014). The histone variant H2A.W defines heterochromatin and promotes chromatin condensation in Arabidopsis. *Cell* 158 (1), 98–109. doi: 10.1016/j.cell.2014.06.006

Yuan, W., Luo, X., Li, Z., Yang, W., Wang, Y., Liu, R., et al. (2016). A cis cold memory element and a trans epigenome reader mediate Polycomb silencing of FLC by vernalization in Arabidopsis. *Nat. Genet.* 48, 1527–1534. doi: 10.1038/ng.3712

Zhang, L., and Ma, H. (2012). Complex evolutionary history and diverse domain organization of SET proteins suggest divergent regulatory interactions. *New Phytol.* 195 (1), 248–263. doi: 10.1111/j.1469-8137.2012.04143.x

Zhou, Y., Romero-Campero, F. J., Gómez-Zambrano, A., Turck, F., and Calonje, M. (2017). H2A monoubiquitination in Arabidopsis thaliana is generally independent of LHP1 and PRC2 activity. *Genome Biol.* 18 (1), 69. doi: 10.1186/s13059-017-1197-z

Zhou, M., Palanca, A. M. S., and Law, J. A. (2018). Locus-specific control of the *de novo* DNA methylation pathway in Arabidopsis by the CLASSY family. *Nat. Genet.* 50 (6), 865–873. doi: 10.1038/s41588-018-0115-y

Conflict of Interest: The authors declare that the research was conducted in the absence of any commercial or financial relationships that could be construed as a potential conflict of interest.

frontiers in Plant Science

ORIGINAL RESEARCH
published: 13 February 2020
doi: 10.3389/fpls.2020.00052

Chromatin Remodeling Protein ZmCHB101 Regulates Nitrate-Responsive Gene Expression in Maize

Xinchao Meng[1†], Xiaoming Yu[1,2†], Yifan Wu[1], Dae Heon Kim[3], Nan Nan[1], Weixuan Cong[1], Shucai Wang[1,4], Bao Liu[1] and Zheng-Yi Xu[1*]*

[1] Key Laboratory of Molecular Epigenetics of the Ministry of Education (MOE), Northeast Normal University, Changchun, China, [2] School of Agronomy, Jilin Agricultural Science and Technology University, Jilin, China, [3] Department of Biology, Sunchon National University, Sunchon, South Korea, [4] College of Life Sciences, Linyi University, Linyi, China

OPEN ACCESS

Edited by:
Rafal Archacki, University of Warsaw, Poland

Reviewed by:
Marco Betti, University of Seville, Spain
Serena Varotto, University of Padova, Italy

***Correspondence:**
Bao Liu
baoliu@nenu.edu.cn
Zheng-Yi Xu
xuzy100@nenu.edu.cn

[†]*These authors have contributed equally to this work*

Specialty section:
This article was submitted to Plant Cell Biology, a section of the journal Frontiers in Plant Science

Received: *08 August 2019*
Accepted: *15 January 2020*
Published: *13 February 2020*

Citation:
Meng X, Yu X, Wu Y, Kim DH, Nan N, Cong W, Wang S, Liu B and Xu Z-Y (2020) Chromatin Remodeling Protein ZmCHB101 Regulates Nitrate-Responsive Gene Expression in Maize. Front. Plant Sci. 11:52. doi: 10.3389/fpls.2020.00052

Nitrate is the main source of nitrogen for plants and an essential component of fertilizers. Rapid transcriptional activation of genes encoding the high-affinity nitrate transport system (HATS) is an important strategy that plants use to cope with nitrogen deficiency. However, the specific transcriptional machineries involved in this process and the detailed transcriptional regulatory mechanism of the core HATS remain poorly understood. ZmCHB101 is the core subunit of the SWI/SNF-type ATP-dependent chromatin remodeling complex in maize. RNA-interference transgenic plants (*ZmCHB101-RNAi*) display abaxially curling leaves and impaired tassel and cob development. Here, we demonstrate that ZmCHB101 plays a pivotal regulatory role in nitrate-responsive gene expression. *ZmCHB101-RNAi* lines showed accelerated root growth and increased biomass under low nitrate conditions. An RNA sequencing analysis revealed that ZmCHB101 regulates the expression of genes involved in nitrate transport, including *ZmNRT2.1* and *ZmNRT2.2*. The NIN-like protein (NLP) of maize, ZmNLP3.1, recognized the consensus nitrate-responsive *cis*-elements (NREs) in the promoter regions of *ZmNRT2.1* and *ZmNRT2.2*, and activated the transcription of these genes in response to nitrate. Intriguingly, well-positioned nucleosomes were detected at NREs in the *ZmNRT2.1* and *ZmNRT2.2* gene promoters, and nucleosome densities were lower in *ZmCHB101-RNAi* lines than in wild-type plants, both in the absence and presence of nitrate. The ZmCHB101 protein bound to NREs and was involved in the maintenance of nucleosome occupancies at these sites, which may impact the binding of ZmNLP3.1 to NREs in the absence of nitrate. However, in the presence of nitrate, the binding affinity of ZmCHB101 for NREs decreased dramatically, leading to reduced nucleosome density at NREs and consequently increased ZmNLP3.1 binding. Our results provide novel insights into the role of chromatin remodeling proteins in the regulation of nitrate-responsive gene expression in plants.

Keywords: chromatin remodeler, nitrate response, transcriptional regulation, nitrate transporter, maize

INTRODUCTION

Maize (*Zea mays*) is one of the most important crops in the world. Approximately 70% of the kernel weight in maize is composed of starch, which is the main source of energy in the human and animal diet. To maximize the yield of maize crop in the field, large quantities of nitrogenous fertilizers are added to the soil during cultivation. Over the past several decades, application of nitrogen (N) fertilizer has significantly increased maize production (Zhang et al., 2011; Sun and Zheng, 2015; Alvarez et al., 2019). As one of the most important macronutrients for plants, N is required for the biosynthesis of proteins, nucleic acids, chlorophyll, ATP, alkaloids, and hormones (Tills and Alloway, 1981; Shadchina and Dmitrieva, 1995; Lam et al., 1996). Therefore, N deficiency limits plant growth and development, thereby reducing crop yield (Chen et al., 2016). However, crops utilize only approximately 30% of the applied N fertilizer (Raun and Johnson, 1999; Sultan, 2003), while the remaining N causes environmental pollution *via* gaseous emission, fertilizer leaching, surface runoff, and denitrification (Good et al., 2004).

In the soil, N is present in two main forms, nitrate and ammonia, both of which are crucial for plant growth and root development (Stitt and Feil, 1999; Zhang et al., 1999). The local stimulatory effect of nitrate on lateral root elongation results from its function as a signal rather than a nutrient (Zhang et al., 1999). Plant nitrate uptake is mediated by low- and high-affinity transport systems that function at high and low external nitrate concentrations, respectively (Huang et al., 1999). In the model plant *Arabidopsis thaliana*, AtNPF6.3 acts as a unique nitrate transporter that mediates both low- and high-affinity nitrate uptake (Ho et al., 2009; Parker and Newstead, 2014). The AtNRT2.1 protein plays a major role in high-affinity nitrate uptake, whereas AtNRT2.2 makes a relatively small contribution (Li et al., 2007). In addition, the nitrate transporter, AtNRT2.5, facilitates nitrate uptake and remobilization in N-starved *A. thaliana* (Lezhneva et al., 2014). Under nitrate-deficient conditions, the activities of high-affinity nitrate transporters and the transcript levels of *AtNRT2.1* and *AtNRT2.2* increase rapidly with nitrate supply (Zhuo et al., 1999; Okamoto et al., 2003); however, both of these genes are subsequently repressed upon prolonged exposure to sufficient nitrate. Restoring nitrate supply stimulates the nitrate uptake capacity of plants; however, accumulation of nitrate and its assimilatory products, including amino acids, in plant cells reduces the expression of *NRT2* genes, and consequently the nitrate uptake capacity of plants (Zhuo et al., 1999; Vidmar et al., 2000). These data suggest the existence of an underlying mechanism that regulates nitrate uptake in accordance with the N demand (Forde, 2002). In maize, an increase in *ZmNRT2.1* and *ZmNRT2.2* transcript levels activates the nitrate uptake capacity (Sabermanesh et al., 2017); however, the mechanism of *ZmNRT* gene transcription regulation remains unclear.

Chromatin remodeling complexes (CRCs) play pivotal roles in nucleosome sliding and occupancy by controlling ATP-dependent alterations in histone-DNA contacts (Peterson and Workman, 2000; Gangaraju and Bartholomew, 2007; Clapier and Cairns, 2009; Narlikar, 2010). The SWITCH (SWI)/SUCROSE NONFERMENTING (SNF) complexes are multi-subunit complexes that contain more than eight proteins (Sarnowska et al., 2016). Based on the type of SNF2 family ATPase subunits, the ATP-dependent CRCs are divided into four subfamilies: SWI2/SNF2, IMITATION SWITCH (ISWI), Mi-2/Chromodomain-Helicase-DNA (CHD)-binding protein (Mi-2/CHD), and INO80 (Sarnowska et al., 2016). Previous studies revealed that SWI3 proteins, the core components of the SWI/SNF CRCs, play essential roles in plant growth and development (Sarnowski et al., 2005; Yu et al., 2016). The *AtSWI3* genes regulate root elongation and leaf and reproductive organ development (Sarnowski et al., 2005). Mutations in either *AtSWI3A* or *AtSWI3B* cause developmental arrest of the embryo at the globular stage, and mutation of *AtSWI3B* leads to the death of macrospores and microspores (Sarnowski et al., 2005; Hurtado et al., 2006). Furthermore, mutations in *AtSWI3D* lead to severe dwarfism and alterations in the number and development of flower organs (Zhou et al., 2003; Sarnowski et al., 2005). The maize SWI3 protein, ZmCHB101, plays an essential role in leaf development and dehydration and abscisic acid responses (Yu et al., 2016; Yu et al., 2018; Yu et al., 2019); however, it is unknown whether SWI/SNF complexes participate in nitrate responses.

In this study, we found that knockdown of *ZmCHB101* expression in maize accelerated root growth and increased biomass under low nitrate conditions. In addition, we found that ZmCHB101 regulates the expression of genes involved in nitrate transport, including *ZmNRT2.1* and *ZmNRT2.2*. Our results also demonstrate that the NIN-like protein (NLP) in maize, ZmNLP3.1, recognizes nitrate-responsive *cis*-elements (NREs) in the promoters of the *ZmNRT2.1* and *ZmNRT2.2* genes, and it activates the expression of these genes in response to nitrate. Intriguingly, well-positioned nucleosomes were detected at NREs, and nucleosome densities were lower in *ZmCHB101-RNAi* transgenic maize lines than in wild-type (WT) plants, both in the absence and presence of nitrate. In the absence of nitrate, ZmCHB101 bound to the NREs and maintained the nucleosome occupancies at these sites, which may impact the binding of ZmNLP3.1. However, in the presence of nitrate, the binding affinity of ZmCHB101 for NREs decreased dramatically, thus reducing the nucleosome density at NREs and consequently increasing the binding of ZmNLP3.1 to these sites.

MATERIALS AND METHODS

Plant Material and Growth Conditions

ZmCHB101-RNAi lines, RS1 and R101, have been described previously (Yu et al., 2016), in which *ZmCHB101* transcript levels were approximately 7% and 16% of that in the WT, respectively. Seeds of the WT and *ZmCHB101-RNAi* lines were sterilized using 1% sodium hypochlorite and incubated on moist filter paper at 28°C for 3 days for germination. Uniform seedlings were chosen and transferred to hydroponic culture in an environmentally controlled chamber with continuous

ventilation for 4 days to deplete the nutrients in seeds. Subsequently, seedlings were removed from endosperms and incubated in modified Hoagland's nutrient solution (Li et al., 2015) containing 0 mM nitrate for 1 day under constant aeration. To determine the effect of nitrate induction, seedlings were grown in Hoagland's nutrient solution containing 0, 0.5, 1, 5, or 15 mM nitrate at 23°C day/18°C night temperature under 16 h light/8 h dark conditions for 5 days. The nutrient solution was renewed daily. Morphological parameters of lateral roots were analyzed using the WinRHIZO software (Regent Instruments Canada Inc., Canada). The experiments were repeated three times, and each experiment was performed using 20 plants per genotype. To perform long-term low nitrate induction, germinated seeds were planted in sand and watered with Hoagland's nutrient solution containing 0.5 or 15 mM nitrate for 6 weeks. To conduct RNA sequencing (RNA-Seq) analysis, total RNA was extracted from the roots of seedlings cultured in nitrate-free nutrient solution for 7 days and then treated with Hoagland's nutrient solution containing 0.5 mM nitrate for 0 or 2 h. Three independent replicates were performed for each sample. The same conditions were used for preparing samples for chromatin immunoprecipitation (ChIP) assay, followed by quantitative PCR (qPCR).

Metabolite Analyses and Enzymatic Assays

ZmCHB101-RNAi lines and WT grown in Hoagland's nutrient solution containing 0.5 or 15 mM nitrate were used for metabolite and enzymatic assays. The amount of total N was measured using Elementar Isoprime 100 vario EL cube (Elementar, German). The amount of nitrate was estimated using Smartchem450 automatic chemical analyzer (Unityscientific, USA). The chlorophyll content of plants was measured as described previously (Yang et al., 2014). Soluble protein content was determined using the Plant Soluble Protein ELISA Kit (Jonln, China). The activity of nitrate reductase (NR), nitrite reductase (NIR), and glutamine synthetase (GS) was analyzed using the NR, NIR, and GS ELISA kits (Plant), respectively (Jonln, China).

Bioinformatics Analyses of RNA-Seq Data

Total RNA was isolated from seedling roots using TRIzol Reagent (Invitrogen, USA), according tothe manufacturer's protocol. Three biological replicates of each sample were used for RNA-Seqlibrary construction and sequenced on the HiSeq2000 platform (Illumina, USA). The raw data werecleaned by removing adaptor sequences and low-quality reads using FASTX-Toolkit version 0.0.13(http://hannonlab.cshl.edu/fastx_toolkit/).At least 110 million clean reads were obtained per library (**Supplementary Table S1**). The clean reads were mapped onto the maizereference genome, B73 RefGen_v3, using Hisat2 (http://ccb.jhu.edu/software/hisat2/index.shtml)with default parameters. The number of Fragments Per Kilobase of transcript per Million mapped reads(FPKM) was used to determine the transcription level of each gene using Cuffdiffv2.0.1. Genes with$|\log_2$fold-change (FC)$|$ > 1 and false discovery rate (FDR) < 0.05 were identified asdifferentially expressed genes (DEGs). Gene Ontology (GO) analysis of all DEGs was performed using the web-based agriGO tool (http://systemsbiology.cau.edu.cn/agriGOv2/). Singular enrichment analysis (SEA) was used for GO enrichment analysis on agriGO. The R package was used to manage, integrate, and visualize the RNA-Seq data.

Plasmid Construction

The coding sequence (CDS) of *ZmNLP3.1* was amplified from a cDNA library by PCR using ZmNLP3.1-F/R gene-specific primers. The CDS of *ZmCHB101* was amplified, as described previously (Yu et al., 2018). To generate a fusion construct of *ZmNLP3.1* with *glutathione S-transferase* (*GST-ZmNLP3.1*), the full-length CDS of *ZmNLP3.1* was cloned into the *pGEX-4T-1* vector using *Sma*I and *Not*I restriction sites. To generate the *ZmNLP3.1* overexpression construct, the *ZmNLP3.1* CDS was cloned downstream of the Cauliflower mosaic virus *35S* promoter in the *pCsV1300* vector using *Xba*I and *Cla*I sites, thus generating the *pro35S:ZmNLP3.1* construct. To generate dual FLAG epitope tagged *ZmNLP3.1* and *ZmCHB101* overexpression constructs (*pro35S:ZmNLP3.1-2×FLAG* and *pro35S:ZmCHB101-2×FLAG*), the CDSs of *ZmNLP3.1* and *ZmCHB101* were cloned into the *pCsV1300* vector separately using *Xba*I and *Cla*I sites. To generate luciferase reporter (LUC) constructs of *ZmNRT2.1* and *ZmNRT2.2* (*proZmNRT2.1:LUC* and *proZmNRT2.2:LUC*), a mutant copy of *ZmNRT2.1* or *ZmNRT2.2* promoter (1 kb) carrying AAAAAACCN$_{10}$CCAAA or GAAAAAAGN$_{10}$GAAAG substitution, respectively, was amplified using the *ZmNRT2.1-MPro*-F/R or *ZmNRT2.2-MPro*-F/R primer pair and inserted upstream of the *LUC* reporter gene; constructs containing an intact copy of each promoter upstream of the *LUC* gene were also generated using the *ZmNRT2.1-Pro*-F/R or *ZmNRT2.2-Pro*-F/R primer pair. To generate *proZmUBQ2*:*GUS* construct, *ZmUBQ2* (*GRMZM2G419891*) promoter sequence was amplified using a sequence-specific primer pair (*ZmUBQ-Pro*-F/R) and cloned in the *pCAMBIA3301* vector upstream of the *β-glucuronidase* (*GUS*) gene using *Nco*I and *Pst*I sites. The sequences of these primers are listed in **Supplementary Table S2**.

Quantitative Real-Time PCR (qRT-PCR)

Total RNA (2 μg) was used to synthesize cDNA with TransScript One-Step gDNA Removal and cDNA Synthesis SuperMix (Transgen Biotech). The qRT-PCR assay was performed using THUNDERBIRD SYBR qPCR Mix (TOYOBO) on the ABI real-time PCR detection system, according to the manufacturer's instructions (ABI StepOnePlus, USA). Three biological replicates in qRT-PCR analysis were performed and each biological replicate was conducted using three technical replicates. The maize *Actin 1* (*ZmACT1*) gene was used as an internal reference. Primers used for qRT-PCR are listed in **Supplementary Table S2**.

Transient Expression in Protoplasts

Plasmid DNA (20 μg) was used to transfect 200 μl of maize protoplasts (2×10^5 cells ml^{-1}), as described previously (Yoo

et al., 2007; Yu et al., 2018). To obtain nitrate-free protoplasts, maize seedlings were watered with nitrate-free Hoagland's nutrient solution (pH 6) containing 0.1% MES, 1% sucrose, 2.5 mM ammonium succinate, and 0.5 mM glutamine and incubated in the dark at 23°C for 15–20 days. To examine the expression levels of nitrate-responsive genes, the isolated maize protoplasts were incubated in W5 solution (0.2 mM MES, 154 mM NaCl, 125 mM $CaCl_2$, and 5 mM KCl) for 12 h and then transferred into W5 solution supplemented with 0.5 mM nitrate for 2 h. The protoplasts were collected by centrifugation at 100 × *g* for 1 min and then used for qRT-PCR or ChIP assay, as described previously (Yu et al., 2018).

ChIP Assay

For H3, H3K4me3 and H3K27me3 ChIP-qPCR assays, root tissues of maize seedlings treated with 0.5 mM nitrate for 0 or 2 h were collected and crosslinked in 1% formaldeyde. ChIP-qPCR was performed as described previously (Huang et al., 2012; Yu et al., 2018). Briefly, chromatin was isolated and sheared to 200–800 bp with the M220 Focused-ultrasonicator (Covaris). And soluble protein was incubated with H3 (Abcam, ab1791), H3K4me3 (Abcam, ab8580), or H3K27me3 (Millipore, 17622) antibody at 4°C. To perform ZmNLP3.1 and ZmCHB101 ChIP-qPCR assays, protoplasts isolated from 15-day-old nitrate-free seedlings were used, as described previously (Huang et al., 2012), with some modifications. The isolated maize protoplasts were transfected with the pro35S:ZmNLP3.1-2×FLAG or pro35S:ZmCHB101-2×FLAG construct, incubated in W5 solution for 12 h, and then treated with or without 0.5 mM nitrate for 2 h. The protoplasts were collected and subjected to crosslinking in 1% formaldehyde. The isolated chromatin was sheared to 200–800 bp fragments using an M220 Focused-ultrasonicator (Covaris, USA). The soluble chromatin was incubated with anti-FLAG antibody (MBL, D153-8) or serum overnight at 4°C. The immunoprecipitates were reverse crosslinked by heating the sample at 65°C for 8 h, and DNA was extracted using the phenol-chloroform extraction method. The ZmNRT2.1 and ZmNRT2.2 gene promoter fragments were amplified by qPCR using sequence-specific primers (**Supplementary Table S2**). The ZmACT1 gene was used as a negative control.

Electrophoretic Mobility Shift Assay (EMSA)

The fusion construct *GST-ZmNLP3.1* or the plasmid expressing GST alone was transformed into Escherichia coli BL21 (DE3) cells. The GST-ZmNLP3.1 and GST proteins were purified with glutathione beads (Xu et al., 2013), according to the manufacturer's protocol. Briefly, 5'-biotinylated probes were synthesized and labeled with biotin by Sangon Biotechnology. Double-stranded probe (50 fmol) was mixed with each purified protein separately in binding buffer and incubated for 10 min. The reaction mixtures were subjected to electrophoresis on a native 6% polyacrylamide gel in 0.5× TBE buffer. DNA in the gel was transferred to a positive charged nylon membrane and detected using the EMSA kit (Beyotime Company), according to the manufacturer's instructions (Ahmad et al., 2019).

Dual-Luciferase Transient Expression System

To examine the expression of the LUC or GUS reporter gene, dual-luciferase transient expression experiments were carried out as described previously (Ahmad et al., 2019). Briefly, the proZmNRT2.1:LUC or proZmNRT2.2:LUC construct was cotransformed with the effector construct pro35S:ZmNLP3.1 as well as proZmUBQ2:GUS into nitrate-free protoplasts. The transformed protoplasts were incubated in nitrate-free solution for 12 h and then treated with 0.5 mM nitrate for 0 or 2 h. After nitrate induction, LUC and GUS activities were measured using a Fluoroskan Finstruments microplate reader (MTX Lab Systems) (Ahmad et al., 2019).

Identification of Putative *Cis*-Regulatory NREs in *ZmNRT2.1* and *ZmNRT2.2* Promoters

To identify *cis*-acting NREs in the promoter regions of *ZmNRT2.1*and *ZmNRT2.2*, 1 kb sequence upstream of the transcription start site (TSS) of bothgenes was searched using EditSeq (https://www.dnastar.com/). Additionally, MEME (http://meme-suite.org/) was run on -303 to -345 bp and -438 to -480 bp of the *ZmNRT2.1* and *ZmNRT2.2* promoters, respectively. Putative NREs were also identified in the promoters of *NIR* genes of Arabidopsis (*Arabidopsis thaliana*), rice (*Oryza sativa*), spinach (*Spinacia oleracea*), silver birch (*Betula pendula*), common bean (*Phaseolus vulgaris*), and sorghum (*Sorghum bicolor*) using default parameters.

RESULTS

ZmCHB101 Regulates Nitrate-Induced Lateral Root Formation and Biomass Accumulation

Previously, we reported that ZmCHB101 may regulate the expression of genes involved in nitrogen compound metabolic process (Yu et al., 2016). To investigate this possibility, the seeds of WT plants and *ZmCHB101-RNAi* lines were incubated on moist filter paper at 28°C for 3 days to allow germination. The seedlings were then transplanted in pure water and grown for 4 days. To obtain nitrate-free seedlings, after removing the endosperm, the seedlings were transferred to Hoagland's nutrient solution without nitrate for 1 day. Subsequently, 0, 0.5, 1, 5, or 15 mM KNO_3 was added to the nutrient solution, and lateral root emergence was observed after 5 days. Both *ZmCHB101-RNAi* lines produced a higher number of and longer lateral roots than the WT plants following treatment with 0.1 or 0.5 mM KNO_3 (**Figures 1A–D**). Notably, these differences between WT plants and *ZmCHB101-RNAi* lines gradually diminished in the presence of 5 or 15 mM KNO_3 (**Figures 1A–D**).

Next, we planted the seeds of WT and *ZmCHB101-RNAi* lines in sand without N and watered them with nutrient solution containing 0.5 or 15 mM nitrate for 6 weeks. Measurement of the dry weight biomass revealed that the two independent

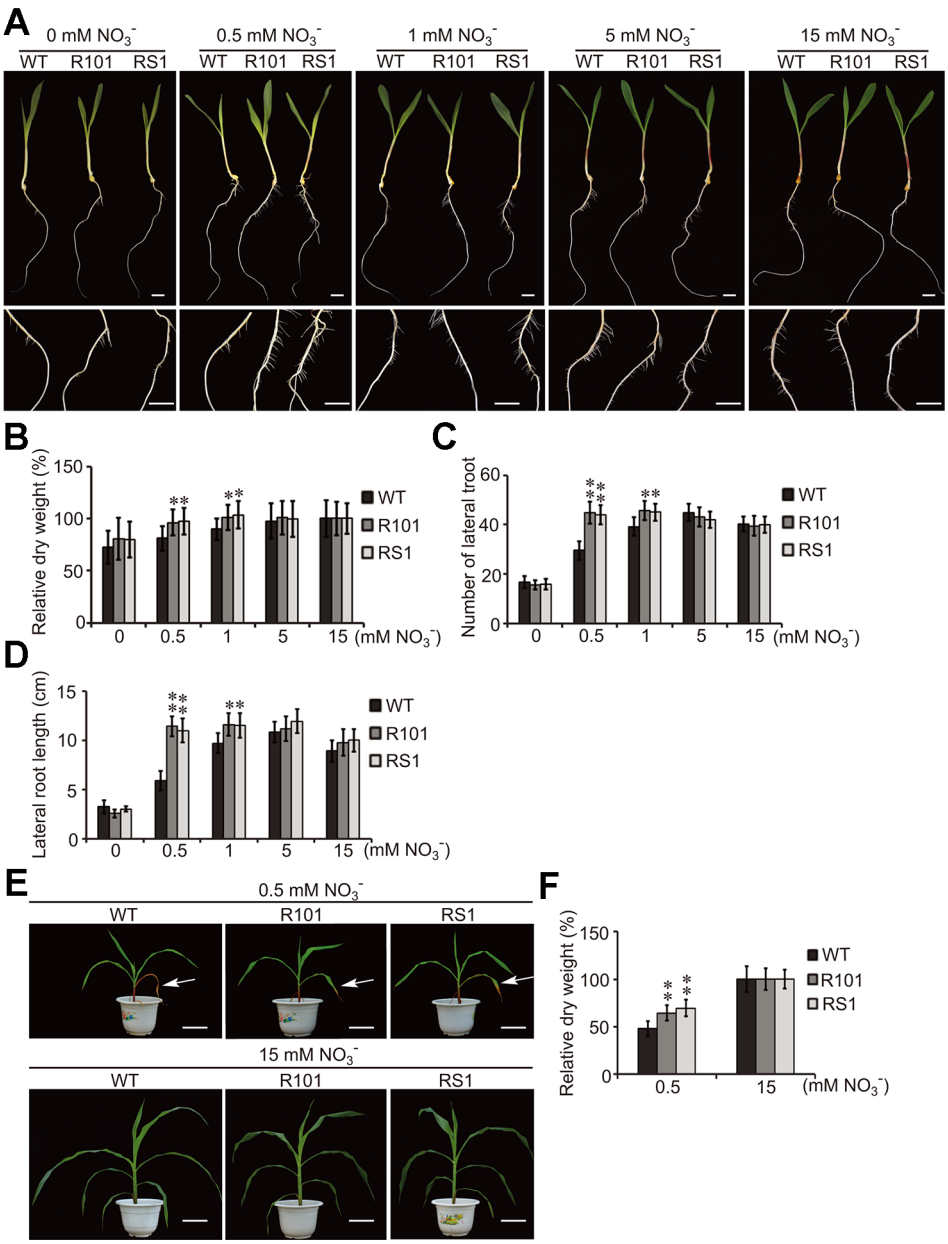

FIGURE 1 | ZmCHB101 plays a negative role in low nitrate response. **(A)** Representative images of seeds at day 5 of nitrate treatment. The germinated seeds were grown in water for 7 days and then transferred to Hoagland's nutrient solution containing 0, 0.5, 1, 5, or 15 mM KNO_3 for 5 days. **(B–D)** Analysis of the phenotypic traits including the dry weight **(B)**, lateral root number **(C)**, and lateral root length **(D)** of wild-type (WT) and *ZmCHB101-RNAi* plants after 5 days nitrate treatment. Data represent mean ± standard deviation (SD) of three biological replicates. 20 seedlings for each genotype for each biological replicate were used to analysis (n = 20). Significant differences are indicated with asterisks (*, $p < 0.05$; **, $p < 0.01$; Student's t-test). **(E)** Images of plants after 6 week nitrate treatment. Seedlings were planted in sand without N for 7 days and then watered with nutrient solution containing 0.5 or 15 mM KNO_3 for 6 weeks. Arrows indicate senescent leaves. **(F)** Dry weight of WT and *ZmCHB101-RNAi* plants measured after 6 weeks nitrate treatment. Data represent mean ± SD of three biological replicates (n = 20). Significant differences are indicated with asterisks (**, $p < 0.01$; Student's t-test). Data in **(A–D)** demonstrate the short-term effect of different nitrate treatments on plant growth, whereas data in **(E, F)** represent the long-term effects.

ZmCHB101-RNAi lines accumulated a higher biomass than WT plants following the 0.5 mM KNO_3 treatment (**Figures 1E, F**). Moreover, leaf senescence due to N deprivation was accelerated in WT plants compared with *ZmCHB101-RNAi* lines under the low nitrate conditions (**Figure 1E**). By contrast, there were no discernable phenotypic differences between the WT and *ZmCHB101-RNAi* lines treated with 15 mM KNO_3 (**Figures 1E, F**). Collectively, these results suggest that ZmCHB101 controls lateral root formation, biomass accumulation, and leaf senescence under low nitrate conditions.

ZmCHB101 Impacts N Metabolic Processes

Nitrate is an important source of N for amino acid and chlorophyll biosynthesis (Jeuffroy et al., 2002; Hirel et al., 2005). Therefore, we compared various physiological parameters of the WT and *ZmCHB101-RNAi* lines, including the contents of N, nitrate, soluble protein, and chlorophyll, as well as the biochemical activities of the nitrate reductase (NR), nitrite reductase (NiR), and glutamine synthetase (GS) enzymes. Following 0.5 mM nitrate treatment, the total N, nitrate, soluble protein, and chlorophyll contents were significantly higher in the *ZmCHB101-RNAi* lines than in the WT plants (**Figure 2A**). In addition, the activities of NR, NIR, and GS enzymes were also significantly higher in the *ZmCHB101-RNAi* lines than in the WT plants (**Figure 2B**). However, following 15 mM nitrate treatment, these physiological features were similar between the WT and *ZmCHB101-RNAi* lines. These results indicate that ZmCHB101 regulates N metabolic processes under low nitrate conditions.

ZmCHB101 Regulates the Expression of Nitrate-Responsive Genes

To gain insight into the potential role of ZmCHB101 in nitrate-responsive gene expression, we conducted an RNA-Seq analysis of WT and R101 plants treated with 0.5 mM KNO_3 for 0 (mock) or 2 h (nitrate condition). RNA-Seq data were mapped onto the maize B73 reference genome, and genes that were differentially expressed between WT and R101 plants were identified based on the following criteria: $|\log_2 FC| > 1$ and FDR < 0.05. A total of 862 and 786 differentially expressed genes (DEGs) were identified under the mock and nitrate conditions, respectively (**Figure 3A** and **Supplementary Table S3**). In addition, a gene ontology analysis revealed that a number of biological terms, including "response to nitrogen compound", "response to stress", and "response to abiotic stimulus", were enriched among the DEGs under the mock condition, whereas terms such as "response to nitrate", "response to nitrogen compound", "nitrate metabolism process", and "nitrate transport" were enriched among the DEGs under the nitrate condition (**Figure 3B** and **Supplementary Table S4**).

Next, we categorized the DEGs identified under each condition into two groups: nitrate-activated and nitrate-repressed (**Figure 3C**). Among the nitrate-activated genes, those encoding high-affinity nitrate transporters (categorized as primary nitrate-responsive genes), such as *ZmNRT2.1* and *ZmNRT2.2*, were activated to a higher level in R101 plants than in WT plants (**Figure 3C**). This result indicates that ZmCHB101 negatively impacts the activation of genes encoding high-affinity nitrate transporters. Similar differences in the expression patterns of other nitrate-activated genes were observed between the WT and R101 plants, including *ZmNNR1* and *ZmNNR2* (encoding the nitrate reductase enzymes; (Wang et al., 2004), *ZmGLN1* (*GRMZM2G098290*, encoding the glutamine synthetase enzyme; (Scheible et al., 2004), *ZmPGD4* (encoding glucose-6-phosphate 1-dehydrogenase; (Scheible et al., 2004), and *GRMZM2G076936* (encoding the ortholog of AtCYP735A2; (Takei et al., 2004; Liu et al., 2017) (**Figure 3C**). However, the expression level of *ZmGDH2*, encoding glutamic dehydrogenase 2 (Turano et al., 1997), was significantly increased under the nitrate condition in WT plants, but this induction was dramatically impaired in R101 plants (**Figure 3C**). Similar expression patterns were observed for the *NRT1/PTR* family (NPF) genes *GRMZM2G076313*, *GRMZM2G012242*, and *GRMZM2G064091*, as well as for the major facilitator superfamily proteins related to nitrate/nitrite transport, *GRMZM5G826658* and *GRMZM2G136523* (Sun and Zheng, 2015; Alvarez et al., 2019), all of which had lower expression levels in R101 plants than in WT plants in the presence of nitrate (**Figure 3C**). Among the genes that were down-regulated in the presence of nitrate, repression of *ZmNRT3* was greater in R101 plants than in WT plants, while the reduced expression fold changes of *GRMZM2G455124* (homolog of *AtNRT2.5*) and *ZmFDX5* (homolog of *AtFD2*) were impaired in R101 plants (Scheible et al., 2004; Sabermanesh et al., 2017; Undurraga et al., 2017). The expression patterns of a few selected genes were confirmed by qRT-qPCR (**Supplementary Figure S1**). Overall, these results indicate that ZmCHB101 regulates the expression of nitrate-responsive genes.

ZmCHB101 Affects Nucleosome Occupancy and Histone Modifications in the Promoters of ZmNRT2.1 and ZmNRT2.2

Based on the RNA-Seq results, we speculated that enhanced activation of *ZmNRT2.1* and *ZmNRT2.2* in *ZmCHB101-RNAi* lines under low nitrate conditions may lead to accelerated lateral root formation and higher biomass accumulation. Because ZmCHB101 impacts gene expression by controlling nucleosome density and/or occupancy (Yu et al., 2016), we speculated that nucleosome density and/or occupancy at the *ZmNRT2.1* and *ZmNRT2.2* loci could be impacted in *ZmCHB101-RNAi* lines. To test this possibility, we performed an H3 chromatin immunoprecipitation-coupled with a quantitative polymerase chain reaction (H3 ChIP-qPCR) experiment. Under the mock condition, well-positioned nucleosomes were detected upstream and downstream of the transcription start sites (TSSs; -1 and +1 nucleosome regions) of *ZmNRT2.1* and *ZmNRT2.2* in the WT line, whereas nucleosome densities at these regions were dramatically reduced in the *ZmCHB101-RNAi* lines (**Figure 4A**). Intriguingly, under the nitrate condition, nucleosome densities at the -1 and +1 regions were dramatically decreased in the WT line and remained at a low level in the *ZmCHB101-RNAi* lines (**Figure 4A**). These phenomena were not observed at the promoter regions of *ZmACT1* or *ZmNRT1.1*, a gene encoding a low-affinity nitrate transporter, which was not induced under the nitrate condition (**Supplementary Figure S2A**). Previous studies revealed that well-positioned nucleosomes are also found within the gene body and 3' (near the transcription termination site) regions of expressed genes (Chen et al., 2017; Mueller et al., 2017). In our experiments, the nucleosome densities within the gene body and 3' (near transcription termination site) regions of

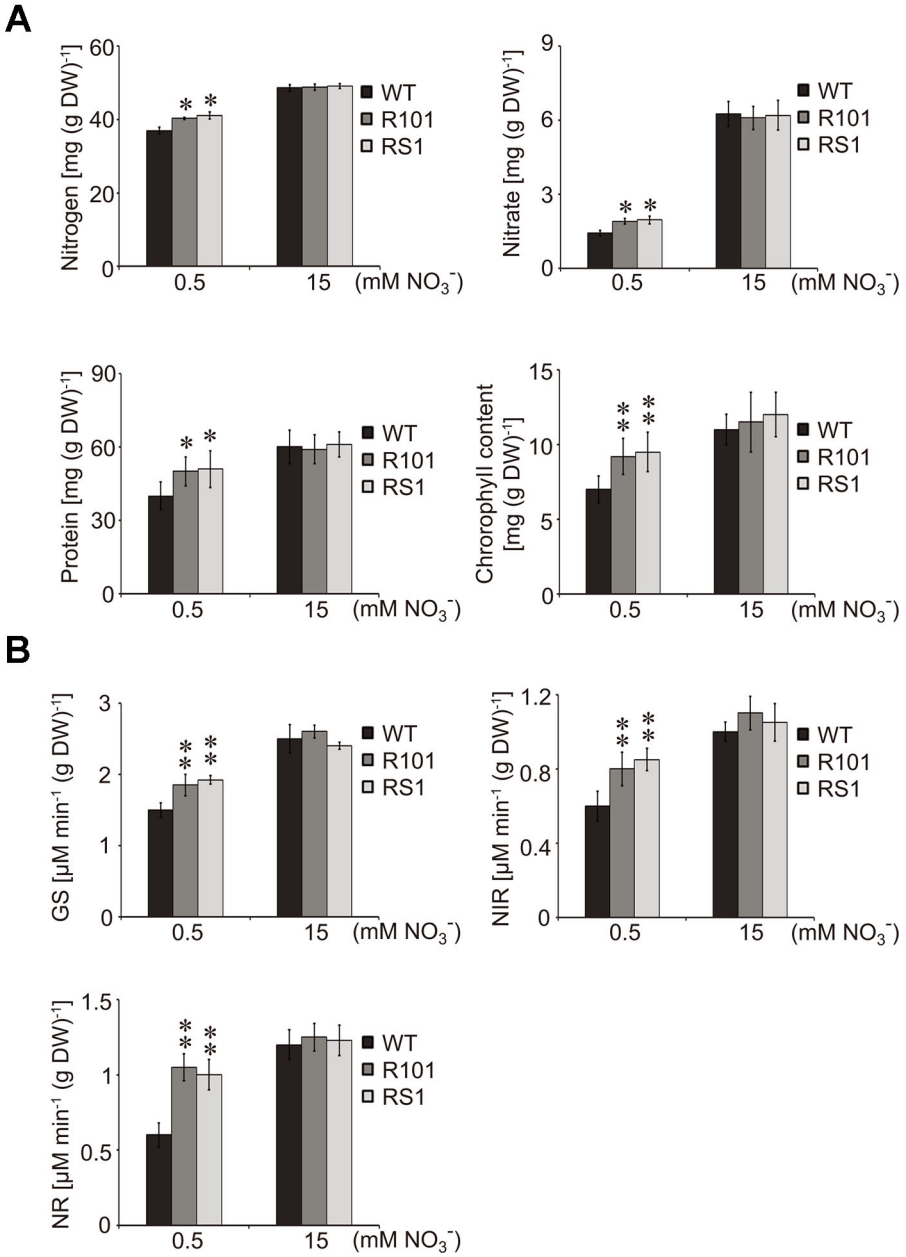

FIGURE 2 | Effects of different concentrations of nitrate on the physiology of maize plants. **(A**, **B)** Analysis of the physiological markers of N status in maize including the contents of N, nitrate, soluble protein, and chlorophyll **(A)** as well as the activities of glutamine synthetase (GS), nitrate reductase (NR), and nitrite reductase (NIR) **(B)**. The WT and *ZmCHB101-RNAi* seedlings were grown in Hoagland's nutrient solution containing 0.5 or 15 mM nitrate for 5 days and used for physiological analysis. Data represent mean ± SD of biological replicates ($n = 3$). Asterisks indicate significant differences (*, $p < 0.05$; **, $p < 0.01$; Student's *t*-test).

ZmNRT2.1 and *ZmNRT2.2* did not differ significantly between the WT and *ZmCHB101-RNAi* lines in either the absence or presence of nitrate (**Supplementary Figures S2B, C**). These results indicate that ZmCHB101 affects the -1 and +1 nucleosome densities of the high-affinity nitrate transporters, *ZmNRT2.1* and *ZmNRT2.2*, but does not alter the nucleosome densities at the gene body and 3' regions of these genes.

A large number of epigenomic analyses have demonstrated that H3K27me3 is associated with strong repression of gene expression, while H3K4me3 is linked to activation of gene expression (Schneider et al., 2004; Turck et al., 2007; Zhang et al., 2007; Vermeulen and Timmers, 2010; Roudier et al., 2011; Sequeira-Mendes et al., 2014; To and Kim, 2014; Wang et al., 2016). Previous studies suggested that *NRT2.1* promoter activity

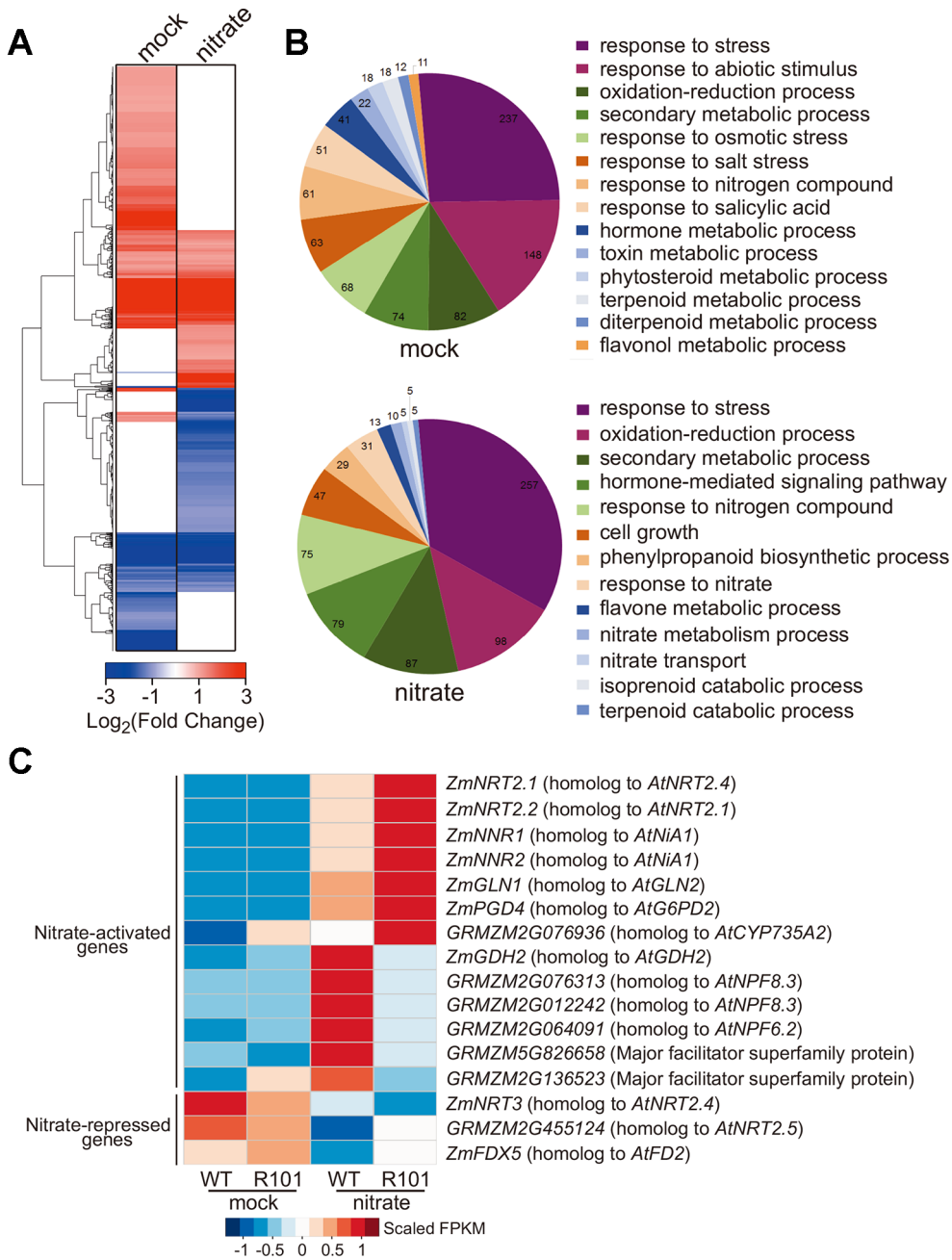

FIGURE 3 | ZmCHB101 regulates transcriptional networks of nitrate-responsive genes in maize roots. **(A, B)** Hierarchical clustering analysis **(A)** and Gene Ontology (GO) enrichment analysis **(B)** of genes differentially expressed between 7-day-old nitrate-free WT and *ZmCHB101-RNAi* line R101 seedlings under the mock and nitrate condition. A total of 862 and 786 differentially expressed genes (DEGs) were identified in the WT vs. R101 comparison under the mock and nitrate condition, respectively. The pie charts in **(B)** show significantly enriched GO terms of DEGs. **(C)** Heatmap of DEGs involved in nitrate metabolism. The color scale indicates the FPKM values. Mock, nitrate treatment for 0 h; nitrate, nitrate treatment for 2 h.

is tightly controlled by H3K27me3 and H3K4me3 in *Arabidopsis* (Bellegarde et al., 2018). Thus, we performed a ChIP-qPCR analysis using anti-H3K4me3 and anti-H3K27me3 antibodies to examine the impact of ZmCHB101 on these two histone modifications. The H3K27me3 levels at the 5', gene body, and 3' regions of *ZmNRT2.1* and *ZmNRT2.2* were slightly lower in the *ZmCHB101-RNAi* lines than in the WT line (**Figures 4B, C**). Nitrate treatment reduced the H3K27me3 levels in the WT plants, and this reduction was even more pronounced in the *ZmCHB101-RNAi* lines (**Figures 4B, C**). By contrast, H3K4me3 levels were moderately higher at the 5', gene body and 3' regions of *ZmNRT2.1* and *ZmNRT2.2* in *ZmCHB101-RNAi* lines than in

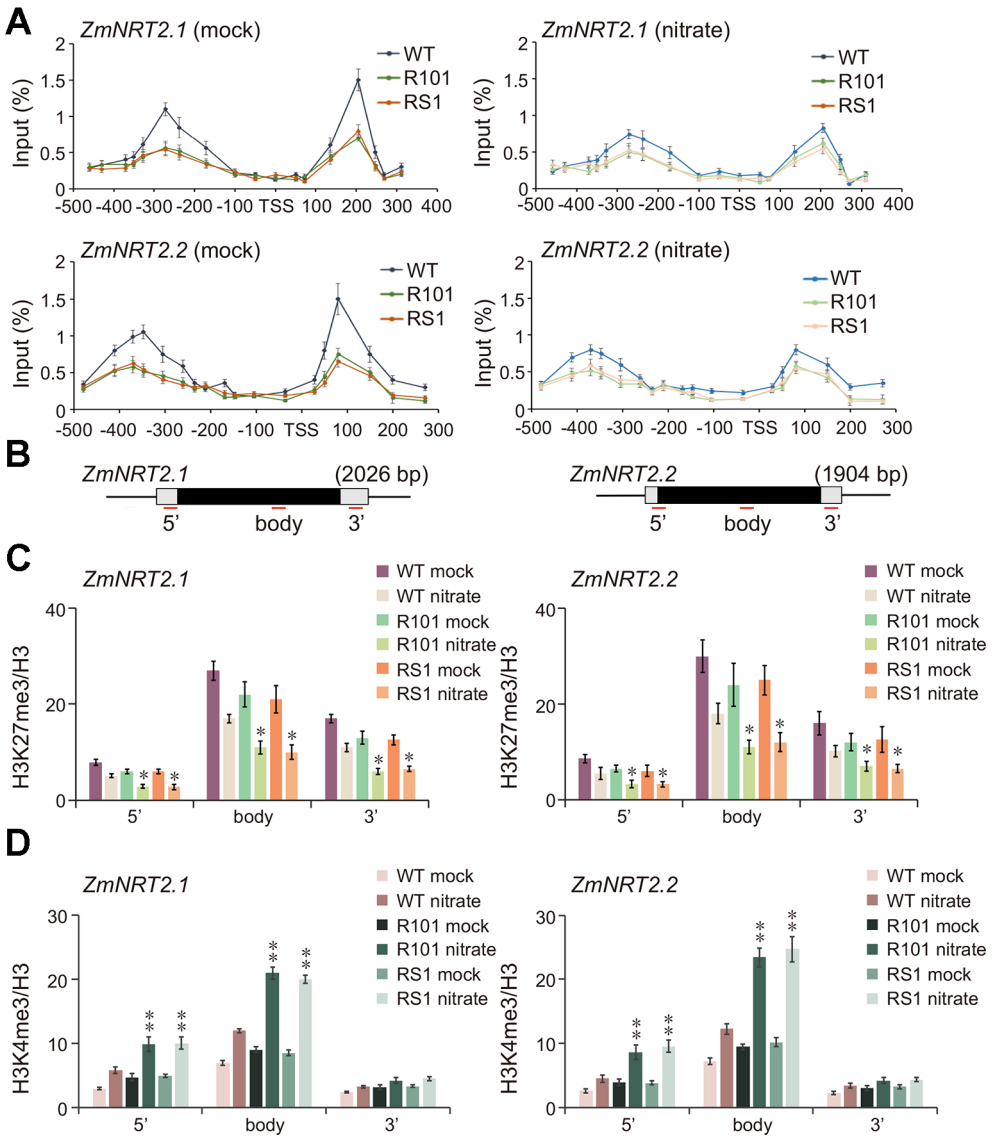

FIGURE 4 | ZmCHB101 affects nucleosome occupancy and histone modification status of *ZmNRT2.1* and *ZmNRT2.2*. 7-day-old nitrate-free seedlings under the mock and nitrate condition were used for chromatin immunoprecipitation and quantitative PCR (ChIP-qPCR) assay. **(A)** ChIP-qPCR using anti-H3 antibody was performed to dissect nucleosome occupancies and densities at -1 and +1 nucleosomes in *ZmNRT2.1* and *ZmNRT2.2* promoters. The X-axis denotes distance from TSS. The Y-axis denotes nucleosome occupancy normalized relative to the input DNA. **(B)** Schematic diagram of *ZmNRT2.1* and *ZmNRT2.2*. The untranslated regions are shown as open boxes and the exons as black boxes. 5', 5' untranslated region; body, gene body region; 3', 3' untranslated region. **(C)** H3K27me3 levels at *ZmNRT2.1* and *ZmNRT2.2*. **(D)** H3K4me3 levels at *ZmNRT2.1* and *ZmNRT2.2*. The Y-axes in **(C, D)** denote relative enrichment normalized to the H3. Data represent mean ± SD of the biological replicates ($n = 3$). Mock, nitrate treatment for 0 h; nitrate, nitrate treatment for 2 h. Asterisks indicate significant differences between WT and RS1 or R101 (*, $p < 0.05$; **, $p < 0.01$; Student's *t*-test).

WT plants (**Figures 4B, D**). Furthermore, the nitrate-induced increase in H3K4me3 levels was greater at the 5' and gene body regions in the *ZmCHB101-RNAi* lines than in the WT line (**Figures 4B, D**).

Next, we examined the binding of ZmCHB101 to the 5', gene body, and 3' regions of *ZmNRT2.1* and *ZmNRT2.2*. To this end, we expressed ZmCHB101-2×FLAG in maize protoplasts and performed a ChIP-qPCR analysis using an anti-FLAG antibody. As shown in **Supplementary Figure S3**, ZmCHB101-2×FLAG, but not FLAG, was strongly associated with the 5' region of *ZmNRT2.1* and *ZmNRT2.2*, but its binding ability became weaker at the gene body and 3' regions. Taken together, these results suggest that ZmCHB101 impacts the nucleosome densities at regions proximal to the TSS and affects the H3K27me3 and H3K4me3 statuses throughout the whole genic regions of *ZmNRT2.1* and *ZmNRT2.2*.

NREs Are Essential for the Expression of *ZmNRT2.1* and *ZmNRT2.2*

Since ZmCHB101 regulates nucleosome densities at the promoter regions of *ZmNRT2.1* and *ZmNRT2.2*, we performed a bioinformatic analysis of these promoters using EditSeq (Arnold and Clewley, 1997; Toplak et al., 2012) and detected consensus NREs (5'-GACtCTTN$_{10}$AAG-3'; (Konishi and Yanagisawa, 2010; Konishi and Yanagisawa, 2014) in the promoter regions of both genes (**Figure 5A**). Subsequently, we examined the expression levels of nitrate-responsive genes in nitrate-free maize protoplasts. After 2 h of nitrate induction, key nitrate-responsive genes such as *ZmNRT2.1*, *ZmNRT2.2*, *ZmNNR1*, and *ZmNNR2* were significantly activated relative to the mock condition (**Supplementary Figure S4**). Next, to determine whether the consensus NRE sequence is required for nitrate-responsive gene activation, we co-transfected nitrate-free maize mesophyll protoplasts with *proZmUBQ2:GUS* and the *proZmNRT2.1:LUC* or *proZmNRT2.2:LUC* construct containing normal or mutant NREs in the *ZmNRT2.1* or *ZmNRT2.2* gene promoter. The *proZmUBQ2:GUS* construct was used as a control for evaluating transfection efficiencies. In protoplasts transfected with the normal *proZmNRT2.1:LUC* or *proZmNRT2.2:LUC* construct, the activity of LUC was dramatically higher in the nitrate condition than in the mock condition (**Figures 5B, C**). However, LUC activity was not detected in protoplasts transformed with plasmids containing the mutant form of the *ZmNRT2.1* or *ZmNRT2.2* gene promoter (**Figures 5B, C**).

ZmNLP3.1 plays an essential role in the regulation of nitrate signaling and assimilation processes. It was reported previously that ectopic expression of *ZmNLP3.1* in *nlp7-1* mutant *Arabidopsis* plants restores the N-deficient phenotypes, including shoot biomass, root morphology, and nitrate assimilation under nitrate-replete conditions (Wang et al., 2018). Moreover, nitrate-mediated induction of the *NRT2.1*, *NIA1*, and *NiR1* transcripts is recovered in the *35S::ZmNLP3.1/nlp7-1* transgenic lines (Wang et al., 2018). To determine whether ZmNLP3.1 participates in the regulation of *ZmNRT2.1* and *ZmNRT2.2* expression, we co-transfected maize protoplasts with *ZmNLP3.1*, *proZmUBQ2:GUS*, and *proZmNRT2.1:LUC* or *proZmNRT2.2:LUC*. The activity of LUC was greatly induced under the nitrate condition (**Figure 5D**). Intriguingly, LUC activity was higher in protoplasts expressing *ZmNLP3.1* than in those expressing empty vector (**Figure 5D**). These results indicate that ZmNLP3.1 regulates the expression of *ZmNRT2.1* and *ZmNRT2.2* in response to nitrate. Next, we performed electrophoretic mobility shift assays to determine whether ZmNLP3.1 binds directly to the NREs of *ZmNRT2.1* and *ZmNRT2.2*. The full-length GST-tagged ZmNLP3.1 protein (GST-ZmNLP3.1) was capable of binding to probes containing consensus ZmNLP3.1-binding motifs; however, mutations of the NREs in the *ZmNRT2.1* or *ZmNRT2.2* gene promoter abolished the binding of ZmNLP3.1 to these regions (**Figure 5E**). These results indicate that ZmNLP3.1 binds to NREs located in the promoter regions of *ZmNRT2.1* and *ZmNRT2.2*, and activates the expression of these genes in response to nitrate.

ZmCHB101 Impacts the Binding of ZmNLP3.1 to *ZmNRT2.1* and *ZmNRT2.2* Promoters

To determine the molecular interplay between ZmCHB101 and ZmNLP3.1, we transiently expressed ZmNLP3.1-2×FLAG in WT, RS1, and R101 protoplasts, and performed ChIP-qPCR analyses using an anti-FLAG antibody. In the absence of nitrate (mock), ZmNLP3.1 did not bind to NREs (P1) or non-NREs (P2) located in the *ZmNRT2.1* or *ZmNRT2.2* promoter regions of WT protoplasts (**Figures 6A, B**); however, in *ZmCHB101-RNAi* lines, ZmNLP3.1 bound to P1 but not P2 (**Figures 6A, B**). In the presence of 0.5 mM nitrate, ZmNLP3.1 bound to P1 in WT protoplasts, although the level of binding was dramatically higher in the *ZmCHB101-RNAi* lines (**Figures 6A, B**). Subsequently, we performed an additional ChIP-qPCR analysis of ZmCHB101-2×FLAG in WT protoplasts and found that ZmCHB101 could bind to NREs in the absence of nitrate. However, this binding activity was significantly reduced in the presence of 0.5 mM nitrate (**Figure 6C**). Overall, these results indicate that ZmCHB101 impacts the binding of ZmNLP3.1 to NREs *via* an unknown mechanism (**Figure 7**).

DISCUSSION

Nitrate uptake is a highly regulated process. Maximizing nitrate uptake during seedling development is important because it has a major influence on plant growth and yield. In nature, the concentrations of seed-derived free amino acids in root and shoot tissues are initially high but decrease rapidly until maintaining a constant level 8 days after imbibition. The root nitrate uptake capacity then increases until shoot N content is stabilized (Sabermanesh et al., 2017). One possible method to improve the efficiency of N uptake is to enhance the nitrate uptake capacity of plants because nitrate is the predominant form of N available in the soil in most agricultural areas (Miller et al., 2007). Plant nitrate uptake is mediated by low- and high-affinity transport systems, which are thought to operate at high and low external nitrate concentrations, respectively (Kronzucker et al., 1995; Okamoto et al., 2003; Kotur et al., 2013). In *Arabidopsis*, AtNRT2.1 and AtNRT2.2 mediate high-affinity nitrate uptake; AtNRT2.1 is thought to be responsible for the majority of high-affinity nitrate transport (Li et al., 2007). Following a nitrate starvation period, the high-affinity nitrate transport activities and transcript levels of *AtNRT2.1* and *AtNRT2.2* increase rapidly after replenishing the nitrate supply but are later repressed with prolonged exposure to sufficient nitrate. In this study, *ZmCHB101-RNAi* lines showed enhanced lateral root numbers and biomass accumulation under low nitrate conditions; however, this phenomenon disappeared gradually under high nitrate conditions. In addition, the expression levels of *ZmNRT2.1* and *ZmNRT2.2* were higher in the *ZmCHB101-RNAi* lines than in the WT plants under low nitrate conditions. These results indicate that the high-affinity nitrate transport system is activated more strongly in the *ZmCHB101-RNAi* lines than in the WT line.

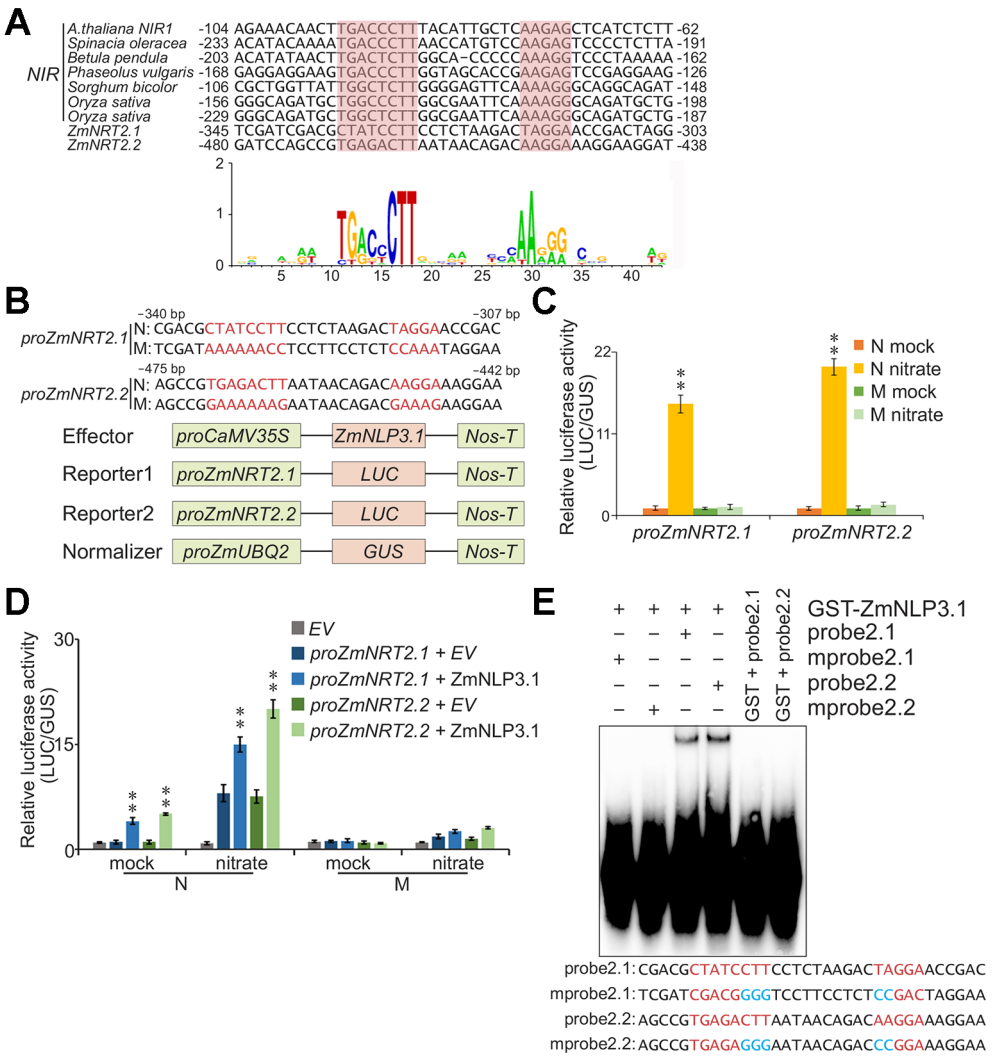

FIGURE 5 | ZmNLP3.1 binds to the promoter regions of *ZmNRT2.1* and *ZmNRT2.2 via* the recognition of NREs and activates gene transcription. **(A)** Nucleotides sequences of nitrate-responsive *cis*-elements (NREs) found in the flanking regions of *ZmNRT2.1* and *ZmNRT2.2*. The NREs of *NIR* genes of *Arabidopsis thaliana*, *Spinacia oleracea*, *Betula pendula*, *Phaseolus vulgaris*, *Sorghum bicolor*, and *Oryza sativa* are indicated. The consensus sequence of NRE is displayed using the sequence logo generation program WebLogo (Crooks et al., 2004). The *p*-values for the prediction of NREs in *ZmNRT2.1* and *ZmNRT2.2* gene promoters were 2.78e-6 and 1.29e-7, respectively. **(B–D)** Transcriptional activation of *ZmNRT2.1* and *ZmNRT2.2* by ZmNLP3.1 *via* recognition of the consensus sequence. **(B)** Schematic representation of the intact and mutant NREs in *ZmNRT2.1* and *ZmNRT2.2* promoters. N: normal *ZmNRT2.1* or *ZmNRT2.2* promoter sequence harboring the motif CTATCCTTN$_{10}$TAGAA or TGAGACTTN$_{10}$AAGGA, respectively. M: variants of the *ZmNRT2.1* or *ZmNRT2.2* promoter harboring mutant NREs (AAAAAACCN$_{10}$CCAAA or GAAAAAAGN$_{10}$GAAAG, respectively). **(C)** Nitrate-induced expression of *ZmNRT2.1* and *ZmNRT2.2* genes in protoplasts, depending on the NRE sequences. Nitrate-free protoplasts were transformed with *proZmNRT2.1* or *proZmNRT2.2* and normalizer, incubated for 12 h, and then treated with 0.5 mM nitrate for 0 or 2 h. Mock, nitrate treatment for 0 h; nitrate, nitrate treatment for 2 h. N and M indicate the normal and mutant promoter sequences of *ZmNRT2.1* or *ZmNRT2.2*, respectively, as shown in **(B)**. The ratio of LUC activity to *β-glucuronidase* (GUS) activity was calculated. Data represent mean ± SD (n = 3). Asterisks indicate significant differences between mock and nitrate conditions (**, $p < 0.01$; Student's *t*-test). **(D)** Transcriptional activation of *ZmNRT2.1* or *ZmNRT2.2* by ZmNLP3.1 relies on NRE sequences. The *proCaMV35S:ZmNLP3.1* vector was cotransformed with a reporter construct containing either *ZmNRT2.1* or *ZmNRT2.2* promoter and normalizing plasmids in nitrate-free protoplasts. After 12 h incubation, followed by treatment with 0.5 mM nitrate for 0 or 2 h, the LUC and GUS activity was determined. Data represent mean ± SD (n = 3). Mock, nitrate treatment for 0 h; nitrate, nitrate treatment for 2 h. Asterisks indicate significant differences between *EV* and ZmNLP3.1 (**, $p < 0.01$; Student's *t*-test). **(E)** Electrophoretic mobility shift assay (EMSA) for analyzing the binding of ZmNLP3.1 to *ZmNRT2.1* and *ZmNRT2.2* promoters. Probe2.1 and probe2.2 denote gene-specific biotin-labeled probes of *ZmNRT2.1* and *ZmNRT2.2* promoters, respectively. In mutant probe 2.1 (mProbe2.1), the sequence CTATCCTTN$_{10}$TAGA in the *ZmNRT2.1* promoter was changed to CGACGGGGN$_{10}$CCGAC. Similarly, in mprobe2.2, the sequence TGAGACTTN$_{10}$AAGGA in the *ZmNRT2.2* promoter was changed to TGAGAGGGN$_{10}$CCGGA.

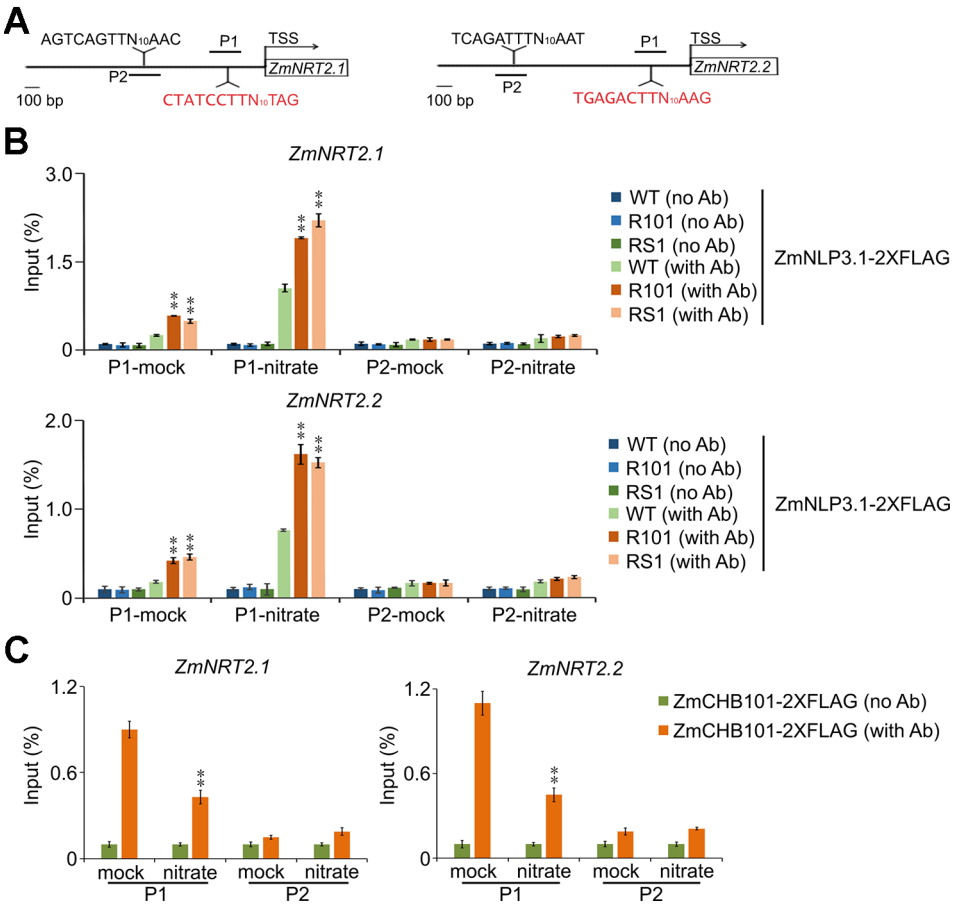

FIGURE 6 | Knockdown of *ZmCHB101* enhances the binding of ZmNLP3.1 to the promoter regions of *ZmNRT2.1* and *ZmNRT2.2*. **(A)** Schematic representation of *ZmNRT2.1* and *ZmNRT2.2* promoters showing the ZmNLP3.1-binding site (P1) and non-ZmNLP3.1-binding site (P2). The NREs located at the -1 nucleosome position are indicted in red. **(B)** The binding of ZmNLP3.1 to NREs in *ZmNRT2.1* and *ZmNRT2.2* promoters was enhanced in *ZmCHB101-RNAi* lines. Nitrate-free WT and *ZmCHB101-RNAi* protoplasts were transformed with *pro35S:ZmNLP3.1-2×FLAG* and then treated with 0.5 mM nitrate for 0 or 2 h. ChIP-qPCR was performed using anti-FLAG antibody. The binding of ZmNLP3.1 to NREs in *ZmNRT2.1* and *ZmNRT2.2* promoters was enhanced in *ZmCHB101-RNAi* protoplasts compared with WT protoplasts. Asterisks indicate significant differences between WT and R101 or RS1 (**, $p < 0.01$; Student's *t*-test). **(C)** Nitrate treatment dissociates ZmCHB101 from the -1 nucleosome position in *ZmNRT2.1* and *ZmNRT2.2* promoters. WT protoplasts were transformed with *pro35S:ZmCHB101-2×FLAG* and then treated with 0.5 mM nitrate for 0 or 2 h. ChIP-qPCR was performed using anti-FLAG antibody. Mock, nitrate treatment for 0 h; nitrate, nitrate treatment for 2 h. Asterisks indicate significant differences between mock and nitrate conditions (**, $p < 0.01$; Student's *t*-test).

Nitrate sensing activates signaling pathways that impinge upon molecular, metabolic, physiological, and developmental responses, both locally and at the whole plant level. However, some gaps still exist in our understanding of how nitrate signaling affects biological processes in plants. Previous studies demonstrated that the SWI/SNF CRC is a central regulatory module in plants that controls biological processes such as cell cycle progression and hormone signaling (Jerzmanowski, 2007; Reyes, 2014; Sarnowska et al., 2016). However, whether the SWI/SNF complex participates in nitrate signaling remains unknown. We showed previously that the ZmCHB101 protein regulates different biological processes in maize, including dehydration stress responses, abscisic acid responses, and shoot and root development (Yu et al., 2016; Yu et al., 2018). In this study, RNA-Seq analyses revealed that ZmCHB101 functions in different biological processes, including "response to nitrogen compound", "response to stress", and "response to abiotic stress". This result, together with the results of previous studies, indicates that ZmCHB101 acts as a general SWI/SNF CRC that participates in different physiological processes. Since we did not have a ZmCHB101-specific antibody, we tried to identify possible targets of ZmCHB101 using RNA-Seq. The expression levels of *ZmNRT2.1* and *ZmNRT2.2*, encoding high-affinity nitrate transporters, were higher in *ZmCHB101-RNAi* lines than in the WT line, identifying them as possible targets of ZmCHB101. Furthermore, ZmCHB101 bound directly to *ZmNRT2.1* and *ZmNRT2.2*, and impacted the chromatin status, indicating that it plays a key role in maintaining nucleosome occupancies at core consensus NREs located in the promoter regions of *ZmNRT2.1* and *ZmNRT2.2* to inhibit their expression. However, upon nitrate induction, ZmCHB101 was likely removed from these NREs, resulting in a dramatic

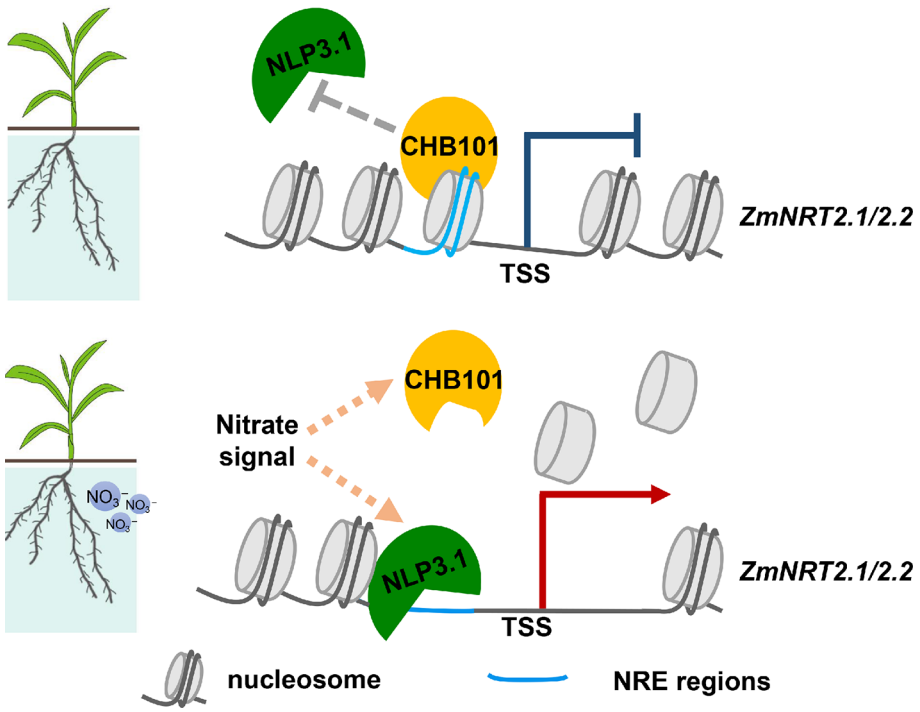

FIGURE 7 | The role of ZmCHB101 in nitrate response in maize. Under nitrate deprivation condition, the ZmCHB101 protein bound to the nitrate-responsive *cis*-elements (NREs) and maintained the nucleosome occupancies at these sites, thereby may impact the binding of ZmNLP3.1 to NREs, and suppresses the expression of *ZmNRT2.1* and *ZmNRT2.2*. In the presence of nitrate, the binding affinity of ZmCHB101 for NREs decreased dramatically, thus decreasing the nucleosome density at NREs and consequently increasing the binding of ZmNLP3.1 to NREs, thus activate the expression of *ZmNRT2.1* and *ZmNRT2.2*.

reduction in nucleosome densities at these loci. These results indicate that, while ZmCHB101 maintains nucleosome occupancies at these loci, some unknown nucleosome remodeling factors reduce the nucleosome densities. Reduction of nucleosome densities further facilitates the binding of ZmNLP3.1 to NREs, which activates gene transcription. Since ZmCHB101 and ZmNLP3.1 antibodies are not currently available, we were unable to determine the mechanism by which ZmCHB101 plays a negative role in ZmNLP3.1-mediated gene expression of *ZmNRT2.1* and *ZmNRT2.2*. Further studies are required to elucidate the *in vivo* molecular interplay between ZmCHB101 and ZmNLP3.1 in response to nitrate.

A genome-wide nucleosome occupancy map of maize constructed *via* sequencing of mononucleosomal DNA generated by MNase digestion revealed that nucleosome organization is associated with the plasticity of gene transcriptional status (Chen et al., 2017). The 5' and 3' nucleosome depleted regions become more pronounced as the gene expression level increases (Chen et al., 2017). In addition, the distances between the +1 and -1 nucleosomes and the TSS show a positive correlation with the level of gene expression (Chen et al., 2017). In our current study, the NREs in the promoters of *ZmNRT2.1* and *ZmNRT2.2* were located at -1 nucleosome, indicating that ZmNLP3.1-mediated gene expression is coupled with chromatin remodeling processes. In addition, the *in vivo* binding affinity of ZmNLP3.1 for NREs was dramatically lower in WT plants than in *ZmCHB101-RNAi* lines, both in the absence and presence of nitrate. Moreover, nucleosome densities were dramatically lower in *ZmCHB101-RNAi* lines than in WT plants. Overall, these results indicate that ZmCHB101 is responsible for the maintenance of nucleosomes at NREs in the absence of nitrate. Previously, we proposed that ZmCHB101 is responsible for removing the -1 and +1 nucleosomes from stress-responsive gene promoters (Yu et al., 2018). Because CRCs perform multiple functions, including nucleosome sliding, eviction, and replacement (Clapier and Cairns, 2009), we deduce that ZmCHB101 also plays different roles during transcriptional regulation.

DATA AVAILABILITY STATEMENT

Data generated in this study are deposited in NCBI Sequence Read Archive (accession number PRJNA541335).

AUTHOR CONTRIBUTIONS

Z-YX and BL devised and supervised the project. XM, XY, Z-YX, and BL designed the experiments. XM, XY, YW, DK, NN, WC,

and SW performed experiments and analyzed the data. XM, XY, Z-YX, and BL wrote the manuscript.

FUNDING

The work was supported by the National Natural Science Foundation of China (#31601311 to Z-YX), the Natural Science Foundation of Jilin Province of China (#20180101233JC to Z-YX), Science and Technology Innovation Development Project of Jilin City (#201831781 to XY), and the Fundamental Research Fund for the Central Universities (#2412018BJ002 to Z-YX) and the National Research Foundation of Korea, Ministry of Science and ICT (#2017R1A4A1015594 and #2017R1C1B2009362 to DK).

SUPPLEMENTARY MATERIAL

The Supplementary Material for this article can be found online at: https://www.frontiersin.org/articles/10.3389/fpls.2020.00052/full#supplementary-material

REFERENCES

Ahmad, R., Liu, Y., Wang, T. J., Meng, Q., Yin, H., Wang, X., et al. (2019). GOLDEN2-LIKE transcription factors regulate *WRKY40* expression in response to abscisic acid. *Plant Physiol.* 179, 1844–1860. doi: 10.1104/pp.18.01466

Alvarez, L., Sanchez-Hevia, D., Sanchez, M., and Berenguer, J. (2019). A new family of nitrate/nitrite transporters involved in denitrification. *Int. Microbiol.* 22, 19–28. doi: 10.1007/s10123-018-0023-0

Arnold, C., and Clewley, J. P. (1997). From ABI sequence data to *LASERGENE*'s EDITSEQ. *Methods Mol. Biol.* 70, 65–74. doi: 10.1385/0-89603-358-9:65

Bellegarde, F., Herbert, L., Sere, D., Caillieux, E., Boucherez, J., Fizames, C., et al. (2018). Polycomb repressive complex 2 attenuates the very high expression of the Arabidopsis gene *NRT2.1*. *Sci. Rep.* 8, 7905. doi: 10.1038/s41598-018-26349-w

Chen, Q., Mu, X., Chen, F., Yuan, L., and Mi, G. (2016). Dynamic change of mineral nutrient content in different plant organs during the grain filling stage in maize grown under contrasting nitrogen supply. *Eur. J. Agron.* 80, 137–153. doi: 10.1016/j.eja.2016.08.002

Chen, J., Li, E., Zhang, X., Dong, X., Lei, L., Song, W., et al. (2017). Genome-wide nucleosome occupancy and organization modulates the plasticity of gene transcriptional status in Maize. *Mol. Plant* 10, 962–974. doi: 10.1016/j.molp.2017.05.001

Clapier, C. R., and Cairns, B. R. (2009). The biology of chromatin remodeling complexes. *Annu. Rev. Biochem.* 78, 273–304. doi: 10.1146/annurev.biochem.77.062706.153223

Crooks, G. E., Hon, G., Chandonia, J. M., and Brenner, S. E. (2004). WebLogo: a sequence logo generator. *Genome Res.* 14, 1188–1190. doi: 10.1101/gr.849004

Forde, B. G. (2002). The role of long-distance signalling in plant responses to nitrate and other nutrients. *J. Exp. Bot.* 53, 39–43. doi: 10.1093/jexbot/53.366.39

Gangaraju, V. K., and Bartholomew, B. (2007). Mechanisms of ATP dependent chromatin remodeling. *Mutat. Res-Fundam Mol. Mech. Mutagen.* 618, 3–17. doi: 10.1016/j.mrfmmm.2006.08.015

Good, A. G., Shrawat, A. K., and Muench, D. G. (2004). Can less yield more? Is reducing nutrient input into the environment compatible with maintaining crop production? *Trends Plant Sci.* 9, 597–605. doi: 10.1016/j.tplants.2004.10.008

Hirel, B., Andrieu, B., Valadier, M.-H., Renard, S., Quillere, I., Chelle, M., et al. (2005). Physiology of maize II: identification of physiological markers representative of the nitrogen status of maize (*Zea mays*) leaves during grain filling. *Physiol. Plant.* 124, 178–188. doi: 10.1111/j.1399-3054.2005.00511.x

Ho, C. H., Lin, S. H., Hu, H. C., and Tsay, Y. F. (2009). CHL1 functions as a nitrate sensor in plants. *Cell* 138, 1184–1194. doi: 10.1016/j.cell.2009.07.004

Huang, N. C., Liu, K. H., Lo, H. J., and Tsay, Y. F. (1999). Cloning and functional characterization of an Arabidopsis nitrate transporter gene that encodes a constitutive component of low-affinity uptake. *Plant Cell.* 11, 1381–1392. doi: 10.1105/tpc.11.8.1381

Huang, M., Li, H., Zhang, L., Gao, F., Wang, P., Hu, Y., et al. (2012). Plant 45S rDNA clusters are fragile sites and their instability is associated with epigenetic alterations. *PloS One* 7, e35139. doi: 10.1371/journal.pone.0035139

Hurtado, L., Farrona, S., and Reyes, J. C. (2006). The putative SWI/SNF complex subunit BRAHMA activates flower homeotic genes in *Arabidopsis thaliana*. *Plant Mol. Biol.* 62, 291–304. doi: 10.1007/s11103-006-9021-2

Jerzmanowski, A. (2007). SWI/SNF chromatin remodeling and linker histones in plants. *Biochim. Biophys. Acta* 1769, 330–345. doi: 10.1016/j.bbaexp.2006.12.003

Jeuffroy, M. H., Ney, B., and Ourry, A. (2002). Integrated physiological and agronomic modelling of N capture and use within the plant. *J. Exp. Bot.* 53, 809–823. doi: 10.1093/jexbot/53.370.809

Konishi, M., and Yanagisawa, S. (2010). Identification of a nitrate-responsive cis-element in the Arabidopsis *NIR1* promoter defines the presence of multiple cis-regulatory elements for nitrogen response. *Plant J.* 63, 269–282. doi: 10.1111/j.1365-313X.2010.04239.x

Konishi, M., and Yanagisawa, S. (2014). Emergence of a new step towards understanding the molecular mechanisms underlying nitrate-regulated gene expression. *J. Exp. Bot.* 65, 5589–5600. doi: 10.1093/jxb/eru267

Kotur, Z., Siddiqi, Y. M., and Glass, A. D. M. (2013). Characterization of nitrite uptake in *Arabidopsis thaliana*: evidence for a nitrite-specific transporter. *New Phytol.* 200, 201–210. doi: 10.1111/nph.12358

Kronzucker, H. J., Glass, A. D. M., and Yaeesh Siddiqi, M. (1995). Nitrate induction in spruce: an approach using compartmental analysis. *Planta* 196, 683–690. doi: 10.1007/BF01106761

Lam, H. M., Coschigano, K. T., Oliveira, I. C., Melo-Oliveira, R., and Coruzzi, G. M. (1996). The molecular-genetics of nitrogen assimilation into amino acids in higher plants. *Annu. Rev. Plant Physiol. Plant Mol. Biol.* 47, 569–593. doi: 10.1146/annurev.arplant.47.1.569

Lezhneva, L., Kiba, T., Feria-Bourrellier, A. B., Lafouge, F., Boutet-Mercey, S., Zoufan, P., et al. (2014). The Arabidopsis nitrate transporter NRT2.5 plays a role in nitrate acquisition and remobilization in nitrogen-starved plants. *Plant J.* 80, 230–241. doi: 10.1111/tpj.12626

Li, W., Wang, Y., Okamoto, M., Crawford, N. M., Siddiqi, M. Y., and Glass, A. D. (2007). Dissection of the *AtNRT2.1:AtNRT2.2* inducible high-affinity nitrate transporter gene cluster. *Plant Physiol.* 143, 425–433. doi: 10.1104/pp.106.091223

Li, F., Chung, T., Pennington, J. G., Federico, M. L., Kaeppler, H. F., Kaeppler, S. M., et al. (2015). Autophagic recycling plays a central role in maize nitrogen remobilization. *Plant Cell.* 27, 1389–1408. doi: 10.1105/tpc.15.00158

Liu, K.-H., Niu, Y., Konishi, M., Wu, Y., Du, H., Sun Chung, H., et al. (2017). Discovery of nitrate-CPK-NLP signalling in central nutrient-growth networks. *Nature* 545, 311–316. doi: 10.1038/nature22077

Miller, A. J., Fan, X., Orsel, M., Smith, S. J., and Wells, D. M. (2007). Nitrate transport and signalling. *J. Exp. Bot.* 58, 2297–2306. doi: 10.1093/jxb/erm066

Mueller, B., Mieczkowski, J., Kundu, S., Wang, P., Sadreyev, R., Tolstorukov, M. Y., et al. (2017). Widespread changes in nucleosome accessibility without changes in nucleosome occupancy during a rapid transcriptional induction. *Genes Dev.* 31, 451–462. doi: 10.1101/gad.293118.116

Narlikar, G. J. (2010). A proposal for kinetic proof reading by ISWI family chromatin remodeling motors. *Curr. Opin. Chem. Biol.* 14, 660–665. doi: 10.1016/j.cbpa.2010.08.001

Okamoto, M., Vidmar, J. J., and Glass, A. D. M. (2003). Regulation of *NRT1* and *NRT2* gene families of *Arabidopsis thaliana*: responses to nitrate provision. *Plant Cell Physiol.* 44, 304–317. doi: 10.1093/pcp/pcg036

Parker, J. L., and Newstead, S. (2014). Molecular basis of nitrate uptake by the plant nitrate transporter NRT1.1. *Nature* 507, 68–6+. doi: 10.1038/nature13116

Peterson, C. L., and Workman, J. L. (2000). Promoter targeting and chromatin remodeling by the SWI/SNF complex. *Curr. Opin. Genet. Dev.* 10, 187–192. doi: 10.1016/S0959-437X(00)00068-X

Raun, W. R., and Johnson, G. V. (1999). Improving nitrogen use efficiency for cereal production. *Agron. J.* 91, 357. doi: 10.2134/agronj1999.00021962009100030001x

Reyes, J. C. (2014). The many faces of plant SWI/SNF complex. *Mol. Plant* 7, 454–458. doi: 10.1093/mp/sst147

Roudier, F., Ahmed, I., Berard, C., Sarazin, A., Mary-Huard, T., Cortijo, S., et al. (2011). Integrative epigenomic mapping defines four main chromatin states in Arabidopsis. *EMBO J.* 30, 1928–1938. doi: 10.1038/emboj.2011.103

Sabermanesh, K., Holtham, L. R., George, J., Roessner, U., Boughton, B. A., Heuer, S., et al. (2017). Transition from a maternal to external nitrogen source in maize seedlings. *J. Integr. Plant Biol.* 59, 261–274. doi: 10.1111/jipb.12525

Sarnowska, E., Gratkowska, D. M., Sacharowski, S. P., Cwiek, P., Tohge, T., Fernie, A. R., et al. (2016). The role of SWI/SNF chromatin remodeling complexes in hormone crosstalk. *Trends Plant Sci.* 21, 594–608. doi: 10.1016/j.tplants.2016.01.017

Sarnowski, T. J., Rios, G., Jasik, J., Swiezewski, S., Kaczanowski, S., Li, Y., et al. (2005). SWI3 subunits of putative SWI/SNF chromatin-remodeling complexes play distinct roles during Arabidopsis development. *Plant Cell.* 17, 2454–2472. doi: 10.1105/tpc.105.031203

Scheible, W. R., Morcuende, R., Czechowski, T., Fritz, C., Osuna, D., Palacios Rojas, N., et al. (2004). Genome-wide reprogramming of primary and secondary metabolism, protein synthesis, cellular growth processes, and the regulatory infrastructure of Arabidopsis in response to nitrogen. *Plant Physiol. Bioch.* 136, 2483–2499. doi: 10.1104/pp.104.047019

Schneider, R., Bannister, A. J., Myers, F. A., Thorne, A. W., Crane-Robinson, C., and Kouzarides, T. (2004). Histone H3 lysine 4 methylation patterns in higher eukaryotic genes. *Nat. Cell Biol.* 6, 73–77. doi: 10.1038/ncb1076

Sequeira-Mendes, J., Aragueez, I., Peiro, R., Mendez-Giraldez, R., Zhang, X., Jacobsen, S. E., et al. (2014). The functional topography of the *Arabidopsis* genome is organized in a reduced number of linear motifs of Chromatin States. *Plant Cell.* 26, 2351–2366. doi: 10.1105/tpc.114.124578

Shadchina, T. M., and Dmitrieva, V. V. (1995). Leaf chlorophyll content as a possible diagnostic mean for the evaluation of plant nitrogen uptake from the soil. *J. Plant Nutr.* 18, 1427–1437. doi: 10.1080/01904169509364992

Stitt, M., and Feil, R. (1999). Lateral root frequency decreases when nitrate accumulates in tobacco transformants with low nitrate reductase activity: consequences for the regulation of biomass partitioning between shoots and root. *Plant Soil.* 215, 143–153. doi: 10.1023/A:1004676605336

Sultan, S. E. (2003). Phenotypic plasticity in plants: a case study in ecological development. *Evol. Dev.* 5, 25–33. doi: 10.1046/j.1525-142X.2003.03005.x

Sun, J., and Zheng, N.(2015). Molecular mechanism underlying the Plant NRT1.1 dual-affinitynitrate transporter. *Front. Physiol.* 6,386. doi: 10.3389/fphys.2015.00386

Takei, K., Yamaya, T., and Sakakibara, H. (2004). Arabidopsis *CYP735A1* and *CYP735A2* encode cytokinin hydroxylases that catalyze the biosynthesis of *trans*-Zeatin. *J. Biol. Chem.* 279, 41866–41872. doi: 10.1074/jbc.M406337200

Tills, A. R., and Alloway, B. J. (1981). The effect of ammonium and nitrate nitrogen sources on copper uptake and amino acid status of cereals. *Plant Soil.* 62, 279–290. doi: 10.1007/BF02374091

To, T. K., and Kim, J. M.(2014). Epigenetic regulation of gene responsiveness in*Arabidopsis*. *Front. Plant Sci.* 4,6. doi: 10.3389/fpls.2013.00548

Toplak, I., Lazic, S., Lupulovic, D., Prodanov-Radulovic, J., Becskei, Z., Dosen, R., et al. (2012). Study of the genetic variability of porcine circovirus type 2 detected in Serbia and Slovenia. *Acta Vet Hung.* 60, 409–420. doi: 10.1556/AVet.2012.035

Turano, F. J., Thakkar, S. S., Fang, T., and Weisemann, J. M. (1997). Characterization and expression of NAD(H)-dependent glutamate dehydrogenase genes in Arabidopsis. *Plant Physiol.* 113, 1329–1341. doi: 10.1104/pp.113.4.1329

Turck, F., Roudier, F., Farrona, S., Martin-Magniette, M.-L., Guillaume, E., Buisine, N., et al. (2007). Arabidopsis TFL2/LHP1 specifically associates with genes marked by trimethylation of histone H3 lysine 27. *PloS Genet.* 3, 855–866. doi: 10.1371/journal.pgen.0030086

Undurraga, S. F., Ibarra-Henriquez, C., Fredes, I., Alvarez, J. M., and Gutierrez, R. A. (2017). Nitrate signaling and early responses in Arabidopsis roots. *J. Exp. Bot.* 68, 2541–2551. doi: 10.1093/jxb/erx041

Vermeulen, M., and Timmers, H. T. M. (2010). Grasping trimethylation of histone H3 at lysine 4. *Epigenomics* 2, 395–406. doi: 10.2217/epi.10.11

Vidmar, J. J., Zhuo, D., Siddiqi, M. Y., Schjoerring, J. K., Touraine, B., and Glass, A. D. (2000). Regulation of high-affinity nitrate transporter genes and high-affinity nitrate influx by nitrogen pools in roots of barley. *Plant Physiol.* 123, 307–318. doi: 10.1104/pp.123.1.307

Wang, R., Tischner, R., Gutierrez, R. A., Hoffman, M., Xing, X., Chen, M., et al. (2004). Genomic analysis of the nitrate response using a nitrate reductase-null mutant of Arabidopsis. *Plant Physiol.* 136, 2512–2522. doi: 10.1104/pp.104.044610

Wang, H., Liu, C. M., Cheng, J. F., Liu, J., Zhang, L., He, C. S., et al. (2016). Arabidopsis flower and embryo developmental genes are repressed in seedlings by different combinations of Polycomb group proteins in association with distinct Sets of Cis-regulatory elements. *PloS Genet.* 12, 25. doi: 10.1371/journal.pgen.1005771

Wang, Z., Zhang, L., Sun, C., Gu, R., Mi, G., and Yuan, L. (2018). Phylogenetic, expression and functional characterizations of the maize *NLP* transcription factor family reveal a role in nitrate assimilation and signaling. *Physiol. Plant.* 163, 269–281. doi: 10.1111/ppl.12696

Xu, Z.-Y., Kim, S. Y., Hyeon, D. Y., Kim, D. H., Dong, T., Park, Y., et al. (2013). The *Arabidopsis* NAC transcription factor ANAC096 cooperates with bZIP-type transcription factors in dehydration and osmotic stress responses. *Plant Cell.* 25, 4708–4724. doi: 10.1105/tpc.113.119099

Yang, C., Zhao, L., Zhang, H., Yang, Z., Wang, H., Wen, S., et al. (2014). Evolution of physiological responses to salt stress in hexaploid wheat. *Proc. Natl. Acad. Sci. USA.* 111, 11882–11887. doi: 10.1073/pnas.1412839111

Yoo, S. D., Cho, Y. H., and Sheen, J. (2007). *Arabidopsis* mesophyll protoplasts: a versatile cell system for transient gene expression analysis. *Nat. Protoc.* 2, 1565–1572. doi: 10.1038/nprot.2007.199

Yu, X., Jiang, L., Wu, R., Meng, X., Zhang, A., Li, N., et al. (2016). The core subunit of a chromatin-remodeling complex, ZmCHB101, plays essential roles in maize growth and development. *Sci. Rep.* 6, 38504. doi: 10.1038/srep38504

Yu, X., Meng, X., Liu, Y., Li, N., Zhang, A., Wang, T.-J., et al. (2018). The chromatin remodeler ZmCHB101 impacts expression of osmotic stress-responsive genes in maize. *Plant Mol. Biol.* 97, 451–465. doi: 10.1007/s11103-018-0751-8

Yu, X., Meng, X., Liu, Y., Wang, X., Wang, T. J., Zhang, A., et al. (2019). The chromatin remodeler ZmCHB101 impacts alternative splicing contexts in response to osmotic stress. *Plant Cell Rep.* 38, 131–145. doi: 10.1007/s00299-018-2354-x

Zhang, H., Jennings, A., Barlow, P. W., and Forde, B. G. (1999). Dual pathways for regulation of root branching by nitrate. *Proc. Natl. Acad. Sci. USA.* 96, 6529–6534. doi: 10.1073/pnas.96.11.6529

Zhang, X., Germann, S., Blus, B. J., Khorasanizadeh, S., Gaudin, V., and Jacobsen, S. E. (2007). The Arabidopsis LHP1 protein colocalizes with histone H3 Lys27 trimethylation. *Nat. Struct. Mol. Biol.* 14, 869–871. doi: 10.1038/nsmb1283

Zhang, F., Cui, Z., Fan, M., Zhang, W., Chen, X., and Jiang, R. (2011). Integrated soil-crop system management: reducing environmental risk while increasing crop productivity and improving nutrient use efficiency in China. *J. Environ. Qual.* 40, 1051–1057. doi: 10.2134/jeq2010.0292

Zhou, C., Miki, B., and Wu, K. (2003). *CHB2*, a member of the *SWI3* gene family, is a global regulator in *Arabidopsis*. *Plant Mol. Biol.* 52, 1125–1134. doi: 10.1023/B:PLAN.0000004305.60407.8b

Zhuo, D., Okamoto, M., Vidmar, J. J., and Glass, A. D. (1999). Regulation of a putative high-affinity nitrate transporter (*Nrt2;1At*) in roots of *Arabidopsis thaliana*. *Plant J.* 17, 563–568. doi: 10.1046/j.1365-313X.1999.00396.x

Conflict of Interest: The authors declare that the research was conducted in the absence of any commercial or financial relationships that could be construed as a potential conflict of interest.

frontiers in Plant Science

REVIEW
published: 19 February 2020
doi: 10.3389/fpls.2020.00085

The FACT Histone Chaperone: Tuning Gene Transcription in the Chromatin Context to Modulate Plant Growth and Development

*Klaus D. Grasser**

Cell Biology & Plant Biochemistry, Biochemistry Centre, University of Regensburg, Regensburg, Germany

FACT is a heterodimeric histone chaperone consisting of the SSRP1 and SPT16 proteins and is conserved among eukaryotes. It interacts with the histones H2A-H2B and H3-H4 as well as with DNA. Based on *in vitro* and *in vivo* studies mainly in yeast and mammalian cells, FACT can mediate nucleosome disassembly and reassembly and thus facilitates in the chromatin context DNA-dependent processes including transcription, replication and repair. In plants, primarily the role of FACT related to RNA polymerase II transcription has been examined. FACT was found to associate with elongating *Arabidopsis* RNA polymerase II (RNAPII) as part of the transcript elongation complex and it was identified as repressor of aberrant intragenic transcriptional initiation. *Arabidopsis* mutants depleted in FACT subunits exhibit various defects in vegetative and reproductive development. Strikingly, FACT modulates important developmental transitions by promoting expression of key repressors of these processes. Thus, FACT facilitates expression of *DOG1* and *FLC* adjusting the switch from seed dormancy to germination and from vegetative to reproductive development, respectively. In the central cell of the female gametophyte, FACT can facilitate DNA demethylation especially within heterochromatin, and thereby contributes to gene imprinting during *Arabidopsis* reproduction. This review discusses results particularly from the plant perspective about the contribution of FACT to processes that involve reorganisation of nucleosomes with a main focus on RNAPII transcription and its implications for diverse areas of plant biology.

Keywords: SSRP1, Pob3, SPT16, histone chaperone, *Arabidopsis*, chromatin

OPEN ACCESS

Edited by:
Sara Farrona, National University of Ireland Galway, Ireland

Reviewed by:
Aline Valeska Probst, Centre National de la Recherche Scientifique (CNRS), France
Jordi Moreno-Romero, Centre for Research in Agricultural Genomics (CRAG), Spain
Kristiina Irma Helena Himanen, University of Helsinki, Finland

***Correspondence:**
Klaus D. Grasser
Klaus.Grasser@ur.de

Specialty section:
This article was submitted to Plant Cell Biology, a section of the journal Frontiers in Plant Science

Received: *22 November 2019*
Accepted: *21 January 2020*
Published: *19 February 2020*

Citation:
Grasser KD (2020) The FACT Histone Chaperone: Tuning Gene Transcription in the Chromatin Context to Modulate Plant Growth and Development. Front. Plant Sci. 11:85. doi: 10.3389/fpls.2020.00085

CHAPERONING HISTONES

In eukaryotes, the nuclear DNA is packaged into nucleosomes, which represent the basic repeat unit of chromatin. The nucleosome contains 147 bp of DNA wrapped around an octamer composed of two copies each of the four core histones H2A, H2B, H3, and H4. Adjacent nucleosomes are connected by linker DNA of variable length (10–80 bp depending on cell type and species) that typically associates with linker histones such as H1 (McGhee and Felsenfeld, 1980; Luger and Richmond, 1998; Kornberg and Lorch, 1999). The general stability of nucleosome particles imposes major obstacles to transcription and other DNA-dependent processes (Li et al., 2007). Therefore,

different mechanisms have evolved that facilitate chromatin transcription by destabilising/disassembly of nucleomes (Henikoff, 2008; Zhou et al., 2019). In the regulation of nucleosome dynamics, in addition to other factors so-called histone chaperones are critically involved. Histone chaperones are a heterogeneous class of proteins that functionally interact with core histones to assemble/disassemble nucleosome particles without consuming energy in form of ATP and they are not necessarily part of the final product (De Koning et al., 2007). There are various types of histone chaperones that contribute to different chromatin-related processes including transcription, replication, and DNA repair (Das et al., 2010; Avvakumov et al., 2011; Gurard-Levin et al., 2014; Hammond et al., 2017). Often histone chaperones are classified as either H2A-H2B or H3-H4 chaperones, reflecting their preferential interaction with different core histones. Some histone chaperones even display selectivity towards specific H3 or H2A isoforms such as replicative or replacement variants (De Koning et al., 2007; Hammond et al., 2017). Beyond that histone chaperones have been functionally linked with the occurrence of certain post-translational modifications of core histones and thus with the establishment, maintenance and propagation of specific chromatin states (Avvakumov et al., 2011).

Due to the extensive evolutionary conservation of the structure of the nucleosome particle, many of the histone chaperones that have been studied in detail in yeast and metazoa also occur in plants. Thus, a variety of H2A-H2B and H3-H4 chaperones have been identified throughout the plant kingdom (Tripathi et al., 2015; Zhou et al., 2015; Kumar and Vasudevan, 2020). By modulating local chromatin structure histone chaperones were found to contribute to the regulation of plant growth and development (Ramirez-Parra and Gutierrez, 2007; Otero et al., 2014; Takatsuka and Umeda, 2015; Zhou et al., 2015). Moreover, tuning of chromatin states by histone chaperones to mediate altered gene expression programs can assist plants to cope more efficiently with environmental stress conditions (Zhu et al., 2013; Liu et al., 2015; Probst and Mittelsten Scheid, 2015).

In this article, the current knowledge about the histone chaperone FACT will be summarised, particularly its role in *Arabidopsis*, as most studies in plants were performed using this model. At first, though the discovery of FACT and its mode of action in yeast and metazoa is introduced.

DISCOVERY OF FACT AND ITS MOLECULAR ROLE IN CHROMATIN TRANSACTIONS

Originally, FACT (FAcilitates Chromatin Transcription) was identified in yeast and mammalian cells (Brewster et al., 1998; Orphanides et al., 1998; Orphanides et al., 1999; Wittmeyer et al., 1999). Its name originates from the finding that FACT promoted *in vitro* transcription from reconstituted chromatin templates by destabilising nucleosomes, facilitating RNA polymerase II passage during elongation (Orphanides et al., 1998; Orphanides et al., 1999; Belotserkovskaya et al., 2003). Over the years it became clear that besides chromatin transcription, FACT is also involved in other chromatin-dependent processes such as replication, recombination, and repair (Belotserkovskaya et al., 2004; Singer and Johnston, 2004; Winkler and Luger, 2011; Formosa, 2012; Gurova et al., 2018), and hence, the established name may well stand more broadly for facilitates chromatin transactions. FACT is a heterodimer consisting of the SSRP1 (Structure-Specific Recognition Protein 1; termed Pob3 in yeast) and SPT16 (SuPpressor of Ty 16). The main feature of FACT is its ability to disassemble and reassemble nucleosomes, and thus its involvement in overcoming and maintaining the nucleosomal barrier to DNA-dependent processes occurring in the chromatin context. Accordingly, FACT can interact with various nucleosomal targets including H2A-H2B dimers, H3-H4 tetramers and DNA (Jamai et al., 2009; Winkler et al., 2011; Hondele et al., 2013; Kemble et al., 2015). The nature of FACT-histone interactions has been further elucidated in a recent cryo-EM study of human FACT in complex with partially assembled sub-nucleosomes (Liu et al., 2020). This work illustrates that structure of FACT resembles a unicycle, consisting of a saddle and fork that is engaged in extensive interactions of SSRP1 and SPT16 with nucleosomal DNA and all histones. Competition between FACT and DNA for histone binding seems to be critical for reversible nucleosome reorganisation and uncoiling of the nucleosomal DNA from the histone core that generally leads to increased DNA accessibility (Xin et al., 2009; Hondele et al., 2013; Kemble et al., 2015; Tsunaka et al., 2016; Valieva et al., 2016; Wang et al., 2018). Following transient nucleosome destabilisation, for instance, during passage of transcribing RNA polymerase II, FACT promotes nucleosome reassembly that is important to maintain proper chromatin signature and to prevent aberrant transcriptional initiation from cryptic promoters (Kaplan et al., 2003; Mason and Struhl, 2003; Cheung et al., 2008; Jamai et al., 2009; Wang et al., 2018). Further intriguing molecular and structural details of numerous studies on yeast and metazoan FACT are summarised in various excellent review articles (Belotserkovskaya et al., 2004; Winkler and Luger, 2011; Formosa, 2012; Gurova et al., 2018).

BASIC FACTS ABOUT PLANT FACT

The FACT heterodimer consisting of SSRP1 (71.6 kDa) and SPT16 (120.6 kDa) was demonstrated by reciprocal coimmunoprecipitation from *Arabidopsis* cells (Duroux et al., 2004). SPT16 comprises an N-terminal domain, a dimerisation domain, a middle domain, and an acidic C-terminal domain (**Figure 1**), and the overall domain organisation of plant SPT16 closely resembles the counterparts of other eukaryotes (**Supplementary Figure S1**). SSRP1 contains an N-terminal domain that mediates dimerisation with SPT16, a middle domain, an acidic domain, and a C-terminal HMG-box domain (**Figure 1**). Metazoan SSRP1 differs from the plant orthologues by a more pronounced C-terminal extension, while the fungal orthologues lack the HMG-box domain (**Supplementary Figure S2**) that in yeast is provided by separate small HMGB-box proteins termed Nhp6a/b (Formosa, 2012; Gurova et al., 2018). Proteins closely related to *Arabidopsis*

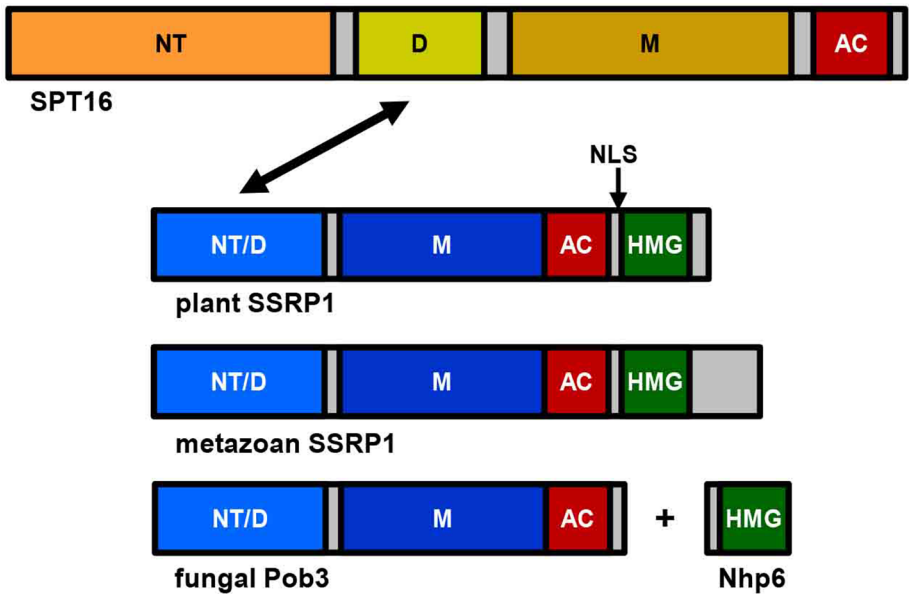

FIGURE 1 | Schematic representation of the FAcilitates Chromatin Transcription (FACT) subunits SPT16 and SSRP1. While the overall structure of SPT16 is essentially conserved throughout eukaryotes, there are differences in the C-terminal region of SSRP1 (Pob3 in fungi). SPT16 consists of N-terminal domain (NT), dimerisation domain (D), middle domain (M), and acidic C-terminal domain (AC), while SSRP1/Pob3 proteins of different eukaryotes are composed of N-terminal domain (that is required for heterodimerisation (NT/D) with SPT16, indicated by an arrow), middle domain (M), acidic region (AC), and HMG-box domain (HMG), which in case of yeast Pob3 is provided by the separate protein(s) Nhp6a/b. Plant SSRP1 contains a nuclear localisation signal (NLS, indicated by an arrow) within a short basic region linking the acidic domain and the HMG-box (Röttgers et al., 2000).

SSRP1 and SPT16 are encoded by monocot and dicot plants, as well as by *Selaginella* and *Physcomitrella* (**Figure 2**).

Since SSRP1 contains an HMG-box domain that typically mediates DNA-interactions (Antosch et al., 2012; Malarkey and Churchill, 2012), the DNA-binding properties of maize SSRP1 were examined. These experiments revealed that SSRP1 does not interact with DNA sequence-specifically, but according to a binding-site selection assay, it binds preferentially to sequences containing deformable dinucleotide steps (Röttgers et al., 2000). In line with this finding, mediated by its HMG-box domain SSRP1 can bend linear DNA and bind selectively to certain DNA structures (Röttgers et al., 2000; Pfab et al., 2018b). Furthermore, SSRP1 is phosphorylated by protein kinase CK2 and phosphorylation of two residues C-terminal of the HMG-box domain modulates the structure-specific interaction with DNA (Krohn et al., 2003). The HMG-box domain of SSRP1 is not only important for DNA-binding, but contributes also to nucleosome interactions (Lichota and Grasser, 2001; Pfab et al., 2018b). In view of the relevance of the HMG-box domain for *in vitro* DNA/nucleosome interactions, it was surprising that based on fluorescence recovery after photobleaching experiments intact SSRP1 and SSRP1 lacking its HMG-box domain (termed SSRP1ΔHMG) displayed the same mobility within nuclei of *Arabidopsis* cells. Beyond that, expression of SSRP1ΔHMG was almost as efficient as that of intact SSRP1 in supporting normal growth and development of the otherwise nonviable *ssrp1-1* mutant (Pfab et al., 2018b). This suggested that the HMG-box domain, which is conserved among SSRP1 proteins of plants and metazoa, is not critical in *Arabidopsis* under standard growth conditions. Possibly, FACT containing SSRP1ΔHMG (or intact SSRP1) functionally interacts with small abundant HMGB proteins similar to the mechanism reported for yeast FACT. Yeast Pob3 lacks the C-terminal HMG-box domain (thus structurally resembling *Arabidopsis* SSRP1ΔHMG; cf. **Figure 1**) and the HMG-box function is provided by small Nhp6a/b HMG-box proteins (Brewster et al., 2001; Formosa et al., 2001). However, fusing a C-terminal HMG-box domain to Pob3 is insufficient for full, Nhp6-independent activity. Both yeast FACT containing the Pob3-HMG fusion and human FACT were dependent on the presence of Nhp6 for efficient nucleosome reorganisation (McCullough et al., 2018). Collectively, these findings suggest that SSRP1-SPT16 of plants/metazoa may need assistance of small HMGB proteins in a way analogous to the cooperation of Pob3/SPT16 with Nhp6 in yeast. However, this issue requires further investigations.

Both SSRP1 and SPT16 are nuclear proteins and are ubiquitously expressed in all/most *Arabidopsis* tissues, but expression is not detectable in certain terminally differentiated cells such as mature trichoblasts or cells of the root cap (Duroux et al., 2004; Ikeda et al., 2011; Pfab et al., 2018a). Consistent with the enrichment of SSRP1 in the highly micrococcal nuclease-sensitive fraction of chromatin (Lichota and Grasser, 2001), both SSRP1 and SPT16 are detected by indirect immunofluorescence microscopy in the euchromatin of interphase nuclei, but not in heterochromatic chromocenters (Duroux et al., 2004). Using chromatin immunoprecipitation SSRP1-SPT16 was detected

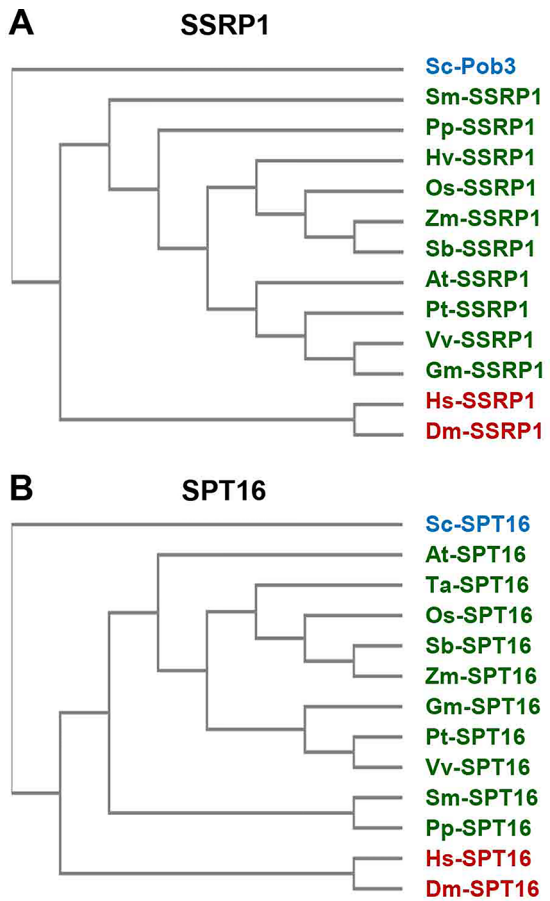

FIGURE 2 | Sequence similarity of FAcilitates Chromatin Transcription (FACT) subunits. The amino acid sequences of SSRP1 **(A)** and SPT16 **(B)** proteins from various organisms (*Arabidopsis thaliana (At), Drosophila melanogaster (Dm), Glycine max (Gm), Homo sapiens (Hs), Hordeum vulgare (Hv), Oryza sativa (Os), Physcomitrella patens (Pp), Populus trichocarpa (Pt), Saccharomyces cerevisiae (Sc), Selaginella moellendorfii (Sm), Sorghum bicolor (Sb), Triticum aestivum (Ta), Vitis vinifera (Vv), Zea mays (Zm)*) were aligned by multiple sequence alignment (cf. **Supplementary Figures S1, S2**) using Clustal Omega (https://www.ebi.ac.uk/Tools/msa/clustalo/) that served to cluster the sequences (unweighted pair group method with arithmetic mean). The sequences of plants are indicated in green and those of metazoa in red, while the yeast sequence is labelled blue.

along the transcribed region of genes transcribed by RNAPII, but not at loci transcribed by RNA polymerases I and III or intergenic regions. Moreover, association with the chromatin of active protein-coding genes occurred in a transcription-dependent manner (Duroux et al., 2004; Perales and Más, 2007; Lolas et al., 2010; Antosz et al., 2017). In accordance with that an affinity-purification approach combined with mass spectrometry demonstrated that FACT efficiently copurified with elongating RNAPII (CTD-phosphorylated at residues S2P, S5P) from *Arabidopsis* cells as well as with known transcript elongation factors including TFIIS, SPT4/SPT5 and PAF1C (Antosz et al., 2017). Moreover, *SSRP1* and *SPT16* genetically interact with *TFIIS* encoding a modulator of RNAPII activity and with *HUB1/2*, encoding factors catalysing elongation-related mono-ubiquitination of histone H2B (Lolas et al., 2010; Antosz et al., 2017). Taken together these findings indicate a role of *Arabidopsis* FACT in RNAPII transcriptional elongation (Van Lijsebettens and Grasser, 2014; Zhou et al., 2015; Grasser and Grasser, 2018), in line with the function of FACT as regulator of mRNA synthesis in other organisms (Reinberg and Sims, 2006; Formosa, 2012; Gurova et al., 2018), although the exact mechanism *in vivo* is still obscure.

Intriguing insight provided a study analysing genome-wide intragenic transcriptional initiation from cryptic promoters in *Arabidopsis*. Thousands of discrete, mostly exonic transcriptional start site positions were mapped in *ssrp1* and *spt16* mutants and the majority of these sites were detected in both mutants (Nielsen et al., 2019). This suggested that FACT is required for repression of aberrant intragenic transcript initiation, whereas no evidence was found for an involvement in repression of cryptic transcription by other elongation factors such as PAF1C, Elongator and the SDG8 H3K36-methyltransferase. At FACT-repressed intragenic start sites an enrichment of the RNAPII elongation signature H3K4me1 was detected that may contribute to suppress intragenic transcriptional initiation (Nielsen et al., 2019). Since FACT has been implicated in repressing cryptic transcription also in other organisms (Kaplan et al., 2003; Mason and Struhl, 2003; Cheung et al., 2008; Jamai et al., 2009), ensuring transcriptional fidelity by restricting transcript initiation to promoters may be a key function of FACT.

FACT IN PLANT GROWTH AND DEVELOPMENT

In various organisms including *Arabidopsis*, FACT is essential for viability (Cao et al., 2003; Lolas et al., 2010; Formosa, 2012; Frost et al., 2018). *Arabidopsis* mutant plants expressing reduced amounts of SSRP1 or SPT16 similarly show various defects in vegetative and reproductive development. Thus, the mutant plants display an increased number of leaves and inflorescences as well as altered leaf architecture (Lolas et al., 2010). In addition, these plants are early bolting, have abnormal flower morphology and a severely reduced seed set. The early bolting phenotype is associated with reduced expression of the floral repressor *FLC* in *ssrp1* and *spt16* plants relative to the wild type controls (Lolas et al., 2010). Germination assays with freshly harvested seeds demonstrated that in contrast to the wild type control, *ssrp1* mutant seeds germinated efficiently without stratification (**Figure 3**), indicating reduced seed dormancy (Michl-Holzinger et al., 2019). In line with this phenotype, *ssrp1* seeds exhibit decreased transcript levels of the *DOG1* gene, which is a known quantitative trait locus of seed dormancy. Introduction of an additional copy of *DOG1* into *ssrp1* resulted in increased *DOG1* transcript levels and consistently in more robust seed dormancy (Michl-Holzinger et al., 2019). Therefore, SSRP1 is required for efficient expression of *DOG1* and FACT is a modulator of seed dormancy in *Arabidopsis*. These

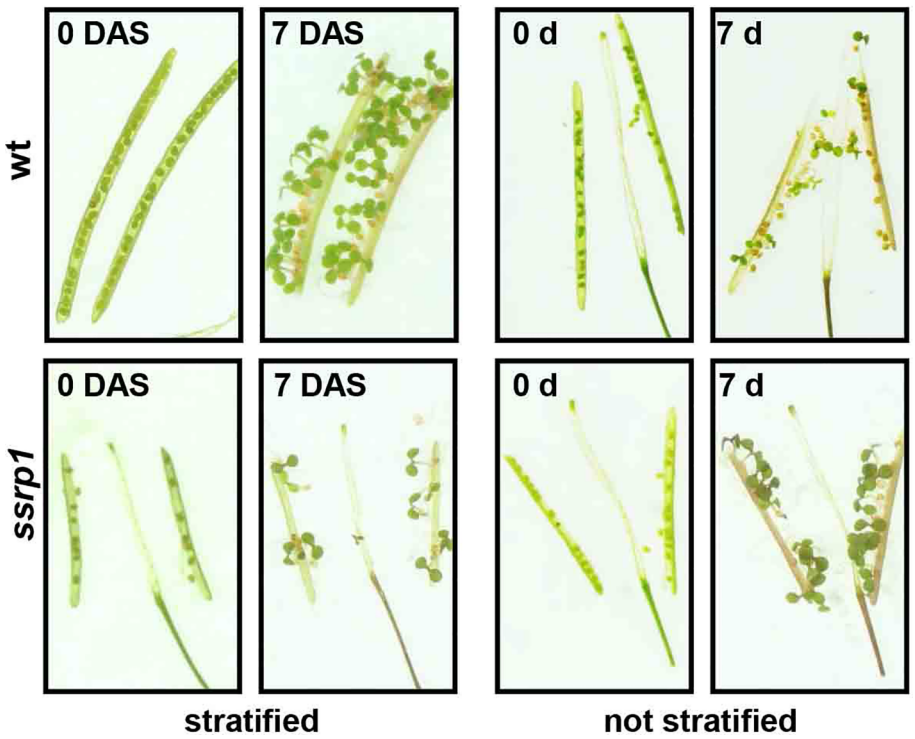

FIGURE 3 | Reduced dormancy of *ssrp1* seeds. Germination assays with opened siliques harvested 14 days after flowering. They are shown at day 0 and 7 days after incubation, either with or without prior stratification. Note the smaller siliques of *ssrp1* containing a severely reduced number of seeds compared to wt. After stratification almost all seeds germinate, whereas without stratification wt seeds germinate inefficiently (< 50%), whereas *ssrp1* seeds due to reduced seed dormancy germinate efficiently (~90%).

findings reveal that FACT is involved in two of the most important plant developmental switches, namely, the transition from seed dormancy to germination and from vegetative to reproductive development. Interestingly, both processes in addition to FACT are regulated by other modulators of transcriptional elongation and chromatin structure. Thus, factors including FACT, PAF1C, SWR1, SDG8 and HUB1/2 contribute to the expression of *FLC* in the induction to flowering (He et al., 2004; Oh et al., 2004; Zhao et al., 2005; Choi et al., 2007; Cao et al., 2008; Lázaro et al., 2008; Lolas et al., 2010), while factors such as FACT, TFIIS, H2B-monoubiquitinases, and H3-methylases influence the expression of *DOG1* in the switch from seed dormancy to germination (Liu et al., 2007; Zheng et al., 2012; Molitor et al., 2014; Michl-Holzinger et al., 2019). Furthermore, FACT was identified as cofactor of the transcriptional regulation of circadian rhythms in *Arabidopsis*. Initially, it was observed that FACT rhythmically associates with the circadian oscillator gene *TOC1* (Perales and Más, 2007). Subsequently, protein interactions were detected between FACT, elongating RNAPII and clock-related components termed LNKs. By interaction between LNKs and the MYB factor RVE8 the transcription machinery is recruited to target promoters, leading to rhythmic occupancy of clock gene promoters (Ma et al., 2018). FACT could be involved in this scenario facilitating the transition from RNAPII transcript initiation to productive elongation.

Recent transcript profiling of 10-day-old *Arabidopsis ssrp1* and *spt16* seedlings in comparison to the wild type demonstrated that a relatively small subset of genes is differentially expressed in the mutants (Pfab et al., 2018a). The alterations in the transcript profile of both mutants relative to wild type were very similar, consistent with the function of SSRP1 and SPT16 as a heterodimer. Among the downregulated genes, those encoding enzymes of anthocyanin biosynthesis were remarkably overrepresented. Upon exposure to moderate high-light stress several of the anthocyanin biosynthetic genes were induced in the *ssrp1/spt16* plants to a lesser extent than in the wild type, and accordingly the mutant plants depleted in FACT accumulated lower amounts of anthocyanin pigments. Expression of SSRP1 and SPT16 was increased under these conditions (Pfab et al., 2018a). Therefore, FACT is required for transcriptional induction leading to anthocyanin accumulation in response to light stress.

A special role of FACT that was discovered in *Arabidopsis* is its involvement in parent-of-origin specific gene expression (genomic imprinting). Initially, SSRP1 was found to be required for DNA demethylation and activation/repression of parentally imprinted genes in the central cell of the female gametophyte (Ikeda et al., 2011). The authors proposed that SSRP1 might contribute to altering the chromatin state, facilitating demethylation by the DNA demethylase DEMETER

(DME). Subsequently, bimolecular complementation assays indicated that SSRP1 and SPT16 colocalised with DME in the nucleus. Genome-wide analyses demonstrated that SSRP1 and SPT16 are required for demethylation at over half the DME-mediated demethylation sites in the central cell (Frost et al., 2018). DME demethylation sites that are particularly dependent on FACT occur in heterochromatic domains with high nucleosome occupancy and are enriched in H3K9me2 and H3K27me1 marks, whereas euchromatic DME targets apparently can be demethylated by the enzyme without assistance of FACT (Frost et al., 2018). Therefore, FACT may be required for DME targeting by facilitating its access to heterochromatic sites, but the exact molecular role of FACT in this process is unknown. Moreover, the authors suggest that the mode of FACT action in conjunction with DME during reproduction differs from that during transcriptional elongation.

PERSPECTIVES

There is substantial evidence that FACT in yeast and metazoa is involved in addition to transcription in various other DNA-dependent processes including replication, recombination and repair. To date essentially the role of plant FACT in transcription has been addressed, and therefore, broader approaches are required to gain insight to which extent it contributes to additional biologically crucial processes in plants. Open questions regarding FACT include how it is recruited to its target sites in chromatin. Analyses in yeast, for instance, indicate that FACT associates with the transcribed regions of all active RNAPII-transcribed genes (Mayer et al., 2010). However, various studies suggest that the absence of FACT causes rather moderate changes in gene expression of relatively small subsets of genes (Gurova et al., 2018). This raises the question, of why the transcription of certain genes is more dependent on FACT than the majority of other genes. Which gene characteristics determine the requirement for FACT action? There exist many potentially influencing parameters including DNA sequence, chromatin structural features, inducibility and expression level of the gene, RNAPII density and elongation rate, as well as cotranscriptional mRNA processing. Perhaps a combination of these and additional parameters defines the requirement of FACT for efficient transcription. Finally, because of the various functions of FACT in nucleosome reorganisation in different biological contexts it appears likely that FACT activity is regulated, but currently this is largely obscure. Although many facts about FACT have been elucidated in recent years, there remain important open questions.

AUTHOR CONTRIBUTIONS

KG wrote the manuscript.

FUNDING

German Research Foundation (DFG) through grants SFB960/A6 and Gr1159/14-2.

ACKNOWLEDGMENTS

The author thanks Philipp Michl-Holzinger for providing the images of **Figure 3** and critical reading of the manuscript and Simon Obermeyer for bioinformatics analyses. Our research is funded by the German Research Foundation (DFG) through grants SFB960/A6 and Gr1159/14-2.

SUPPLEMENTARY MATERIAL

The Supplementary Material for this article can be found online at: https://www.frontiersin.org/articles/10.3389/fpls.2020.00085/full#supplementary-material

REFERENCES

Antosch, M., Mortensen, S. A., and Grasser, K. D. (2012). Plant proteins containing high mobility group box DNA-binding domains modulate different nuclear processes. *Plant Physiol.* 159, 875–883. doi: 10.1104/pp.112.198283

Antosz, W., Pfab, A., Ehrnsberger, H. F., Holzinger, P., Köllen, K., Mortensen, S. A., et al. (2017). Composition of the Arabidopsis RNA polymerase II transcript elongation complex reveals the interplay between elongation and mRNA processing factors. *Plant Cell* 29, 854–870. doi: 10.1105/tpc.16.00735

Avvakumov, N., Nourani, A., and Côté, J. (2011). Histone chaperones: modulators of chromatin marks. *Mol. Cell* 41, 502–514. doi: 10.1016/j.molcel.2011.02.013

Belotserkovskaya, R., Oh, S., Bondarenko, V. A., Orphanides, G., Studitsky, V. M., and Reinberg, D. (2003). FACT facilitates transcription-dependent nucleosome alteration. *Science* 301, 1090–1093. doi: 10.1126/science.1085703

Belotserkovskaya, R., Saunders, A., Lis, J. T., and Reinberg, D. (2004). Transcription through chromatin: understanding a complex FACT. *Biochim. Biophys. Acta* 1677, 87–99. doi: 10.1016/j.bbaexp.2003.09.017

Brewster, N. K., Johnston, G. C., and Singer, R. A. (1998). Characterization of the CP complex, an abundant dimer of Cdc68 and Pob3 that regulates yeast transcriptional activation and chromatin repression. *J. Biol. Chem.* 273, 21972–21979. doi: 10.1074/jbc.273.34.21972

Brewster, N. K., Johnston, G. C., and Singer, R. A. (2001). A bipartite yeast SSRP1 analog comprised of Pob3 and Nhp6 proteins modulates transcription. *Mol. Cell. Biol.* 21, 3491–3502. doi: 10.1128/MCB.21.10.3491-3502.2001

Cao, S., Bendall, H., Hicks, G. G., Nashabi, A., Sakano, H., Shinkai, Y., et al. (2003). The high-mobility-group box protein SSRP1/T160 is essential for cell viability in day 3.5 mouse embryos. *Mol. Cell. Biol.* 23, 5301–5307. doi: 10.1128/MCB.23.15.5301-5307.2003

Cao, Y., Dai, Y., Cui, S., and Ma, L. (2008). Histone H2B monoubiquitination in the chromatin of FLOWERING LOCUS C regulates flowering time in Arabidopsis. *Plant Cell* 20, 2586–2602. doi: 10.1105/tpc.108.062760

Cheung, V., Chua, G., Batada, N. N., Landry, C. R., Michnick, S. W., Hughes, T. R., et al. (2008). Chromatin- and transcription-related factors repress transcription from within coding regions throughout the Saccharomyces cerevisiae genome. *PloS Biol.* 6, e277. doi: 10.1371/journal.pbio.0060277

Choi, K., Park, C., Lee, J., Oh, M., Noh, B., and Lee, I. (2007). Arabidopsis homologs of components of the SWR1 complex regulate flowering and plant development. *Development* 134, 1931–1941. doi: 10.1242/dev.001891

Das, C., Tyler, J. K., and Churchill, M. E. (2010). The histone shuffle: histone chaperones in an energetic dance. *Trends Biochem. Sci.* 35, 476–489. doi: 10.1016/j.tibs.2010.04.001

De Koning, L., Corpet, A., Haber, J. E., and Almouzni, G. (2007). Histone chaperones: an escort network regulating histone traffic. *Nat. Struct. Mol. Biol.* 14, 997–1007. doi: 10.1038/nsmb1318

Duroux, M., Houben, A., Ruzicka, K., Friml, J., and Grasser, K. D. (2004). The chromatin remodelling complex FACT associates with actively transcribed regions of the Arabidopsis genome. *Plant J.* 40, 660–671. doi: 10.1111/j.1365-313X.2004.02242.x

Formosa, T., Eriksson, P., Wittmeyer, J., Ginn, J., Yu, Y., and Stillman, D. J. (2001). Spt16-Pob3 and the HMG protein Nhp6 combine to form the nucleosome-binding factor SPN. *EMBO J.* 20, 3506–3517. doi: 10.1093/emboj/20.13.3506

Formosa, T. (2012). The role of FACT in making and breaking nucleosomes. *Biochim. Biophys. Acta* 1819, 247–255. doi: 10.1016/j.bbagrm.2011.07.009

Frost, J. M., Kim, M. Y., Park, G. T., Hsieh, P. H., Nakamura, M., Lin, S. J. H., et al. (2018). FACT complex is required for DNA demethylation at heterochromatin during reproduction in Arabidopsis. *Proc. Natl. Acad. Sci. U.S.A.* 115, E4720–E4729. doi: 10.1073/pnas.1713333115

Grasser, M., and Grasser, K. D. (2018). The plant RNA polymerase II elongation complex: A hub coordinating transcript elongation and mRNA processing. *Transcription* 9, 117–122. doi: 10.1080/21541264.2017.1356902

Gurard-Levin, Z. A., Quivy, J. P., and Almouzni, G. (2014). Histone chaperones: assisting histone traffic and nucleosome dynamics. *Ann. Rev. Biochem.* 83, 487–517. doi: 10.1146/annurev-biochem-060713-035536

Gurova, K., Chang, H. W., Valieva, M. E., Sandlesh, P., and Studitsky, V. M. (2018). Structure and function of the histone chaperone FACT - Resolving FACTual issues. *Biochim. Biophys. Acta* 1861, 892–904. doi: 10.1016/j.bbagrm.2018.07.008

Hammond, C. M., Strømme, C. B., Huang, H., Patel, D. J., and Groth, A. (2017). Histone chaperone networks shaping chromatin function. *Nat. Rev. Mol. Cell Biol.* 18, 141–158. doi: 10.1038/nrm.2016.159

He, Y., Doyle, M. R., and Amasino, R. M. (2004). PAF1-complex-mediated histone methylation of FLOWERING LOCUS C chromatin is required for the vernalization-responsive, winter-annual habit in Arabidopsis. *Genes Dev.* 18, 2774–2784. doi: 10.1101/gad.1244504

Henikoff, S. (2008). Nucleosome destabilization in the epigenetic regulation of gene expression. *Nat. Rev. Genet.* 9, 15–26. doi: 10.1038/nrg2206

Hondele, M., Stuwe, T., Hassler, M., Halbach, F., Bowman, A., Zhang, E. T., et al. (2013). Structural basis of histone H2A–H2B recognition by the essential chaperone FACT. *Nature* 499, 111–114. doi: 10.1038/nature12242

Ikeda, Y., Kinoshita, Y., Susaki, D., Ikeda, Y., Iwano, M., Takayama, S., et al. (2011). HMG domain containing SSRP1 is required for DNA demethylation and genomic imprinting in Arabidopsis. *Dev. Cell* 21, 589–596. doi: 10.1016/j.devcel.2011.08.013

Jamai, A., Puglisi, A., and Strubin, M. (2009). Histone chaperone Spt16 promotes redeposition of the original H3-H4 histones evicted by elongating RNA polymerase. *Mol. Cell* 35, 377–383. doi: 10.1016/j.molcel.2009.07.001

Kaplan, C. D., Laprade, L., and Winston, F. (2003). Transcription elongation factors repress transcription initiation from cryptic sites. *Science* 301, 1096–1099. doi: 10.1126/science.1087374

Kemble, D. J., McCullough, L. L., Whitby, F. G., Formosa, T., and Hill, C. P. (2015). FACT disrupts nucleosome structure by binding H2A-H2B with conserved peptide motifs. *Mol. Cell* 60, 294–306. doi: 10.1016/j.molcel.2015.09.008

Kornberg, R. D., and Lorch, Y. (1999). Twenty-five years of the nucleosome, fundamental particle of the eukaryotic chromosome. *Cell* 98, 285–294. doi: 10.1016/S0092-8674(00)81958-3

Krohn, N. M., Stemmer, C., Fojan, P., Grimm, R., and Grasser, K. D. (2003). Protein kinase CK2 phosphorylates the high mobility group domain protein SSRP1, inducing the recognition of UV-damaged DNA. *J. Biol. Chem.* 278, 12710–12715. doi: 10.1074/jbc.M300250200

Kumar, A., and Vasudevan, D. (2020). Structure-function relationship of H2A-H2B specific plant histone chaperones. *Cell Stress Chaperones In Press* 25, 1–17. doi: 10.1007/s12192-019-01050-7

Lázaro, A., Gómez-Zambrano, A., López-González, L., Piñeiro, M., and Jarillo, J. A. (2008). Mutations in the Arabidopsis SWC6 gene, encoding a component of the SWR1 chromatin remodelling complex, accelerate flowering time and alter leaf and flower development. *J. Exp. Bot.* 59, 653–666. doi: 10.1093/jxb/erm332

Li, B., Carey, M., and Workman, J. L. (2007). The role of chromatin during transcription. *Cell* 128, 707–719. doi: 10.1016/j.cell.2007.01.015

Lichota, J., and Grasser, K. D. (2001). Differential chromatin association and nucleosome binding of the maize HMGA, HMGB, and SSRP1 proteins. *Biochemistry* 40, 7860–7867. doi: 10.1021/bi010548y

Liu, Y., Koornneef, M., and Soppe, W. J. (2007). The absence of histone H2B monoubiquitination in the Arabidopsis hub1 (rdo4) mutant reveals a role for chromatin remodeling in seed dormancy. *Plant Cell* 19, 433–444. doi: 10.1105/tpc.106.049221

Liu, J., Feng, L., Li, J., and He, Z. (2015). Genetic and epigenetic control of plant heat responses. *Front. Plant Sci.* 6, 267. doi: 10.3389/fpls.2015.00267

Liu, Y., Zhou, K., Zhang, N., Wei, H., Tan, Y. Z., Zhang, Z., et al. (2020). FACT caught in the act of manipulating the nucleosome. *Nature* 577, 426–431. doi: 10.1038/s41586-019-1820-0

Lolas, I. B., Himanen, K., Grønlund, J. T., Lynggaard, C., Houben, A., Melzer, M., et al. (2010). The transcript elongation factor FACT affects Arabidopsis vegetative and reproductive development and genetically interacts with HUB1/2. *Plant J.* 61, 686–697. doi: 10.1111/j.1365-313X.2009.04096.x

Luger, K., and Richmond, T. J. (1998). DNA binding within the nucleosome core. *Curr. Opin. Struct. Biol.* 8, 33–40. doi: 10.1016/S0959-440X(98)80007-9

Ma, Y., Gil, S., Grasser, K. D., and Mas, P. (2018). Targeted recruitment of the basal transcriptional machinery by LNK clock components controls the circadian rhythms of nascent RNAs in Arabidopsis. *Plant Cell* 30, 907–924. doi: 10.1105/tpc.18.00052

Malarkey, C. S., and Churchill, M. E. (2012). The high mobility group box: the ultimate utility player of a cell. *Trends Biochem. Sci.* 37, 553–562. doi: 10.1016/j.tibs.2012.09.003

Mason, P. B., and Struhl, K. (2003). The FACT complex travels with elongating RNA polymerase II and is important for the fidelity of transcriptional initiation *in vivo*. Mol. *Cell. Biol.* 23, 8323–8333. doi: 10.1128/MCB.23.22.8323-8333.2003

Mayer, A., Lidschreiber, M., Siebert, M., Leike, K., Söding, J., and Cramer, P. (2010). Uniform transitions of the general RNA polymerase II transcription complex. *Nat. Struct. Mol. Biol.* 17, 1272–1278. doi: 10.1038/nsmb.1903

McCullough, L. L., Connell, Z., Xin, H., Studitsky, V. M., Feofanov, A. V., Valieva, M. E., et al. (2018). Functional roles of the DNA-binding HMGB domain in the histone chaperone FACT in nucleosome reorganization. *J. Biol. Chem.* 293, 6121–6133. doi: 10.1074/jbc.RA117.000199

McGhee, J. D., and Felsenfeld, G. (1980). Nucleosome structure. *Ann. Rev. Biochem.* 49, 1115–1156. doi: 10.1146/annurev.bi.49.070180.005343

Michl-Holzinger, P., Mortensen, S. A., and Grasser, K. D. (2019). The SSRP1 subunit of the histone chaperone FACT is required for seed dormancy in Arabidopsis. *J. Plant Physiol.* 236, 108. doi: 10.1016/j.jplph.2019.03.006

Molitor, A. M., Bu, Z., Yu, Y., and Shen, W. H. (2014). Arabidopsis AL PHD-PRC1 complexes promote seed germination through H3K4me3-to-H3K27me3 chromatin state switch in repression of seed developmental genes. *PloS Genet.* 10, e1004091. doi: 10.1371/journal.pgen.1004091

Nielsen, M., Ard, R., Leng, X., Ivanov, M., Kindgren, P., Pelechano, V., et al. (2019). Transcription-driven chromatin repression of intragenic transcription start sites. *PloS Genet.* 15, e1007969. doi: 10.1371/journal.pgen.1007969

Oh, S., Zhang, H., Ludwig, P., and van Nocker, S. (2004). A mechanism related to the yeast transcriptional regulator Paf1c is required for expression of the Arabidopsis FLC/MAF MADS box gene family. *Plant Cell* 16, 2940–2953. doi: 10.1105/tpc.104.026062

Orphanides, G., LeRoy, G., Chang, C.-H., Luse, D. S., and Reinberg, D. (1998). FACT, a factor that facilitates transcript elongation through nucleosomes. *Cell* 92, 105–116. doi: 10.1016/S0092-8674(00)80903-4

Orphanides, G., Wu, W.-H., Lane, W. S., Hampsey, M., and Reinberg, D. (1999). The chromatin-specific transcription elongation factor FACT comprises human SPT16 and SSRP1 proteins. *Nature* 400, 284–288. doi: 10.1038/22350

Otero, S., Desvoyes, B., and Gutierrez, C. (2014). Histone H3 dynamics in plant cell cycle and development. *Cytogenet. Genome Res.* 143, 114–124. doi: 10.1159/000365264

Perales, M., and Más, P. (2007). A functional link between rhythmic changes in chromatin structure and the Arabidopsis biological clock. *Plant Cell* 19, 2111–2123. doi: 10.1105/tpc.107.050807

Pfab, A., Breindl, M., and Grasser, K. D. (2018a). The Arabidopsis histone chaperone FACT is required for stress-induced expression of anthocyanin biosynthetic genes. *Plant Mol. Biol.* 96, 367–374. doi: 10.1007/s11103-018-0701-5

Pfab, A., Grønlund, J. T., Holzinger, P., Längst, G., and Grasser, K. D. (2018b). The Arabidopsis histone chaperone FACT: role of the HMG-box domain of SSRP1. *J. Mol. Biol.* 430, 2747–2759. doi: 10.1016/j.jmb.2018.06.046

Probst, A. V., and Mittelsten Scheid, O. (2015). Stress-induced structural changes in plant chromatin. *Curr. Opin. Plant Biol.* 27, 8–16. doi: 10.1016/j.pbi.2015.05.011

Röttgers, K., Krohn, N. M., Lichota, J., Stemmer, C., Merkle, T., and Grasser, K. D. (2000). DNA-interactions and nuclear localisation of the chromosomal HMG domain protein SSRP1 from maize. *Plant J.* 23, 395–405. doi: 10.1046/j.1365-313x.2000.00801.x

Ramirez-Parra, E., and Gutierrez, C. (2007). The many faces of chromatin assembly factor 1. *Trends Plant Sci.* 12, 570–576. doi: 10.1016/j.tplants.2007.10.002

Reinberg, D., and Sims, R. J. (2006). de FACTo nucleosome dynamics. *J. Biol. Chem.* 281, 23297–23301. doi: 10.1074/jbc.R600007200

Singer, R. A., and Johnston, G. C. (2004). The FACT chromatin modulator: genetic and structure/function relationships. *Biochem. Cell Biol.* 82, 419–427. doi: 10.1139/o04-050

Takatsuka, H., and Umeda, M. (2015). Epigenetic control of cell division and cell differentiation in the root apex. *Front. Plant Sci.* 6, 1178. doi: 10.3389/fpls.2015.01178

Tripathi, A. K., Singh, K., Pareek, A., and Singla-Pareek, S. L. (2015). Histone chaperones in Arabidopsis and rice: genome-wide identification, phylogeny, architecture and transcriptional regulation. *BMC Plant Biol.* 15, 42. doi: 10.1186/s12870-015-0414-8

Tsunaka, Y., Fujiwara, Y., Oyama, T., Hirose, S., and Morikawa, K. (2016). Integrated molecular mechanism directing nucleosome reorganization by human FACT. *Genes Dev.* 30, 673–686. doi: 10.1101/gad.274183.115

Valieva, M. E., Armeev, G. A., Kudryashova, K. S., Gerasimova, N. S., Shaytan, A. K., Kulaeva, O. I., et al. (2016). Large-scale ATP-independent nucleosome unfolding by a histone chaperone. *Nat. Struct. Mol. Biol.* 23, 1111–1116. doi: 10.1038/nsmb.3321

Van Lijsebettens, M., and Grasser, K. D. (2014). Transcript elongation factors: shaping transcriptomes after transcript initiation. *Trends Plant Sci.* 19, 717–726. doi: 10.1016/j.tplants.2014.07.002

Wang, T., Liu, Y., Edwards, G., Krzizke, D., Scherman, H., and Luger, K. (2018). The histone chaperone FACT modulates nucleosome structure by tethering its components. *Life Sci. Alliance* 1, e201800107. doi: 10.26508/lsa.201800107

Winkler, D. D., and Luger, K. (2011). The histone chaperone FACT: structural insights and mechanisms for nucleosome reorganization. *J. Biol. Chem.* 286, 18369–18374. doi: 10.1074/jbc.R110.180778

Winkler, D. D., Muthurajan, U. M., Hieb, A. R., and Luger, K. (2011). Histone chaperone FACT coordinates nucleosome interaction through multiple synergistic binding events. *J. Biol. Chem.* 286, 41883–41892. doi: 10.1074/jbc.M111.301465

Wittmeyer, J., Joss, L., and Formosa, T. (1999). Spt16 and Pob3 of Saccharomyces cerevisiae form an essential, abundant heterodimer that is nuclear, chromatin-associated, and copurifies with DNA polymerase a. *Biochemistry* 38, 8961–8971. doi: 10.1021/bi982851d

Xin, H., Takahata, S., Blanksma, M., McCullough, L., Stillman, D. J., and Formosa, T. (2009). yFACT induces global accessibility of nucleosomal DNA without H2A-H2B displacement. *Mol. Cell* 35, 365–376. doi: 10.1016/j.molcel.2009.06.024

Zhao, Z., Yu, Y., Meyer, D., Wu, C., and Shen, W.-H. (2005). Prevention of early flowering by expression of FLOWERING LOCUS C requires methylation of histone H3K36. *Nat. Cell Biol.* 7, 1256–1260. doi: 10.1038/ncb1329

Zheng, J., Chen, F., Wang, Z., Cao, H., Li, X., Deng, X., et al. (2012). A novel role for histone methyltransferase KYP/SUVH4 in the control of Arabidopsis primary seed dormancy. *New Phytol.* 193, 605–616. doi: 10.1111/j.1469-8137.2011.03969.x

Zhou, W., Zhu, Y., Dong, A., and Shen, W.-H. (2015). Histone H2A/H2B chaperones: from molecules to chromatin-based functions in plant growth and development. *Plant J.* 83, 78–95. doi: 10.1111/tpj.12830

Zhou, K., Gaullier, G., and Luger, K. (2019). Nucleosome structure and dynamics are coming of age. *Nat. Struct. Mol. Biol.* 26, 3–13. doi: 10.1038/s41594-018-0166-x

Zhu, Y., Dong, A., and Shen, W. H. (2013). Histone variants and chromatin assembly in plant abiotic stress responses. *Biochim. Biophys. Acta* 1819, 343–348. doi: 10.1016/j.bbagrm.2011.07.012

Conflict of Interest: The author declares that the research was conducted in the absence of any commercial or financial relationships that could be construed as a potential conflict of interest.

frontiers in Plant Science

REVIEW
published: 21 February 2020
doi: 10.3389/fpls.2020.00125

Insights Into the Function of the NuA4 Complex in Plants

Loreto Espinosa-Cores†, Laura Bouza-Morcillo†, Javier Barrero-Gil, Verónica Jiménez-Suárez, Ana Lázaro, Raquel Piqueras, José A. Jarillo and Manuel Piñeiro**

Centro de Biotecnología y Genómica de Plantas, Universidad Politécnica de Madrid (UPM) - Instituto Nacional de Investigación y Tecnología Agraria y Alimentaria (INIA), Madrid, Spain

OPEN ACCESS

Edited by:
Sara Farrona, National University of Ireland Galway, Ireland

Reviewed by:
Konstantinos Vlachonasios, Aristotle University of Thessaloniki, Greece
Piotr Andrzej Ziolkowski, Adam Mickiewicz University, Poland

***Correspondence:**
José A. Jarillo
jarillo@inia.es
Manuel Piñeiro
pineiro@inia.es

†These authors have contributed equally to this work

Specialty section:
This article was submitted to Plant Cell Biology, a section of the journal Frontiers in Plant Science

Received: *22 November 2019*
Accepted: *28 January 2020*
Published: *21 February 2020*

Citation:
Espinosa-Cores L, Bouza-Morcillo L, Barrero-Gil J, Jiménez-Suárez V, Lázaro A, Piqueras R, Jarillo JA and Piñeiro M (2020) Insights Into the Function of the NuA4 Complex in Plants. Front. Plant Sci. 11:125. doi: 10.3389/fpls.2020.00125

Chromatin remodeling plays a key role in the establishment and maintenance of gene expression patterns essential for plant development and responses to environmental factors. Post-translational modification of histones, including acetylation, is one of the most relevant chromatin remodeling mechanisms that operate in eukaryotic cells. Histone acetylation is an evolutionarily conserved chromatin signature commonly associated with transcriptional activation. Histone acetylation levels are tightly regulated through the antagonistic activity of histone acetyltransferases (HATs) and histone deacetylases (HDACs). In plants, different families of HATs are present, including the MYST family, which comprises homologs of the catalytic subunit of the Nucleosome Acetyltransferase of H4 (NuA4) complex in yeast. This complex mediates acetylation of histones H4, H2A, and H2A.Z, and is involved in transcriptional regulation, heterochromatin silencing, cell cycle progression, and DNA repair in yeast. In Arabidopsis and, other plant species, homologs for most of the yeast NuA4 subunits are present and although the existence of this complex has not been demonstrated yet, compelling evidence supports the notion that this type of HAT complex functions from mosses to angiosperms. Recent proteomic studies show that several Arabidopsis homologs of NuA4 components, including the assembly platform proteins and the catalytic subunit, are associated *in vivo* with additional members of this complex suggesting that a NuA4-like HAT complex is present in plants. Furthermore, the functional characterization of some Arabidopsis NuA4 subunits has uncovered the involvement of these proteins in the regulation of different plant biological processes. Interestingly, for most of the mutant plants deficient in subunits of this complex characterized so far, conspicuous defects in flowering time are observed, suggesting a role for NuA4 in the control of this plant developmental program. Moreover, the participation of Arabidopsis NuA4 homologs in other developmental processes, such as gametophyte development, as well as in cell proliferation and stress and hormone responses, has also been reported. In this review, we summarize the current state of knowledge on plant putative NuA4 subunits and discuss the latest progress concerning the function of this chromatin modifying complex.

Keywords: chromatin, histone acetylation, NuA4, TIP60, SWR1, Arabidopsis, development, flowering time

INTRODUCTION

In eukaryotic organisms, DNA is present in the nucleus in a highly compacted structure known as chromatin, in which nucleosomes are the basic structural units. Each nucleosome encompasses a histone octamer (two H2A-H2B dimers and an H3-H4 tetramer), and 147 bp of DNA wrapped around the histone octamer (Luger et al., 1997). However, the fact that DNA is packaged into the nucleus complicates the access of nuclear machinery that mediates different cellular processes such as transcription, replication or DNA repair (Luger et al., 2012). Chromatin needs to be relaxed by remodelers to allow these processes to take place, making the structure of nucleosomes very dynamic (Venkatesh and Workman, 2015). In particular, the reorganization of chromatin is pivotal for the establishment of gene expression patterns that drive developmental programs and environmental responses in eukaryotes (Xiao et al., 2017). Chromatin remodeling can be carried out by complexes that i) use ATP hydrolysis to alter the interaction between the DNA and the histone octamer non-covalently (Clapier et al., 2017); ii) catalyze the exchange of canonical histones by histone variants, which have specialized functions and differ in sequence from the canonical histones (Talbert and Henikoff, 2017); and iii) are involved in the covalent modification of histones and DNA, which affect the condensation status of chromatin (Bhaumik et al., 2007). The post-translational modification (PTM) of histones occurs mostly in the amino-terminal tails, and is one of the most important mechanisms to regulate chromatin dynamics. These covalent modifications include, among others, lysine (K) acetylation, ubiquitination, and methylation, arginine methylation, and phosphorylation (Bannister and Kouzarides, 2011). In addition, DNA is also a methylation target (Law and Jacobsen, 2010). Many of these modifications have functions in transcription, and some may also accomplish roles in DNA repair, replication or chromatin condensation (Kouzarides, 2007).

The combination and crosstalk among different PTMs constitutes a histone code that sets the basis for epigenetic transcriptional regulation and adds an extra level of regulation overlying those mediated by transcription factors (Strahl and Allis, 2000; Rothbart and Strahl, 2014). Some histone modifications such as trimethylation of lysine 27 in histone H3 (H3K27me3) and H3K9me2 are commonly associated with transcriptional repression (Shahbazian and Grunstein, 2007; Schuettengruber et al., 2017), whereas H3 and H4 acetylation, H3K4me3, and H3K36me3 are marks linked to transcriptionally active states (Pokholok et al., 2005; Black et al., 2012). PTMs act as recruitment platforms for effector proteins that modify the transcriptional status of underlying genes. However, histone acetylation has an additional physical effect on chromatin structure. The addition of a negatively charged acetyl group to K has been proposed to neutralize the positive charge of K in histones. This reduces the affinity of the histone tail for the DNA and contributes to release the interaction between histones and DNA, and to open the chromatin (Barnes et al., 2019). Due to its great impact on a myriad of cellular and developmental processes, the antagonistic action of two classes of enzymes, histone deacetylases (HDACs), and histone acetyltransferases (HATs), has been the subject of a growing number of studies (Liu et al., 2014; Hu et al., 2019).

HATs are evolutionarily conserved from yeast to humans, including plants, and they usually function as multiprotein complexes defined by the catalytic subunit responsible for the transfer of acetyl groups to K residues (Lee and Workman, 2007). There are at least four families of HATs including GNAT (Gcn5-related N-acetyltransferase), MYST (MOZ, YbF2, Sas2, Tip60-like), p300/CREB-binding protein (CBP), and $TAF_{II}250$ families. Eukaryotic genomes usually contain multiple members of each family illustrating their relevance for chromatin function. For example, in *Arabidopsis thaliana* twelve HATs have been identified. Three of them belong to the GNAT-MYST superfamily, five to the p300/CBP family, two to the $TAF_{II}250$, and two more to the MYST family (Berr et al., 2011; Liu et al., 2016).

The MYST family of HATs is the largest one and is present in all eukaryotes. One of the best characterized complexes included in this family is the yeast Nucleosome Acetyltransferase of Histone H4 (NuA4) complex, highly conserved in eukaryotes. NuA4 is involved in different genomic processes such as DNA damage repair and transcription, heterochromatin silencing, cell cycle progression, and chromosome stability (Clarke et al., 1999; Doyon and Côté, 2004; Lee and Workman, 2007; Lu et al., 2009; Uprety et al., 2012; Bruzzone et al., 2018; Hodges et al., 2019). NuA4 was initially described in yeast to acetylate nucleosomal histones at specific gene promoters (Ginsburg et al., 2009), although later studies showed that this complex is also present in actively transcribed coding sequences (Steunou et al., 2016). Besides acetylating histone H4, NuA4 also acts on histone H2A (Boudreault et al., 2003) and the variant H2A.Z (Millar et al., 2006; Valdés-Mora et al., 2012). In mammals and flies, NuA4 evolved into a hybrid complex known as TIP60 (Cai et al., 2003), formed by subunits that in yeast belong to NuA4 and the ATP-dependent SWI2/SNF2-Related 1 chromatin remodeling complex (SWR1), that mediates the exchange of histone H2A by the histone variant H2A.Z (Voss and Thomas, 2009). NuA4 also acetylates non-histone protein substrates in yeast and metazoans, ascribing to this complex additional roles in controlling metabolism, autophagy, and homeostasis (Lin et al., 2009; Narita et al., 2019).

Most of the yeast NuA4 subunits are widely conserved in plants where more than one homolog for members of the complex are frequently found. This is the case of *Arabidopsis thaliana,* in which many NuA4 components, including the putative catalytic subunits HISTONE ACETYLTRANSFERASE OF THE MYST FAMILY (HAM1/2) (Latrasse et al., 2008), are duplicated. Recent proteomic analyses performed with Arabidopsis homologs of NuA4 subunits have revealed that most of the components of this complex associate to each other *in vivo* (Bieluszewski et al., 2015; Tan et al., 2018; Crevillén et al., 2019). In plants, mutants for different NuA4 subunits characterized so far display pleiotropic vegetative and reproductive alterations, such as abnormal flowering time (Latrasse et al., 2008; Umezawa et al., 2013; Xiao et al., 2013; Bu et al., 2014; Xu et al., 2014; Bieluszewski et al., 2015; Gómez-

Zambrano et al., 2018; Peng et al., 2018; Crevillén et al., 2019), suggesting the involvement of NuA4 in the control of central plant developmental processes through acetylation-mediated regulation of gene expression. In this review, we discuss the possible existence of NuA4 in plants, and describe the biological functions carried out by different homolog subunits of NuA4 studied in Arabidopsis. We speculate with future directions of the research aimed at confirming the conservation of this HAT complex in plants and characterizing its role in the control of gene expression to regulate different plant developmental programs and environmental responses.

ORGANIZATION OF THE NuA4 COMPLEX: LESSONS FROM YEAST AND METAZOANS

The structure and molecular architecture of yeast NuA4 have been characterized by cryo-electron microscopy as well as by studying the interactions between the different subunits (Chittuluru et al., 2011; Wang et al., 2018a). Yeast NuA4 comprises 13 subunits including the catalytic subunit Esa1, together with Enhancer of polycomb-like1 (Epl1), the inhibitor of growth (ING) factor Yng2, Esa1-associated factor 6 (Eaf6), Transcription-associated protein 1 (Tra1), Eaf1, Eaf3, Eaf5, Eaf7, Actin-related protein 4 (Arp4), Actin1 (Act1), Yeast all fused gene from chromosome 9 (Yaf9), and SWR1 COMPLEX 4 (Swc4)/Eaf2 subunits (**Table 1**). Interestingly, most of the components of this 1.0-MDa complex are shared with other chromatin remodeling complexes. For instance, Swc4, Yaf9, Arp4, and Act1 are members of SWR1, and therefore are also involved in the exchange of H2A-H2B by H2A.Z-H2B dimers (Gerhold and Gasser, 2014). Tra1 is also part of the recruitment module in SAGA and SAGA-like (SLIK)/SALSA complexes (Helmlinger and Tora, 2017). Arp4 and Act1 are additionally present in the INO80 ATP-dependent chromatin remodeling complex (Chen et al., 2013), while Eaf3 is a component of the Reduced Potassium Dependency-3 Small (Rpd3S) HDAC complex (Carrozza et al., 2005; Keogh et al., 2005), and Eaf6 is also found in the yeast NuA3 (Taverna et al., 2006), HUMAN ACETYLASE BINDING TO ORC1 (HBO1) (Avvakumov et al., 2012), and MONOCYTIC LEUKEMIC ZINC-FINGER PROTEIN (MOZ)/MOZ RELATED FACTOR (MORF) HAT complexes (Yang and Ullah, 2007). Even the catalytic subunit in metazoans complexes is not exclusively present in TIP60 since it can also be found in HBO1 and MOZ HATs (Xu et al., 2016). Highlighting the strong conservation of this complex throughout evolution, most of the NuA4 subunits display high homology with the TIP60 HAT complex in *Homo sapiens*, in which twelve out of the thirteen subunits are conserved (**Table 1**) (Cai et al., 2003; Doyon and Côté, 2004).

Interestingly, the biochemical isolation of two NuA4 subcomplexes lacking the full array of subunits has been reported in yeast: the Piccolo (Boudreault et al., 2003), and the Trimer Independent of NuA4 involved in Transcription Interactions with Nucleosomes (TINTIN) (Rossetto et al., 2014; Wang et al., 2018a). Both subcomplexes work independently of the core NuA4 and have specific functions

TABLE 1 | NuA4 conserved subunits from yeast to humans.

	NuA4 conserved subunits				
	S. cerevisiae	***A. thaliana***	***O. sativa***	***D. melanogaster* (TIP60)**	***H. sapiens* (TIP60)**
Piccolo NuA4	Epl1	AtEPL1A (AT1G16690) AtEPL1B (AT1G79020)	Os09g0284600 Os08g0338900	E(Pc)	EPC1
	Eaf6	AtEAF6 (AT4G14385)	Os12g0298600 Os01g0233400	Eaf6	EAF6
	Yng2	AtING1 (AT3G24010) AtING2 (AT1G54390)	Os03g0143600 Os03g0748200	ING3	ING3
	Esa1	AtHAM1 (AT5G64610) AtHAM2 (AT5G09740)	Os07g0626600	TIP60	TIP60
Assembly platform	Tra1	AtTRA1 (AT4G36080) AtTRA2 (AT2G17930)	Os07g0645100	dTRA1	TRRAP
	Eaf1	AtEAF1A (AT3G24880) AEAF1B (AT3G24870)	Os08g0177300	Domino/p400	Domino/p400
TINTIN	Eaf5	-			
	Eaf7	AtEAF7 (AT1G26470)	Os05g0512500	MRGBP	MRGBP
	Eaf3	AtMRG1 (AT4G37280) AtMRG2 (AT1G02740)	OsMRG701 (Os04g0101300) OsMRG702 (Os11g0545600)	MRG15	MRG15
SWR1 shared module	Swc4	AtSWC4 (AT2G47210)	Os05g0540800	DMAP1	DMAP1
	Yaf9	AtYAF9A (AT5G45600) AtYAF9B (AT2G18000)	Os06g0137300	GAS41	GAS41
	Act1	8, including AT2G37620 and AT3G53750	Os03g0718150	Act88F	Act1
	Arp4	AtARP4 (AT1G18450) AtARP4A (AT1G73910)	Os08g0137200	BAP55	BAF53

Composition of NuA4-like complexes from model organisms such as S. cerevisiae, D. melanogaster, H. sapiens (Doyon and Côté, 2004; Sapountzi et al., 2006), A thaliana and O sativa are included. Annotations for Arabidopsis and rice NuA4 homolog proteins come from the Arabidopsis Information Resource (TAIR) (https://www.arabidopsis.org/) and the Rice Annotation Project Database (https://rapdb.dna.affrc.go.jp/index.html), respectively.

(Mitchell et al., 2008). A recent study has addressed the spatial structure of NuA4 by performing single-particle electron microscopy. This approach has revealed that NuA4 has a trilobal structure with a central core and two lobes. The central core contains Tra1, the Piccolo module and Eaf1, while lobe 1 is formed by the TINTIN sub-module, and lobe 2 is composed of the four subunits shared with SWR1 (Setiaputra et al., 2018). Studies carried out in parallel performed cryoelectron microscopy and released the crystal structure of the Piccolo NuA4 core complex unveiling the histone H4 acetylation mechanism in the context of the nucleosome (Xu et al., 2016). This type of approach is shedding light on how this multisubunit complex assembles with the nucleosomal substrate to regulate gene expression.

A Small Version of NuA4: the Piccolo NuA4 Complex

The yeast Piccolo NuA4 is composed of Esa1, Epl1, Yng2, and Eaf6 subunits (**Table 1**). This complex is responsible for the non-targeted Esa1-mediated acetylation of chromatin, and also for the interaction of NuA4 with the nucleosome core particle (Chittuluru et al., 2011). Esa1 is the only essential acetyltransferase in *Saccharomyces cerevisiae* (Allard et al., 1999). This subunit alone is able to acetylate free histones while it acetylates nucleosomal H4, H2A, and H2A.Z histones *in vivo* when is present in Piccolo NuA4 complex (Keogh et al., 2006; Millar et al., 2006; Lu et al., 2009; Mehta et al., 2010). Esa1 contains a chromodomain (CHD) at the N-terminus and a C-terminal MYST domain. Mutations in the CHD domain, which is required to acetylate nucleosomes *in vitro* but not free histones, are lethal (Doyon and Côté, 2004; Steunou et al., 2016). Esa1 was originally described to be required for double-strand breaks repair (Bird et al., 2002; Lee and Workman, 2007). In addition, as a component of Piccolo NuA4, this subunit has a role in transcriptional regulation of ribosomal protein genes (Uprety et al., 2015) and autophagy response (Yi et al., 2012).

The Epl1 subunit is essential for the interaction of the Piccolo NuA4 complex with nucleosomes (Chittuluru et al., 2011). This is the yeast ortholog of the human EPC1/2 paralogs and the *Drosophila melanogaster* Enhancer of Polycomb (E(Pc)) protein, originally described as an enhancer of trithorax and polycomb mutations (Searle and Pillus, 2018). Epl1 bears two differentiated domains: the C-terminus, which connects Epl1 and the Piccolo complex to the rest of NuA4 through Eaf1, and the EPcA domain in the N-terminus, which physically interacts with the rest of subunits of the Piccolo complex. A short region of the EPcA domain is required for binding to nucleosomes and histone H2A tail, an interaction necessary for the acetylation of nucleosomal H4 (Steunou et al., 2016). The EPcA domain interacts with Esa1 promoting its activation. Then, Esa1 binds the nucleosome through its CHD domain, projecting its catalytic pocket towards the N-terminal tail of H4. The acetylation occurs through a double recognition mechanism of a short sequence of the histone H4 N-terminal tail and the spatial orientation of the histone after the binding of Esa1 with the nucleosome (Xu et al., 2016).

Yng2 is also critical for the Piccolo NuA4 HAT activity on nucleosomes *in vitro* and histone H4 acetylation *in vivo* (Steunou et al., 2016). This subunit belongs to the highly conserved ING tumor suppressor family (Aguissa-Touré et al., 2011) and contains a Plant Homeo-Domain (PHD) and a short polybasic region at its C-terminal domain (Guérillon et al., 2013). The PHD domain binds H3K4me3 near the transcription start sites (TSS) of active genes (Peña et al., 2006). The recognition of H3K4me3 by Yng2 both at the promoter and coding sequences of genes has been proposed to recruit NuA4 to gene promoter regulatory regions. Subsequently, Yng2 positions the Piccolo complex for the acetylation of specific K residues of H4 and H2A histones, providing to this complex the function of maintaining the basal levels of H4 and H2A acetylation (Chittuluru et al., 2011).

The fourth Piccolo subunit, Eaf6, is a small 13-kDa protein without known domains except for a putative leucine zipper region (Doyon and Côté, 2004). The contribution of Eaf6 to the transcriptional regulation mediated by NuA4 has not been fully addressed and awaits further characterization. Recent observations reveal that Eaf6 (in humans, CENP-28) is also present at the centromere, and participates in the induction of centromeric transcription (Molina et al., 2016), possibly acting independently of NuA4.

The Assembly Platform of NuA4 Contains Eaf1 and Tra1 Subunits

Among the subunits of yeast NuA4, Eaf1 is, together with Epl1, the only subunit present exclusively in this complex (**Table 1**) (Auger et al., 2008; Wang et al., 2018a). Eaf1 directly contacts multiple subunits and occupies the central portion of the NuA4 core. This protein has been proposed to be the assembly platform of NuA4 (Mitchell et al., 2008). In fact, the removal of Eaf1 subunit results in the loss of NuA4 integrity and the collapse of the full complex (Mitchell et al., 2008; Setiaputra et al., 2018). This protein contains a SANT (Swi3, Ada2, N-Cor, and TFIIIB) domain involved in interactions with DNA and histone tails, and also shows structural similarities with p400/Domino, a subunit of TIP60 (**Table 1**) (Cai et al., 2003). Eaf1 directly binds Tra1 through its SANT domain and both proteins constitute the assembly platform of NuA4. Eaf1 also contains a Helicase/SANT-associated (HSA) domain that interacts with the Epl1 C-terminus and bridges the Piccolo module to the rest of NuA4 (Wang et al., 2018a).

Tra1, known as TRRAP in humans, is another important and conserved subunit of the central core of the yeast NuA4 (**Table 1**). There are few demonstrated interactions between this large protein and the rest of NuA4 components, and is located in the opposite domain of the Piccolo complex (Chittuluru et al., 2011). This subunit belongs to the Phosphatidylinositol-3 kinase-related kinase (PIKK) family and is an essential protein since its deletion is lethal in yeast and mammals (Helmlinger et al., 2011; Berg et al., 2018). Recent analysis of the three-dimensional structure of this protein by electron microscopy indicates that Tra1 has a rigid structure, highly conserved in both SAGA and NuA4 complexes (Cheung and Díaz-Santín, 2019).

The TINTIN Complex

TINTIN is a NuA4 subcomplex composed of Eaf3, Eaf5, and Eaf7 subunits in yeast (**Table 1**) (Cheng and Côté, 2014; Rossetto et al., 2014; Wang et al., 2018a). This complex is tethered to NuA4 through the interaction of Eaf5 with Eaf1. In turn, Eaf7 connects Eaf5 with Eaf3 (Auger et al., 2008; Rossetto et al., 2014). Mutants of these subunits do not show the same phenotypic alterations as the other subunits of the complex, suggesting that TINTIN may have additional functions to those exerted by NuA4 (Mitchell et al., 2008). TINTIN appears more enriched over coding regions than in promoters, suggesting its possible role in transcriptional elongation (Rossetto et al., 2014). Additional TINTIN co-transcriptional roles in mRNA processing, termination, and quality control have been reported revealing some connections with the mRNA splicing machinery and the nuclear exosome (Bhat et al., 2015).

Eaf3 and the human MORF4-related gene on chromosome 15 (MRG15) homolog belong to the Morf Related Gene (MRG) protein family and act as H3K36me3 "readers" (**Table 1**) (Reid et al., 2004). The Eaf3 subunit contains different specific domains: a CHD domain at its N-terminus responsible for binding H3K36 methylated residues, a putative DNA binding region, and a large highly conserved MRG domain. Eaf3 seems to be crucial for proper histone acetylation toward the 3′ end of actively transcribed coding sequences in a process that does not affect the association of the TINTIN complex with these regions (Steunou et al., 2016).

In the Eaf5 protein no functional domains have been identified, and its role does not seem to be critical for NuA4 or TINTIN complexes since the loss-of-function of this protein does not cause abnormal phenotypes in yeast (Mitchell et al., 2008; Rossetto et al., 2014). Moreover, the gene is absent in higher eukaryotes, including plants (Doyon and Côté, 2004; Doyon et al., 2004). Conversely, the third TINTIN subunit, Eaf7, is widely conserved from yeast to humans (**Table 1**) (Sathianathan et al., 2016). In humans, the Eaf7 homolog, MRG/MORF4L-binding protein (MRGBP), forms dimers with MRG15 independently of the TIP60 complex, possibly constituting the human TINTIN subcomplex (Cheng and Côté, 2014; Bhat et al., 2015).

Accessory NuA4 Subunits Shared With SWR1

Four yeast NuA4 proteins, Yaf9, Swc4, Arp4, and Act1, are also present in the chromatin remodeling complex SWR1 (**Table 1**) (Altaf et al., 2010), suggesting a functional interplay between both remodelers. Indeed, NuA4-dependent acetylation of nucleosomal histones H4 and H2A directly promotes the incorporation of H2A.Z by SWR1 (Altaf et al., 2010). Once incorporated, H2A.Z is also acetylated by NuA4 (Millar et al., 2006; Valdés-Mora et al., 2012). Yaf9 contributes to the functions of both NuA4 and SWR1, and it has been implicated in transcriptional regulation, histone acetylation, DNA repair, chromosome segregation, cellular resistance to microtubule depolymerization, and response to spindle stress (Klein et al., 2018). Yaf9 contains a YEATS (Yaf9, ENL, AF9, Taf14, Sas5) domain, an evolutionarily conserved module that binds histones H3 and H4 *in vitro* (Wang et al., 2009), and that also recognizes H3K27ac in nucleosomes, guiding the replacement of H2A-H2B dimers with H2A.Z-H2B by SWR1 at gene promoters (Klein et al., 2018).

Swc4/Eaf2 contains an N-terminal SANT domain that recognizes both histones and DNA, and a C-terminal Yaf9-interacting domain (Bittner et al., 2004). This subunit is the homolog of the human DNA methyltransferase-associated protein 1 (DMAP1; **Table 1**) (Rountree et al., 2000), suggesting an interplay of Swc4 with the DNA methylation pathways. The fact that Swc4 deletion in yeast did not broadly affect global acetylation levels of histone H4 suggests that it may regulate site-specific roles of NuA4, likely mediating the recruitment of both NuA4 and SWR1 to target genes and coupling acetylation and H2A.Z deposition (Zhou et al., 2010).

The ARP4 protein is a member of the ARP superfamily, a branch of an ancient and highly divergent family of proteins present in all eukaryotes and whose primary sequences display homology to actins (Kandasamy et al., 2005). Nuclear actins (N-actins) control different nucleic acid transitions as part of chromatin remodeling complexes (Olave et al., 2002). Actin and Arp4 form a conjugated pair, and despite being widely conserved in eukaryotes, their structures and roles within the chromatin remodeling complexes have remained obscure until recently (Cao et al., 2016). N-actins and Arp4 are incorporated into different chromatin regulatory complexes through a common motif, the HSA domain (Szerlong et al., 2008). Yeast Arp4 is involved in DNA repair, and it has been suggested to interact with acetylated H4 tails (Bird et al., 2002). Altogether, these observations suggest that the shared subunits between SWR1 and NuA4 may cooperatively enable the association of these complexes with chromatin.

GROWING EVIDENCE FOR THE PRESENCE OF NuA4 IN PLANTS

The existence of a putative NuA4-like complex in plants remains an open question nowadays since this complex has not been purified or characterized yet in any plant species. There are gene homologs for most of the yeast NuA4 subunits in plant genomes, but not for Eaf5 (**Table 1** and **Figure 1**). Many of these genes appear duplicated in the Arabidopsis genome, suggesting that this complex might be also present in plants. However, knowledge concerning the function of the putative plant NuA4 is very limited. Only during the last years the study of Arabidopsis mutants deficient for particular NuA4 subunits has started to reveal functions for these homologs in several biological processes (Latrasse et al., 2008; Umezawa et al., 2013; Bu et al., 2014; Xu et al., 2014; Bieluszewski et al., 2015; Gómez-Zambrano et al., 2018; Peng et al., 2018; Crevillén et al., 2019). Nevertheless, the presence of NuA4 homologs within different multisubunit chromatin remodeling complexes (Latrasse et al., 2008; Bieluszewski et al., 2015; Lin et al., 2017; Tan et al., 2018) may complicate the interpretation of the phenotypic alterations

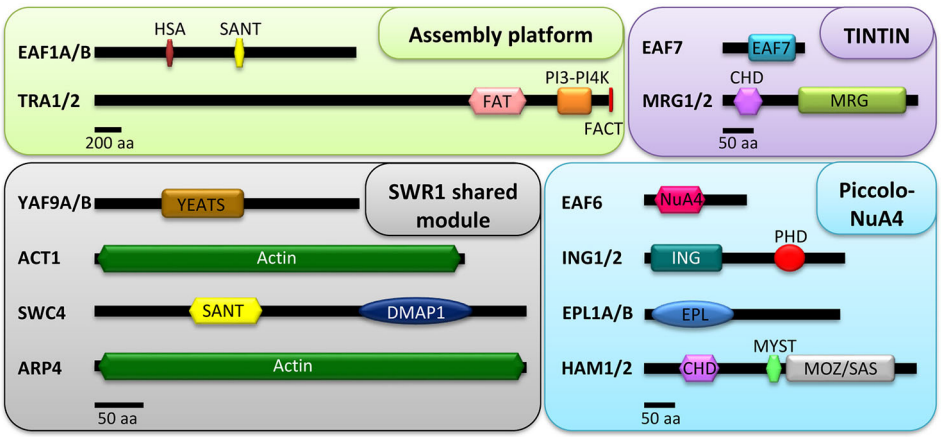

FIGURE 1 | Conserved domains of the putative NuA4 subunits in plants. Proteins are grouped according to the different sub-modules of the complex: assembly platform, Piccolo NuA4, TINTIN, and SWR1 shared module. The modular architecture of the proteins was extracted from multiple alignments with the web servers HMMER v2.1 (Finn et al., 2011) and SMART (Letunic and Bork, 2018). Scale bars are indicated for the proteins of each sub-module. For the assembly platform, 200 aa; for Piccolo NuA4, TINTIN, and the SWR1 shared module, 50 aa.

observed in some of these mutants. In any case, a picture is beginning to emerge showing the involvement of various components of this HAT complex in the regulation of a variety of plant biological processes, such as flowering initiation, gametophyte development, cell proliferation, stress, growth, and hormone responses among others (Latrasse et al., 2008; Umezawa et al., 2013; Bu et al., 2014; Xu et al., 2014; Bieluszewski et al., 2015; Gómez-Zambrano et al., 2018; Peng et al., 2018; Crevillén et al., 2019).

As discussed above, Eaf1, together with Tra1, fulfills the role of the assembly platform of the yeast NuA4 (Auger et al., 2008; Wang et al., 2018a). In plants, the Eaf1 subunit is widely conserved and particularly in *A. thaliana* a couple of tandem repeated *EAF1* homologs, *AtEAF1A* (AT3G24880) and *AtEAF1B* (AT3G24870), exist and have already been analyzed (**Table 1** and **Figure 1**). These genes share 98.5% identity in their coding regions and are equally expressed in mature rosette leaves (Bieluszewski et al., 2015). AtEAF1 proteins have also been proposed to function as the scaffold platform of the putative plant NuA4 (Bieluszewski et al., 2015). Besides, Tra1 is also conserved in Arabidopsis and two genes, *AtTRA1A* (AT4G36080) and *AtTRA1B* (AT2G17930), encode homologs of the yeast and the mammalian counterparts (Lu et al., 2009), supporting that the assembly platform for NuA4 is present in plants (**Table 1** and **Figure 1**). The two AtEAF1 proteins contain highly conserved HSA and SANT domains (**Figure 1**), which are also present in the yeast Eaf1 subunit, *H. sapiens* p400 and several plant homologs of PHOTOPERIOD-INDEPENDENT EARLY FLOWERING 1 (PIE1), the proposed catalytic subunit of plant SWR1 (Noh and Amasino, 2003; Bieluszewski et al., 2015). The HSA domain is a common feature of the platform subunits of the chromatin remodeling complexes SWR1, NuA4, and the hybrid complex TIP60-p400 (Szerlong et al., 2008), and is thought to provide the assembly surface for the shared submodule between NuA4 and SWR1 (Auger et al., 2008; Szerlong et al., 2008).

Besides the conservation of NuA4 subunits, recent works have provided additional evidence for the occurrence of this HAT complex in plants. By using the Arabidopsis homologs of yeast Swc4 and Arp4, AtSWC4 and AtARP4, as baits in affinity purification experiments followed by tandem mass spectrometry (AP-MS/MS), hints for the physical association of these proteins with AtEAF1 were revealed. Interestingly, homologs for the rest of NuA4 subunits, including the other assembly platform protein AtTRA1 (specifically AtTRA1B), were also pulled down in these proteomic assays, suggesting that all these NuA4 components coexist in multimeric complexes in Arabidopsis (**Figure 2**). According to the presence of SWC4 and ARP4 in other chromatin remodeling complexes, subunits of SWR1 and INO80 were also identified (Bieluszewski et al., 2015). Furthermore, co-immunoprecipitation experiments have demonstrated that both YAF9 homologs present in Arabidopsis, AtYAF9A and AtYAF9B, physically interact with AtEAF1B through the HSA domain (**Figure 2**) (Bieluszewski et al., 2015), and that AtYAF9A is also able to interact with AtEAF1A in pulldown assays (Crevillén et al., 2019).

Additional AP-MS experiments have uncovered that both AtEAF1 and AtTRA1 immunoprecipitate as well when other putative subunits of NuA4, including HAM1 and HAM2 (Arabidopsis Esa1 homologs), and the two EPL homologs, AtEPL1A and AtEPL1B, were used as baits (**Figure 2**) (Tan et al., 2018), consistent with a crucial role of both AtEAF1 homologs as assembly platforms for NuA4. Furthermore, these proteomic analyses revealed that not only AtEAF1 but also ten additional conserved subunits of NuA4 were copurified with tagged versions of AtHAMs and AtEPLs in Arabidopsis (**Figure 2**) (Tan et al., 2018). Confirmation for these observations came from Co-IP experiments performed in

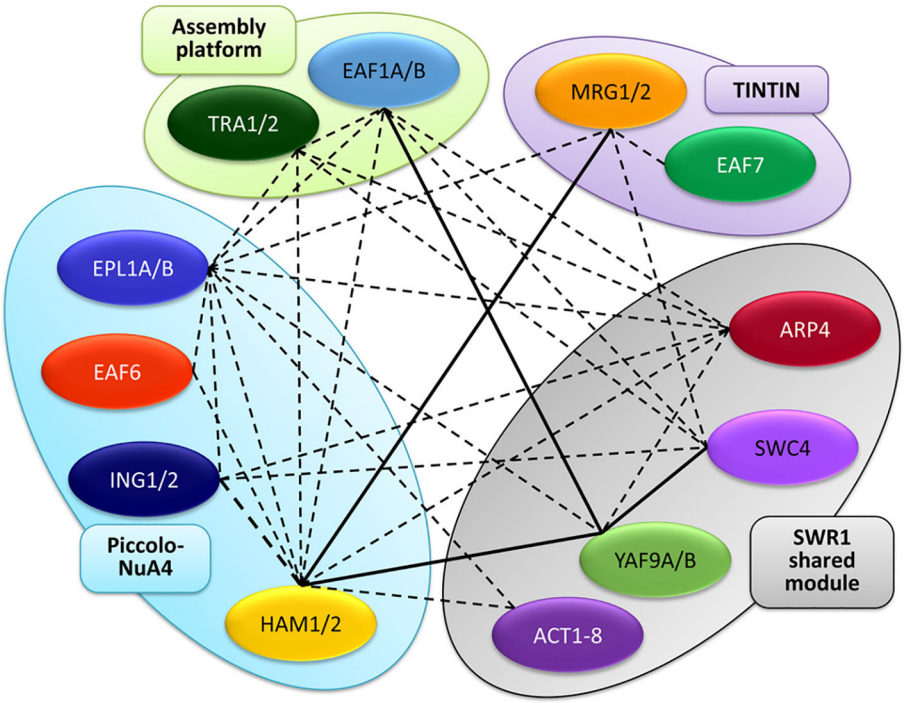

FIGURE 2 | Interaction map among NuA4 subunits in *A. thaliana*. The different homologs are grouped into the different sub-modules of the complex, similarly to **Figure 1**. Continuous lines represent interactions demonstrated by pair-wise protein-protein experiments, whereas dotted lines depict interactions revealed in proteomic experiments.

N. benthamiana leaves that demonstrated a physical interaction between AtHAM1 and AtYAF9A proteins *in vivo* (Crevillén et al., 2019). Intriguingly, AtTRA1 homologs were also pulled down in proteomic assays performed using either the SWR1 subunit ARP6 (Sijacic et al., 2019) or the SWR1-interacting protein MBD9 (Methyl-CpG-binding domain 9) (Potok et al., 2019) as baits, further supporting an intricate functional relationship between Arabidopsis SWR1 and NuA4 complexes. Altogether, these observations reinforce our hypothesis that a putative NuA4 exists in plants and may be closely linked with SWR1.

Emerging Roles of NuA4 in the Control of Plant Biological Processes

The functional characterization of putative Arabidopsis NuA4 components has revealed the involvement of these subunits in the control of a variety of plant biological processes ranging from different aspects of growth and development to stress responses. Interestingly, the emerging picture unveils the implication of a putative plant NuA4 in the regulation of the floral transition, as shown by the abnormal flowering time phenotypes observed in the mutants affected in most of the NuA4 subunits characterized so far (Xiao et al., 2013; Bu et al., 2014; Xu et al., 2014; Bieluszewski et al., 2015; Gómez-Zambrano et al., 2018; Crevillén et al., 2019). This trend strongly argues for a role of NuA4 in the control of plant developmental programs, and particularly, flowering time, a phase transition with important implications in plant adaptation and reproductive success (**Figure 3**).

The Piccolo and NuA4 Catalytic Subunits HAM1/2 of Arabidopsis Are Involved in the Control of Developmental Responses

MYST family acetyltransferases have been identified in several plant species. The Arabidopsis genome contains two closely related homologs of the yeast Esa1 protein, HAM1 (AT5G64610) and HAM2 (AT5G09740) (**Table 1** and **Figure 1**) (Latrasse et al., 2008). Their transcripts are constitutively expressed in all tissues, with higher expression levels found in shoot apical meristems, mainly during the floral transition (Earley et al., 2007; Latrasse et al., 2008). In contrast to Arabidopsis, *Solanum lycopersicum* contains only one MYST protein, SlHAM1 (Cigliano et al., 2013). Similar to *AtHAM1* and *AtHAM2*, *SlHAM1* is expressed in all organs, but mainly in flowers and fruits, suggesting that it could accomplish the same developmental role as its Arabidopsis homologs. Phylogenetic analyses have shown that plant HAMs are distributed in two clades, one of which includes both tomato and Arabidopsis proteins while the other comprises two HAM proteins from monocots, including maize and rice. This separation indicates

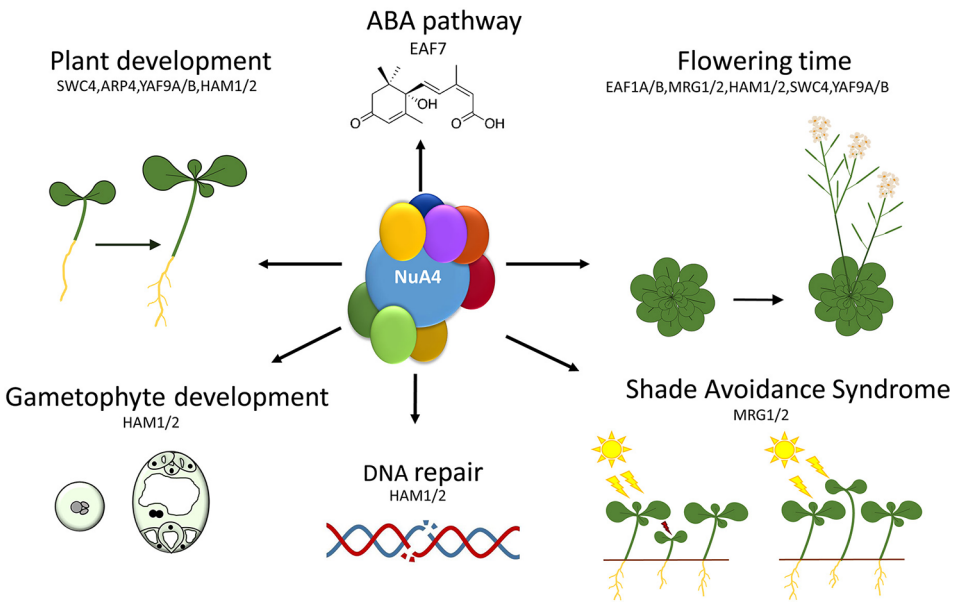

FIGURE 3 | Functions of the putative NuA4 subunits in different plant biological responses. Particular NuA4 subunits are involved in a number of developmental processes such as flowering transition, gametophyte development or hypocotyl growth, as well as in cell proliferation processes and stress responses or in hormone signaling transduction pathways.

that a single ancestral *HAM* gene gave rise to *HAM* homologs in monocots and dicots, occurring a specific event of duplication at the origin of the expansion of this family in Arabidopsis and maize (Cigliano et al., 2013).

Both HAM1 and HAM2 catalytic subunits have been functionally analyzed (**Figure 3**) and shown to specifically acetylate K5 residues of the histone H4 both *in vitro* and *in vivo* (Earley et al., 2007). The high sequence similarity between HAM1 and HAM2 suggests that a functional redundancy could exist for these proteins (Latrasse et al., 2008; Xiao et al., 2013). Consistent with this, Arabidopsis mutants lacking only one of the HAM proteins do not display noticeable phenotypic alterations when grown under standard conditions. However, *ham1 ham2* double mutants are lethal due to severe defects in the development of male and female gametophytes (**Figure 3**) (Latrasse et al., 2008). Although this embryo lethality hampered the complete functional characterization of *HAM* genes, some pieces of information have been inferred by assessing sesquimutants (Latrasse et al., 2008), double heterozygous mutants (Li et al., 2018), and knockdown and over-expression lines of both *HAM1* and *HAM2* (Xiao et al., 2013). Interestingly, total H4 acetylation levels were reduced in knock-down *ham* lines and increased in HAM1-overexpressors, corroborating that HAM1 functions as HAT *in planta* (Xiao et al., 2013). In addition, *ham1/ham1 ham2/HAM2* and *ham1/HAM1 ham2/ham2* sesquimutant plants display smaller siliques and lower seed number compared to wild-type (wt), as well as unfertilized ovules in some of the analyzed fruits. Furthermore, only 60% of the pollen grains are viable in the anthers of the sesquimutants. These results confirm that both proteins work redundantly to regulate gametophyte development (Latrasse et al., 2008).

Besides its function in gametogenesis, HAM1 and HAM2 also regulate flowering time (**Figure 3**), since *ham* knock-down or *ham1/HAM1 ham2/HAM2* double heterozygous plants in *FRIGIDA* (*FRI*) background (Xiao et al., 2013; Li et al., 2018) displayed an early flowering time phenotype that is accompanied by a reduction in the expression levels of the floral repressors *FLC* and *MADS-BOX AFFECTING FLOWERING GENES 3/4* (*MAF3/4*) (Xiao et al., 2013). These are negative regulators of the floral integrators *SUPPRESSOR OF OVEREXPRESSION OF CO 1* (*SOC1*) and *FT*, the latter being part of the florigen (Andrés and Coupland, 2012). Chromatin immunoprecipitation (ChIP) analyses demonstrated a substantial reduction in H4K5ac and H4ac levels in different regions of *FLC* and *MAF3/4* genes in the knock-down transgenic lines, consistent with the low expression levels observed for these flowering genes. In contrast, *HAM* overexpression lines displayed the opposite behavior, showing late flowering, increased levels of *FLC* and *MAF3/4*, and higher H4ac levels in these genes. Thus, HAM1 and HAM2 regulate H4 acetylation in the genomic region of these floral repressors, modulating their activation and, consequently, the timing of flowering (Xiao et al., 2013). This is in agreement with previous observations that revealed that flowering time and the expression levels of the floral repressor *FLC* are finely tuned by changes in histone acetylation (revised in He, 2012).

On top of being part of NuA4, HAM proteins are associated *in vivo* with components of the PWWPs-EPCRs-ARIDs-TRBs

(PEAT) complex (Tan et al., 2018), which mediates histone deacetylation and heterochromatin condensation. Interestingly, a recent study described that HAM1 protein also co-immunoprecipitates with FRI (Li et al., 2018). This flowering regulator defines the FRI complex (FRI-C), which is key to promote *FLC* expression and delay the floral transition. According to these observations, HAM1, recruited together with the FRI-C and a number of chromatin remodeling complexes, is part of the FRI supercomplex (FRI^{SC}), which is enriched in the TSS region of *FLC* to mediate its transcriptional activation (**Figure 4A**) (Li et al., 2018). However, it remains to be elucidated if HAM-mediated histone acetylation at the *FLC* locus (Xiao et al., 2013) is functionally related with this FRI^{SC}.

In addition to gene transcriptional regulation, histone acetylation is also related to DNA damage repair processes in yeast and mammals (House et al., 2014). In Arabidopsis, the role of HAM1 and HAM2 in DNA damage repair is conserved (**Figure 3**). Single *ham1* and *ham2* mutants display little or no clear phenotypical alterations when grown under normal conditions, but suffer more DNA damage than wt plants when they were exposed to ultraviolet (UV)-B irradiation (Campi et al., 2012). This suggests that plant HAM proteins conserve a functional role in DNA damage repair. In Arabidopsis, HAM1 appears to play a predominant role in this response since *ham1* mutant plants are more affected by UV-B irradiation than those that are defective in *HAM2* (Campi et al., 2012).

The data discussed above support the involvement of HAM proteins in the control of both developmental processes and DNA repair in plants (**Figure 3**). However, the presence of HAM proteins in additional Arabidopsis multiprotein chromatin remodeling complexes hinders the interpretation of the phenotypic alterations observed in *ham* mutants that could be affecting the function of other complexes (Li et al., 2018; Tan et al., 2018), in addition to NuA4. Future studies will contribute to clarify the implication of this HAT complex in the transcriptional control of biological processes and to ascribe specific NuA4-dependent roles for HAM proteins in plants. For that reason, it will be essential to address the implication of additional Arabidopsis Piccolo subunits (EPL1A/B, ING1/2, and EAF6) in the regulation of those processes. In Arabidopsis there are two homologs of yeast Epl1, *AtEPL1A* (AT1G16690) and *AtEPL1B* (AT1G79020) (**Table 1**). Both genes are located in chromosome 1 and are 67% identical with a highly conserved EPL domain (**Figure 1**) (Perry, 2006). EPL proteins are well conserved in plants, and one homolog has been described in maize (*ZmEpl101)* and in other plant species such as soybean, tomato, potato, wheat, and barley (Springer et al., 2002). However, the function of these proteins in plants remains completely unknown.

Piccolo ING homologs are conserved across the plant kingdom and share a similar architecture, with a C-terminal PHD finger module (**Figure 1**). Homologs of ING were found in the moss *Physcomitrella patens*, the monocot *Oryza sativa*, the dicot *Medicago truncatula,* and in the woody plant *Populus trichocarpa* (He et al., 2005; Lee et al., 2009). In Arabidopsis there are two PHD-containing proteins homologs of yeast Yng2 named AtING1 (AT3G24010) and AtING2 (AT1G54390) (**Table 1**) (He et al., 2005; Lee et al., 2009). Both *AtING1* and *AtING2* are ubiquitously expressed, although at low levels. The corresponding proteins are nuclear localized and hold the ability to bind H3K4me2/3 marks, as it has been described in PHD-containing proteins in yeast and mammals, where they can

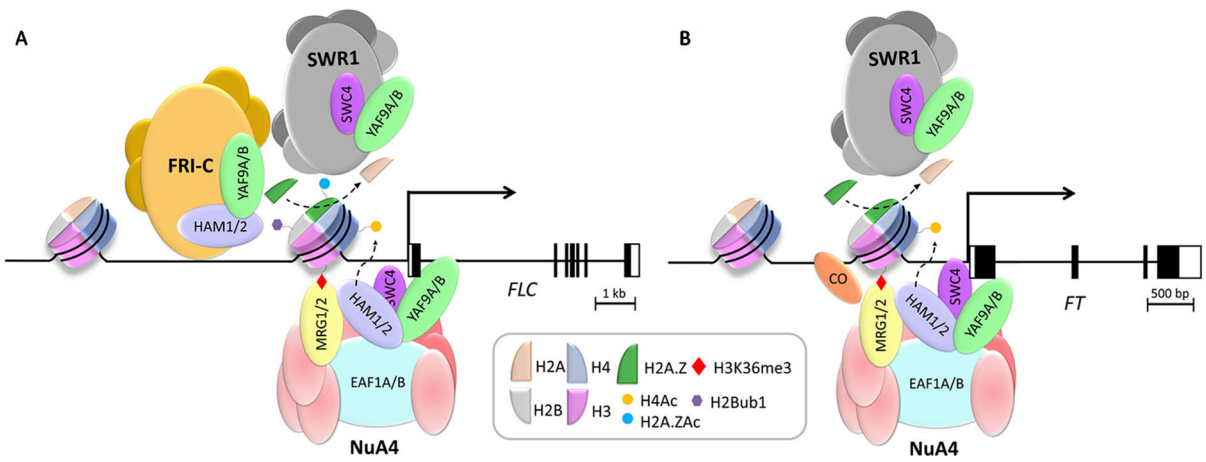

FIGURE 4 | Working models for the NuA4-dependent activation of the flowering time master regulators *FLC* and *FT*. **(A)** H2A.Z deposition mediated by SWR1 and histone H4 and H2A.Z acetylation performed by the putative NuA4 catalytic subunits HAM1/2 in genomic regions surrounding *FLC* TSS are required for *FLC* expression. FRI-C, together with HAM1 and a plethora of chromatin remodelers and transcriptional regulators assist in the recruitment of SWR1 to *FLC* chromatin, fine tuning *FLC* expression by facilitating the incorporation of H2A.Z and histone PTMs. **(B)** HAM1/2 mediate H4K5 acetylation at *FT* chromatin promoting its transcriptional activation. HAM1/2 interact with MRG1/2 proteins as subunits of NuA4. MRGs recognize enriched H3K36me3 regions at *FT* chromatin, and *via* their MRG domain, physically interact with CO to enhance *FT* activation under LD inductive photoperiods. On the other hand, SWR1 mediates the deposition of H2A.Z at the TSS of *FT* chromatin, modulating its expression. See text for details. Scale bars refer to the size of coding regions of the genes from their respective TSS.

recruit either HAT or HDAC complexes (Lee et al., 2009). In plants, these histone binding modules are involved in the regulation of developmental processes and defense responses among others (Mouriz et al., 2015). However, the function of AtING proteins remains unknown, although a physical interaction of ING2 with Histone Deacetylase Complex 1 (HDC1), an important component of the plant HDAC machinery, has been reported (Perrella et al., 2016). Similarly, the functional roles of AtEAF6, the fourth member of Arabidopsis Piccolo encoded by AT4G14385, have not been defined yet. Further studies are needed to clarify the functions of these putative NuA4 components that accompany HAM proteins in the putative plant Piccolo NuA4 complex.

The Assembly Platform Subunit EAF1 Is Also Involved in the Regulation of Plant Development

Further to the roles of the catalytic NuA4 subunit, HAM proteins, recent reports have shed light on the role of AtEAF1 in the control of plant developmental processes (Bieluszewski et al., 2015). Knockout plants for *AtEAF1B* display an acceleration of flowering associated with a reduction in the expression of *FLC* and lower histone acetylation levels near the 5' end of this locus (**Figure 4A**). Besides, these *eaf1b* mutant plants show a reduction in H4K5ac levels in the chromatin of other master regulators of flowering such as *FT*, *CONSTANS* (*CO)* and *SOC1 (***Figure 4B**) (Bieluszewski et al., 2015). Interestingly, the physical interaction of AtEAF1 with AtYAF9A and AtYAF9B is in agreement with the early flowering phenotype shared by *Ateaf1b*, *Atyaf9a,* and *Atyaf9a Atyaf9b* mutant plants (see below). The acceleration of flowering observed in all these mutants can be attributed to decreased *FLC* expression mainly due to the reduction of its H4 acetylation levels (**Figure 4A**) (Zacharaki et al., 2012; Bieluszewski et al., 2015; Crevillén et al., 2019). Although the location in tandem of both *AtEAF1* homologs in the genome has prevented the isolation of *eaf1a eaf1b* double mutants, the observations regarding *eaf1b* mutants (Bieluszewski et al., 2015) support the involvement of this putative NuA4 subunit in the regulation of flowering time. The alteration of histone acetylation levels displayed by plants deficient in *EAF1* is again consistent with the existence of a functional NuA4 in plants and its participation in developmental regulation.

Developmental and Stress-Related Functions Associated to Homologs of Putative Plant TINTIN Complex Subunits

In Arabidopsis there are two homologous proteins for the MRG family, namely AtMRG1 (AT4G37280) and AtMRG2 (AT1G02740) (**Table 1**). Both share nearly 50% identity and 65% similarity in their amino acids sequence. As their human and yeast counterparts, both Arabidopsis proteins conserve the CHD motif that binds H3K4me3 and H3K36me3, and the MRG domain (**Figure 1**) (Bu et al., 2014; Xu et al., 2014; Xie et al., 2015). Arabidopsis *MRG1* and *MRG2* genes are ubiquitously expressed in all tissues but mainly in roots, inflorescences, and the vasculature of cotyledons and true leaves (Bu et al., 2014; Xu et al., 2014). Moreover, the corresponding proteins are nuclear localized, close to euchromatic regions (Xu et al., 2014).

AtMRG1 and *AtMRG2* are functionally redundant in the control of flowering time in Arabidopsis since plants defective in only one of the *MRG* genes do not display any phenotypic alteration in comparison to wt, while *mrg1 mrg2* double mutant plants show late flowering and low expression levels of the flowering integrator gene *FT* specifically under long-day (LD) conditions, suggesting a link with the photoperiod-dependent flowering pathway (Bu et al., 2014; Xu et al., 2014). In this pathway, the activation of *FT* is critical and promoted by the transcription factor CO in LD. Only under these conditions CO protein is stabilized in the afternoon, allowing the induction of *FT* expression (Song et al., 2015). Interestingly, MRG1/2 proteins physically interact with CO *via* their MRG domain to activate *FT* expression (Bu et al., 2014). In fact, a model of functional interdependence between CO and MRG1/2 has been proposed, in which CO directly binds the *FT* promoter and recruits MRG1/2 proteins to *FT* locus. In addition, the CHDs present in MRG1/2 allow these proteins to bind regions of the *FT* promoter enriched in H3K4me3 and H3K36me3 marks. In this way, MRG1/2 proteins stabilize the binding of CO to the *FT* promoter region, eventually controlling *FT* activation (**Figure 4B**) (Bu et al., 2014). Intriguingly, in addition to regulating *FT*, MRG1 and MRG2 are also needed to fine tune *FLC* expression since *mrg1 mrg2* double mutant plants display reduced expression levels of this floral repressor. The significance of this regulation for the control of flowering time is unclear given that this double mutant is late-flowering, and this delay cannot be explained by low *FLC* expression levels (Xu et al., 2014).

Arabidopsis MRG proteins also interact with HAM1 and HAM2 (Xu et al., 2014). This interaction is conserved through evolution since in yeast, the MYST HAT Esa1 associates with Eaf3 to specifically target gene promoter regions for transcriptional activation (Eisen et al., 2001). *mrg1 mrg2* double mutants show a reduction in acetylation levels of histone H3 and histone H4K5 at their target genes, and particularly in *FT* (Xu et al., 2014). Therefore, according to the current working model, MRG1 and MRG2 preferably bind H3K36me3 at the promoter region of their target genes and recruit HATs HAM1/2 to increase histone acetylation levels, making these loci more accessible for transcriptional activation (**Figure 4B**) (Xu et al., 2014).

MRG1 and MRG2 also function as positive regulators of shade-induced hypocotyl elongation responses (**Figure 3**) (Peng et al., 2018). Plants grown in high-density conditions adapt their development to ensure its accessibility to sunlight. This is known as shade avoidance syndrome (SAS), where the most characteristic phenotypic response is hypocotyl elongation (Ballaré and Pierik, 2017). Plants defective in both *MRG1* and *MRG2* are affected in SAS response since they display a shorter hypocotyl length compared to wt plants when they are grown under shade, while there are no differences under standard white light or dark conditions (Peng et al., 2018). PHYTOCHROME-INTERACTING FACTOR 7 (PIF7) also plays a crucial role in this response, since *pif7* mutants display shorter hypocotyls only

when they are grown under shade conditions (Li et al., 2012). Interestingly, MRG2 and PIF7 proteins physically interact, and in response to shade PIF7 recruits MRG1/2 to the promoter of the target loci to regulate the expression of shade-responsive genes (Peng et al., 2018). In turn, MRG1/2 proteins bind H3K4me3 and H3K36me3 marks and recruit HAT complexes to promote histone acetylation, inducing the expression of genes mediating SAS (Peng et al., 2018).

Arabidopsis MRG proteins have also been implicated in the flowering response to ambient temperature (Pajoro et al., 2017), although it is currently unclear whether this function of MRGs is linked to NuA4 activity. In Arabidopsis, genome-wide approaches have shown that genes differentially spliced in response to fluctuating ambient temperature are enriched in H3K36me3 (Pajoro et al., 2017). Interestingly, Arabidopsis *mrg1 mrg2* mutant plants are less sensitive to the high ambient temperature acceleration of flowering observed in wt plants, suggesting that MRG1/2 could mediate the H3K36me3-dependent regulation of alternative splicing that occurs under warm temperature (Pajoro et al., 2017). Based on these observations, it is tempting to speculate that a link might exist between the activity of NuA4 and alternative splicing in response to environmental cues. However, it is not possible to rule out that this role of MRG proteins is NuA4-independent, and further research will be necessary to explore the implication of this HAT complex in mRNA maturation in plants.

MRG proteins are conserved across the plant kingdom, and their function has been addressed not only in Arabidopsis but also in other plant species. The rice genome contains two *MRG* genes, *OsMRG701* and *OsMRG702* (**Table 1**), the latter being involved in the floral transition since knockdown mutants for this gene display a late flowering phenotype under both LD and short-day (SD) conditions (Jin et al., 2015). Interestingly, this mutant shows similar developmental alterations to those observed in brassinosteroid (BR)-deficient plants. These defects are related to the ability of MRG702 to bind chromatin and regulate the expression of BR biosynthesis genes. Like other MRG family proteins, MRG702 also directly binds the chromatin of target genes in an H3K36me3-dependent manner (Jin et al., 2015).

On the other hand, AT1G26470 encodes AtEAF7 in Arabidopsis, the homologous protein of yeast Eaf7 and human MRGBP (**Table 1** and **Figure 1**) (Ito et al., 2018). AtEAF7 is also known as SNS1 (SnRK2-SUBSTRATE 1) since it is a target of SnRK2 (Umezawa et al., 2013), a protein kinase involved in abscisic acid (ABA) signaling pathway (Hirayama and Umezawa, 2010). In response to ABA, SnRK2 is activated and phosphorylates a variety of protein substrates, including AtEAF7/SNS1 (Umezawa et al., 2013). Plants deficient in *AtEAF7/SNS1* display a conspicuous inhibition of post-germination growth when they are grown in the presence of ABA, while they grow normally in the absence of this phytohormone (Umezawa et al., 2013). In comparison to wt, ABA-responsive genes appeared upregulated in *Ateaf7/sns1* seedlings treated with ABA. Thus, AtEAF7/SNS1 has been proposed to act as a negative regulator of ABA signaling pathway in Arabidopsis at the post-germination stage (**Figure 3**) (Umezawa et al., 2013).

Although evidence for the physical interaction between AtEAF7 and MRG1/2 is still lacking, the dimers between AtEAF7 and MRG1/2 might work in plants as a functional homolog of the TINTIN complex with both NuA4-dependent and -independent functions. Given the role of AtEAF7 in the ABA signaling pathway (Umezawa et al., 2013), it will be interesting to investigate the possible implication of MRG1/2 in abiotic stress responses mediated by this hormone. In addition, emerging evidence has unveiled the participation of alternative splicing mechanisms in ABA-mediated responses (Laloum et al., 2018). Besides, SnRK2 kinases have been shown to regulate the phosphorylation status of several plant splicing factors (Laloum et al., 2018), suggesting a link between these two processes that might implicate Arabidopsis homologs of the TINTIN subunits, an issue that will need to be thoroughly explored in the future.

Accessory Subunits of NuA4 Shared With SWR1 Also Regulate Developmental Programs

Arabidopsis SWR1 is involved in the control of plant stress responses and developmental processes, particularly in the regulation of flowering time. Mutations affecting different SWR1 subunits cause an acceleration of flowering due to reduced *FLC* expression (Jarillo and Piñeiro, 2015). Consistently, loss of function mutants in the genes encoding different isoforms of H2A.Z in Arabidopsis display similar phenotypes (Coleman-Derr and Zilberman, 2012), indicating that SWR1 is required to control flowering time mainly through the deposition of H2A.Z histone variant in regulatory regions of *FLC* (Martín-Trillo et al., 2006; Deal et al., 2007; Jarillo and Piñeiro, 2015). Arabidopsis homologs of the four shared subunits between SWR1 and NuA4 complexes (YAF9, SWC4, ARP4, and ACT1) have been characterized, revealing that their loss of function confers in most of them pleiotropic phenotypic alterations similar to other *swr1* mutants.

Two genes encoding YEATS domain-containing homologs to the yeast Yaf9 are present in the Arabidopsis genome, *AtYAF9A* (AT5G45600) and *AtYAF9B* (AT5G18000) (**Table 1** and **Figure 1**) (Zacharaki et al., 2012; Bieluszewski et al., 2015; Crevillén et al., 2019). The YEATS domain of Yaf9 has been defined as a selective reader of H3K27ac in yeast, and the recognition of this histone modification by Yaf9 leads to the exchange of the H2A histone variant for H2A.Z (Klein et al., 2018). In Arabidopsis, both YAF9A/B proteins can recognize unmodified histone H3 and also H3K9ac and H3K27ac, suggesting that the ability of the YEATS domain to bind acetylated H3 is conserved in plants and could participate in the recruitment of YAF9 to chromatin (Crevillén et al., 2019). *YAF9A* is highly expressed in different organs of the plant, while high expression levels of *YAF9B* were only detected in young flowers and roots (Zacharaki et al., 2012; Crevillén et al., 2019). The proteins encoded by both genes are located in the nucleus, consistent with YAF9 proteins being present in chromatin remodeling

complexes (Crevillén et al., 2019). Plants deficient in *YAF9A* display a slight but significant acceleration of flowering in both LD and SD. However, plants defective in *YAF9B* behave like wt (Crevillén et al., 2019). Interestingly, *yaf9a yaf9b* double mutant plants show pleiotropic developmental phenotypic alterations in comparison to wt plants, such as accelerated senescence and chlorotic leaves with reduced chlorophyll content, conspicuous early flowering under both LD and SD conditions, and reduced organ and plant size due to lower endoreduplication levels (Bieluszewski et al., 2015; Crevillén et al., 2019). Results derived from transcriptomic analyses with *yaf9a yaf9b* plants are in agreement with their pleiotropic phenotypic alterations. These mutants show more than 2000 differentially expressed genes, including some related to cell size and growth regulation, systemic acquired response, and also to flowering time regulation (Crevillén et al., 2019). Altogether, these data indicate that the Arabidopsis *YAF9A* and *YAF9B* genes have partially redundant roles in the regulation of developmental processes, including the initiation of reproductive growth.

According to their early flowering, both *yaf9a* and *yaf9a yaf9b* plants have reduced *FLC* transcript levels, while in *yaf9b* no alterations are observed in *FLC* expression (Zacharaki et al., 2012; Bieluszewski et al., 2015; Crevillén et al., 2019). Interestingly, crosses of *flc* plants with *yaf9a* or *yaf9a yaf9b* reveal an additive effect between the corresponding genes, suggesting that *YAF9* genes regulate this developmental transition through both *FLC*-dependent and -independent mechanisms (Crevillén et al., 2019). The downstream floral integrators *FT* and *SOC1* are upregulated in *yaf9a* and *yaf9a yaf9b* mutants, consistent with the early flowering observed in these plants (Zacharaki et al., 2012; Bieluszewski et al., 2015; Crevillén et al., 2019).

In Arabidopsis, SWR1 is necessary for the activation of *FLC via* the exchange of H2A by the histone variant H2A.Z in the chromatin of this locus (Martín-Trillo et al., 2006; Deal et al., 2007). However, no change in H2A.Z levels were found between wt and *yaf9a yaf9b* double mutant plants at *FLC* chromatin, suggesting that YAF9 proteins are not required for H2A.Z deposition at this locus, and that YAF9 proteins also regulate flowering in an SWR1-independent manner. Supporting this conclusion, the combination of *swr1* mutants with *yaf9a* and *yaf9a yaf9b* revealed an additive effect on flowering time (Crevillén et al., 2019). *yaf9a yaf9b* double mutants also show a distinct genetic interaction with *FRI* in comparison with other subunits of SWR1. As discussed above, the FRI-C delays flowering by promoting *FLC* expression (Choi et al., 2011; Crevillén and Dean, 2011; Li et al., 2018). When combined with *FRI* alleles, *yaf9a yaf9b* mutations partially suppress this late flowering and the high expression levels of *FLC*. This is in contrast with the flowering time phenotype observed in lines carrying an active *FRI* allele introgressed into other *swr1* mutants, where the suppression of the *FRI* late-flowering phenotype is complete (Choi et al., 2005). These observations corroborate that *FRI* requires an active SWR1 to regulate *FLC* expression, and further support the notion that YAF9 also regulates *FLC* expression *via* SWR1-independent mechanisms (**Figure 4A**) (Crevillén et al., 2019).

ChIP experiments demonstrated that *FLC* is a direct target of YAF9, and that the effect of this protein on *FLC* expression is mediated by changes in chromatin organization since the acetylation levels of both histone H4 and the histone variant H2A.Z were decreased in this locus in *yaf9a* and *yaf9a yaf9b* mutants (**Figure 4A**) (Zacharaki et al., 2012; Bieluszewski et al., 2015; Crevillén et al., 2019). These results reveal for the first time in plants a possible link between H2A.Z acetylation and gene expression that will have to be analyzed in detail in future works. *FT* is also a direct target of YAF9 (**Figure 4B**) (Crevillén et al., 2019), although its expression was upregulated in the *yaf9a yaf9b* double mutant. Despite this increased expression, levels of histone H4ac are moderately reduced at the *FT* locus in these mutant plants (Bieluszewski et al., 2015). In contrast to the *FLC* gene, no changes in H2A.Zac levels were observed in *FT* chromatin in *YAF9* defective plants (Crevillén et al., 2019), revealing that the role of YAF9 in H2A.Z modification could be locus specific and highlighting the complexity of chromatin-mediated regulation of gene expression in plants.

YAF9A also participates in the control of flowering time through the photoperiod-dependent pathway. This NuA4 subunit interacts with the circadian clock component CIRCADIAN CLOCK ASSOCIATED 1 (CCA1) which recruits MUT9P-LIKE-KINASE 4 (MLK4) to the *GIGANTEA* (*GI*) promoter. This protein complex that contains YAF9 and MLK4 acts to induce *GI* expression through phosphorylation of histone H2A at serine 95, H2A.Z deposition, and histone H4 acetylation in the chromatin of this flowering locus (Su et al., 2017). These observations illustrate how the coordinated action of different histone marks and chromatin remodeling complexes establishes patterns of gene expression required for an appropriate regulation of developmental processes such as flowering time.

Another NuA4 subunit shared with SWR1 is SWC4. Arabidopsis SWC4, encoded by AT2G47210, was recently found associated with SWR1 in plants (Gómez-Zambrano et al., 2018) (**Table 1**). Like its yeast and mammalian counterparts, AtSWC4 contains a SANT/Myb_DMAP1 domain in N-terminal position and a DMAP1 domain in the C-terminus (**Figure 1**) (Gómez-Zambrano et al., 2018). The first one is involved in the interaction with DNA, histones, and other proteins, while the second one mediates protein-protein interactions (Zhou et al., 2010). As in yeast, AtSWC4 physically interacts with both AtYAF9A and AtYAF9B in the nucleus (Bieluszewski et al., 2015; Gómez-Zambrano et al., 2018), suggesting the conservation of this common submodule in plants. *SWC4* is widely expressed but shows higher transcript levels in proliferating tissues including roots, flowers, and floral buds, and participates in the regulation of different developmental processes. This NuA4 subunit seems to be essential for Arabidopsis embryo development given that *swc4* knockout mutant plants are embryo-lethal. Furthermore, SWC4 also takes part in the regulation of post-embryonic processes since plants with reduced levels of *SWC4* expression (*swc4i*)

grown under both LD and SD conditions display pleiotropic phenotypic alterations in both vegetative and reproductive development such as curly leaves, symptoms of accelerated leaf senescence, and reduced plant and organ size due to a defective balance between cell proliferation and expansion. Additionally, consistent with the early flowering phenotype of *yaf9* mutants, *SWC4* knock-down lines displayed a slight acceleration of flowering concomitantly with *FT* upregulation under LD conditions (Gómez-Zambrano et al., 2018). Many of these morphological and developmental alterations resemble those observed in several Arabidopsis mutants defective in SWR1 function (Choi et al., 2005; Deal et al., 2005; Martín-Trillo et al., 2006; Choi et al., 2007; Deal et al., 2007; Lázaro et al., 2008; Jarillo and Piñeiro, 2015; Crevillén et al., 2019).

Transcriptomic analyses have revealed the misregulation of a wide range of genes in the *SWC4* knockdown plants, which is consistent with the pleiotropic phenotypic alterations observed in these lines. Among the differentially expressed genes in *swc4i* lines, upregulated transcripts were three times more frequent than those downregulated, suggesting a role for SWC4 in gene silencing (Gómez-Zambrano et al., 2018). Differentially expressed genes include some loci involved in primary and secondary metabolism, response to stimulus and stress, post-embryonic development, cell-cycle control, cell differentiation, and growth (Gómez-Zambrano et al., 2018). Interestingly, this transcriptomic analysis revealed a wider overlap with that of the *yaf9a yaf9b* plants than with those of mutants affected in other SWR1 subunits like *pie1*, *arp6,* or *swc6* (Crevillén et al., 2019), suggesting that AtYAF9 and AtSWC4 share a number of functions, and both may have additional roles to those performed by SWR1. In agreement with this idea and similarly to *yaf9a yaf9b* mutant plants (Crevillén et al., 2019), *SWC4* knock-down plants show lower endoreduplication levels (Gómez-Zambrano et al., 2018). This is consistent with YAF9 proteins and SWC4 being part of the same functional submodule. Nevertheless, a significant overlap was still noticeable between the RNA-seq data of *swc4i* lines and transcriptomic profiles of other *swr1* mutants (Gómez-Zambrano et al., 2018; Crevillén et al., 2019). Moreover, ChIP-seq analyses performed in *swc4i* plants identified more than 5000 genes with reduced levels of H2A.Z. Interestingly, these loci significantly overlap with the upregulated genes in *SWC4* deficient plants, consistent with the association of AtSWC4 with SWR1. Based on these results, SWC4 has been proposed to be necessary for the recruitment of SWR1 and H2A.Z deposition to specific loci through the recognition of AT-rich DNA elements that are over-represented in the TSS of target genes. Consistent with previous observations showing that H2A.Z deposition is essential for proper transcriptional regulation of *FT* (Kumar et al., 2012), this master gene of flowering is a direct target of AtSWC4, and is one of the most highly upregulated genes in *swc4i* plants (Gómez-Zambrano et al., 2018), underscoring the relevance of SWR1 activity for modulating floral initiation in Arabidopsis (**Figure 4B**).

Finally, another shared member of SWR1 and NuA4 complexes that has been characterized in Arabidopsis is ARP4 (**Table 1** and **Figure 1**). In Arabidopsis, there are eight classes of ARPs (ARP2-9), and two of them (ARP7 and 8) are plant-specific, while for the rest there are homologs in other eukaryotes. ARP proteins are well conserved in diverse angiosperms and homologs for all ARP classes have been found in the monocot rice (**Table 1**) (Kandasamy et al., 2003). All the Arabidopsis ARP classes are represented by a single gene except for *ARP4*, which has two closely related genes dubbed as *AtARP4* (AT1G18450) and *AtARP4A* (AT1G73910). While *AtARP4A* appears to be poorly expressed, *AtARP4* mRNA is ubiquitously present in all organs and tissues analyzed (Kandasamy et al., 2003). *AtARP4* knockdown plants display morphological alterations like reduction in plant size, smaller and fewer leaves, and atrophied siliques with few seeds and fertility. These plants are also affected in many phases of reproductive development since they display conspicuous alterations in flower development and an early flowering time phenotype specifically under LD, suggesting a possible link with the photoperiodic flowering pathway. This global impact of *AtARP4* deficiency in plant growth and architecture indicates that this gene is involved in the control of several developmental programs (Kandasamy et al., 2005).

ARP4 homologs from Arabidopsis and *Brassica* and tobacco species are nuclear proteins (Kandasamy et al., 2005) and co-purify with multiple putative subunits of INO80, NuA4, SWR1, and SWI/SNF complexes, confirming that ARP4 is part of several nuclear chromatin remodeling complexes in plants. Again, the presence of this protein in multiple complexes may explain the broad range of phenotypic alterations displayed by plants deficient in *ARP4* function. Finally, up to eight isoforms of Act are encoded in the Arabidopsis genome (**Table 1**) (Meagher et al., 2005), but any experimental evidence shedding light on which ones might be involved in the plant NuA4 is still missing.

The Putative NuA4-SWR1 Complexes Merge in Plants, an Evolutionary Perspective

The existence of a functional interplay between the yeast SWR1 and NuA4 chromatin remodeling complexes has been suggested, based on several observations (Billon and Côté, 2013). First, four subunits are shared by both complexes (Altaf et al., 2010). Second, the NuA4-mediated acetylation of H2A and H4 facilitates the replacement of H2A-H2B with H2A.Z-H2B dimers by SWR1 (Altaf et al., 2010). Third, yeast NuA4 is responsible for the acetylation of H2A.Z histone variant after its incorporation into chromatin by SWR1 (Millar et al., 2006). Fourth, NuA4-mediated histone acetylation and H2A.Z deposition are intimately associated in a number of chromatin remodeling processes such as the establishment of heterochromatin boundaries or the activation of expression in subtelomeric regions (Zhou et al., 2010). Finally, in metazoans, homologs of SWR1 and NuA4 form the hybrid TIP60 complex, which is able to acetylate H2A and H4 histones and, at the same time, exchange H2A with H2A.Z (Cai et al., 2003).

Further to the functional link between SWR1 and NuA4 in yeast and animals, recent reports have demonstrated how these

complexes can merge and separate during the transition from unicellular yeast to multicellular hypha in *Candida albicans* (Wang et al., 2018b). During the yeast state of this human pathogen, the catalytic subunit of NuA4 mediates the specific acetylation of the K173 residue in Eaf1. This modification of the NuA4 assembly platform subunit allows the interaction with Yaf9, a shared subunit of NuA4 and SWR1, facilitating the merge of both complexes. In contrast, during hyphal elongation, the acetylation levels of Eaf1 decrease through the action of the histone deacetylase Hda1, which is recruited to chromatin in response to nutritional signals that sustain hyphal elongation. In this state, NuA4 and SWR1 complexes are separated, showing the relevance of the dynamic merge and separation of these complexes in developmental transitions that take place depending on the nutritional status of the fungus (Wang et al., 2018b).

Based on these observations, a plausible scenario is that the merge of SWR1 and NuA4 complexes occurs also in plants. However, compelling experimental evidence supports the notion that plants, from mosses to angiosperms, are most likely to have canonical SWR1 and NuA4 complexes similar to those found in yeast. Most AP–MS approaches using subunits of SWR1 as baits reveal enrichments in SWR1 components and shared subunits with NuA4 among the co-immunoprecipitated proteins. In addition to these proteins, only homologs for the yeast Tra1, present in both NuA4 and SAGA HAT complexes, were recovered in these immunoprecipitation experiments when the SWR1 specific subunit ARP6 was used as bait, but not the NuA4 scaffold (EAF1) nor the catalytic subunit (HAM) (Potok et al., 2019; Sijacic et al., 2019). Based on these results, it is unlikely that these complexes may represent a merge of the Arabidopsis SWR1 and NuA4 complexes, similar to the mammalian TIP60 complex (Cai et al., 2003). In support of this conclusion, the K residue found to be acetylated in *C. albicans* Eaf1 during the transition from yeast to hyphae is not conserved in Arabidopsis, suggesting that this mechanism of separation and merge could be a specific adaptation of polymorphic fungi (Wang et al., 2018b). However, at present we cannot completely rule out the possibility that specific subsets of SWR1, NuA4 or even TIP60-like complexes could establish various combinations of the different homolog subunits that are encoded in the Arabidopsis genome for SWR1 and NuA4 complexes (Gómez-Zambrano et al., 2018) depending on the cell type, the developmental stage or the environmental and growth conditions that plants are exposed to. To precisely address the possible occurrence of distinct SWR1 and TIP60-like complexes, further complex purification approaches using for example Arabidopsis PIE1, the putative catalytic subunit of SWR1, as bait could contribute to elucidate the possible merge of NuA4 and SWR1 in plants.

CONCLUDING REMARKS

Over the last few years, several reports have started to enlighten the possible existence of a functional NuA4 in plants. At least 12 out of the 13 subunits of this complex are conserved in plants, and their functional characterization is providing evidence for the participation of this complex in different developmental processes and environmental responses. However, as for other plant chromatin remodeling complexes, one of the main bottlenecks in the characterization of the putative plant NuA4 is its purification and further crystallization. At the moment, the only information available to support the presence of NuA4 in plants is based on proteomic and individual protein-protein interaction analyses performed in Arabidopsis. While the data gathered until now tend to suggest that most of the components of the complex associate to each other *in vivo*, further complex purification approaches will be needed to clarify the exact biochemical composition of plant NuA4.

Remarkably, most of the NuA4 subunits are duplicated in plants. The functional characterization performed for some of these subunits indicate that different levels of redundancy are found in these couples of paralogs. The combinatorial potential of these homologs either in the full NuA4 complex or in the subcomplexes like Piccolo or TINTIN, is considerable. A plethora of distinct NuA4 chromatin remodelers with specific acetylation properties and functions could be produced in response to environmental factors or developmental cues, increasing plant plasticity that may result in a fitness benefit. Future research is expected to shed light on the possible interplay of the putative plant NuA4 and SWR1 complexes, although no clear evidence for their merge in a TIP60-like complex has been reported so far in Arabidopsis. In fact, current experimental data supports that plants most likely have independent NuA4 and SWR1 complexes, as it happens in yeast. Nevertheless, it is still possible that particular growing conditions, nutritional status, differentiation states or developmental signals may promote the combination of subunits from both complexes in plants, as it has been described in some fungi.

Although knowledge on the function of plant NuA4 is still in its infancy, the study of mutants affected in different NuA4 subunits characterized so far has revealed a number of phenotypic alterations at both vegetative and reproductive stages, suggesting an involvement of NuA4 in the control of central plant developmental programs through acetylation-mediated regulation of gene expression. However, the presence of some of the NuA4 homologs within different multisubunit chromatin remodeling complexes hampers the interpretation of the phenotypic alterations observed in these mutants, or in the combinations between them, complicating at the moment the adscription of functions to particular complexes. Further work is necessary to characterize additional plant NuA4 subunits in order to discriminate the functions that rely on the HAT activity of this complex from those that depend partially or totally on other chromatin remodeling complexes that share components with NuA4. Future comparative genomic and epigenomic analyses concerning mutants affected in specific and non-specific plant NuA4 subunits will allow us to conclude the mechanisms through which NuA4 works in gene expression regulation and the identification of its direct targets, increasing

our understanding on how plant NuA4 functions in different developmental programs and environmental responses, and how this complex interacts with other chromatin remodeling activities.

AUTHOR CONTRIBUTIONS

JJ and MP suggested and designed the article. LE-C, LB-M, JJ, and MP wrote the paper and designed the figures. JB-G, VJ-S, AL, and RP made valuable suggestions for the manuscript. All authors checked and confirmed the final version of the manuscript.

ACKNOWLEDGMENTS

Work in our group is currently funded by grant BIO2016-77559-R from the Spanish Ministry of Economy, Industry, and Competiveness to JJ and MP. LE-C and LB-M are recipients of the FPI fellowships FPI-SGIT-2016-08 from INIA and BES-2017-07992 from the Spanish Ministry of Economy, Industry, and Competiveness, respectively. We thank CONACYT for providing the fellowships 711040 and 740508 to VJ-S. We also acknowledge to the "Severo Ochoa Program for Centres of Excellence in R&D" from the Agencia Estatal de Investigación of Spain (grant SEV-2016-0672 (2017-2021) for supporting the scientific services used in this work.

REFERENCES

Aguissa-Touré, A. H., Wong, R. P., and Li, G. (2011). The ING family tumor suppressors: from structure to function. *Cell Mol. Life Sci.* 68 (1), 45–54. doi: 10.1007/s00018-010-0509-1

Allard, S., Utley, R. T., Savard, J., Clarke, A., Grant, P., Brandl, C. J., et al. (1999). NuA4, an essential transcription adaptor/histone H4 acetyltransferase complex containing Esa1p and the ATM-related cofactor Tra1p. *EMBO J.* 18 (18), 5108–5119. doi: 10.1093/emboj/18.18.5108

Altaf, M., Auger, A., Monnet-Saksouk, J., Brodeur, J., Piquet, S., Cramet, M., et al. (2010). NuA4-dependent acetylation of nucleosomal histones H4 and H2A directly stimulates incorporation of H2A.Z by the SWR1 complex. *J. Biol. Chem.* 285 (21), 15966–15977. doi: 10.1074/jbc.M110.117069

Andrés, F., and Coupland, G. (2012). The genetic basis of flowering responses to seasonal cues. *Nat. Rev. Genet.* 13 (9), 627–639. doi: 10.1038/nrg3291

Auger, A., Galarneau, L., Altaf, M., Nourani, A., Doyon, Y., Utley, R. T., et al. (2008). Eaf1 is the platform for NuA4 molecular assembly that evolutionarily links chromatin acetylation to ATP-dependent exchange of histone H2A variants. *Mol. Cell Biol.* 28 (7), 2257–2270. doi: 10.1128/MCB.01755-07

Avvakumov, N., Lalonde, M. E., Saksouk, N., Paquet, E., Glass, K. C., Landry, A. J., et al. (2012). Conserved molecular interactions within the HBO1 acetyltransferase complexes regulate cell proliferation. *Mol. Cell Biol.* 32 (3), 689–703. doi: 10.1128/MCB.06455-11

Ballaré, C. L., and Pierik, R. (2017). The shade-avoidance syndrome: multiple signals and ecological consequences. *Plant Cell Environ.* 40 (11), 2530–2543. doi: 10.1111/pce.12914

Bannister, A. J., and Kouzarides, T. (2011). Regulation of chromatin by histone modifications. *Cell Res.* 21 (3), 381–395. doi: 10.1038/cr.2011.22

Barnes, C. E., English, D. M., and Cowley, S. M. (2019). Acetylation & Co: an expanding repertoire of histone acylations regulates chromatin and transcription. *Essays Biochem.* 63 (1), 97–107. doi: 10.1042/EBC20180061

Berg, M. D., Genereaux, J., Karagiannis, J., and Brandl, C. J. (2018). The pseudokinase domain of *Saccharomyces cerevisiae* Tra1 is required for nuclear localization and incorporation into the SAGA and NuA4 complexes. *G3 (Bethesda)* 8 (6), 1943–1957. doi: 10.1534/g3.118.200288

Berr, A., Shafiq, S., and Shen, W. H. (2011). Histone modifications in transcriptional activation during plant development. *Biochim. Biophys. Acta* 1809 (10), 567–576. doi: 10.1016/j.bbagrm.2011.07.001

Bhat, W., Ahmad, S., and Côté, J. (2015). TINTIN, at the interface of chromatin, transcription elongation, and mRNA processing. *RNA Biol.* 12 (5), 486–489. doi: 10.1080/15476286.2015.1026032

Bhaumik, S. R., Smith, E., and Shilatifard, A. (2007). Covalent modifications of histones during development and disease pathogenesis. *Nat. Struct. Mol. Biol.* 14 (11), 1008–1016. doi: 10.1038/nsmb1337

Bieluszewski, T., Galganski, L., Sura, W., Bieluszewska, A., Abram, M., Ludwikow, A., et al. (2015). AtEAF1 is a potential platform protein for Arabidopsis NuA4 acetyltransferase complex. *BMC Plant Biol.* 15, 75. doi: 10.1186/s12870-015-0461-1

Billon, P., and Côté, J. (2013). Precise deposition of histone H2A.Z in chromatin for genome expression and maintenance. *Biochim. Biophys. Acta* 1819 (3-4), 290–302. doi: 10.1016/j.bbagrm.2011.10.004

Bird, A. W., Yu, D. Y., Pray-Grant, M. G., Qiu, Q., Harmon, K. E., Megee, P. C., et al. (2002). Acetylation of histone H4 by Esa1 is required for DNA double-strand break repair. *Nature* 419 (6905), 411–415. doi: 10.1038/nature01035

Bittner, C. B., Zeisig, D. T., Zeisig, B. B., and Slany, R. K. (2004). Direct physical and functional interaction of the NuA4 complex components Yaf9p and Swc4p. *Eukaryot. Cell* 3 (4), 976–983. doi: 10.1128/EC.3.4.976-983.2004

Black, J. C., Van Rechem, C., and Whetstine, J. R. (2012). Histone lysine methylation dynamics: establishment, regulation, and biological impact. *Mol. Cell* 48 (4), 491–507. doi: 10.1016/j.molcel.2012.11.006

Boudreault, A. A., Cronier, D., Selleck, W., Lacoste, N., Utley, R. T., Allard, S., et al. (2003). Yeast enhancer of polycomb defines global Esa1-dependent acetylation of chromatin. *Genes Dev.* 17 (11), 1415–1428. doi: 10.1101/gad.1056603

Bruzzone, M. J., Grünberg, S., Kubik, S., Zentner, G. E., and Shore, D. (2018). Distinct patterns of histone acetyltransferase and Mediator deployment at yeast protein-coding genes. *Genes Dev.* 32 (17-18), 1252–1265. doi: 10.1101/gad.312173.118

Bu, Z., Yu, Y., Li, Z., Liu, Y., Jiang, W., Huang, Y., et al. (2014). Regulation of Arabidopsis flowering by the histone mark readers MRG1/2 *via* interaction with CONSTANS to modulate *FT* expression. *PloS Genet.* 10 (9), e1004617. doi: 10.1371/journal.pgen.1004617

Cai, Y., Jin, J., Tomomori-Sato, C., Sato, S., Sorokina, I., Parmely, T. J., et al. (2003). Identification of new subunits of the multiprotein mammalian TRRAP/TIP60-containing histone acetyltransferase complex. *J. Biol. Chem.* 278 (44), 42733–42736. doi: 10.1074/jbc.C300389200

Campi, M., D'Andrea, L., Emiliani, J., and Casati, P. (2012). Participation of chromatin-remodeling proteins in the repair of ultraviolet-B-damaged DNA. *Plant Physiol.* 158 (2), 981–995. doi: 10.1104/pp.111.191452

Cao, T., Sun, L., Jiang, Y., Huang, S., Wang, J., and Chen, Z. (2016). Crystal structure of a nuclear actin ternary complex. *Proc. Natl. Acad. Sci. U.S.A.* 113 (32), 8985–8990. doi: 10.1073/pnas.1602818113

Carrozza, M. J., Li, B., Florens, L., Suganuma, T., Swanson, S. K., Lee, K. K., et al. (2005). Histone H3 methylation by Set2 directs deacetylation of coding regions by Rpd3S to suppress spurious intragenic transcription. *Cell* 123 (4), 581–592. doi: 10.1016/j.cell.2005.10.023

Chen, L., Conaway, R. C., and Conaway, J. W. (2013). Multiple modes of regulation of the human Ino80 SNF2 ATPase by subunits of the INO80 chromatin-remodeling complex. *Proc. Natl. Acad. Sci. U. S. A.* 110 (51), 20497–20502. doi: 10.1073/pnas.1317092110

Cheng, X., and Côté, J. (2014). A new companion of elongating RNA Polymerase II: TINTIN, an independent sub-module of NuA4/TIP60 for nucleosome transactions. *Transcription* 5 (5), e995571. doi: 10.1080/21541264.2014.995571

Cheung, A. C. M., and Díaz-Santín, L. M. (2019). Share and share alike: the role of Tra1 from the SAGA and NuA4 coactivator complexes. *Transcription* 10 (1), 37–43. doi: 10.1080/21541264.2018.1530936

Chittuluru, J. R., Chaban, Y., Monnet-Saksouk, J., Carrozza, M. J., Sapountzi, V., Selleck, W., et al. (2011). Structure and nucleosome interaction of the yeast NuA4 and Piccolo-NuA4 histone acetyltransferase complexes. *Nat. Struct. Mol. Biol.* 18 (11), 1196–1203. doi: 10.1038/nsmb.2128

Choi, K., Kim, S., Kim, S. Y., Kim, M., Hyun, Y., Lee, H., et al. (2005). SUPPRESSOR OF FRIGIDA3 encodes a nuclear ACTIN-RELATED PROTEIN6 required for floral repression in Arabidopsis. *Plant Cell* 17 (10), 2647–2660. doi: 10.1105/tpc.105.035485

Choi, K., Park, C., Lee, J., Oh, M., Noh, B., and Lee, I. (2007). Arabidopsis homologs of components of the SWR1 complex regulate flowering and plant development. *Development* 134 (10), 1931–1941. doi: 10.1242/dev.001891

Choi, K., Kim, J., Hwang, H. J., Kim, S., Park, C., Kim, S. Y., et al. (2011). The FRIGIDA complex activates transcription of FLC, a strong flowering repressor in Arabidopsis, by recruiting chromatin modification factors. *Plant Cell* 23 (1), 289–303. doi: 10.1105/tpc.110.075911

Cigliano, R. A., Sanseverino, W., Cremona, G., Ercolano, M. R., Conicella, C., and Consiglio, F. M. (2013). Genome-wide analysis of histone modifiers in tomato: gaining an insight into their developmental roles. *BMC Genomics* 14, 57. doi: 10.1186/1471-2164-14-57

Clapier, C. R., Iwasa, J., Cairns, B. R., and Peterson, C. L. (2017). Mechanisms of action and regulation of ATP-dependent chromatin-remodelling complexes. *Nat. Rev. Mol. Cell Biol.* 18 (7), 407–422. doi: 10.1038/nrm.2017.26

Clarke, A. S., Lowell, J. E., Jacobson, S. J., and Pillus, L. (1999). Esa1p is an essential histone acetyltransferase required for cell cycle progression. *Mol. Cell Biol.* 19 (4), 2515–2526. doi: 10.1128/mcb.19.4.2515

Coleman-Derr, D., and Zilberman, D. (2012). Deposition of histone variant H2A.Z within gene bodies regulates responsive genes. *PloS Genet.* 8 (10), e1002988. doi: 10.1371/journal.pgen.1002988

Crevillén, P., and Dean, C. (2011). Regulation of the floral repressor gene FLC: the complexity of transcription in a chromatin context. *Curr. Opin. Plant Biol.* 14 (1), 38–44. doi: 10.1016/j.pbi.2010.08.015

Crevillén, P., Gómez-Zambrano, A., López, J. A., Vázquez, J., Piñeiro, M., and Jarillo, J. A. (2019). Arabidopsis YAF9 histone readers modulate flowering time through NuA4-complex-dependent H4 and H2A.Z histone acetylation at FLC chromatin. *New Phytol.* 222 (4), 1893–1908. doi: 10.1111/nph.15737

Deal, R. B., Kandasamy, M. K., McKinney, E. C., and Meagher, R. B. (2005). The nuclear actin-related protein ARP6 is a pleiotropic developmental regulator required for the maintenance of FLOWERING LOCUS C expression and repression of flowering in Arabidopsis. *Plant Cell* 17 (10), 2633–2646. doi: 10.1105/tpc.105.035196

Deal, R. B., Topp, C. N., McKinney, E. C., and Meagher, R. B. (2007). Repression of flowering in Arabidopsis requires activation of FLOWERING LOCUS C expression by the histone variant H2A.Z. *Plant Cell* 19 (1), 74–83. doi: 10.1105/tpc.106.048447

Doyon, Y., and Côté, J. (2004). The highly conserved and multifunctional NuA4 HAT complex. *Curr. Opin. Genet. Dev.* 14 (2), 147–154. doi: 10.1016/j.gde.2004.02.009

Doyon, Y., Selleck, W., Lane, W. S., Tan, S., and Côté, J. (2004). Structural and functional conservation of the NuA4 histone acetyltransferase complex from yeast to humans. *Mol. Cell Biol.* 24 (5), 1884–1896. doi: 10.1128/mcb.24.5.1884-1896.2004

Earley, K. W., Shook, M. S., Brower-Toland, B., Hicks, L., and Pikaard, C. S. (2007). In vitro specificities of Arabidopsis co-activator histone acetyltransferases: implications for histone hyperacetylation in gene activation. *Plant J.* 52 (4), 615–626. doi: 10.1111/j.1365-313X.2007.03264.x

Eisen, A., Utley, R. T., Nourani, A., Allard, S., Schmidt, P., Lane, W. S., et al. (2001). The yeast NuA4 and Drosophila MSL complexes contain homologous subunits important for transcription regulation. *J. Biol. Chem.* 276 (5), 3484–3491. doi: 10.1074/jbc.M008159200

Finn, R. D., Clements, J., and Eddy, S. R. (2011). HMMER web server: interactive sequence similarity searching. *Nucleic Acids Res.* 39, W29–W37. doi: 10.1093/nar/gkr367

Gómez-Zambrano, A., Crevillén, P., Franco-Zorrilla, J. M., López, J. A., Moreno-Romero, J., Roszak, P., et al. (2018). Arabidopsis SWC4 binds DNA and recruits the SWR1 complex to modulate histone H2A.Z deposition at key regulatory genes. *Mol. Plant* 11 (6), 815–832. doi: 10.1016/j.molp.2018.03.014

Gerhold, C. B., and Gasser, S. M. (2014). INO80 and SWR complexes: relating structure to function in chromatin remodeling. *Trends. Cell Biol.* 24 (11), 619–631. doi: 10.1016/j.tcb.2014.06.004

Ginsburg, D. S., Govind, C. K., and Hinnebusch, A. G. (2009). NuA4 lysine acetyltransferase Esa1 is targeted to coding regions and stimulates transcription elongation with Gcn5. *Mol. Cell Biol.* 29 (24), 6473–6487. doi: 10.1128/MCB.01033-09

Guérillon, C., Larrieu, D., and Pedeux, R. (2013). ING1 and ING2: multifaceted tumor suppressor genes. *Cell Mol. Life Sci.* 70 (20), 3753–3772. doi: 10.1007/s00018-013-1270-z

He, G. H., Helbing, C. C., Wagner, M. J., Sensen, C. W., and Riabowol, K. (2005). Phylogenetic analysis of the ING family of PHD finger proteins. *Mol. Biol. Evol.* 22 (1), 104–116. doi: 10.1093/molbev/msh256

He, Y. (2012). Chromatin regulation of flowering. *Trends Plant Sci.* 17 (9), 556–562. doi: 10.1016/j.tplants.2012.05.001

Helmlinger, D., and Tora, L. (2017). Sharing the SAGA. *Trends Biochem. Sci.* 42 (11), 850–861. doi: 10.1016/j.tibs.2017.09.001

Helmlinger, D., Marguerat, S., Villén, J., Swaney, D. L., Gygi, S. P., Bähler, J., et al. (2011). Tra1 has specific regulatory roles, rather than global functions, within the SAGA co-activator complex. *EMBO J.* 30 (14), 2843–2852. doi: 10.1038/emboj.2011.181

Hirayama, T., and Umezawa, T. (2010). The PP2C-SnRK2 complex: the central regulator of an abscisic acid signaling pathway. *Plant Signal Behav.* 5 (2), 160–163. doi: 10.4161/psb.5.2.10460

Hodges, A. J., Plummer, D. A., and Wyrick, J. J. (2019). NuA4 acetyltransferase is required for efficient nucleotide excision repair in yeast. *DNA Repair (Amst)* 73, 91–98. doi: 10.1016/j.dnarep.2018.11.006

House, N. C., Koch, M. R., and Freudenreich, C. H. (2014). Chromatin modifications and DNA repair: beyond double-strand breaks. *Front. Genet.* 5, 296. doi: 10.3389/fgene.2014.00296

Hu, Y., Lu, Y., Zhao, Y., and Zhou, D. X. (2019). Histone acetylation dynamics integrates metabolic activity to regulate plant response to stress. *Front. Plant Sci.* 10, 1236. doi: 10.3389/fpls.2019.01236

Ito, S., Kayukawa, N., Ueda, T., Taniguchi, H., Morioka, Y., Hongo, F., et al. (2018). MRGBP promotes AR-mediated transactivation of KLK3 and TMPRSS2 *via* acetylation of histone H2A.Z in prostate cancer cells. *Biochim. Biophys. Acta Gene Regul. Mech.* 1861 (9), 794–802. doi: 10.1016/j.bbagrm.2018.07.014

Jarillo, J. A., and Piñeiro, M. (2015). H2A.Z mediates different aspects of chromatin function and modulates flowering responses in Arabidopsis. *Plant J.* 83 (1), 96–109. doi: 10.1111/tpj.12873

Jin, J., Shi, J., Liu, B., Liu, Y., Huang, Y., Yu, Y., et al. (2015). MORF-RELATED GENE702, a reader protein of trimethylated histone H3 lysine 4 and histone H3 lysine 36, is involved in brassinosteroid-regulated growth and flowering time control in rice. *Plant Physiol.* 168 (4), 1275–1285. doi: 10.1104/pp.114.255737

Kandasamy, M. K., McKinney, E. C., and Meagher, R. B. (2003). Cell cycle-dependent association of Arabidopsis actin-related proteins AtARP4 and AtARP7 with the nucleus. *Plant J.* 33 (5), 939–948. doi: 10.1046/j.1365-313x.2003.01691.x

Kandasamy, M. K., Deal, R. B., McKinney, E. C., and Meagher, R. B. (2005). Silencing the nuclear actin-related protein AtARP4 in Arabidopsis has multiple effects on plant development, including early flowering and delayed floral senescence. *Plant J.* 41 (6), 845–858. doi: 10.1111/j.1365-313X.2005.02345.x

Keogh, M. C., Kurdistani, S. K., Morris, S. A., Ahn, S. H., Podolny, V., Collins, S. R., et al. (2005). Cotranscriptional set2 methylation of histone H3 lysine 36 recruits a repressive Rpd3 complex. *Cell* 123 (4), 593–605. doi: 10.1016/j.cell.2005.10.025

Keogh, M. C., Mennella, T. A., Sawa, C., Berthelet, S., Krogan, N. J., Wolek, A., et al. (2006). The *Saccharomyces cerevisiae* histone H2A variant Htz1 is acetylated by NuA4. *Genes Dev.* 20 (6), 660–665. doi: 10.1101/gad.1388106

Klein, B. J., Ahmad, S., Vann, K. R., Andrews, F. H., Mayo, Z. A., Bourriquen, G., et al. (2018). Yaf9 subunit of the NuA4 and SWR1 complexes targets histone H3K27ac through its YEATS domain. *Nucleic Acids Res.* 46 (1), 421–430. doi: 10.1093/nar/gkx1151

Kouzarides, T. (2007). Chromatin modifications and their function. *Cell* 128 (4), 693–705. doi: 10.1016/j.cell.2007.02.005

Kumar, S. V., Lucyshyn, D., Jaeger, K. E., Alos, E., Alvey, E., Harberd, N. P., et al. (2012). Transcription factor PIF4 controls the thermosensory activation of flowering. *Nature* 484 (7393), 242–245. doi: 10.1038/nature10928

Lázaro, A., Gómez-Zambrano, A., López-González, L., Piñeiro, M., and Jarillo, J. A. (2008). Mutations in the Arabidopsis SWC6 gene, encoding a component of the SWR1 chromatin remodelling complex, accelerate

flowering time and alter leaf and flower development. *J. Exp. Bot.* 59 (3), 653–666. doi: 10.1093/jxb/erm332

Laloum, T., Martin, G., and Duque, P. (2018). Alternative Splicing Control of Abiotic Stress Responses. *Trends Plant Sci.* 23 (2), 140–150. doi: 10.1016/j.tplants.2017.09.019

Latrasse, D., Benhamed, M., Henry, Y., Domenichini, S., Kim, W., Zhou, D. X., et al. (2008). The MYST histone acetyltransferases are essential for gametophyte development in Arabidopsis. *BMC Plant Biol.* 8, 121. doi: 10.1186/1471-2229-8-121

Law, J. A., and Jacobsen, S. E. (2010). Establishing, maintaining and modifying DNA methylation patterns in plants and animals. *Nat. Rev. Genet.* 11 (3), 204–220. doi: 10.1038/nrg2719

Lee, K. K., and Workman, J. L. (2007). Histone acetyltransferase complexes: one size doesn't fit all. *Nat. Rev. Mol. Cell Biol.* 8 (4), 284–295. doi: 10.1038/nrm2145

Lee, W. Y., Lee, D., Chung, W. I., and Kwon, C. S. (2009). Arabidopsis ING and Alfin1-like protein families localize to the nucleus and bind to H3K4me3/2 *via* plant homeodomain fingers. *Plant J.* 58 (3), 511–524. doi: 10.1111/j.1365-313X.2009.03795.x

Letunic, I., and Bork, P. (2018). 20 years of the SMART protein domain annotation resource. *Nucleic Acids Res.* 46 (D1), D493–D496. doi: 10.1093/nar/gkx922

Li, L., Ljung, K., Breton, G., Schmitz, R. J., Pruneda-Paz, J., Cowing-Zitron, C., et al. (2012). Linking photoreceptor excitation to changes in plant architecture. *Genes Dev.* 26 (8), 785–790. doi: 10.1101/gad.187849.112

Li, Z., Jiang, D., and He, Y. (2018). FRIGIDA establishes a local chromosomal environment for FLOWERING LOCUS C mRNA production. *Nat. Plants* 4 (10), 836–846. doi: 10.1038/s41477-018-0250-6

Lin, Y. Y., Lu, J. Y., Zhang, J., Walter, W., Dang, W., Wan, J., et al. (2009). Protein acetylation microarray reveals that NuA4 controls key metabolic target regulating gluconeogenesis. *Cell* 136 (6), 1073–1084. doi: 10.1016/j.cell.2009.01.033

Lin, C. L., Chaban, Y., Rees, D. M., McCormack, E. A., Ocloo, L., and Wigley, D. B. (2017). Functional characterization and architecture of recombinant yeast SWR1 histone exchange complex. *Nucleic Acids Res.* 45 (12), 7249–7260. doi: 10.1093/nar/gkx414

Liu, X., Yang, S., Zhao, M., Luo, M., Yu, C. W., Chen, C. Y., et al. (2014). Transcriptional repression by histone deacetylases in plants. *Mol. Plant* 7 (5), 764–772. doi: 10.1093/mp/ssu033

Liu, X., Yang, S., Yu, C. W., Chen, C. Y., and Wu, K. (2016). Histone acetylation and plant development. *Enzymes* 40, 173–199. doi: 10.1016/bs.enz.2016.08.001

Lu, P. Y., Lévesque, N., and Kobor, M. S. (2009). NuA4 and SWR1-C: two chromatin-modifying complexes with overlapping functions and components. *Biochem. Cell Biol.* 87 (5), 799–815. doi: 10.1139/O09-062

Luger, K., Mäder, A. W., Richmond, R. K., Sargent, D. F., and Richmond, T. J. (1997). Crystal structure of the nucleosome core particle at 2.8 Å resolution. *Nature* 389 (6648), 251–260. doi: 10.1038/38444

Luger, K., Dechassa, M. L., and Tremethick, D. J. (2012). New insights into nucleosome and chromatin structure: an ordered state or a disordered affair? *Nat. Rev. Mol. Cell Biol.* 13 (7), 436–447. doi: 10.1038/nrm3382

Martín-Trillo, M., Lázaro, A., Poethig, R. S., Gómez-Mena, C., Piñeiro, M. A., Martínez-Zapater, J. M., et al. (2006). EARLY IN SHORT DAYS 1 (ESD1) encodes ACTIN-RELATED PROTEIN 6 (AtARP6), a putative component of chromatin remodelling complexes that positively regulates FLC accumulation in Arabidopsis. *Development* 133 (7), 1241–1252. doi: 10.1242/dev.02301

Meagher, R. B., Deal, R. B., Kandasamy, M. K., and McKinney, E. C. (2005). Nuclear actin-related proteins as epigenetic regulators of development. *Plant Physiol.* 139 (4), 1576–1585. doi: 10.1104/pp.105.072447

Mehta, M., Braberg, H., Wang, S., Lozsa, A., Shales, M., Solache, A., et al. (2010). Individual lysine acetylations on the N terminus of *Saccharomyces cerevisiae* H2A.Z are highly but not differentially regulated. *J. Biol. Chem.* 285 (51), 39855–39865. doi: 10.1074/jbc.M110.185967

Millar, C. B., Xu, F., Zhang, K., and Grunstein, M. (2006). Acetylation of H2A.Z Lys 14 is associated with genome-wide gene activity in yeast. *Genes Dev.* 20 (6), 711–722. doi: 10.1101/gad.1395506

Mitchell, L., Lambert, J. P., Gerdes, M., Al-Madhoun, A. S., Skerjanc, I. S., Figeys, D., et al. (2008). Functional dissection of the NuA4 histone acetyltransferase reveals its role as a genetic hub and that Eaf1 is essential for complex integrity. *Mol. Cell Biol.* 28 (7), 2244–2256. doi: 10.1128/MCB.01653-07

Molina, O., Vargiu, G., Abad, M. A., Zhiteneva, A., Jeyaprakash, A. A., Masumoto, H., et al. (2016). Epigenetic engineering reveals a balance between histone modifications and transcription in kinetochore maintenance. *Nat. Commun.* 7, 13334. doi: 10.1038/ncomms13334

Mouriz, A., López-Gonzalez, L., Jarillo, J. A., and Piñeiro, M. (2015). PHDs govern plant development. *Plant Signal Behav.* 10 (7), e993253. doi: 10.4161/15592324.2014.993253

Narita, T., Weinert, B. T., and Choudhary, C. (2019). Functions and mechanisms of non-histone protein acetylation. *Nat. Rev. Mol. Cell Biol.* 20 (3), 156–174. doi: 10.1038/s41580-018-0081-3

Noh, Y. S., and Amasino, R. M. (2003). PIE1, an ISWI family gene, is required for FLC activation and floral repression in Arabidopsis. *Plant Cell* 15 (7), 1671–1682. doi: 10.1105/tpc.012161

Olave, I. A., Reck-Peterson, S. L., and Crabtree, G. R. (2002). Nuclear actin and actin-related proteins in chromatin remodeling. *Annu. Rev. Biochem.* 71, 755–781. doi: 10.1146/annurev.biochem.71.110601.135507

Pajoro, A., Severing, E., Angenent, G. C., and Immink, R. G. H. (2017). Histone H3 lysine 36 methylation affects temperature-induced alternative splicing and flowering in plants. *Genome Biol.* 18 (1), 102. doi: 10.1186/s13059-017-1235-x

Peña, P. V., Davrazou, F., Shi, X., Walter, K. L., Verkhusha, V. V., Gozani, O., et al. (2006). Molecular mechanism of histone H3K4me3 recognition by plant homeodomain of ING2. *Nature* 442 (7098), 100–103. doi: 10.1038/nature04814

Peng, M., Li, Z., Zhou, N., Ma, M., Jiang, Y., Dong, A., et al. (2018). Linking PHYTOCHROME-INTERACTING FACTOR to Histone Modification in Plant Shade Avoidance. *Plant Physiol.* 176 (2), 1341–1351. doi: 10.1104/pp.17.01189

Perrella, G., Carr, C., Asensi-Fabado, M. A., Donald, N. A., Paldi, K., Hannah, M. A., et al. (2016). The histone deacetylase complex 1 protein of Arabidopsis has the capacity to interact with multiple proteins including histone 3-binding proteins and histone 1 variants. *Plant Physiol.* 171 (1), 62–70. doi: 10.1104/pp.15.01760

Perry, J. (2006). The Epc-N domain: a predicted protein-protein interaction domain found in select chromatin associated proteins. *BMC Genomics* 7, 6. doi: 10.1186/1471-2164-7-6

Pokholok, D. K., Harbison, C. T., Levine, S., Cole, M., Hannett, N. M., Lee, T. I., et al. (2005). Genome-wide map of nucleosome acetylation and methylation in yeast. *Cell* 122 (4), 517–527. doi: 10.1016/j.cell.2005.06.026

Potok, M. E., Wang, Y., Xu, L., Zhong, Z., Liu, W., Feng, S., et al. (2019). Arabidopsis SWR1-associated protein methyl-CpG-binding domain 9 is required for histone H2A.Z deposition. *Nat. Commun.* 10 (1), 3352. doi: 10.1038/s41467-019-11291-w

Reid, J. L., Moqtaderi, Z., and Struhl, K. (2004). Eaf3 regulates the global pattern of histone acetylation in *Saccharomyces cerevisiae*. *Mol. Cell Biol.* 24 (2), 757–764. doi: 10.1128/mcb.24.2.757-764.2004

Rossetto, D., Cramet, M., Wang, A. Y., Steunou, A. L., Lacoste, N., Schulze, J. M., et al. (2014). Eaf5/7/3 form a functionally independent NuA4 submodule linked to RNA polymerase II-coupled nucleosome recycling. *EMBO J.* 33 (12), 1397–1415. doi: 10.15252/embj.201386433

Rothbart, S. B., and Strahl, B. D. (2014). Interpreting the language of histone and DNA modifications. *Biochim. Biophys. Acta* 1839 (8), 627–643. doi: 10.1016/j.bbagrm.2014.03.001

Rountree, M. R., Bachman, K. E., and Baylin, S. B. (2000). DNMT1 binds HDAC2 and a new co-repressor, DMAP1, to form a complex at replication foci. *Nat. Genet.* 25 (3), 269–277. doi: 10.1038/77023

Sapountzi, V., Logan, I. R., and Robson, C. N. (2006). Cellular functions of TIP60. *Int. J. Biochem. Cell Biol.* 38 (9), 1496–1509. doi: 10.1016/j.biocel.2006.03.003

Sathianathan, A., Ravichandran, P., Lippi, J. M., Cohen, L., Messina, A., Shaju, S., et al. (2016). The Eaf3/5/7 Subcomplex Stimulates NuA4 Interaction with Methylated Histone H3 Lys-36 and RNA Polymerase II. *J. Biol. Chem.* 291 (40), 21195–21207. doi: 10.1074/jbc.M116.718742

Schuettengruber, B., Bourbon, H. M., Di Croce, L., and Cavalli, G. (2017). Genome regulation by polycomb and trithorax: 70 years and counting. *Cell* 171 (1), 34–57. doi: 10.1016/j.cell.2017.08.002

Searle, N. E., and Pillus, L. (2018). Critical genomic regulation mediated by Enhancer of Polycomb. *Curr. Genet.* 64 (1), 147–154. doi: 10.1007/s00294-017-0742-3

Setiaputra, D., Ahmad, S., Dalwadi, U., Steunou, A. L., Lu, S., Ross, J. D., et al. (2018). Molecular architecture of the essential yeast histone acetyltransferase complex NuA4 redefines its multimodularity. *Mol. Cell Biol.* 38 (9), e00570-17. doi: 10.1128/MCB.00570-17

Shahbazian, M. D., and Grunstein, M. (2007). Functions of site-specific histone acetylation and deacetylation. *Annu. Rev. Biochem.* 76, 75–100. doi: 10.1146/annurev.biochem.76.052705.162114

Sijacic, P., Holder, D. H., Bajic, M., and Deal, R. B. (2019). Methyl-CpG-binding domain 9 (MBD9) is required for H2A.Z incorporation into chromatin at a subset of H2A.Z-enriched regions in the Arabidopsis genome. *PloS Genet.* 15 (8), e1008326. doi: 10.1371/journal.pgen.1008326

Song, Y. H., Shim, J. S., Kinmonth-Schultz, H. A., and Imaizumi, T. (2015). Photoperiodic flowering: time measurement mechanisms in leaves. *Annu. Rev. Plant Biol.* 66, 441–464. doi: 10.1146/annurev-arplant-043014-115555

Springer, N. M., Danilevskaya, O. N., Hermon, P., Helentjaris, T. G., Phillips, R. L., Kaeppler, H. F., et al. (2002). Sequence relationships, conserved domains, and expression patterns for maize homologs of the polycomb group genes E(z), esc, and E(Pc). *Plant Physiol.* 128 (4), 1332–1345. doi: 10.1104/pp.010742

Steunou, A. L., Cramet, M., Rossetto, D., Aristizabal, M. J., Lacoste, N., Drouin, S., et al. (2016). Combined action of histone reader modules regulates NuA4 local acetyltransferase function but not its recruitment on the genome. *Mol. Cell Biol.* 36 (22), 2768–2781. doi: 10.1128/MCB.00112-16

Strahl, B. D., and Allis, C. D. (2000). The language of covalent histone modifications. *Nature* 403 (6765), 41–45. doi: 10.1038/47412

Su, Y., Wang, S., Zhang, F., Zheng, H., Liu, Y., Huang, T., et al. (2017). Phosphorylation of histone H2A at serine 95: a plant-specific mark involved in flowering time regulation and H2A.Z deposition. *Plant Cell* 29 (9), 2197–2213. doi: 10.1105/tpc.17.00266

Szerlong, H., Hinata, K., Viswanathan, R., Erdjument-Bromage, H., Tempst, P., and Cairns, B. R. (2008). The HSA domain binds nuclear actin-related proteins to regulate chromatin-remodeling ATPases. *Nat. Struct. Mol. Biol.* 15 (5), 469–476. doi: 10.1038/nsmb.1403

Talbert, P. B., and Henikoff, S. (2017). Histone variants on the move: substrates for chromatin dynamics. *Nat. Rev. Mol. Cell Biol.* 18 (2), 115–126. doi: 10.1038/nrm.2016.148

Tan, L. M., Zhang, C. J., Hou, X. M., Shao, C. R., Lu, Y. J., Zhou, J. X., et al. (2018). The PEAT protein complexes are required for histone deacetylation and heterochromatin silencing. *EMBO J.* 37 (19), e98770. doi: 10.15252/embj.201798770

Taverna, S. D., Ilin, S., Rogers, R. S., Tanny, J. C., Lavender, H., Li, H., et al. (2006). Yng1 PHD finger binding to H3 trimethylated at K4 promotes NuA3 HAT activity at K14 of H3 and transcription at a subset of targeted ORFs. *Mol. Cell* 24 (5), 785–796. doi: 10.1016/j.molcel.2006.10.026

Umezawa, T., Sugiyama, N., Takahashi, F., Anderson, J. C., Ishihama, Y., Peck, S. C., et al. (2013). Genetics and phosphoproteomics reveal a protein phosphorylation network in the abscisic acid signaling pathway in *Arabidopsis thaliana*. *Sci. Signal* 6 (270), rs8. doi: 10.1126/scisignal.2003509

Uprety, B., Lahudkar, S., Malik, S., and Bhaumik, S. R. (2012). The 19S proteasome subcomplex promotes the targeting of NuA4 HAT to the promoters of ribosomal protein genes to facilitate the recruitment of TFIID for transcriptional initiation *in vivo*. *Nucleic Acids Res.* 40 (5), 1969–1983. doi: 10.1093/nar/gkr977

Uprety, B., Sen, R., and Bhaumik, S. R. (2015). Eaf1p is required for recruitment of NuA4 in targeting TFIID to the promoters of the ribosomal protein genes for transcriptional initiation *in vivo*. *Mol. Cell Biol.* 35 (17), 2947–2964. doi: 10.1128/MCB.01524-14

Valdés-Mora, F., Song, J. Z., Statham, A. L., Strbenac, D., Robinson, M. D., Nair, S. S., et al. (2012). Acetylation of H2A.Z is a key epigenetic modification associated with gene deregulation and epigenetic remodeling in cancer. *Genome Res.* 22 (2), 307–321. doi: 10.1101/gr.118919.110

Venkatesh, S., and Workman, J. L. (2015). Histone exchange, chromatin structure and the regulation of transcription. *Nat. Rev. Mol. Cell Biol.* 16 (3), 178–189. doi: 10.1038/nrm3941

Voss, A. K., and Thomas, T. (2009). MYST family histone acetyltransferases take center stage in stem cells and development. *Bioessays* 31 (10), 1050–1061. doi: 10.1002/bies.200900051

Wang, A. Y., Schulze, J. M., Skordalakes, E., Gin, J. W., Berger, J. M., Rine, J., et al. (2009). Asf1-like structure of the conserved Yaf9 YEATS domain and role in H2A.Z deposition and acetylation. *Proc. Natl. Acad. Sci. U.S.A.* 106 (51), 21573–21578. doi: 10.1073/pnas.0906539106

Wang, X., Ahmad, S., Zhang, Z., Côté, J., and Cai, G. (2018a). Architecture of the *Saccharomyces cerevisiae* NuA4/TIP60 complex. *Nat. Commun.* 9 (1), 1147. doi: 10.1038/s41467-018-03504-5

Wang, X., Zhu, W., Chang, P., Wu, H., Liu, H., and Chen, J. (2018b). Merge and separation of NuA4 and SWR1 complexes control cell fate plasticity in *Candida albicans*. *Cell Discovery* 4, 45. doi: 10.1038/s41421-018-0043-0

Xiao, J., Zhang, H., Xing, L., Xu, S., Liu, H., Chong, K., et al. (2013). Requirement of histone acetyltransferases HAM1 and HAM2 for epigenetic modification of FLC in regulating flowering in Arabidopsis. *J. Plant Physiol.* 170 (4), 444–451. doi: 10.1016/j.jplph.2012.11.007

Xiao, J., Jin, R., and Wagner, D. (2017). Developmental transitions: integrating environmental cues with hormonal signaling in the chromatin landscape in plants. *Genome Biol.* 18 (1), 88. doi: 10.1186/s13059-017-1228-9

Xie, T., Zmyslowski, A. M., Zhang, Y., and Radhakrishnan, I. (2015). Structural basis for multi-specificity of MRG domains. *Structure* 23 (6), 1049–1057. doi: 10.1016/j.str.2015.03.020

Xu, Y., Gan, E. S., Zhou, J., Wee, W. Y., Zhang, X., and Ito, T. (2014). Arabidopsis MRG domain proteins bridge two histone modifications to elevate expression of flowering genes. *Nucleic Acids Res.* 42 (17), 10960–10974. doi: 10.1093/nar/gku781

Xu, P., Li, C., Chen, Z., Jiang, S., Fan, S., Wang, J., et al. (2016). The NuA4 core complex acetylates nucleosomal histone H4 through a double recognition mechanism. *Mol. Cell* 63 (6), 965–975. doi: 10.1016/j.molcel.2016.07.024

Yang, X. J., and Ullah, M. (2007). MOZ and MORF, two large MYSTic HATs in normal and cancer stem cells. *Oncogene* 26 (37), 5408–5419. doi: 10.1038/sj.onc.1210609

Yi, C., Ma, M., Ran, L., Zheng, J., Tong, J., Zhu, J., et al. (2012). Function and molecular mechanism of acetylation in autophagy regulation. *Science* 336 (6080), 474–477. doi: 10.1126/science.1216990

Zacharaki, V., Benhamed, M., Poulios, S., Latrasse, D., Papoutsoglou, P., Delarue, M., et al. (2012). The Arabidopsis ortholog of the YEATS domain containing protein YAF9a regulates flowering by controlling H4 acetylation levels at the FLC locus. *Plant Sci.* 196, 44–52. doi: 10.1016/j.plantsci.2012.07.010

Zhou, B. O., Wang, S. S., Xu, L. X., Meng, F. L., Xuan, Y. J., Duan, Y. M., et al. (2010). SWR1 complex poises heterochromatin boundaries for antisilencing activity propagation. *Mol. Cell Biol.* 30 (10), 2391–2400. doi: 10.1128/MCB.01106-09

Conflict of Interest: The authors declare that the research was conducted in the absence of any commercial or financial relationships that could be construed as a potential conflict of interest.

frontiers in Plant Science

REVIEW
published: 05 March 2020
doi: 10.3389/fpls.2020.00181

Who Rules the Cell? An Epi-Tale of Histone, DNA, RNA, and the Metabolic Deep State

Jeffrey Leung[1*] *and Valérie Gaudin*[2*]

[1] *Institut Jean-Pierre Bourgin, ERL3559 CNRS, INRAE, Versailles, France,* [2] *Institut Jean-Pierre Bourgin, UMR1318 INRAE-AgroParisTech, Université Paris-Saclay, Versailles, France*

Epigenetics refers to the mode of inheritance independent of mutational changes in the DNA. Early evidence has revealed methylation, acetylation, and phosphorylation of histones, as well as methylation of DNA as part of the underlying mechanisms. The recent awareness that many human diseases have in fact an epigenetic basis, due to unbalanced diets, has led to a resurgence of interest in how epigenetics might be connected with, or even controlled by, metabolism. The Next-Generation genomic technologies have now unleashed torrents of results exposing a wondrous array of metabolites that are covalently attached to selective sites on histones, DNA and RNA. Metabolites are often cofactors or targets of chromatin-modifying enzymes. Many metabolites themselves can be acetylated or methylated. This indicates that the acetylome and methylome can actually be deep and pervasive networks to ensure the nuclear activities are coordinated with the metabolic status of the cell. The discovery of novel histone marks also raises the question on the types of pathways by which their corresponding metabolites are replenished, how they are corralled to the specific histone residues and how they are recognized. Further, atypical cytosines and uracil have also been found in eukaryotic genomes. Although these new and extensive connections between metabolism and epigenetics have been established mostly in animal models, parallels must exist in plants, inasmuch as many of the basic components of chromatin and its modifying enzymes are conserved. Plants are chemical factories constantly responding to stress. Plants, therefore, should lend themselves readily for identifying new endogenous metabolites that are also modulators of nuclear activities in adapting to stress.

Keywords: metabolites, epigenetics, acetylation, methylation, histone, acetyl-coenzyme A, S-adenosylmethionine

OPEN ACCESS

Edited by:
Iva Mozgova,
Czech Academy of Sciences, Czechia

Reviewed by:
Keqiang Wu,
National Taiwan University, Taiwan
Yuhai Cui,
Agriculture and Agri-Food Canada, Canada
Hans-Wilhelm Nuetzmann,
University of Bath, United Kingdom

****Correspondence:***
Jeffrey Leung
jeffrey.leung@inrae.fr
Valérie Gaudin
valerie.gaudin@inrae.fr

Specialty section:
This article was submitted to Plant Cell Biology, a section of the journal Frontiers in Plant Science

Received: *26 November 2019*
Accepted: *06 February 2020*
Published: *05 March 2020*

Citation:
Leung J and Gaudin V (2020) Who Rules the Cell? An Epi-Tale of Histone, DNA, RNA, and the Metabolic Deep State. Front. Plant Sci. 11:181. doi: 10.3389/fpls.2020.00181

INTRODUCTION

One of the earliest observations redolent of epigenetics was made around 1915 when W. Bateson and C. Pellew made crosses between three "rogue" varieties of pea with its wild-type counterpart. The "rogues" bred offspring of exclusively "rogues", while the expected wild-type segregants vanished forever (it should be understood that "rogue" at the time was not referring to a specific

phenotype, but any off-type with respect to the parent, equivalent to our modern usage of "mutant"). Unusual heritable traits were again noted in the 1950s, more frequently and in different organisms, owing probably to the flourishing discipline of Mendelian genetics. These exceptional cases reported silenced alleles that can go on silencing another allele in *trans*. The causes were variously described as "paramutations" or "transvection effects" (with the benefit of hindsight, each of them represents likely one specific aspect of epigenetics involving *trans*-acting sRNAs). At about that time, the influential embryologist, C. Waddington, also remarked that many developmental traits were not fixed, but subjected to alteration by the environmental conditions (developmental pluripotency). One example was the vein patterns of the *Drosophila* wing, which can be altered by high temperatures during development, yielding a particular *crossveinless* phenotype. If these flies were then maintained for several generations at high temperatures, their progeny became all stably *crossveinless*, even when subsequent generations were returned to normal temperatures. Waddington articulated his ideas on developmental plasticity by using the metaphor of a rugged "epigenetic landscape". He envisioned that each successive stage of developmental "decisions", likened to a ball rolling down the landscape, can be nudged by environmental cues to deviate from its original path down a different furl (pathway). The landscape itself was also not static, but can change shape, as its floppy crust (can be equated with chromatin) is suspended over numerous genes whose actions are similar to those of pulleys, tugging asynchronously at the landscape. The term "epigenetics" was coined by Waddington as a nod to the existence of phenotypic determinants above the well-accepted Mendelian entity later called genes (Slack, 2002; Stam and Mittelsten Scheid, 2005; Noble, 2015).

These ideas did not gain immediate traction, as they of course conjured up Lamarckian inheritance, a forbidden fruit in the Mendelian Eden. Ironically, some of the molecular components for his model were already being discovered by his contemporaries at Cambridge University, his alma mater where he taught embryology. Between the 1950 and 1970s, Cambridge was the scientific mecca for some of the most brash and brilliant minds that ever united under the same proverbial roof, trying to understand life's workings by blurring the intellectual divide between biology, chemistry and physics (https://qesp.org/james-watson-francis-crick-maurice-wilkins-and-rosalind-franklin/). This new reductionist approach, called molecular biology, was inaugurated there by a series of ground-breaking discoveries (e.g. the double-helix) and equally reverberating technical achievements–the most notable being DNA sequencing–that laid down the path for today's genomics. In fact, the Watson–Crick DNA structure, with its full mechanistic implications for Mendelian inheritance, was published 4 years ahead of Waddington's matured ideas in his book The Strategy of the Gene [reviewed by (Slack, 2002)]! Following the wake of the double-helix, acetylation on histones was also turning up a mere 100 km from Cambridge. These fractions of histone hydrolysates might have been annoying to work with, as they would thwart routine precipitations, owing to their increased hydrophobicity (Phillips, 1963). With the inexorable progress of molecular biology–debuting in the late 70s rsquo;s and its eclosion into the now cutting-edge genomics–epigenetics and the other lesser-used sobriquets like paramutations are understood to involve the same phenomenon of phenotypic changes without DNA mutations. These (epi-)phenotypes are caused by rearranged chromatin landscape triggered by chemical attachments to the DNA and histones, or in some gene-silencing systems, through the intermediate steps of *trans*-acting small RNAs that recruit the DNA- and histone-modifying enzymes. The reconfigured chromatin landscape, in turn, leads to altered accessibility to the genes underneath by the transcriptional machinery.

A current resurgence of excitement in epigenetics surrounds the question of how it can be extensively controlled by metabolism. This seemingly esoteric question is in fact revived by the awareness that unbalanced diets can cause many diseases due to deregulated epigenetic mechanisms, leading then, of course, to misexpression of genes (Kinnaird et al., 2016). Some cancers have been traced to malfunctioning RNA-modifying enzymes and the enthusiasm to understand the RNA code was buoyed by the hopes of developing treatments targeting the modifying enzymes. Along the way, the field of "epitranscriptomics" dedicated to understanding RNA modifications was launched (Saletore et al., 2012). Many of the metabolites are also donors, inducers, inhibitors, substrates, and co-factors of chromatin remodeling enzymes. There are over 260 sites on the animal histones (H1, H2A, H2B, H3, and H4) that are known to be modified post-translationally [**Figure 1**; see (Huang et al., 2014; Sabari et al., 2017)] and probably nearly so for plant histones. Benefitting from the Next-Generation technologies, the number of potential sites and the type of chemical adducts are rapidly expanding. One generality is that the vast majority of the histone modifications belongs to the class called short-chain acylation, defined by a thioester bond [R-C(=O)-S-R'] that links one molecule (e.g. lysine in a histone) to the next (e.g. acyl adducts) (**Figure 1**). For example, the widely-studied acetyl adduct is linked to the ε-amine of the lysine (K) by acylation. The other less-known acyl groups are distinctive by their hydrocarbon chain length, hydrophobicity or net electrical charges.

In plants, studies directly addressing the functional relationships between metabolism and epigenetics are still relatively rare (Shen et al., 2015; Shen et al., 2016). But because many metabolites, histones, and modifying enzymes are highly conserved, the general principles derived from studies of other models should nevertheless provide useful clues into plants. On the other hand, because the lifestyle of plants is different from these other organisms, experimental confirmation or refutation is still ultimately desirable, if not necessary. In particular, plants produce myriads of secondary metabolites, many of which are implicated in defense against pathogens and abiotic stresses, as well as being immensely important for human health. Plants should thus be an excellent model to address the question of how these metabolites can relay environmental changes to the nucleus, a timely topic in view of global warming. This review will articulate mainly around acetylation and methylation, as they provide most of the current knowledge. This owes to the fact that most of their relevant modifying enzymes are known. It generally holds that the overall cellular concentrations of acetyl-coenzyme A (acetyl-CoA) and S-adenosylmethionine are the

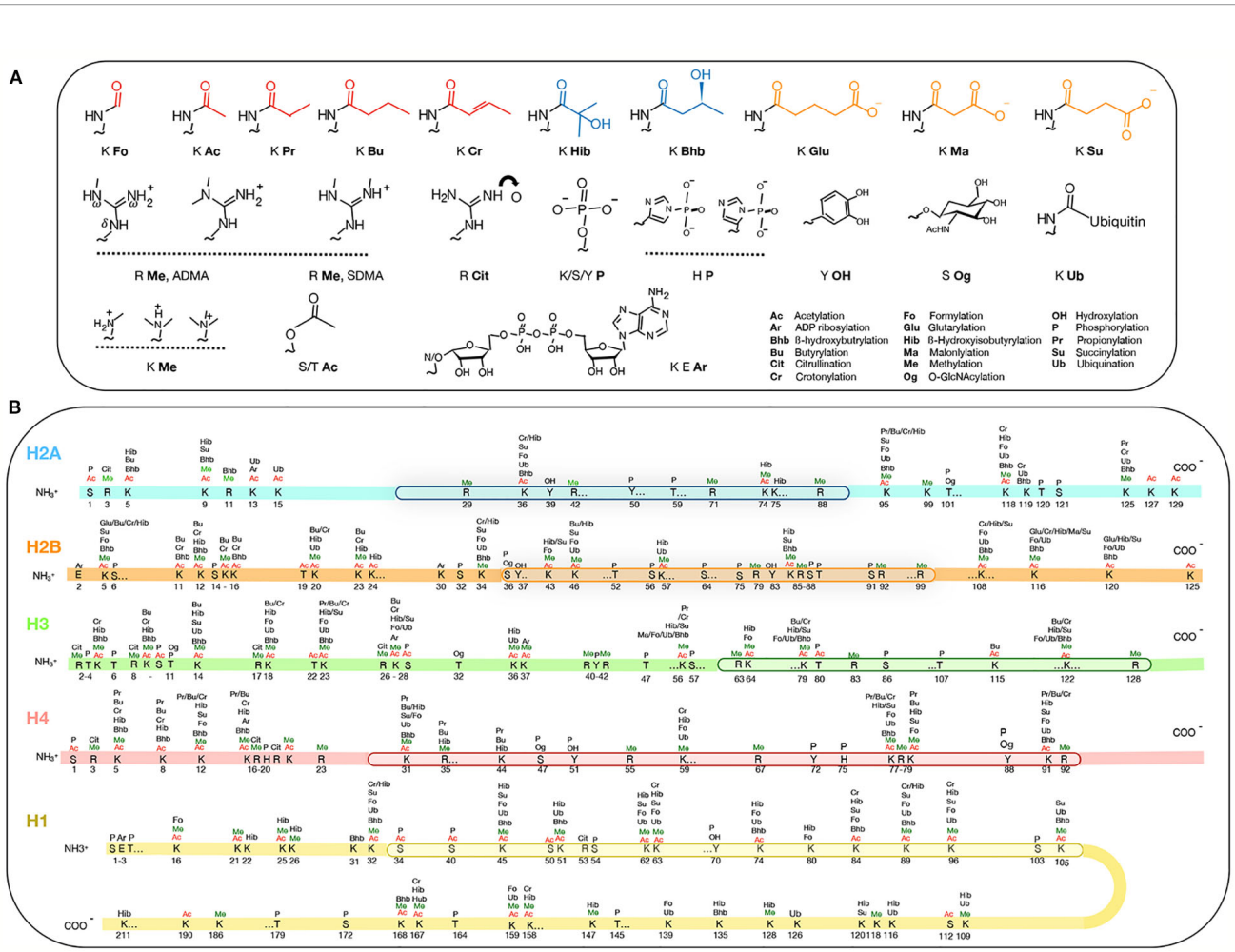

FIGURE 1 | Post-translational modification of histones. **(A)** Metabolites attached to histones. The top row shows acyl groups that are hydrophobic (red), polar (blue) and charged (orange) attachments. **(B)** The types and amino acid positions of the modifications on the core and the linker H1 histones. The globular domains (by which the histones themselves interact) are boxed. Figure is modified from Huang et al., 2014; Sabari et al., 2017.

rate-limiting suppliers of, respectively, acetyl and methyl groups. So far, the literature available on the potential competitors for these two adducts in both plant and animal models is frequently limited to DNA and proteins (e.g. chromatin and the overall proteome). Plant epigenetics elevated to the scale of epigenomics will need to step outside the provinces of just protein and DNA. The complete acetylome and methylome in a cell must include all molecules requiring these same adducts for functioning. For this reason, we are broadening this discussion here to include epi-transcriptomics and "epi-metabolites", by drawing in examples from both plant and non-plant models. One thing we try to avoid is lengthy coverage on how histone acetylation, histone methylation, and DNA methylation specifically influence plant development, especially flowering, as these areas have been amply covered. To help orientate non-experts, the following reviews should be highly informative: Zilberman et al. (2007), Law and Jacobsen (2010), Liu et al. (2010), Matzke and Mosher (2014), Liu et al. (2016), Trindade et al. (2017), Wang and Kohler (2017) and Friedrich et al. (2019).

In Plants, are the Cellular Concentrations of Acetyl-CoA Commensurate With the Level of Histone Acetylation?

Acetyl is used by cells as the basic currency for circulating two-carbon units in metabolic cycles. In eukaryotes, it comes exclusively from acetyl-CoA (**Figure 2A**) and several plant homologs of acetyl-CoA biosynthetic genes have been reported: pyruvate decarboxylase, acetaldehyde dehydrogenase, acetyl-CoA synthase, plastid pyruvate dehydrogenase, and ATP-citrate lyase. (https://portal.nifa.usda.gov/web/crisprojectpages/0187429-how-is-acetyl-coa-generated-in-plants.html). Many of these have not been extensively studied.

In other model organisms (e.g., yeast, mammals), the global level of acetylated histones has been shown to be correlated positively with that of acetyl-CoA in the cell. This suggests that acetyl-CoA availability likely represents the bottleneck. Acetyl-CoA itself is not membrane permeable so that within a compartmentalized cell, there are likely local heterogeneities in

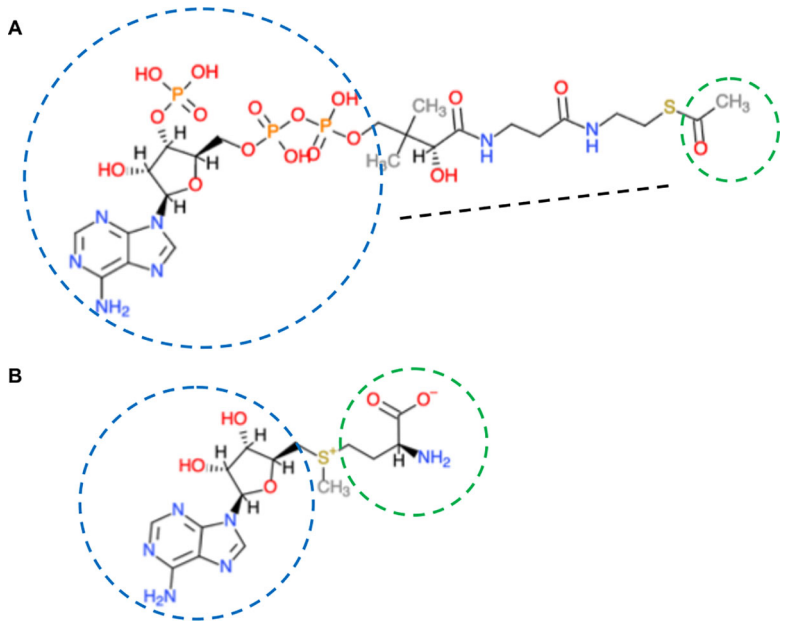

FIGURE 2 | Co-enzyme A and S-adenosylmethionine structures. **(A)** Co-enzyme A. Composed of an aliphatic chain (black dotted line), joined to adenosine diphosphate (blue circle). The sulfhydryl group (–SH) at one end is the most reactive. It can bond with, via the thioester with carboxylic acids (RCOOH), the most important is acetic acid (CH3COOH; acetyl is in green circle). Co-enzyme A has two major functions-as an energy carrier because of the high-energy phosphates and to transport two-carbon units in the form of acetyl between various biological molecules. **(B)** S-adenosylmethionine is synthesized from ATP (adenosyl in blue) and the sulfur-containing amino acid methionine (green circle). The activated methyl group (red) is linked to the sulfur (yellow). Chemical molecules were derived from ChemDoodle Web Component 2D Sketcher.

concentrations. Its flux among the subcellular compartments is accomplished rather by the membrane-permeable citrate and pyruvate, generated from the TCA cycle in the mitochondria (**Figure 3**). It has been hypothesized that membrane compartmentalization could in fact contribute to target specificity of some acetyltransferases (van Roermund et al., 1995; Jonas et al., 2010; Kistler and Broz, 2015; Sivanand et al., 2018; Wang et al., 2019).

Chen et al. (2017) have identified mutations in the Arabidopsis *ACETYL-COA CARBOXYLASE 1* (*ACC1*) locus, whose encoded enzyme converts cytosolic acetyl-CoA into malonyl-CoA required for the elongation of fatty acids produced in the plastids. While *acc1* null mutants are embryo lethal, leaky mutants show variable symptoms of vegetative growth defects in addition to a reduced stature, coined collectively as "bonsai phenotypes" (Fatland et al., 2005). The leaky *ACC1–5* contained about 50% higher amount of acetyl-CoA, and this is correlated with a global 50%–70% increase in histone acetylation over hundreds of chromosomal sites.

This semi-randomness in acetyl distribution over the chromosomes is somewhat expected, but at the level of individual histones, the lysine acetylation pattern showed a surprisingly strong bias. Instead of many lysines being eligible recipients owing to the higher acetyl-CoA import into the nucleus, the only notable beneficiary was H3K27. Seven other lysines (H3K9/14/18 and H4K5/8/12/16), known sites of acetylation, had levels indistinguishable from that of the wild type. Although there are many other possible target lysines or even arginines that have not been examined, this small size sample is nonetheless sufficient to hint at a rather strong selectivity in H3K27 to be acetylated. The underlying reason for this bias is not known.

The cytosolic acetyl-CoA biosynthetic enzyme ATP-citrate lyase (ACL) mentioned above is composed of two distinct subunits, ACLA and ACLB. The holoenzyme is a hetero-octomer composed of four subunits each of the A and B. Genetic analysis on *acl* mutants, because of their severe phenotypes or even lethality, indicated that the ACL complex represents a rate-limiting step or "non-redundant" generator of cytosolic acetyl-CoA (Fatland et al., 2005). This interpretation is consistent with the observation that hyperacetylation at H3K27 in *ACC1* can be partially blocked by expressing a ß-estradiol inducible artificial microRNA targeted against *ACLA*. Thus, it is clear that acetyl-CoA homeostasis and the global histone acetylation levels are intrinsically linked. This further implies that acetyl-CoA in the cytosol can cross the nuclear membrane, possibly by passive diffusion via the pore complexes (Shen et al., 2015).

Genetic and biochemical analyses on eight of the 12 acetyltransferases in Arabidopsis revealed that the hyperacetylation of H3K27 in *ACC1* depended on *At3g54610*, the single-copy gene encoding the nuclear histone acetyltransferase (HAT) GCN5/HAG1 [hereafter GCN5; for classification and descriptions of HATs, see (Shen et al., 2015)]. The argument that GCN5 is the major writer of H3K27ac is reinforced by the observations that the (hyper)acetylation at H3K27 in *aac1-5* was

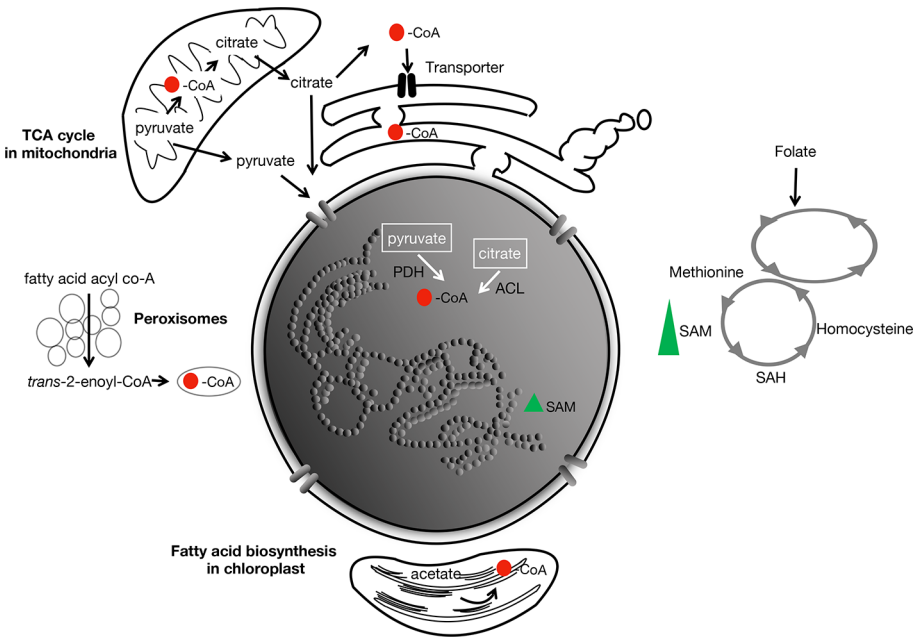

FIGURE 3 | Main metabolites involved in acetylation and methylation in the cell. CoA is produced by the TCA cycle in the mitochondria, and during fatty-acid biosynthesis in the chloroplast and peroxisomes. Its redistribution to the different subcellular compartments is hypothesized to be by diffusion (as pyruvate and citrate from the mitochondria) across membranes, or perhaps through nuclear pores. In animals, transporters of acetyl-CoA in the endoplasmic reticulum has been described (Jonas et al., 2010; Hirabayashi et al., 2013). Red spot, acetyl; PDH, pyruvate dehydrogenase; ACL, ATP-citrate lyase. SAM, the rate-limiting methyl group supplier is derived from methionine and the folate cycle. Green triangle, SAM.

abolished in the double mutant *gcn5 aac1–5*. This was also accompanied by partial reversion of one of the phenotypes, "leaf fusion", observed in the single mutant *aac1–5* (Chen et al., 2017).

How Does Acetyl-CoA Metabolism Link Up to Chromatin? Early Clues From Genetic Analyses

In Arabidopsis, genetic screens for suppressors of gene silencing based on altered expression of reporter transgenes *ProRD29:LUC* and *Pro35S:NPTII* (confers the kanamycin resistance) had identified loci in metabolism. One suppressor mutant showed kanamycin-sensitivity (due to hypermethylation of the *NPTII* gene), but still expressing *LUC*. The suppressor mutation was mapped to *At3g51840,* whose gene sequence predicted a peroxisomal acyl-CoA oxidase 4 (ACX4) involved in fatty acid ß-oxidation (Wang et al., 2019). Acyl-CoA oxidases in general act on CoA derivatives of fatty acids. In the case of ACX4, it catalyzes the conversion of fatty acid acyl-CoA [chemical formula: –C(O)–fatty acid] to *trans*-2-enoyl CoA, which is eventually converted into acetyl-CoA [chemical formula: –C–(O)–CH_3] (**Figures 2A** and **3**). This is thought to be the predominant way by which the rate of acetyl-CoA flux is controlled through ß-oxidation in peroxisomes. The acetyl-CoA level was lower in this mutant than in the wild type. By specific antibody staining in nuclei cytological spreads, histones H2B, H3, and H4 were all found to have lower than wild-type levels of acetylation levels. When histone H3 was analyzed in detail, again, some bias in the target lysines was detected. It was found that H3K9ac, H3K18ac, and H3K23ac were moderately reduced, those of H3K14Ac and H3K27Ac were unchanged. Over-expression of the above-mentioned *ACLA* and *ACLB* simultaneously (to reconstitute the complete cytosolic biosynthetic complex), but not the subunits individually, led to the rescue of the kanamycin-sensitivity of *acx4*. These results uncovered that ß-oxidation of fatty acids in peroxisome is interlocked with the regulation of histone acetylation and DNA methylation relevant to gene silencing.

The control of circadian rhythm in animals depends on one of the central regulators of circadian rhythm, CLOCK (Circadian Locomotor Output Cycle Kaput), which unexpectedly turns out to be a specific histone acetyltransferase (Doi et al., 2006; Eckel-Mahan and Sassone-Corsi, 2013). We mentioned this here because it was largely this finding that consolidated the idea that the epigenetic regulatory mechanisms are fundamentally controlled by metabolism. Counterbalancing CLOCK's activity are the repressors, PER and CRY. These can form heterodimers in the cytosol, then migrate into the nucleus where they physically block the CLOCK complex from binding to target chromatin sites. PER2:CRY1 dimerization is sensitive to the level of polyamines. And in the mouse, the decline in polyamines is correlated with the lengthening of the circadian period (Zwighaft et al., 2015). Polyamines also stimulate histone acetylation in several mammalian cell types, although the mechanistic contour remains hazy (Hobbs and Gilmour, 2000).

Metabolic Status of the Cell and Histone Deacetylases

The cofactor nicotinamide adenosine dinucleotide [NAD(+)] was initially discovered as an electron carrier (becomes NADH) in the oxidation of carbohydrates. The involvement of NAD(+) in histone modification is just beginning to be explored in plants. In combination with the *de novo* synthetic pathway (from aspartic acid), Arabidopsis has a salvage pathway in which nicotinate mononucleotide is regenerated from nicotinamide. In animals, the Sirtuin-Like proteins SIRT 1 and SIRT6 form a class of histone deacetylases whose activities depend on NAD(+) (so-called class III HDACs). Sirtuins are activated at times of energy deficit and reduced carbohydrate energy, associating with high NAD(+) levels. The activities of SIRT seem to be, moreover, limited by NAD(+) availability (Pacholec et al., 2010; Gerhart-Hines et al., 2011; Hirschey et al., 2011; Fischer et al., 2012). Like acetyl-CoA, the levels of NAD(+) could, therefore, act as a signal that communicates the cellular redox status to the chromatin, through activating specific SIRT's (in mammals, these are SIRT1, SIRT6, and SIRT7).

Mammalian HDACs are inhibited by ß-hydroxybutyrate, a ketone that has been known primarily as a circulating source of energy in response to fasting. ß-hydroxybutyrate can thus logically act as a trigger inside cells to increase the global levels of histone acetylation and the expression of numerous genes, particularly those encoding oxidative stress-protection factors (Shimazu et al., 2013). Whether ß-hydroxybutyrate exists in this form freely in plants is not conclusive, but poly-ß-hydroxybutyrate is present (Tsuda et al., 2016). Whether this can metabolize to ß-hydroxybutyrate is not known.

Polyamines and Histones Cooperate in Remodeling the Chromatin Structure

Polyamines are aliphatic compounds of low molecular weight bearing more than one amino group. Because of the amino groups, at physiological pH, these compounds are therefore polycations. The four most abundant, or universal, polyamines are putrescine, spermine, spermidine, and cadaverine, which are found in disparate ratios in virtually all cellular life forms, ranging from prokaryotes (e.g. Mycoplasma, *E. coli*, Salmonella, etc.) to humans.

In eukaryotes, one of the earliest roles attributed to polyamines is that they interact with the chromatin (Morgan et al., 1987). Polyamines are ancient molecules that played a role in packaging DNA and RNA in simple cells and viruses. Although most of the demonstrations on polyamine–DNA interactions have been done *in vitro*, there are genetic evidences, especially obtained from yeast, entirely consistent with these interpretations.

The mutation *gcn5* disrupts the yeast homologous histone acetyltransferase and impairs the transcriptional activation of many target genes (Xue-Franzen et al., 2010). The mutant is also hypersensitive to oxidative stress and shows retarded growth (Pollard et al., 1999). In genetic screens for extragenic suppressor mutations, the *gcn5* phenotypes were found to be partially restored to those of the wild type by the overexpression of *ARG3. ARG3* does not encode chromatin-related proteins, but ornithine decarbamylase, which converts the non-protein amino acid ornithine to citrulline, an intermediate in the urea cycle as well as an arginine derivative found in histones (**Figure 1**). Because ornithine is the limiting step in polyamine biosynthesis, its catabolic conversion into citrulline competes with its alternative production of polyamine. This led to the hypothesis that polyamine deficiency caused by *ARG3* overexpression should suppress the histone acetyltransferase deficiency. This was indeed confirmed. Similarly, another mutation, the loss-of-function *spe1* can also partially reverse the effect of *gcn5* based on reporter-gene expression assays (e.g. *HO-lacZ*, *SUC2-lacZ*, etc.). *SPE1* encodes ornithine decarboxylase, which converts ornithine into putrescine, a precursor for the biosynthesis of other polyamines. Finally, combining *spe1* and a semi-dominant allele of histone H4 (*hhf2-7*; which impairs nucleosome-mediated gene repression) almost completely alleviated GCN5-dependent expression of the reporter gene. These results, together, provide strong genetic proofs that the normal roles of polyamines include the repression of gene expression through interactions with nucleosomes. *In vitro*, spermidine can efficiently promote oligomerization of nucleosomes onto DNA. Core histones acetylation attenuates this process (Pollard et al., 1999).

Both core histones and polyamines seem to be common targets of transglutaminases (Folk et al., 1980; Ballestar et al., 1996). These enzymes catalyze the additions of amine groups to the amino acid glutamine. Histones are easily cross-linked or modified by polyamines *in vitro* and raises the possibility that they are transglutaminase substrates *in vivo* (Nunomura et al., 2003). Human histone proteins directly purified from HeLa cells do show abundantly linked putrescine, spermidine or spermine (Yu et al., 2015). More unexpected is that serotonin, a neural transmitter as well as a trophic factor that helps neurons to grow, is added by a specific transglutaminase onto glutamine 5 of H3 (Farrelly et al., 2019). And this modification can take place only if H3K4 is already trimethylated, attesting to the functional specificity of this serotonin mark. It is also worthwhile to emphasize that this discovery portents that other neural transmitters, such as dopamine and histamine, could well be histone marks (Cervantes and Sassone-Corsi, 2019). Serotonin (Erland and Saxena, 2017), dopamine (Bell and Janzen, 1971) and histamine (Sanchez-Perez et al., 2018) (https://www.britannica.com/science/histamine) all exist in plants, portending the astonishing diversity of adducts that are still waiting to be uncovered.

Mechanisms of Acetylation of Metabolites and Histones Hint at Early Co-Evolution

Genomic-scale analysis of "acetylome" has found that many non-histone proteins, including those in organelles, are acetylated. Some of the acetylated non-histone proteins have been described in Shen et al. (2015), as potential stakeholders of the same acetyl-CoA source.

Beyond proteins, the more intriguing point is that many metabolites themselves are targets of acetylation, prompting some to call these epi-metabolites (Showalter et al., 2017). For

examples, some amino acids, neurotransmitters or polysaccharides such as glucosamine and muramic acid are all substrates of acetyl-CoA-dependent acetyltransferases (Engelke et al., 2004; Vetting et al., 2005; Han et al., 2012; Showalter et al., 2017; Christensen et al., 2019).

Acetyltransferase activities have been reported to co-purify from mammalian cell extracts that can acetylate *in vitro* both histones and polyamines, although the nature of these proteins is not known (Wong et al., 1991; Matthews, 1993). Equally intriguing is whether some acetyltransferases can modify both histones and metabolites, with implications for the evolution of this class of enzymes. One recent discovery is that the activity of the human H3 acetyltransferase, PCAF, can be enhanced towards histone H3 (10 μM) by the presence of low concentrations (<5 μM) of N^8-monoacetylspermidine i*n vitro*. It was hypothesized that the PCAF Bromodomain is able to bind N^8-monoacetylspermidine, which then increases the affinity of the acetyltransferase towards H3. In the presence of high spermidine concentrations (>15 μM), PCAF switches substrate preference, exhibiting N^8-spermidine acetyltransferase activity over that of histone, resulting in N^8-monoacetylspermidine (Burgio et al., 2016).

So far, there is no polyamine deacetylase known from eukaryotes. However, acetylpolyamine amidohydrolases (APAH) with deacetylase activity had been isolated from the soil bacterium *Mycoplana ramosa* (formerly *bullata*) (Fujishiro et al., 1988; Sakurada et al., 1996). These enzymes, dimeric, have a strong affinity towards acetylated spermine, N^1– and N^8 – isoforms of spermidine, cadaverine, and putrescine. The APAH has been crystallized and its structure resembles that of a HDAC–like oligomer. In fact, APAH displayed significant activity towards L–Lys (ε–acetyl)–coumarin, the small *in vitro* substrate for HDAC, but reduced activity towards the larger HDAC test substrate acetyl–L–Arg–L–His–L–Lys(ε–acetyl)–L–Lys(ε–acetyl)–coumarin. Dimerization is important, because the interface creates an "L"-shaped active site tunnel would allow only substrates that are sufficiently narrow and flexible to enter. These results also hint at the possibility that a comparable dimeric HDAC could catalyze polyamine deacetylation in eukaryotes (Lombardi et al., 2011). The implication is that prokaryotic polyamine deacetylases might have been the predecessors that eventually evolved into eukaryotic histone deacetylases.

Histone Methylation and Metabolic Cofactors

Methylation of histones and DNA is well known, but their methylation status is coordinated with the metabolism. On a genome-scale, methylome will need to explore beyond histones and DNA, by taking into account of other cellular elements, including RNA and metabolites.

Approximately 1% of the genes in several reference eukaryotic genomes, ranging from Arabidopsis to mammals, encode proteins with motifs characteristics of methyltransferases (Katz et al., 2003). This relatively large number of predicted methyltransferases suggests there might be an equally large trove of corresponding methylated substrates yet to be discovered. By far, the most characterized methyl acceptors are histones (**Figure 1**) and DNA, with direct consequences on the epigenetic regulation of gene expression.

The universal methyl ($–CH_3$) donor is S-adenosylmethionine (SAM) (**Figure 2**). SAM originates from folate-dependent one-carbon metabolism (the transfer of one-carbon units) (**Figure 3**). The vitamin B_{12}-dependent methionine synthase uses 5-methyl-tetrahydrofolate (5-CH_3-THF) as the one-carbon donor for the methylation of homocysteine to methionine, the precursor of SAM. Removal of the methyl moiety from SAM results in S-adenosylhomocysteine, which is a competitive inhibitor of methyltransferases. On the other hand, decarboxylation of SAM to S-adenosyl-methioninamine contributes the α-aminopropionyl group to the biosynthesis of spermine and spermidine, as well as being the precursor of certain amino acids and ethylene (Miyazaki and Yang, 1987; Roje, 2006).

Histone methylation is carried out by families of transferases represented by SUPPRESSOR OF VARIEGATION SU(VAR)3-9, ENHANCER OF ZESTE [E(Z)], TRITHORAX (Trx), and ASH1 (absent, small, or homeotic discs 1). These protein families share a common stretch of 130 aa, called the SET domain, an acronym based on the founding members of the first three families, identified in Drosophila by genetic screens for modifiers of variegating phenotypes (see section *HETEROCHROMATIN PROTEIN1 and Histones-Collaborators or Competitors?*). Histone methyltransferases in Arabidopsis can control the expression of genes with functions in metabolism. For example, the SET-domain SDG8 catalyzes H3K36me3 in gene bodies, inducing high-level expression of a specific set of light- and/or carbon-responsive genes important for photosynthesis, metabolism and energy production (Li et al., 2015).

The catalytic activities of histone demethylases are directly dependent on metabolites as co-factors. The first type is the amine oxidases, represented by the Lysine-Specific Demethylase1 (LSD1), whose activities require flavin adenine dinucleotide (FAD). In Arabidopsis, several homologs (e.g. *FLD*, *LDL1*, *LDL2*) play a prominent role in flowering time through the suppression of *FLC* (Jiang D. et al., 2007; Liu et al., 2007).

In mammals, histone demethylases have extremely broad functions, covering many metabolic pathways. For example, high carbohydrates will stimulate FAD accumulation, which can then activate LSD1 and also the deacetylase Sirtuin. Thus, it seems that nutrient signals are transduced by at least two epigenetic pathways, implicating both demethylation and deacetylation. LSD1 is known to demethylate the repressive mark H3K4me2 on the fatty acid synthase gene, to activate its expression. But it can also inhibit glucogenesis by demethylating the active mark H3K4me2 on *FBP1* and *G6Pase* (Nakao et al., 2019). LSD1 and many other epigenetic components are also implicated in DNA metabolism, in which chromatin structures at double-strand breaks are remodeled to allow DNA-repair machinery to access the spatially confined region surrounding the double-strand DNA break [for example, see (Wei et al., 2012)].

The other class of demethylases is a complex family of proteins characterized by the Jumonji C (JmjC) domain, with members targeting specific histone lysines at different methylation states. Their catalytic activities need ferrous iron [Fe(II)] and 2-oxoglutarate (2-OG). Because Fe(II) is sensitive to reactive oxygen species (ROS) produced during aerobic metabolism and oxidative stress, JmjC activities might thus be modulated by Fe(II) availability.

There is also a sizeable number of arginine (R) residues on H3 and H4 that are targets of methylation [which will not be enumerated here; for details, see (Zhang and Reinberg, 2001; Liu et al., 2010; Ahmad and Cao, 2012)] (**Figure 1B**). The essential point here is that this amino acid bears three guanidino nitrogen atoms (CH_5N_3)–two terminal nitrogens designated as ω and one internal designated as δ (**Figure 1A).** Contingent on the methylation positions on the nitrogens, one isomer generated is called SDMA, or symmetric dimethylarginine, in which each of the two ω guanidino nitrogens is bound to one methyl group; the other is designated ADMA, or ω-N^G, N^G asymmetric dimethylarginine, in which two methyl groups replace the two hydrogens of the same ω guanidino nitrogen atom. These dimethylarginine isomers, ADMA and SDMA, seem to generate contrasting biological readouts. In mammals, ADMA at H4R3 is associated with transcriptional activation (Wang et al., 2001), whereas SDMA at the identical position is a repressive mark (Zhao et al., 2009). The regulatory readouts dictated by these modifications do not stop here, but subsequent proteolysis of the methylated proteins liberates ADMA and SDMA. ADMA (but not SDMA) then turns into a metabolite inhibitor of the endothelial nitric oxide synthase (Xuan et al., 2016). Arabidopsis arginine methyltransferase homologs exist (Liu et al., 2010), it is likely that ADMA might also act as a metabolic inhibitor.

DNA Modifications–Reversible Methylation, Novel Bases, Double-Strand DNA Break, Gene Silencing

Studies on DNA modification have been largely focusing on methylcytosine. It was first reported in 1925 in *Mycobacterium tuberculosis*, but it is now widespread in most model organisms, except *C. elegans.* DNA methylation is found on nucleotides (N^6-)methyladenine, (N^4- and N^5-)methylcytosines (Ratel et al., 2006). In Arabidopsis, N^5-methylcytosines are abundant and present in CG, CHG and CHH sequence contexts. These marks are catalyzed and maintained by a battery of enzymes leading to restructured chromatin (e.g. MET1, DDM1, SWI2/SNF2, CMT2, CMT3, DRM2, etc.). The present-day technologies, however, are not of sufficient resolution to pinpoint the specific function of the individual types of methylated nucleotides. For now, it appears that it is rather the optimal levels of DNA methylation are important for plant growth (Dowen et al., 2012; Zhang et al., 2018; Gonzales and Vera, 2019).

Double-strand DNA breaks (DSB), which is mechanistically associated with DNA repair and recombination, is best correlated with low DNA methylation levels. In meiosis, during which recombination has been explored in detail, it starts with a double strand break (DSB) introduced in the chromosomal DNA by SPO11-1, SPO11-2, and MTOPVIB in a topoisomerase IV-like complex. Sequencing the oligonucleotides recovered from SPO11-1 revealed hotspots that are clearly low in cytosine methylation, gene-rich, and tend to exclude nucleosomes as ascertained by micrococcal nuclease digestion (Choi et al., 2018). Similar analyses had also been carried out in maize, by taking advantage of the RAD51 protein, which binds to sequences near DSBs (He et al., 2017). These RAD51-bound sequences are not skewed towards gene-rich regions but rather dispersed throughout the genome, including centromeric and pericentromeric regions. In fact, 75% of DSBs are derived from repetitive DNAs and retrotransposons. Despite these differences relative to Arabidopsis, maize DSBs are also found in DNA regions of low methylation as well as being nucleosome-free (He et al., 2017).

DNA methylation is reversed by demethylases belonging to a family of DNA glycosylases but the relationship with metabolism has not been firmly established, especially in plants. In animals, one enzyme family is called TEN-ELEVEN TRANSLOCATION METHYLCYTOSINE DIOXYGENASEs (TETs). TET converts 5-methylcytosine to 5-hydroxymethylcytosine, 5-formylcytosine, and 5-carboxylcytosine; all of these unusual base derivatives have been found in the mouse genome (Ito et al., 2011) (**Figure 4**). TET activities–like those of histone deacetylases and demethylases–share the cofactors Fe^{2+} and α-ketoglutarate. Another link between DNA methylation/demethylation and metabolism is through vitamin C. Its simple addition to the culture medium can induce extensive epigenetic reprogramming, converting mouse fibroblast cells back into pluripotent or stem cells; the efficiency of this conversion is TET1-dependent (Pera, 2013).

The above methyl-cytosine derivatives are not the only novelties found in mammalian genomes. In fact, eukaryotic nuclear DNA could be more extensively modified than we realize (https://en.wikipedia.org/wiki/DNA). For now, most of the modified bases have only been reported in microorganisms, such as bacteria and phages, but some of the "exotic" modifications might still turn up in eukaryotic genomes: Uracil was first found in the genomic DNA of Plasmodium, but it is now present on at least two human chromosomes (Shu et al., 2018) (**Table 1**). Obviously, how all of these unusual bases are maintained and escape correction mechanisms is not known. Neither do we know whether a parallel exists in plants.

Sulfamethazine, an inhibitor of folate synthesis, can suppress gene-silencing in plants (Zhang et al., 2012). In the same genetic screens for suppressors that would release the silenced expression of the double reporters (*LUC* and *NPTII*) in the mutant *ros1* (*Repressor of Silencing 1*), extragenic suppressor mutations mapping to *FOLYLPOLYGLUTAMATE SYNTHETASE 1* (*FPGS1*) were identified (Zhou et al., 2013). *In vivo*, folate can be polyglutamylated and FPGS catalyzes the sequential conjugation of additional *r*-linked Glu residues to the initial Glu. The *fpgs* mutation reduced the total folate abundance and DNA methylation in all three cytosine contexts, as well as the

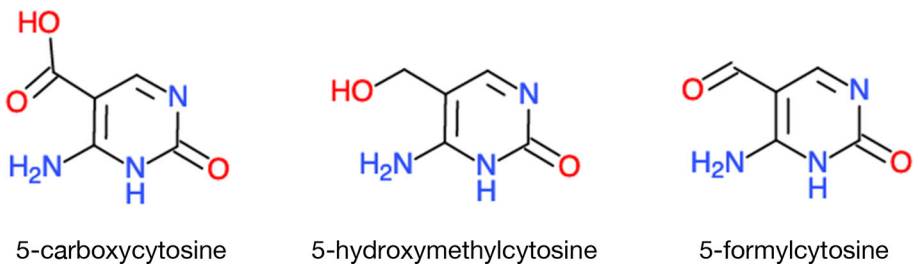

FIGURE 4 | A sample of unusual bases in eukaryotic DNA. TET DNA demethylases, instead of simply removing the methyl groups, they leave in their wake rearranged nucleotides. Chemical molecules were derived from ChemDoodle Web Component 2D Sketcher.

TABLE 1 | Modifications and substitutions of DNA bases.

Bases	Modifications
Adenosine	N^6-carbamoyl-methyladenine
Guanine	7-methylguanine
Cytosine	N^4-methylcytosine
	5-carboxylcytosine
	5-formylcytosine
	5-glycosylhydroxymethylcytosine
	5-hydroxycytosine
Thymidine	α-glutamylthymidine
	α-putrescinylthymine
Uracil and modifications	ß-glucopyranosyloxymethyluracil (base J)
	uracil
	5-dihydroxypentauracil
	5-hydroxymethyldeoxyuracil
Others	deoxyarchaeosine
	2,6-diaminopurine

level of the repressive mark H3K9me2. Similar to the example of vitamin C in animal cells, here, adding to the plant medium a stable form of folate (5-formyltetrahydrofolate, 5-CHO-THF) could revert the short-root phenotype and the recovery of kanamycin resistance from the reporter *NPTII*. This treatment also restored the level of H3K9me2. Moreover, the addition of 5-CHO-THF to the wild-type plants also increased the DNA methylation level, but that of H3K9me2 remained constant. These results suggest that the level of DNA methylation during normal development of the plant is directly limited by folate, with a secondary consequence on histone methylation. Over-expressing methionine synthase, to increase the precursor to SAM, represses resistance to *Pseudomonas syringae* DC3000 and genome-wide increase in DNA methylation, reinforcing the importance of folate one-carbon metabolism for correct DNA methylation and its dynamics in responding to stress stimuli (Gonzales and Vera, 2019).

The locus *SUPPRESSOR OF DRM2 CMT3* (*SDC*) is silenced conjointly by the DRM2- and CMT3-mediated methylation pathways. Thus, while *SDC* is expressed in the double mutant *drm2 cmt3*, it is silenced in the wild-type and also in each of the two respective single mutants. Using the transgene *SDCpro-GFP* as the reporter, which was silenced in the WT and *cmt3* background, one mutant was identified with alleviated reporter gene suppression in the WT background. The mutation was mapped to the gene (*MTHFD1*) encoding METHYLENETETRAHYDROFOLATE DEHYDROGENASE/METHENYLTETRAHYDROFOLATE CYCLOHYDROLASE 1 involved in the interconversion of three key folate intermediates, and other functions including the production of purine, pyrimidine, and SAM (Groth et al., 2016). This mutation led to the genome-wide loss of CHG and CHH methylation, reduced H3K9me and re-activation of mobile elements. The actual cause of these consequences, however, may not be the mere results of diminished folate pools, because, in contrast to *fpgs1* above, applied 5-formyltetrahydrofalte (5-CHO-THF) led to rather root growth inhibition of the *mthfd1-1* (but not on WT seedlings). Treatment with 5-CHO-THF as well as 5-CH_3-THF did not rescue the DNA methylation defects in *mthfd1-1*. The authors have attributed the cause to be inhibition of methionine synthase.

In human cells, a fraction of the MTHFD1 is recruited to chromatin by a direct interaction with the histone acetyl reader Bromodomain-containing protein 4 (BRD4), whose deregulation has been linked to oncogenesis (Sdelci et al., 2019). Thus, besides SAM production, the MTHFD1 protein itself, involved in nuclear folate metabolism, can be a component of chromatin complexes that directly influence gene expression.

Epi-Transcriptomics-m^{6}A, With Links to TCA Cycle, Methylated DNA and Acetylated Histones

RNA containing modified bases had been noted since the 1970s (Desrosiers et al., 1974). Because mapping modified RNA bases was labor-intensive (https://bitesizebio.com/13550/a-short-history-of-sequencing-part-1-from-the-first-proteins-to-the-human-genome/), it took a backseat to the easier task of determining the actual sequences themselves, aided by the technical advances in DNA sequencing. In the process of copying the RNA into cDNA by supplying the standard nucleotides in the *in vitro* reactions, any chance of following up on modified RNA bases quickly dropped out of the radar, which lasted over 3 decades.

Over 150 different chemical modifications are known, most of them are in structural RNAs (e.g. tRNA, rRNA), but a few are

also present in mRNA (http://modomics.genesilico.pl/ and http://mods.rna.albany.edu). The prevailing idea is that these modifications determine the post-transcriptional fate of the RNA (Boccaletto et al., 2018; Hu et al., 2019). But it is likely that at least some of the modifications on RNA, particularly methylation, can compete with the demands by DNA and histones. Only m^6A will be discussed here.

The m^6A found in DNA is also a major mark on total RNA (0.1% to 0.2% of the nucleotide). It maps preferentially to the transcription start sites, the stop codon, and the 3' UTR. Compared to its counterpart on DNA, for which the functions are speculative with the possible exception of double-strand breaks, we have better ideas about its effects on RNA. The first-ever hint of its functional importance at the whole-organism level was distilled from disrupting the gene *MTA* (At4g10760), encoding the mRNA adenosine methyltransferase, in Arabidopsis (Zhong et al., 2008). Homozygous T-DNA insertion mutant embryos are white and fail to mature beyond the globular stage, indicating that the optimal m^6A level must be connected with a number of elementary metabolic networks.

The levels of m^6A in RNA are positively correlated with transcript stability. This may be one mechanism to enhance the half-life of selective mRNAs. This hypothesis is clearly supported by a mammalian model system, in which viral infection stimulated the binding of a specific RNA m^6A demethylase, ALKBH5, to an important transcript–the α-ketoglutarate dehydrogenase (*OGHD*) mRNA. This binding is correlated with blocking viral infection. ALKBH5 is a methylated protein, and demethylation at its R107 inactivates its catalytic activity (Liu et al., 2019). In this alternative scenario, the *OGHD* mRNA became hypermethylated as well as stabilized as the result. The higher OGHD also stimulated the production of the metabolite, itaconate, an intermediate of the TCA cycle, required for viral replication. RNA m^6A demethylases are actually α-ketoglutarate-dependent dioxygenases, indicating their catalytic activities are linked to those of the TCA. They can erase not only methyl but also alkyl groups on their diverse types of targets. For example, in animals, ALKBH1 can act on RNA, DNAs, and histones. This dioxygenase also targets several m^1A methylated tRNAs in the mitochondria, influencing organellar translation (Kawarada et al., 2017; Muller et al., 2018).

In Arabidopsis, there are 13 different ALKBHs. Most of them are localized in the nucleus and in the cytoplasm, except ALKBH1D, which is chloroplastic (Mielecki et al., 2012). ALKBH10B is the principal mRNA m^6A eraser influencing floral transition by controlling the transcript levels of *SPL3*, *SPL9* and *FLOWERING LOCUS T* (Duan et al., 2017). ALKBH9B also seems to play roles in plant defense against pathogens (Martinez-Perez et al., 2017). In rice, *ALKBH1*, *ALKBH6*, *ALKBH8B*, and *ALKBH10A* were found to be differentially regulated by drought, cold or ABA. All of these observations are consistent with the notion that these ∝-ketoglutarate-dependent demethylases may have roles as environmental sensors (Hu et al., 2019). Thus, there seems to be a possible coordinated switch of the chromatin towards more of an active state by demethylation of DNA, RNA, histones, coupled to acetylation of histones.

Metabolite Methylation: Functions and Influence on Chromatin State

In mammals, methylation of phosphotidylethanolamine (a phospholipid) was experimentally shown to divert methylation from histones and a protein phosphatase2A. This overall process is thought to reflect optimization of sulfur metabolism as well as transcriptional regulation of sulfur and the expression of genes involved in phospholipid metabolism (Ye et al., 2017). These biochemical results prove that metabolites are parts of the global methylome by competing for SAM away from histones and non-histone proteins.

Plants are metabolite factories (Fang et al., 2019), yet their potential connection with epigenetics has hardly been explored. Examples of well-known metabolites are methyl-salicylic acid and methyl-jasmonate, with broad physiological effects on development and plant–environment interactions (Vogt, 2010; Hu et al., 2017). *O*-methyltransferases have been implicated in lignin biosynthesis (Zhong et al., 1998) and in modifying flavonoids as well as esters with aromatic vicinal dihydroxyl groups (Ibdah et al., 2003). Methylation of certain anthocyanins alters the intensity of pigment hues, generating their diversity in stability and functions, likely related to their function as protectants against UV, pigmentation, antioxidation or attractants of insects (Du et al., 2015). In Arabidopsis and the cyanobacterium *Synechococcus*, trimethylation of glycine yields glycinebetaine, which confers tolerance to experimental stresses that include low temperature, drought and high salinity (Waditee et al., 2005). The enhanced salt tolerance in the case of *Synechococcus* can be dramatic, as illustrated by the transgenic expression of two glycine methyltransferases that enabled the cells to grow in 0.6 M NaCl, converting a fresh-water organism into a marine species (Waditee et al., 2005). Methylglycine also exists in mammalian cells, which converts the amino acid into an oncometabolite. *N*-methylglycine or sarcosine stimulates the invasion and aggressiveness of prostate cancer cells (Sreekumar et al., 2009). *1*-Methylnicotinamide is known to be a developmental regulator of prostacyclin synthesis in mammals (Chlopicki et al., 2007). More recently, this metabolite is also found to be required to maintain stem cells in their embryonic state by competing with the deposition of H3K27me3 marks (Sperber et al., 2015). Even the SAM-independent methyl donor, folate, itself, can be methylated, which is the active form of vitamin B9 used by the human body in circulation. As it is generally thought that the number of metabolites vastly outnumbers that of proteins (Li and Snyder, 2011), metabolites could turn out to be extremely tenacious competitors for SAM, and thereby, also chromatin structures.

Arsenate induces the accumulation of several methylated/citrullinated proteins [FUS, EWS, and TAF15; see (Tanikawa et al., 2018)]; arsenate is itself inactivated by methylation (Tseng, 2009). Methylhalides (organic halogens) are produced by a large number of ecosystems, crops, and biota. Likewise, the terrestrial source of methyl iodide can account for 80-110x10^9 tons of

iodine per year (https://www.sciencedirect.com/topics/chemistry/methyl-halides) (Carpenter, 2015). Despite little is known about their biological roles, there are nonetheless methyltransferases that have already been identified in plants, such as *Endocladia muricata* (marine red alga), *Phellinus promaceus* (white rot fungus) or *Mesembryanthemum crystallanium* (ice plant), that can use SAM to methylate organic ions such as the anions iodide, chloride, bromide (Wuosmaa and Hager, 1990) and the amino acid alanine (Barkla and Vera-Estrella, 2015), possibly associated with various adaptive functions. Along with the thinking of diets in humans being linked to epigenetics and diseases, one wonders whether plants metabolites, liberated after being ingested by the organism, can directly be used by the animal epi-genome as well. This hypothetical scenario is plausible; it would be analogous to horizontal gene transfer (bacteria taking up free DNA) or interspecific exchanges of small regulatory RNAs between pathogens and plants [for an example, see (Hudzik et al., 2020)].

Heterochromatin Protein1 and Histones-Collaborators or Competitors?

The methyl marks on histones are "read" by protein modules, which then translate them into specific gene expression profiles. One of the better-characterized methyl-lysine readers in plants is LIKE HETEROCHROMATIN PROTEIN1 (LHP1), a Chromo domain protein in the Polycomb Repressive Complex 1 (PRC1). The mutant *lhp1* displays pleiotropic phenotypes that include abnormal rosette leaves, smaller plant stature, partial sterility, early flowering and a terminal flower (Gaudin et al., 2001; Kotake et al., 2003). The mutation has an impact on general metabolism: in a genetic screen for mutants affected in the synthesis of glucosinolates, *tub8* was identified. Intriguingly, this mutation turned out to be allelic to *lhp1* (Kim et al., 2004).

While a "reader" has an important role in translating a histone mark into a cellular function, histones and (L)HP1 may also have complicated relationships in that they compete for the same metabolites for adducts. LHP1 binds to trimethylated H3K27, which is a euchromatin mark *in vivo* (Turck et al., 2007; Zhang et al., 2007) and sensitive to the cytosolic level of acetyl-CoA. The name LHP1 had been inspired by its notable sequence similarity to the founder HETEROCHROMATIN PROTEIN1 (HP1) of Drosophila. HP1 was identified as *Su(var)205*, a suppressor mutation of Position Effect Variegation (PEV) (Tschiersch et al., 1994; Lloyd et al., 1999; Elgin and Reuter, 2013). For clarity, PEV describes the variegation of a phenotype caused by a wild-type gene's abnormal juxtaposition to heterochromatin brought about by either chromosomal rearrangement or transposition. One model suggests that heterochromatin can spread from HP1-bound sites to adjacent regions with stochastic endpoints, suppressing the expression of neighboring genes in some cells but not in others. Modifiers of PEV almost always corresponded to deleted or disrupted loci encoding histone, chromatin proteins and components in RNA interference. One surprising result, at least at the time, from these genetic screens was the discovery of *SUPPRESSOR OF ZESTE5* [*Su(z)5*]. Instead of a mutation in yet another locus encoding a chromatin-related protein, *Su(z)5* turned out to impair the synthesis of SAM (Larsson et al., 1996). With hindsight, it is obvious that SAM is the limiting methyl donor for a wide range of molecules, including chromatin proteins and metabolites. But in the absence of this knowledge at the time, PEV suppression was hypothesized by the authors to be linked to the reduced levels of certain polyamines, which was empirically confirmed.

In vivo, the Arabidopsis LHP1 is found in nuclear speckles (Gaudin et al., 2001; Kotake et al., 2003), which represent an example of non-membrane bodies. However, whether these speckles reflect the intrinsic ability of LHP1 to self-aggregate and to undergo liquid–liquid phase separation, or coerced into foci by association with other cellular components, is not known. We raised this possibility because the Drosophila and one of the human homologs have an intrinsic ability to phase separate *in vitro* (Larson et al., 2017; Strom et al., 2017). In the latter case, the *in vitro* phase separation HP1 isoform α was correlated with phosphorylation on the protein's N-terminal extension, or alternatively, by the presence of certain ligands including non-specific DNA and spermine (Larson et al., 2017). This phase separation into protein droplets has been interpreted by the authors as recapitulating the key role of HP1 as nucleation sites for chromatin condensation and spreading that occur *in vivo*. HP1α and the Drosophila homolog are endowed with an ability to self-assemble into a large oligomer, and nucleating around charged molecules. However, the *in vivo* physiochemical conditions facilitating these particular HP1s to assume gel-like droplets are still a matter of debate [see (Richter et al., 2008) for an example of conditions]. Because spermine and other polyamines are abundant metabolites in cells and can condense nucleic acids, these polycations may ease HP1 into molecular crowding and local phase separation.

There are covalent modifications on histones–acetylation, methylation, citrullination, and formylation–that are also predicted on all three human HP1 isoforms (LeRoy et al., 2009; Wiese et al., 2019). Most of the target lysines are conserved in the Arabidopsis LHP1 (**Figure 5**). The role of histone formylation in influencing gene expression is not completely understood despite that protein formylation in eukaryotes is widespread (Wisniewski et al., 2008). Nonetheless, formylation of histones (**Figure 1**), and chromatin proteins such as High-Mobility Group (HMG) and HP1 homologs, adds an additional point of convergence between epigenetics and metabolism. Deformylases (Meinnel et al., 1996) and formyl-binding chemosensory receptors (Dahlgren et al., 2016) exist in animals, suggesting dedicated metabolic and signaling processes, likely in responding to stressful stimuli. The metazoan HP1s are also recruited to damaged DNA; thus, it has been proposed that formyl donors could come from 3'-formylphosphate, a highly reactive intermediate generated from oxidation of the 5'-deoxyribose in the damaged DNA (Jiang T. et al., 2007; Ayoub et al., 2008; LeRoy et al., 2009; Luijsterburg et al., 2009). Are these processes also inherent to normal development? For example, would (L)HP1 be involved in the repair of hundreds of double-strand breaks generated regularly during meiosis? We have also mentioned that LSD histone

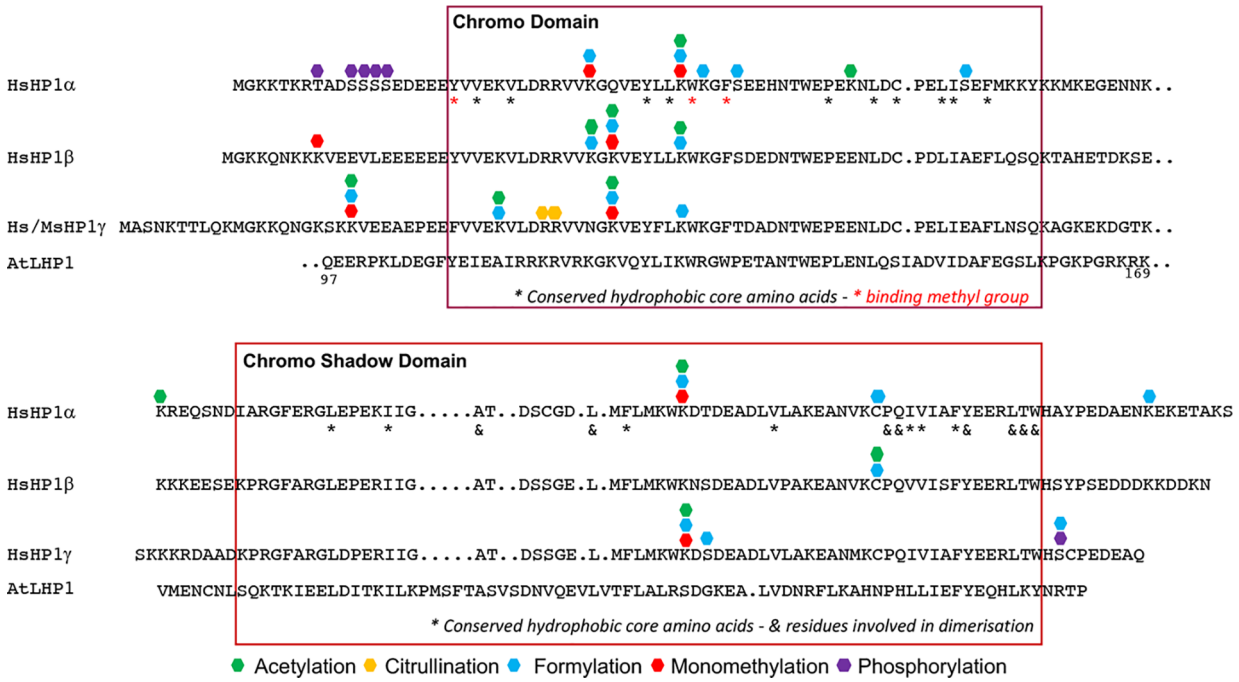

FIGURE 5 | Modified residues in Chromo and Chromo Shadow domains of HP1 family. The figure was adapted from Gaudin et al. (2001); LeRoy et al. (2009); Wiese et al. (2019). Conserved residues involved in methyl lysine binding and hydrophobic cores were deduced from Nielsen et al. (2002); Fischle et al. (2003).

demethylases are huddled around sites of DNA damages (section *Histone Methylation and Metabolic Cofactors*), whether there is functional cooperation with (L)HP1 in DNA repair is not known.

SUMMARY AND PROSPECTS

In his book, "Who Rules the World?", the acclaimed MIT linguist, Noam Chomsky, weighs in on the question of how the term of the global discourse is set. The "Who" is somewhat of an abstraction, but generally personified as a "Deep State", a kind of sprawling network that knows how to control the most "vital strategic points".

One vital strategy evolved in cells to coordinate complex workings is epigenetics, the powerful driving force behind multicellularity, pluripotency and the capacity to adapt to new environmental niches (**Figure 6**). In just the last few years, torrents of never before seen modifications have been revealed in the genomes of animals. Most of these newer adducts in **Figure 1** are beyond the remit of this review, but it does reveal the sprawling network of possible interactions between epigenetics and metabolites. Neither can **Figure 1**–already detail-rich– be exhaustive, as new modifications are being continually discovered.

The newer sequencing technologies are also identifying novel modifications on RNA and DNA. Cytosines modified by formylation, carboxylation or hydroxylation have now been found in the human genome. These discoveries also immediately raise questions on how these marks influence the local DNA structure? What are the instructions encoded by such modified DNA? Do they mark special sites on the DNA, such as

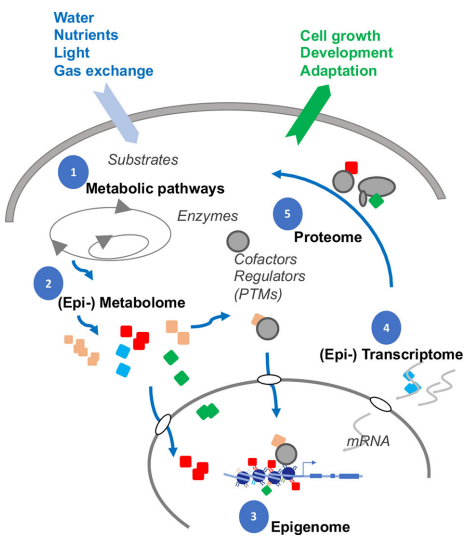

FIGURE 6 | Interplay between DNA, RNA, chromatin and metabolites. Gene expression is dynamically modulated by feedback with interdependent subcellular systems (numbered). Many metabolites (colored symbols) are substrates for chemical attachments. The cellular compositions of the metabolites are likely altered, as adaptation, to nutrient and water availability, light perception, gas exchange, and interactions with the rhizosphere. In turn, the metabolites themselves can attach, either covalently (adducts) or by electrostatic interactions (cofactors), to proteins, RNAs, and chromatin to shape the final gene expression profiles in responding to changing developmental and environmental stimuli (output arrow).

breakpoints? Do these DNA modifications influence the local deposition of histone marks? If so, are there particular histone marks that might be more susceptible?

We have dealt mainly with the donors, acetyl-CoA, and SAM, but it is clear that their implications are deep. Acetyl-CoA is the starting point of fatty acid synthesis and membranous structures from carbohydrates. Acetyl-CoA in the cytosol is fed into the synthesis of a plethora of small chemicals, many of which have proven to be important for plant growth, development and responding to environmental cues. Methylation also regulates many cellular processes. We are familiar with methyl-jasmonate and methyl-salicylic acid. But in fact, myriads of small molecules can exist in methylated variants, suggesting that all of them, could have an impact on altering epigenetic regulation by competing for SAM. How the novel metabolites are replenished, by which pathways, is of obvious interest.

How specific gene expression patterns emerged from the complex interactions between chromatin and the immense arrays of metabolites (**Figure 6**) will be a daunting, but an extremely timely, question concerning food security, as we attempt to rationally design crops that can adapt better to drought and high temperatures. We are still largely in the awakening phase of discovering and cataloging the types of modifications. Identifying and characterizing the roster of proteins that interact with specific metabolites will be equally a critical step towards understanding how the metabolites may influence epigenetics. Because metabolites are of such diverse biochemical and physical nature, functional analyses will require dedicated techniques of sufficient spatial resolution, sensitivity, and discrimination that will permit tracking a single class of metabolites in a single cell before we can correlate them to the nuclear output.

AUTHOR CONTRIBUTIONS

JL and VG conceived the review. JL wrote the manuscript. VG revised the manuscript. JL and VG designed the figures.

ACKNOWLEDGMENTS

IJPB benefits from the support of the LabEx Saclay Plant Sciences-SPS (ANR-17-EUR-0007).

REFERENCES

Ahmad, A., and Cao, X. (2012). Plant PRMTs broaden the scope of arginine methylation. *J. Genet. Genomics* 39, 195–208. doi: 10.1016/j.jgg.2012.04.001

Ayoub, N., Jeyasekharan, A. D., Bernal, J. A., and Venkitaraman, A. R. (2008). HP1-beta mobilization promotes chromatin changes that initiate the DNA damage response. *Nature* 453, 682–686. doi: 10.1038/nature06875

Ballestar, E., Abad, C., and Franco, L. (1996). Core histones are glutaminyl substrates for tissue transglutaminase. *J. Biol. Chem.* 271, 18817–18824. doi: 10.1074/jbc.271.31.18817

Barkla, B. J., and Vera-Estrella, R. (2015). Single cell-type comparative metabolomics of epidermal bladder cells from the halophyte *Mesembryanthemum crystallinum*. *Front. Plant Sci.* 6, 435. doi: 10.3389/fpls.2015.00435

Bell, E. A., and Janzen, D. H. (1971). Medical and ecological considerations of L-dopa and 5-HTP in seeds. *Nature* 229, 136–137. doi: 10.1038/229136a0

Boccaletto, P., Machnicka, M. A., Purta, E., Platkowski, P., Baginski, B., Wirecki, T. K., et al. (2018). MODOMICS: a database of RNA modification pathways. 2017 update. *Nucl. Acid Res.* 46, D303–D307.

Burgio, G., Corona, D. F., Nicotra, C. M., Carruba, G., and Taibi, G. (2016). P/CAF-mediated spermidine acetylation regulates histone acetyltransferase activity. *J. Enzyme Inhib. Med. Chem.* 31, 75–82. doi: 10.1080/14756366.2016.1205045

Carpenter, L. J. (2015). "Biogeochemical cycles," in *Encyclopedia of Atmospheric Sciences*. Eds. G. North, J. Pyle and F. Zhang, (Academic Press: Elsevier), 205–219.

Cervantes, M., and Sassone-Corsi, P. (2019). Modification of histone proteins by serotonin in the nucleus. *Nature* 567, 464–465. doi: 10.1038/d41586-019-00532-z

Chen, C., Li, C., Wang, Y., Renaud, J., Tian, G., Kambhampati, S., et al. (2017). Cytosolic acetyl-CoA promotes histone acetylation predominantly at H3K27 in Arabidopsis. *Nat. Plants* 3, 814–824. doi: 10.1038/s41477-017-0023-7

Chlopicki, S., Swies, J., Mogielnicki, A., Buczko, W., Bartus, M., Lomnicka, M., et al. (2007). 1-Methylnicotinamide (MNA), a primary metabolite of nicotinamide, exerts anti-thrombotic activity mediated by a cyclooxygenase-2/prostacyclin pathway. *Br. J. Pharmacol.* 152, 230–239. doi: 10.1038/sj.bjp.0707383

Choi, K., Zhao, X., Tock, A. J., Lambing, C., Underwood, C. J., Hardcastle, T. J., et al. (2018). Nucleosomes and DNA methylation shape meiotic DSB frequency in Arabidopsis thaliana transposons and gene regulatory regions. *Genome Res.* 28, 532–546. doi: 10.1101/gr.225599.117

Christensen, D. G., Xie, X., Basisty, N., Byrnes, J., McSweeney, S., Schilling, B., et al. (2019). Post-translational protein acetylation: an elegant mechanism for bacteria to dynamically regulate metabolic functions. *Front. Microbiol.* 10, 1604. doi: 10.3389/fmicb.2019.01604

Dahlgren, C., Gabl, M., Holdfeldt, A., Winther, M., and Forsman, H. (2016). Basic characteristics of the neutrophil receptors that recognize formylated peptides, a danger-associated molecular pattern generated by bacteria and mitochondria. *Biochem. Pharmacol.* 114, 22–39. doi: 10.1016/j.bcp.2016.04.014

Desrosiers, R., Friderici, K., and Rottman, F. (1974). Identification of methylated nucleosides in messenger RNA from Novikoff hepatoma cells. *Proc. Natl. Acad. Sci. U. S. A.* 71, 3971–3975. doi: 10.1073/pnas.71.10.3971

Doi, M., Hirayama, J., and Sassone-Corsi, P. (2006). Circadian regulator CLOCK is a histone acetyltransferase. *Cell* 125, 497–508. doi: 10.1016/j.cell.2006.03.033

Dowen, R. H., Pelizzola, M., Schmitz, R. J., Lister, R., Dowen, J. M., Nery, J. R., et al. (2012). Widespread dynamic DNA methylation in response to biotic stress. *Proc. Natl. Acad. Sci. U. S. A.* 109, E2183–E2191. doi: 10.1073/pnas.1209329109

Du, H., Wu, J., Ji, K. X., Zeng, Q. Y., Bhuiya, M. W., Su, S., et al. (2015). Methylation mediated by an anthocyanin, *O*-methyltransferase, is involved in purple flower coloration in Paeonia. *J. Exp. Bot.* 66, 6563–6577. doi: 10.1093/jxb/erv365

Duan, H. C., Wei, L. H., Zhang, C., Wang, Y., Chen, L., Lu, Z., et al. (2017). ALKBH10B is an RNA N^6-methyladenosine demethylase affecting Arabidopsis floral transition. *Plant Cell* 29, 2995–3011. doi: 10.1105/tpc.16.00912

Eckel-Mahan, K., and Sassone-Corsi, P. (2013). Metabolism and the circadian clock converge. *Physiol. Rev.* 93, 107–135. doi: 10.1152/physrev.00016.2012

Elgin, S. C., and Reuter, G. (2013). Position-effect variegation, heterochromatin formation, and gene silencing in Drosophila. *Cold Spring Harb Perspect. Biol.* 5, a017780. doi: 10.1101/cshperspect.a017780

Engelke, U. F., Liebrand-van Sambeek, M. L., de Jong, J. G., Leroy, J. G., Morava, E., Smeitink, J. A., et al. (2004). N-acetylated metabolites in urine: proton nuclear magnetic resonance spectroscopic study on patients with inborn errors of metabolism. *Clin. Chem.* 50, 58–66. doi: 10.1373/clinchem.2003.020214

Erland, L. A. E., and Saxena, P. K. (2017). Beyond a neurotransmitter: the role of serotonin in plants. *Neurotransmitter* 4, e1538.

Fang, C., Fernie, A. R., and Luo, J. (2019). Exploring the diversity of plant metabolism. *Trends Plant Sci.* 24, 83–98. doi: 10.1016/j.tplants.2018.09.006

Farrelly, L. A., Thompson, R. E., Zhao, S., Lepack, A. E., Lyu, Y., Bhanu, N. V., et al. (2019). Histone serotonylation is a permissive modification that enhances TFIID binding to H3K4me3. *Nature* 567, 535–539. doi: 10.1038/s41586-019-1024-7

Fatland, B. L., Nikolau, B. J., and Wurtele, E. S. (2005). Reverse genetic characterization of cytosolic acetyl-CoA generation by ATP-citrate lyase in Arabidopsis. *Plant Cell* 17, 182–203. doi: 10.1105/tpc.104.026211

Fischer, F., Gertz, M., Suenkel, B., Lakshminarasimhan, M., Schutkowski, M., and Steegborn, C. (2012). Sirt5 deacylation activities show differential sensitivities to nicotinamide inhibition. *PLoS One* 7, e45098. doi: 10.1371/journal.pone.0045098

Fischle, W., Wang, Y., Jacobs, S. A., Kim, Y., Allis, C. D., and Khorasanizadeh, S. (2003). Molecular basis for the discrimination of repressive methyl-lysine marks in histone H3 by Polycomb and HP1 chromodomains. *Genes Dev.* 17, 1870–1881. doi: 10.1101/gad.1110503

Folk, J. E., Park, M. H., Chung, S. I., Schrode, J., Lester, E. P., and Cooper, H. L. (1980). Polyamines as physiological substrates for transglutaminases. *J. Biol. Chem.* 255, 3695–3700.

Friedrich, T., Faivre, L., Baurle, I., and Schubert, D. (2019). Chromatin-based mechanisms of temperature memory in plants. *Plant Cell Environ.* 42, 762–770. doi: 10.1111/pce.13373

Fujishiro, K., Ando, M., and Uwajima, T. (1988). Crystallization and some properties of acetylpolyamine amidohydrolase from *Mycoplana bullata*. *Biochem. Biophys. Res. Comm.* 157, 1169–1174. doi: 10.1016/S0006-291X(88)80997-5

Gaudin, V., Libault, M., Pouteau, S., Juul, T., Zhao, G., Lefebvre, D., et al. (2001). Mutations in LIKE HETEROCHROMATIN PROTEIN 1 affect flowering time and plant architecture in Arabidopsis. *Development* 128, 4847–4858.

Gerhart-Hines, Z., Dominy, J. E.Jr., Blattler, S. M., Jedrychowski, M. P., Banks, A. S., Lim, J. H., et al. (2011). The cAMP/PKA pathway rapidly activates SIRT1 to promote fatty acid oxidation independently of changes in NAD(+). *Mol. Cell* 44, 851–863. doi: 10.1016/j.molcel.2011.12.005

Gonzales, B., and Vera, P. (2019). Folate metabolism interferes with plant immunity through 1C methionine synthase-directed genome-wide DNA methylation enhancement. *Mol. Plant* 12, 1227–1242. doi: 10.1016/j.molp.2019.04.013

Groth, M., Moissiard, G., Wirtz, M., Wang, H., Garcia-Salinas, C., Ramos-Parra, P. A., et al. (2016). MTHFD1 controls DNA methylation in Arabidopsis. *Nat. Commun.* 7, 11640. doi: 10.1038/ncomms11640

Han, Q., Robinson, H., Ding, H., Christensen, B. M., and Li, J. (2012). Evolution of insect arylalkylamine *N*-acetyltransferases: structural evidence from the yellow fever mosquito, *Aedes aegypti*. *Proc. Natl. Acad. Sci. U.S.A.* 109, 11669– 11674. doi: 10.1073/pnas.1206828109

He, Y., Wang, M., Dukowic-Schulze, S., Zhou, A., Tiang, C. L., Shilo, S., et al. (2017). Genomic features shaping the landscape of meiotic double-strand-break hotspots in maize. *Proc. Natl. Acad. Sci. U. S. A.* 114, 12231–12236. doi: 10.1073/pnas.1713225114

Hirabayashi, Y., Nomura, K. H., and Nomura, K. (2013). The acetyl-CoA transporter family SLC33. *Mol. Aspects Med.* 34, 586–589. doi: 10.1016/j.mam.2012.05.009

Hirschey, M. D., Shimazu, T., Huang, J. Y., Schwer, B., and Verdin, E. (2011). SIRT3 regulates mitochondrial protein acetylation and intermediary metabolism. *Cold Spring Harb Symp. Quant. Biol.* 76, 267–277. doi: 10.1101/sqb.2011.76.010850

Hobbs, C. A., and Gilmour, S. K. (2000). High levels of intracellular polyamines promote histone acetyltransferase activity resulting in chromatin hyperacetylation. *J. Cell Biochem.* 77, 345–360. doi: 10.1002/(SICI)1097-4644(20000601)77:3<345::AID-JCB1>3.0.CO;2-P

Hu, J., Manduzio, S., and Kang, H. (2019). Epitranscriptomic RNA Methylation in plant development and abiotic stress responses. *Front. Plant Sci.* 10, 500. doi: 10.3389/fpls.2019.00500

Hu, Y., Jiang, Y., Han, X., Wang, H., Pan, J., and Yu, D. (2017). Jasmonate regulates leaf senescence and tolerance to cold stress: crosstalk with other phytohormones. *J. Exp. Bot.* 68, 1361–1369. doi: 10.1093/jxb/erx004

Huang, H., Sabari, B. R., Garcia, B. A., Allis, C. D., and Zhao, Y. (2014). SnapShot: histone modifications. *Cell* 159, 458–458e1. doi: 10.1016/j.cell.2014.09.037

Hudzik, C., Hou, Y., Ma, W., and Axtell, M. J. (2020). Exchange of small regulatory RNAs between plants and their pests. *Plant Physiol.* 182, 51–62. doi: 10.1104/pp.19.00931.

Ibdah, M., Zhang, X. H., Schmidt, J., and Vogt, T. (2003). A novel Mg^{2+}-dependent *O*-methyltransferase in the phenylpropanoid metabolism of *Mesembryanthemum crystallinum*. *J. Biol. Chem.* 278, 43961–43972. doi: 10.1074/jbc.M304932200

Ito, S., Shen, L., Dai, Q., Wu, S. C., Collins, L. B., Swenberg, J. A., et al. (2011). Tet proteins can convert 5-methylcytosine to 5-formylcytosine and 5-carboxylcytosine. *Science* 333, 1300–1303. doi: 10.1126/science.1210597

Jiang, D., Yang, W., He, Y., and Amasino, R. M. (2007). Arabidopsis relatives of the human lysine-specific Demethylase1 repress the expression of *FWA* and *FLOWERING LOCUS C* and thus promote the floral transition. *Plant Cell* 19, 2975–2987. doi: 10.1105/tpc.107.052373

Jiang, T., Zhou, X., Taghizadeh, K., Dong, M., and Dedon, P. C. (2007). *N*-formylation of lysine in histone proteins as a secondary modification arising from oxidative DNA damage. *Proc. Natl. Acad. Sci. U. S. A.* 104, 60–65. doi: 10.1073/pnas.0606775103

Jonas, M. C., Pehar, M., and Puglielli, L. (2010). AT-1 is the ER membrane acetyl-CoA transporter and is essential for cell viability. *J. Cell Sci.* 123, 3378–3388. doi: 10.1242/jcs.068841

Katz, J. E., Dlakic, M., and Clarke, S. (2003). Automated identification of putative methyltransferases from genomic open reading frames. *Mol. Cell Proteomics* 2, 525–540. doi: 10.1074/mcp.M300037-MCP200

Kawarada, L., Suzuki, T., Ohira, T., Hirata, S., Miyauchi, K., and Suzuki, T. (2017). ALKBH1 is an RNA dioxygenase responsible for cytoplasmic and mitochondrial tRNA modifications. *Nucl. Acids Res.* 45, 7401–7415. doi: 10.1093/nar/gkx354

Kim, J. H., Durrett, T. P., Last, R. L., and Jander, G. (2004). Characterization of the Arabidopsis TU8 glucosinolate mutation, an allele of *TERMINAL FLOWER2*. *Plant Mol. Biol.* 54, 671–682. doi: 10.1023/B:PLAN.0000040897.49151.98

Kinnaird, A., Zhao, S., Wellen, K. E., and Michelakis, E. D. (2016). Metabolic control of epigenetics in cancer. *Nat. Rev. Cancer* 16, 694–707. doi: 10.1038/nrc.2016.82

Kistler, H. C., and Broz, K. (2015). Cellular compartmentalization of secondary metabolism. *Front. Microbiol.* 6, 68. doi: 10.3389/fmicb.2015.00068

Kotake, T., Takada, S., Nakahigashi, K., Ohto, M., and Goto, K. (2003). Arabidopsis *TERMINAL FLOWER 2* gene encodes a heterochromatin protein 1 homolog and represses both *FLOWERING LOCUS T* to regulate flowering time and several floral homeotic genes. *Plant Cell Physiol.* 44, 555–564. doi: 10.1093/pcp/pcg091

Larson, A. G., Elnatan, D., Keenen, M. M., Trnka, M. J., Johnston, J. B., Burlingame, A. L., et al. (2017). Liquid droplet formation by HP1∝ suggests a role for phase separation in heterochromatin. *Nature* 547, 236–240. doi: 10.1038/nature22822

Larsson, J., Zhang, J., and Rasmuson-Lestander, A. (1996). Mutations in the *Drosophila melanogaster* gene encoding S-adenosylmethionine synthetase suppress position-effect variegation. *Genetics* 143, 887–896.

Law, J. A., and Jacobsen, S. E. (2010). Establishing, maintaining and modifying DNA methylation patterns in plants and animals. *Nat. Rev. Genet.* 11, 204–220. doi: 10.1038/nrg2719

LeRoy, G., Weston, J. T., Zee, B. M., Young, N. L., Plazas-Mayorca, M. D., and Garcia, B. A. (2009). Heterochromatin protein 1 is extensively decorated with histone code-like post-translational modifications. *Mol. Cell Proteomics* 8, 2432–2442. doi: 10.1074/mcp.M900160-MCP200

Li, X., and Snyder, M. (2011). Metabolites as global regulators: a new view of protein regulation. *Bioessays* 33, 485–489. doi: 10.1002/bies.201100026

Li, Y., Mukherjee, I., Thum, K. E., Tanurdzic, M., Katari, M. S., Obertello, M., et al. (2015). The histone methyltransferase SDG8 mediates the epigenetic modification of light and carbon responsive genes in plants. *Genome Biol.* 16, 79. doi: 10.1186/s13059-015-0640-2

Liu, F., Quesada, V., Crevillen, P., Baurle, I., Swiezewski, S., and Dean, C. (2007). The Arabidopsis RNA-binding protein FCA requires a lysine-specific demethylase 1 homolog to downregulate FLC. *Mol. Cell* 28, 398–407. doi: 10.1016/j.molcel.2007.10.018

Liu, C., Lu, F., Cui, X., and Cao, X. (2010). Histone methylation in higher plants. *Ann. Rev. Plant Biol.* 61, 395–420. doi: 10.1146/annurev.arplant.043008.091939

Liu, X., Yang, S., Yu, C.-W., Chen, C.-Y., and Wu, K. (2016). Histone acetylation and plant development. *Enzymes* 40, 173–199. doi: 10.1016/bs.enz.2016.08.001

Liu, Y., You, Y., Lu, Z., Yang, J., Li, P., Liu, L., et al. (2019). N^6-methyladenosine RNA modification-mediated cellular metabolism rewiring inhibits viral replication. *Science* 365, 1171–1176. doi: 10.1126/science.aax4468

Lloyd, V. K., Sinclair, D. A., and Grigliatti, T. A. (1999). Genomic imprinting and position-effect variegation in *Drosophila melanogaster*. *Genetics* 151, 1503–1516.

Lombardi, P. M., Angell, H. D., Whittington, D. A., Flynn, E. F., Rajashankar, K. R., and Christianson, D. W. (2011). Structure of prokaryotic polyamine deacetylase reveals evolutionary functional relationships with eukaryotic histone deacetylases. *Biochemistry* 50, 1808–1817. doi: 10.1021/bi101859k

Luijsterburg, M. S., Dinant, C., Lans, H., Stap, J., Wiernasz, E., Lagerwerf, S., et al. (2009). Heterochromatin protein 1 is recruited to various types of DNA damage. *J. Cell Biol.* 185, 577–586. doi: 10.1083/jcb.200810035

Martinez-Perez, M., Aparicio, F., Lopez-Gresa, M. P., Belles, J. M., Sanchez-Navarro, J. A., and Pallas, V. (2017). Arabidopsis m(6)A demethylase activity

modulates viral infection of a plant virus and the m(6)A abundance in its genomic RNAs. *Proc. Natl. Acad. Sci. U. S. A.* 114, 10755–10760. doi: 10.1073/pnas.1703139114

Matthews, H. R. (1993). Polyamines, chromatin structure and transcription. *Bioessays* 15, 561–566. doi: 10.1002/bies.950150811

Matzke, M. A., and Mosher, R. A. (2014). RNA-directed DNA methylation: an epigenetic pathway of increasing complexity. *Nat. Rev. Genet.* 15, 394–408. doi: 10.1038/nrg3683

Meinnel, T., Blanquet, S., and Dardel, F. (1996). A new subclass of the zinc metalloproteases superfamily revealed by the solution structure of peptide deformylase. *J. Mol. Biol.* 262, 375–386. doi: 10.1006/jmbi.1996.0521

Mielecki, D., Zugaj, D. L., Muszewska, A., Piwowarski, J., Chojnacka, A., Mielecki, M., et al. (2012). Novel AlkB dioxygenases-alternative models for in silico and in vivo studies. *PLoS One* 7, e30588. doi: 10.1371/journal.pone.0030588

Miyazaki, J. H., and Yang, S. F. (1987). The methionine salvage pathway in relation to ethylene and polyamine biosynthesis. *Physiol. Plant* 69, 366–370. doi: 10.1111/j.1399-3054.1987.tb04302.x

Morgan, J. E., Blankenship, J. W., and Matthews, H. R. (1987). Polyamines and acetylpolyamines increase the stability and alter the conformation of nucleosome core particles. *Biochemistry* 26, 3643–3649. doi: 10.1021/bi00386a058

Muller, T. A., Struble, S. L., Meek, K., and Hausinger, R. P. (2018). Characterization of human AlkB homolog 1 produced in mammalian cells and demonstration of mitochondrial dysfunction in ALKBH1-deficient cells. *Biochem. Biophy. Res. Comm.* 495, 98–103. doi: 10.1016/j.bbrc.2017.10.158

Nakao, M., Anan, K., Araki, H., and Hino, S. (2019). Distinct roles of the NAD^+-Sirt1 and FAD-LSD1 pathways in metabolic response and tissue development. *Trends Endocrinol. Metab.* 30, 409–412. doi: 10.1016/j.tem.2019.04.010

Nielsen, P. R., Nietlispach, D., Mott, H. R., Callaghan, J., Bannister, A., Kouzarides, T., et al. (2002). Structure of the HP1 chromodomain bound to histone H3 methylated at lysine 9. *Nature* 416, 103–107. doi: 10.1038/nature722

Noble, D. (2015). Conrad Waddington and the origin of epigenetics. *J. Exp. Biol.* 218, 816–818. doi: 10.1242/jeb.120071

Nunomura, K., Kawakami, S., Shimizu, T., Hara, T., Nakamura, K., Terakawa, Y., et al. (2003). In vivo cross-linking of nucleosomal histones catalyzed by nuclear transglutaminase in starfish sperm and its induction by egg jelly triggering the acrosome reaction. *Eur. J. biochem./FEBS* 270, 3750–3759. doi: 10.1046/j.1432-1033.2003.03761.x

Pacholec, M., Bleasdale, J. E., Chrunyk, B., Cunningham, D., Flynn, D., Garofalo, R. S., et al. (2010). SRT1720, SRT2183, SRT1460, and resveratrol are not direct activators of SIRT1. *J. Biol. Chem.* 285, 8340–8351. doi: 10.1074/jbc.M109.088682

Pera, M. F. (2013). Epigenetics, vitamin supplements and cellular reprogramming. *Nat. Genet.* 45, 1412–1413. doi: 10.1038/ng.2834

Phillips, D. M. (1963). The presence of acetyl groups of histones. *Biochem. J.* 87, 258–263. doi: 10.1042/bj0870258

Pollard, K. J., Samuels, M. L., Crowley, K. A., Hansen, J. C., and Peterson, C. L. (1999). Functional interaction between GCN5 and polyamines: a new role for core histone acetylation. *EMBO J.* 18, 5622–5633. doi: 10.1093/emboj/18.20.5622

Ratel, D., Ravanat, J. L., Berger, F., and Wion, D. (2006). N^6-methyladenine: the other methylated base of DNA. *Bioessays* 28, 309–315. doi: 10.1002/bies.20342

Richter, K., Nessling, M., and Lichter, P. (2008). Molecular crowding and its potential impact on nuclear function. *Biochim. Biophys. Acta* 1783, 2100–2107. doi: 10.1016/j.bbamcr.2008.07.017

Roje, S. (2006). S-Adenosyl-L-methionine: beyond the universal methyl group donor. *Phytochemistry* 67, 1686–1698. doi: 10.1016/j.phytochem.2006.04.019

Sabari, B. R., Zhang, D., Allis, C. D., and Zhao, Y. (2017). Metabolic regulation of gene expression through histone acylations. *Nat. Rev. Mol. Cell Biol.* 18, 90–101. doi: 10.1038/nrm.2016.140

Sakurada, K., Ohta, T., Fujishiro, K., Hasegawa, M., and Aisaka, K. (1996). Acetylpolyamine amidohydrolase from *Mycoplana ramosa*: gene cloning and characterization of the metal-substituted enzyme. *J. Bacteriol.* 178, 5781–5786. doi: 10.1128/JB.178.19.5781-5786.1996

Saletore, Y., Meyer, K., Korlach, J., Vilfan, I. D., Jaffrey, S., and Mason, C. E. (2012). The birth of the Epitranscriptome: deciphering the function of RNA modifications. *Genome Biol.* 13, 175. doi: 10.1186/gb-2012-13-10-175

Sanchez-Perez, S., Comas-Baste, O., Rabell-Gonzalez, J., Veciana-Nogues, M. T., Latorre-Moratalla, M. L., and Vidal-Carou, M. C. (2018). Biogenic amines in plant-origin foods: are they frequently underestimated in low-histamine diets? *Foods* 7. doi: 10.3390/foods7120205

Sdelci, S., Rendeiro, A. F., Rathert, P., You, W., Lin, J. G., Ringler, A., et al. (2019). MTHFD1 interaction with BRD4 links folate metabolism to transcriptional regulation. *Nat. Genet.* 51, 990–998. doi: 10.1038/s41588-019-0413-z

Shen, Y., Wei, W., and Zhou, D. X. (2015). Histone acetylation enzymes coordinate metabolism and gene expression. *Trends Plant Sci.* 20, 614–621. doi: 10.1016/j.tplants.2015.07.005

Shen, Y., Issakidis-Bourguet, E., and Zhou, D. X. (2016). Perspectives on the interactions between metabolism, redox, and epigenetics in plants. *J. Exp. Bot.* 67, 5291–5300. doi: 10.1093/jxb/erw310

Shimazu, T., Hirschey, M. D., Newman, J., He, W., Shirakawa, K., Le Moan, N., et al. (2013). Suppression of oxidative stress by beta-hydroxybutyrate, an endogenous histone deacetylase inhibitor. *Science* 339, 211–214. doi: 10.1126/science.1227166

Showalter, M. R., Cajka, T., and Fiehn, O. (2017). Epimetabolites: discovering metabolism beyond building and burning. *Curr. Opin. Chem. Biol.* 36, 70–76. doi: 10.1016/j.cbpa.2017.01.012

Shu, X., Liu, M., Lu, Z., Zhu, C., Meng, H., Huang, S., et al. (2018). Genome-wide mapping reveals that deoxyuridine is enriched in the human centromeric DNA. *Nat. Chem. Biol.* 14, 680–687. doi: 10.1038/s41589-018-0065-9

Sivanand, S., Viney, I., and Wellen, K. E. (2018). Spatiotemporal control of acetyl-CoA metabolism in chromatin regulation. *Trends Biochem. Sci.* 43, 61–74. doi: 10.1016/j.tibs.2017.11.004

Slack, J. M. (2002). Conrad Hal Waddington: the last Renaissance biologist? *Nat. Rev. Genet.* 3, 889–895. doi: 10.1038/nrg933

Sperber, H., Mathieu, J., Wang, Y., Ferreccio, A., Hesson, J., Xu, Z., et al. (2015). The metabolome regulates the epigenetic landscape during naive-to-primed human embryonic stem cell transition. *Nat. Cell Biol.* 17, 1523–1535. doi: 10.1038/ncb3264

Sreekumar, A., Poisson, L. M., Rajendiran, T. M., Khan, A. P., Cao, Q., Yu, J., et al. (2009). Metabolomic profiles delineate potential role for sarcosine in prostate cancer progression. *Nature* 457, 910–914. doi: 10.1038/nature07762

Stam, M., and Mittelsten Scheid, O. (2005). Paramutation: an encounter leaving a lasting impression. *Trends Plant Sci.* 10, 283–290. doi: 10.1016/j.tplants.2005.04.009

Strom, A. R., Emelyanov, A. V., Mir, M., Fyodorov, D. V., Darzacq, X., and Karpen, G. H. (2017). Phase separation drives heterochromatin domain formation. *Nature* 547, 241–245. doi: 10.1038/nature22989

Tanikawa, C., Ueda, K., Suzuki, A., Iida, A., Nakamura, R., Atsuta, N., et al. (2018). Citrullination of RGG motifs in FET proteins by PAD4 regulated protein aggregation and ALS susceptibility. *Cell Rep.* 22, 1473–1483. doi: 10.1016/j.celrep.2018.01.031

Trindade, I., Schubert, D., and Gaudin, V. (2017). "Epigenetic regulation of phase transitions in Arabidopsis thaliana," in *Plant Epigenetics, RNA Technologies*. Eds. N. Rajewsky, S. Jurga and J. Barciszewski (Springer International Publishing AG 2017), 359–384.

Tschiersch, B., Hofmann, A., Krauss, V., Dorn, R., Korge, G., and Reuter, G. (1994). The protein encoded by the Drosophila position-effect variegation suppressor gene Su(var)3-9 combines domains of antagonistic regulators of homeotic gene complexes. *EMBO J.* 13, 3822–3831. doi: 10.1002/j.1460-2075.1994.tb06693.x

Tseng, C. H. (2009). A review on environmental factors regulating arsenic methylation in humans. *Toxicol. Appl. Pharmacol.* 235, 338–350. doi: 10.1016/j.taap.2008.12.016

Tsuda, H., Shiraki, M., Inoue, E., and Saito, T. (2016). Generation of poly-beta-hydroxybutyrate from acetate in higher plants: detection of acetoacetyl CoA reductase- and PHB synthase- activities in rice. *J. Plant Physiol.* 201, 9–16. doi: 10.1016/j.jplph.2016.06.007

Turck, F., Roudier, F., Farrona, S., Martin-Magniette, M. L., Guillaume, E., Buisine, N., et al. (2007). Arabidopsis TFL2/LHP1 specifically associates with genes marked by trimethylation of histone H3 lysine 27. *PLoS Genet.* 3, e86. doi: 10.1371/journal.pgen.0030086

van Roermund, C. W., Elgersma, Y., Singh, N., Wanders, R. J., and Tabak, H. F. (1995). The membrane of peroxisomes in *Saccharomyces cerevisiae* is impermeable to NAD(H) and acetyl-CoA under in vivo conditions. *EMBO J.* 14, 3480–3486. doi: 10.1002/j.1460-2075.1995.tb07354.x

Vetting, M. W., de Cavalho, L. P. S., Yu, M., Hegde, S. S., Magnet, S., Roderick, S. L., et al. (2005). Structure and functions of the GNAT superfamily of acetyltransferases. *Arch. Biochem. Biophys.* 433, 212–226. doi: 10.1016/j.abb.2004.09.003

Vogt, T. (2010). Phenylpropanoid biosynthesis. *Mol. Plant* 3, 2–20. doi: 10.1093/mp/ssp106

Waditee, R., Bhuiyan, M. N., Rai, V., Aoki, K., Tanaka, Y., Hibino, T., et al. (2005). Genes for direct methylation of glycine provide high levels of glycinebetaine and abiotic-stress tolerance in Synechococcus and Arabidopsis. *Proc. Natl. Acad. Sci. U. S. A.* 102, 1318–1323. doi: 10.1073/pnas.0409017102

Wang, G., and Kohler, C. (2017). Epigenetic processes in flowering plant reproduction. *J. Exp. Bot.* 68, 797–807. doi: 10.1093/jxb/erw486

Wang, H., Huang, Z. Q., Xia, L., Feng, Q., Erdjument-Bromage, H., Strahl, B. D., et al. (2001). Methylation of histone H4 at arginine 3 facilitating transcriptional activation by nuclear hormone receptor. *Science* 293, 853–857. doi: 10.1126/science.1060781

Wang, L., Wang, C., Liu, X., Cheng, J., Li, S., Zhu, J. K., et al. (2019). Peroxisomal ß-oxidation regulates histone acetylation and DNA methylation in Arabidopsis. *Proc. Natl. Acad. Sci. U. S. A.* 116, 10576–10585. doi: 10.1073/pnas.1904143116

Wei, W., Ba, Z., Gao, M., Wu, Y., Ma, Y., Amiard, S., et al. (2012). A role for small RNAs in DNA double-strand break repair. *Cell* 149, 101–112. doi: 10.1016/j.cell.2012.03.002

Wiese, M., Bannister, A. J., Basu, S., Boucher, W., Wohlfahrt, K., Christophorou, M. A., et al. (2019). Citrullination of HP1gamma chromodomain affects association with chromatin. *Epigenet. Chromatin* 12, 21.

Wisniewski, J. R., Zougman, A., and Mann, M. (2008). *N* epsilon-formylation of lysine is a widespread post-translational modification of nuclear proteins occurring at residues involved in regulation of chromatin function. *Nucl. Acids Res.* 36, 570–577. doi: 10.1093/nar/gkm1057

Wong, L. C., Sharpe, D. J., and Wong, S. S. (1991). High-mobility group and other non histone substrates for nuclear histone N-acetyltransferase. *Biochem. Genet.* 29, 461–475. doi: 10.1007/BF02399688

Wuosmaa, A. M., and Hager, L. P. (1990). Methyl chloride transferase: a carbocation route for biosynthesis of halometabolites. *Science* 249, 160–162. doi: 10.1126/science.2371563

Xuan, C., Tian, Q. W., Li, H., Zhang, B. B., He, G. W., and Lun, L. M. (2016). Levels of asymmetric dimethylarginine (ADMA), an endogenous nitric oxide synthase inhibitor, and risk of coronary artery disease: a meta-analysis based on 4713 participants. *Eur. J. Prev. Cardiol.* 23, 502–510. doi: 10.1177/2047487315586094

Xue-Franzen, Y., Johnsson, A., Brodin, D., Henriksson, J., Burglin, T. R., and Wright, A. P. (2010). Genome-wide characterisation of the Gcn5 histone acetyltransferase in budding yeast during stress adaptation reveals evolutionarily conserved and diverged roles. *BMC Genomics* 11, 200. doi: 10.1186/1471-2164-11-200

Ye, C., Sutter, B. M., Wang, Y., Kuang, Z., and Tu, B. P. (2017). A metabolic function for phospholipid and histone methylation. *Mol. Cell* 66, 180–193 e188. doi: 10.1016/j.molcel.2017.02.026

Yu, C. H., Chou, C. C., Lee, Y. J., Khoo, K. H., and Chang, G. D. (2015). Uncovering protein polyamination by the spermine-specific antiserum and mass spectrometric analysis. *Amino Acids* 47, 469–481. doi: 10.1007/s00726-014-1879-8

Zhang, Y., and Reinberg, D. (2001). Transcription regulation by histone methylation: interplay between different covalent modifications of the core histone tails. *Genes Dev.* 15, 2343–2360. doi: 10.1101/gad.927301

Zhang, X., Germann, S., Blus, B. J., Khorasanizadeh, S., Gaudin, V., and Jacobsen, S. E. (2007). The Arabidopsis LHP1 protein colocalizes with histone H3 Lys27 trimethylation. *Nat. Struct. Mol. Biol.* 14, 869–871. doi: 10.1038/nsmb1283

Zhang, H., Deng, X., Miki, D., Cutler, S., La, H., Hou, Y. J., et al. (2012). Sulfamethazine suppresses epigenetic silencing in Arabidopsis by impairing folate synthesis. *Plant Cell* 24, 1230–1241. doi: 10.1105/tpc.112.096149

Zhang, Q., Liang, Z., Cui, X., Ji, C., Li, Y., Zhang, P., et al. (2018). N^6-methyladenine DNA methylation in Japonica and Indica rice genomes and its association with gene expression, plant development, and stress responses. *Mol. Plant* 11, 1492–1508. doi: 10.1016/j.molp.2018.11.005

Zhao, Q., Rank, G., Tan, Y. T., Li, H., Moritz, R. L., Simpson, R. J., et al. (2009). PRMT5-mediated methylation of histone H4R3 recruits DNMT3A, coupling histone and DNA methylation in gene silencing. *Nat. Struct. Mol. Biol.* 16, 304–311. doi: 10.1038/nsmb.1568

Zhong, R., Morrison, W.H. III, Negrel, J., and Ye, Z. H. (1998). Dual methylation pathways in lignin biosynthesis. *Plant Cell* 10, 2033– 2046. doi: 10.1105/tpc.10.12.2033

Zhong, S., Li, H., Bodi, Z., Button, J., Vespa, L., Herzog, M., et al. (2008). MTA is an Arabidopsis messenger RNA adenosine methylase and interacts with a homolog of a sex-specific splicing factor. *Plant Cell* 20, 1278–1288. doi: 10.1105/tpc.108.058883

Zhou, H. R., Zhang, F. F., Ma, Z. Y., Huang, H. W., Jiang, L., Cai, T., et al. (2013). Folate polyglutamylation is involved in chromatin silencing by maintaining global DNA methylation and histone H3K9 dimethylation in Arabidopsis. *Plant Cell* 25, 2545–2559. doi: 10.1105/tpc.113.114678

Zilberman, D., Gehring, M., Tran, R. K., Ballinger, T., and Henikoff, S. (2007). Genome-wide analysis of *Arabidopsis thaliana* DNA methylation uncovers an interdependence between methylation and transcription. *Nat. Genet.* 39, 61–69. doi: 10.1038/ng1929

Zwighaft, Z., Aviram, R., Shalev, M., Rousso-Noori, L., Kraut-Cohen, J., Golik, M., et al. (2015). Circadian clock control by polyamine levels through a mechanism that declines with age. *Cell Metab.* 22, 874–885. doi: 10.1016/j.cmet.2015.09.011

Conflict of Interest: The authors declare that the research was conducted in the absence of any commercial or financial relationships that could be construed as a potential conflict of interest

frontiers in Plant Science

REVIEW
published: 06 May 2020
doi: 10.3389/fpls.2020.00452

Writing and Reading Histone H3 Lysine 9 Methylation in *Arabidopsis*

*Linhao Xu and Hua Jiang**

Leibniz Institute of Plant Genetics and Crop Plant Research, Gatersleben, Germany

In eukaryotes, histone H3 lysine 9 methylation (H3K9me) mediates the silencing of invasive and repetitive sequences by preventing the expression of aberrant gene products and the activation of transposition. In *Arabidopsis*, while it is well known that dimethylation of histone H3 at lysine 9 (H3K9me2) is maintained through a feedback loop between H3K9me2 and DNA methylation, the details of the H3K9me2-dependent silencing pathway have not been fully elucidated. Recently, the regulation and the function of H3K9 methylation have been extensively characterized. In this review, we summarize work from the recent studies regarding the regulation of H3K9me2, emphasizing the process of deposition and reading and the biological significance of H3K9me2 in *Arabidopsis*.

Keywords: epigenetics, histone, heterochromatin, H3K9 methylation, transcriptional silencing

OPEN ACCESS

Edited by:
Iva Mozgova,
Centre for Biology, Academy of Sciences of the Czech Republic, Czechia

Reviewed by:
Paul Fransz,
University of Amsterdam, Netherlands
Liangsheng Zhang,
Fujian Agriculture and Forestry University, China

***Correspondence:**
Hua Jiang
jiangh@ipk-gatersleben.de

Specialty section:
This article was submitted to Plant Cell Biology, a section of the journal Frontiers in Plant Science

Received: *22 November 2019*
Accepted: *27 March 2020*
Published: *06 May 2020*

Citation:
Xu L and Jiang H (2020) Writing and Reading Histone H3 Lysine 9 Methylation in Arabidopsis. Front. Plant Sci. 11:452. doi: 10.3389/fpls.2020.00452

INTRODUCTION

In eukaryotic cells, chromatin is divided into two major types of compartments: heterochromatin and euchromatin, reflecting the repressive and permissive potential for transcription in these regions, respectively (Ding et al., 2007). Chromatin is rich in repetitive sequences and transposable elements inside and near centromeres, posing a risk for genome instability through their potential for transposition and meiotic recombination. Thus, during the whole life cycle, it is necessary to keep these regions inaccessible, condensed, and transcriptionally silent. Such regions are classified as constitutive heterochromatin (Saksouk et al., 2015). In contrast, facultative heterochromatin refers to regions whose compaction and silencing are dynamic in the life cycle or under stress stimuli, mainly distributed in chromosomal arms (Trojer and Reinberg, 2007).

Chromatin states are modulated by modifications at the N-terminal tails of histones, DNA methylation, and different histone variants (Jenuwein and Allis, 2001). Histone H3K9 methylation is a critical marker for transcriptional silencing and heterochromatin formation, mostly constitutive heterochromatin formation. Methylation states at H3K9 can be mono- (H3K9me1), di- (H3K9me2), or tri- (H3K9me3) methylation. In mammals, H3K9me3 is the most abundant marker in constitutive heterochromatin (Peters et al., 2003; Rice et al., 2003). However, in plants, the modification of H3K9me1 and H3K9me2 is rich in constitutive heterochromatin and only slightly present in facultative chromatin, whereas H3K9me3 is distributed with a high concentration in euchromatin and at expressed genes (Naumann et al., 2005). In *Arabidopsis*, H3K9me3 methylation broadly marks 40% of all genes (Roudier et al., 2009), but only a low level of H3K9me3 can be detected in regions with transposons and pseudogenes (Charron et al., 2009). Thus, the function of H3K9me3 has been altered in *Arabidopsis* compared to H3K9me3 in yeast and mammals.

H3K9me2 is mainly catalyzed by the histone methyltransferases KRYPTONITE (KYP), SUVH5, and SUVH6 in *Arabidopsis* and is maintained through the feedback loop between H3K9me2 and non-CG methylation (Du et al., 2015). Several studies have shown more details of H3K9me2 deposition with the structural analysis of KYP/SUVH5/SUVH6 and their role in H3K9me2 deposition (Du et al., 2014; Li et al., 2018) and other H3K9 methyltransferases (Caro et al., 2012) and cofactors (Yu et al., 2017). The downstream part of H3K9me2-dependent silencing has also been investigated by identifying a novel H3K9 reader (Zhang C. et al., 2018; Zhao et al., 2019). In this article, we review the writing, reading, and biological roles of H3K9 methylation in *Arabidopsis*.

H3K9 METHYLTRANSFERASES IN *ARABIDOPSIS*

Histone lysine methyltransferases usually contain a catalytic SET domain, which is named after three *Drosophila melanogaster* genes, *Su(var)3-9*, *E(z)*, and *Trx* (Jenuwein et al., 1998). In fission yeast, there is only one H3K9 methyltransferase, Clr4/KMT1, which is responsible for all three states of H3K9 methylation (Nakayama et al., 2001; **Figure 1**). In mammals, there are multiple H3K9 methyltransferases with different catalytic activities and target genes (Sims et al., 2003; Dodge et al., 2004; Shinkai and Tachibana, 2011; **Figure 1**). SUV39H1 and SUVH39H2 mono- and dimethylase catalyze di-and trimethylation in constitutive heterochromatic regions, SETDB1 monomethylates at the pericentromeric region, and the heterodimer of G9a and G9a-like protein (GLP) catalyzes di- and trimethylation in euchromatic regions.

In *Arabidopsis*, there are 15 SET-domain proteins that are related to SU(VAR)3-9 (Baumbusch et al., 2001; Lei et al., 2012; Zhang and Ma, 2012; **Figure 1**). Ten of these proteins are classified as SU(VAR)3-9 HOMOLOGS (SUVH1-SUVH9), and the remaining five are classified as SU(VAR)3-9-RELATED proteins (SUVR1-SUVR5) (**Table 1**). Among the nine SUVHs, KYP/SUVH4, SUVH5, and SUVH6 have been well identified as H3K9 methyltransferases responsible for maintaining H3K9 methylation. KYP mediates the majority of H3K9me2 methylation in both constitutive and facultative heterochromatin in *Arabidopsis*, while SUVH5 and SUVH6 only play minor roles in H3K9me2 methylation (Jackson et al., 2002, 2004; Stroud et al., 2014; Li et al., 2018). Crystal structures of KYP, SUVH5, and SUVH6 reveal that the post-SET domain is critical for enzymatic activity (Li et al., 2018); thus, SUVH2 and SUVH9, which lack the post-SET domain, are enzymatically inactive (Johnson et al., 2014). The remaining SUVH1, SUVH3, SUVH7, and SUVH8 were recently reported to function in transcriptional activation but not silencing, expanding the roles of SUVHs in transcriptional regulation (Harris et al., 2018; Xiao et al., 2019). Nevertheless, SUVH7 and SUVH8 are both primarily expressed and imprinted in the endosperm (Gehring et al., 2011; Wolff et al., 2011), indicating an endosperm-specific targeting mechanism favoring a relatively specific chromatin environment. Indeed, SUVH7 has already been shown to play a role in establishing postzygotic hybridization barriers established by H3K9me2 (Wolff et al., 2015; Jiang et al., 2017). Interestingly, computational characterization predicts that SUVH7 and SUVH8 are capable of catalyzing H3K9me1 and H3K9me2 methylation. Two critical residues in the catalytic pocket, Tyr1124 and Phe1209, determine the product specificity in GLP, a G9a-related methyltransferase (Wu et al., 2010). Meanwhile, H3K9me1 or H3K9me2 is correlated with the presence of Tyr in one of the positions and non-Tyr in the other, indicating that the two SUVHs are capable of catalyzing H3K9me1 or H3K9me2. Thus, SUVH7 and SUVH8 may function as methyltransferases for endosperm-specific H3K9me2 deposition. Taken together, KYP, SUVH5, and SUVH6 are the general H3K9 methyltransferases in *Arabidopsis*, and it is possible that SUVH7 and SUVH8 act as endosperm-specific methyltransferases.

Among the five SUVRs, SUVR1, and SUVR2 have shown no HMTase activity in an *in vitro* enzymatic assay, but SUVR4 has HMTase activity to convert H3K9me1 to H3K9me2 (ubiquitin) and H3K9me3 (without ubiquitin) *in vitro* (Thorstensen et al., 2006; Veiseth et al., 2011). The level of H3K9me3 is correlated with the amount of SUVR4-GFP in *Arabidopsis* nuclei, but the effect of genome-wide H3K9mer3 has not been determined (Veiseth et al., 2011). SUVR5 is capable of establishing H3K9me2 in a DNA methylation–independent manner and is involved in the response to environmental or developmental cues (Caro et al., 2012).

TARGETING H3K9 METHYLATION THROUGH BINDING TO METHYLATED DNA

DNA methylation is tightly connected with H3K9 methylation. In *Neurospora crassa*, the H3K9 methyltransferase DIM5 establishes H3K9me3, and then heterochromatin protein 1 (HP1) recognizes H3K9me3 to facilitate the targeting of the DNA methyltransferase DIM2 (Tamaru and Selker, 2003). In mammals, knockout of either *G9a* or *Suv39 H1, Suv39 H2* results in reduced DNA methylation in mice (Ikegami et al., 2007). Moreover, H3K9 methylation is dependent on DNA methylation in human cancer cells (Espada et al., 2004). Likewise, in *Arabidopsis*, KYP, SUVH5, and SUVH6 are primarily recruited to the targets through SET and RING-associated (SRA) domain binding to DNA that is methylated in the CHG context (H stands for any base except G). H3K9me2 is known to recruit the DNA methyltransferases CMT2 and CMT3, which mediate CHH and CHG DNA methylation, respectively, in a feedback loop with H3K9me2 (**Figure 2**; Johnson et al., 2007; Bernatavichute et al., 2008; Du et al., 2012; Zemach et al., 2013; Stroud et al., 2014). Considering the targeting of H3K9 methyltransferases to CHG-methylated DNA, KYP, SUVH5, and SUVH6 have distinct DNA binding preferences. KYP, which is responsible for the majority of H3K9me2, has high affinity to the CWG (W stands for A or T) context but has low affinity to the CCG context (Li et al., 2018). The differential binding affinity is consistent with the phenotype that DNA methylation at CWG is strongly lost in *kyp*, but loss of CCG methylation is very low in *kyp* but high in *suvh5* and *suvh6*.

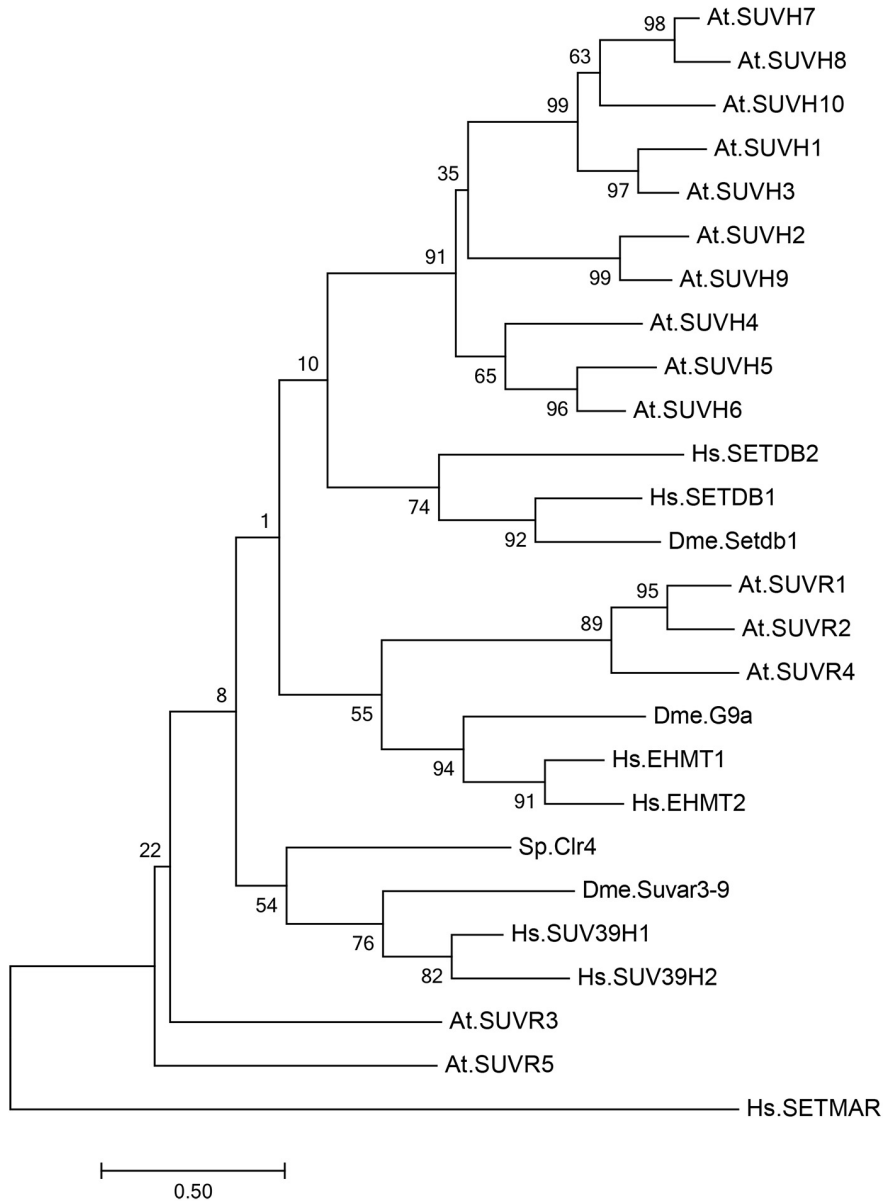

FIGURE 1 | Phylogenetic analysis of SU(VAR)3–9 homologous proteins in *Arabidopsis thaliana*, *Drosophila melanogaster*, *Schizosaccharomyces pombe*, and *Homo sapiens*. Phylogenetic analysis of 15 SU(VAR)3–9 homologous protein sequences from *Arabidopsis thaliana* (At), three SU(VAR)3–9 homologous protein sequences from *Drosophila melanogaster* (Dme), one SU(VAR)3–9 homologous protein sequence from *Schizosaccharomyces pombe* (Sp), and five SU(VAR)3–9 homologous protein sequences from *Homo sapiens* (Hs). The evolutionary history was inferred by using the maximum likelihood method based on the Poisson correction model. Phylogenetic analysis was performed using MEGA 7.0.

Consistent with the *in vivo* consequence of DNA methylation, SUVH5 has a preference for the CCG context, and SUVH6 can bind to both the CWG and CCG contexts, which act as a backup of KYP to ensure H3K9me2 in all CHG contexts (**Figure 2**).

While the feedback loop between CHG DNA methylation is frequently discussed, CG and CHH methylation also contribute to H3K9me2 deposition through SRA domains of KYP, SUVH5, and SUVH6 binding to DNA that is methylated in CG or CHH context. In a large-scale comparative epigenome analysis, *MET1* was indeed found to be required for the maintenance of CMT2-dependent asymmetric CHH methylation at loci with H3K9me2 (Zhang Y. et al., 2018). Moreover, SUVH5 and SUVH6 can bind to DNA that is methylated in the CG context *in vitro* (Li et al., 2018), supporting the view that CG methylation also contributes to H3K9me2 deposition. In addition to CG methylation, it has been known for many years that CHH methylation generated by the RNA-directed DNA methylation (RdDM) pathway is also involved in H3K9me2 deposition (Wierzbicki et al., 2008; Zheng et al., 2009; Shin et al., 2013; Liu Z.W. et al., 2014). Recent biochemical

TABLE 1 | Summary of DNA methyltransferases and SUV methyltransferases in *Arabidopsis thaliana.*

Gene ID	Gene name	Description
AT5G49160	MET1	Maintains CG methylation (Finnegan et al., 1996)
AT4G19020	CMT2	Deposits mainly CHH methylation (Stroud et al., 2014)
AT1G69770	CMT3	Maintains CHG methylation (Lindroth et al., 2001)
AT5G14620	DRM2	Establishes *de novo* CHH methylation (Cao and Jacobsen, 2002)
AT5G04940	SUVH1	Required for transcriptional activation (Harris et al., 2018)
AT2G33290	SUVH2	Recruit RNA polymerase V to establish CHH methylation (Johnson et al., 2008; Johnson et al., 2014)
AT1G73100	SUVH3	Required for transcriptional activation (Harris et al., 2018)
AT5G13960	SUVH4	Maintains H3K9me1/me2 (Jackson et al., 2002)
AT2G35160	SUVH5	Maintains H3K9me1/me2 (Ebbs and Bender, 2006)
AT2G22740	SUVH6	Maintains H3K9me1/me2 (Jackson et al., 2004)
AT1G17770	SUVH7	Paternal-expressed imprinted gene (Gehring et al., 2011; Wolff et al., 2011)
AT2G24740	SUVH8	Maternal-expressed imprinted gene (Gehring et al., 2011; Wolff et al., 2011)
AT4G13460	SUVH9	Recruits RNA polymerase V to establish CHH methylation (Johnson et al., 2008; Johnson et al., 2014)
AT2G05900	SUVH10	Pseudogene (Baumbusch et al., 2001)
AT1G04050	SUVR1	Unknown
AT5G43990	SUVR2	deposits H3K9me1/me2; H4K20me; H3K27me2 (Han et al., 2014)
AT3G03750	SUVR3	Unknown
AT3G04380	SUVR4	Deposits H3K9me2/me3 (Thorstensen et al., 2006; Veiseth et al., 2011)
AT2G23740	SUVR5	Establishes H3K9me2 independently of DNA methylation (Caro et al., 2012)

evidence indeed supports this hypothesis; all three SUVHs can bind to CHH-methylated DNA (**Figure 2**), and there is no sequence preference among the three SUVHs in targeting CHH-methylated DNA (Li et al., 2018).

Apart from the specificity of the SRA domain on the sequence context, other factors may also affect KYP, SUVH5, and SUVH6 targeting to methylated DNA. It was reported that SUVH4 and SUVH5 prefer to control transposable elements, but SUVH4 and SUVH6 prefer to target transcribed inverted repeat sources of dsRNA. Thus, in addition to DNA methylation states, chromatin state may also govern SUVH activities (Ebbs and Bender, 2006).

TARGETING H3K9 METHYLATION INDEPENDENTLY OF DNA METHYLATION

Apart from DNA methylation-dependent H3K9me2 deposition, there are known exceptions. G9a is one of the primary enzymes for H3K9me1 and H3K9me2 and usually interacts with another enzyme, GLP, to form a heteromeric complex that appears to be a functional H3K9 methyltransferase *in vivo* (Shinkai and Tachibana, 2011). In murine embryonic stem cells (mESCs), H3K9me2 at the newly integrated proviral LTR is reduced in cells with G9a silencing. Since there is no H3K9me2 or DNA methylation at the newly integrated region, *G9a* is considered to be responsible for *de novo* H3K9me2 (Leung et al., 2011). In addition to mESCs, G9a-dependent H3K9me2 has also been associated with gene repression in multiple human cell lines (Chen et al., 2009; Liu C. et al., 2014; Yoshida et al., 2015; Kramer, 2016; Scheer and Zaph, 2017).

Similar exceptions also exist in *Arabidopsis*. It was reported that SUVR5 is able to establish H3K9me2 independently of DNA methylation (**Figure 2**; Caro et al., 2012). Unlike KYP/SUVH5/SUVH6, SUVR5 does not have the SRA domain which can bind at methylated DNA but relies on a set of three C2H2 zinc fingers in tandem, which can bind at the sequence context of "TACTAGTA" *in vitro*. This motif also occurs at a minor part of transposable elements (TEs) and surrounds substantial genes losing H3K9me2 in *suvr5*, further supporting the role of zinc fingers in targeting H3K9me2 deposition. While H3K9 methyltransferases in yeast or mammals do not contain zinc fingers, DNA binding proteins recruiting H3K9 methyltransferases contain zinc fingers (Kim and Huang, 2003; Fog et al., 2012; Bian et al., 2015). In mammalian cells, ZNF644 has eight zinc finger motifs and WIZ contains 12 zinc finger motifs that are the binding partners of the G9a-GLP complex (Bian et al., 2015). The N-terminus of ZNF644 interacts with the transcriptional domain (TAD) of G9a, but the C-terminus of WIZ interacts with the TAD of GLP to facilitate the targeting of the G9a-GLP complex at specific genomic loci with the preference of the promoter region (Bian et al., 2015). Thus, it seems that targeting H3K9me2 by the zinc finger domain is a conserved mechanism in plants and mammals, but in plants, the zinc finger domain has been integrated into H3K9 methyltransferase. Interestingly, the combination of zinc fingers and a C-terminal SET domain can be found in all plant species (Caro et al., 2012). Thus, SUVR5 depositing H3K9me2 independently of DNA methylation might be conserved in plants. Another exception in *Arabidopsis* is SUVR4, which can bind to

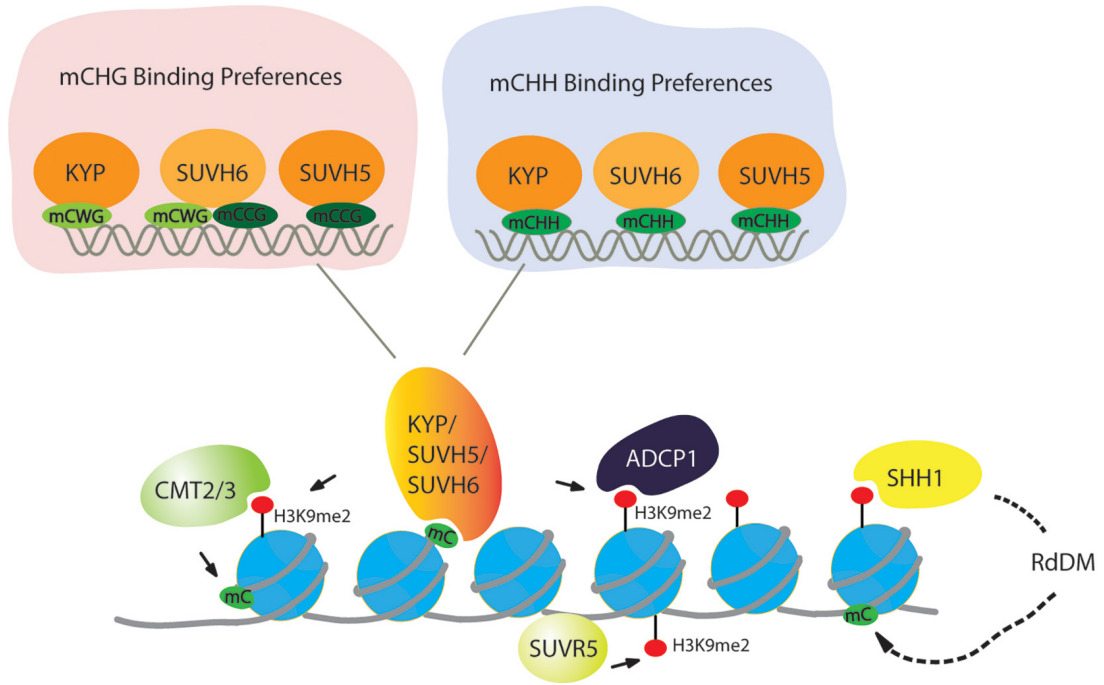

FIGURE 2 | Targeting of H3K9 dimethylation in a DNA methylation-dependent and -independent manner. For DNA methylation, CMT2 and CMT3 recognize the H3K9me2 mark and catalyze DNA methylation in the CHG and CHH context (H = A, T, or C), respectively. For H3K9 methylation, histone methyltransferases KYP/SUVH4, SUVH5, and SUVH6 bind at methylated DNA in the CHG and CHH context to deposit H3K9me2, creating a reinforcing loop between DNA methylation and Histone modification. In the CHG context, KYP has a preference of mCWG (W = A or T), while SUVH5 and SUVH6 have a high affinity to the mCCG. All three SUVHs have similar sequence specificities at mCHH sites. SUVR5 binds to DNA through its zinc finger domain to facilitate H3K9me2 independently of DNA methylation. H3K9me2 is captured by SHH1, then through RdDM pathway to methylate DNA.

ubiquitin through the N-terminal WIYLD domain to facilitate the conversion from H3K9me1 to H3K9me3 *in vitro*, but it is not clear if the WIYLD domain binds to ubiquitin *in vivo* and if this domain binds to histone or other proteins with ubiquitination (Thorstensen et al., 2006; Veiseth et al., 2011). Recently, it was reported that the CRL4DCAF8 ubiquitin ligase is capable of targeting H3 for polyubiquitination at K79 in mice, which may further promote H3K9me2 deposition (Li et al., 2017), suggesting a similar connection between histone ubiquitination and H3K9me3. Taken together, the deposition of H3K9me2 is not only DNA methylation dependent but can also be independent.

OTHER PROTEINS PARTICIPATE IN H3K9 METHYLATION DEPOSITION

The distribution of histone acetylation is usually anti-correlated with histone methylation, such as H3K9Ac and H3K9me2 (Zhou et al., 2010), indicating that the removal of H3K9Ac or relevant protein complexes functions in H3K9me2 deposition. Histone deacetylation is processed by histone deacetylases (HDACs), which play important roles in chromatin regulation (Liu X. et al., 2014). In mammals, SUV39H1 can interact with HDAC1 and HDAC2 (Vaute et al., 2002). Moreover, transcriptional repression by SUV39H1 is abolished by treatment with the HDAC inhibitor trichostatin A (TSA), indicating that the function of SUV39H1 is dependent on HDAC activity (Vaute et al., 2002). Likewise, in *Arabidopsis*, one of the HDACs, HDA6, also physically interacts with H3K9 methyltransferases KYP, SUVH5, and SUVH6, regulating a group of transposable elements and repetitive sequences (Yu et al., 2017). The mutant with compromised HDA6 has reduced H3K9me2 levels compared with the wild type, suggesting that H3K9me2 deposited by KYP, SUVH5, and SUVH6 is partly dependent on HDA6, but it is not clear that H3K9me2 deposition in *Arabidopsis* is dependent on the level of H3K9Ac at the targets or depends on the interaction between HDA6 and KYP/SUVH5/SUVH6, or perhaps both mechanisms exist in *Arabidopsis*, which has not been clearly dissected to date. Given the remaining H3K9me2 level in the *hda6* mutant, it will be interesting to know if other HDACs are also involved in H3K9me2 deposition in the future.

Matrix attachment regions (MARs) are important for chromatin organization and gene expression (Tetko et al., 2006; Zhao et al., 2014). MARs are stretches of AT-rich sequences that guide the binding of DNA to the nuclear matrix by recruiting MAR-binding proteins. Proteins with AT-hook motifs bind to MARs and play roles in regulating H3K9me2 levels. In *Neurospora crassa*, CHAP, a protein with AT-hook motifs, was demonstrated to recognize heterochromatic regions through AT-hook motifs and to recruit the H3K9 methyltransferase DIM5

to targets (Honda et al., 2016). In *Arabidopsis*, overexpression of AT-hook motif nuclear localized 22 (AHL22) causes delayed flowering time by increasing H3K9me2 at MAR located in an intron of the FLOWERING LOCUS T (FT) locus (Xiao et al., 2009; Yun et al., 2012). AHL16 regulates the expression of the floral repressor genes FLOWERING LOCUS C (FLC) and FLOWERING WAGENINGEN (FWA) by adjusting the H3K9me2 level (Xu et al., 2013). Overexpressed AHL10 increases genome-wide H3K9me2 levels in the endosperm of triploid seeds (Jiang et al., 2017). Consistent with the distribution of MARs that are mainly in chromosome arms, TEs that are methylated by H3K9me2 *via* AHL10 in the endosperm of triploid seeds are usually euchromatic AT-rich TEs (Jiang et al., 2017). To date, it has not been determined how AHLs regulate H3K9me2 levels. While there is no direct physical interaction between AHLs and H3K9 methyltransferase in *Arabidopsis*, AHLs usually interact with HDAC complexes both *in vitro* and *in vivo*, such as AHL22 interacting with HDA1, HDA6, and HDA9 (Xiao et al., 2009) and AHL16 interacting with FVE and MSI5, which are core components of the HDA6 complex (Gu et al., 2011; Xu et al., 2013). Thus, it is possible that AHLs participate in H3K9me2 deposition through interaction with HDACs, especially HDA6. Nevertheless, other chromatin-relevant proteins also occur in AHL complexes, such as SUVH9 in the AHL10 complex. Apart from interacting with the DDR complex and mediating Pol V recruitment in RdDM (Johnson et al., 2014; Liu Z.W. et al., 2014), SUVH9 also interacts with MORC6 and its two close homologs, MORC1 and MORC2, required for heterochromatin condensation and formation of 3D chromatin architecture at SUPPRESSOR OF DRM1 DRM2 CMT3 (SDC) and Solo-LTR loci (Jing et al., 2016). Recently, the mammalian nuclear matrix protein scaffold attachment factor B (SAFB) was found to participate in stabilizing heterochromatin architecture partially through phase separation, which is a phenomenon in which different biological molecules spontaneously separate into two coexisting liquid phases and result in miscellaneous non-membrane-bound cellular compartments. Depletion of SAFB results in more interchromosomal interactions around pericentromeric heterochromatin and a decrease in genomic compartmentalization, which could result from the decondensation of pericentromeric heterochromatin (Huo et al., 2020). Thus, it is also possible that AHLs and MARs participate in H3K9me2 regulation by affecting heterochromatin architecture and phase separation.

H3K9 READERS IN *ARABIDOPSIS*

H3K9 methylation recruits downstream effectors containing specific reader domains to further mediate gene silencing. In metazoans, heterochromatin protein 1 (HP1) is known to read the trimethylated lysine 9 residue of histone H3 (H3K9me3) (Bannister et al., 2001; Jacobs et al., 2001), which is a hallmark histone modification for transcriptionally silenced heterochromatin in mammals (Zeng et al., 2010). HP1 contains a conserved chromodomain (CD) at the N-terminus and a chromo shadow domain (CSD) at the C-terminus (Li et al., 2002). CD is able to directly bind to H3K9me3 (Jacobs et al., 2001). Based on sequence similarity and early biochemistry analyses, the homolog of HP1 in *Arabidopsis*, LIKE HETEROCHROMATIN PROTEIN 1 (LHP1) was first proposed to be the H3K9me reader that mediates H3K9me2-dependent heterochromatic silencing, as it was shown to bind H3K9me2 *in vitro* (Jackson et al., 2002). Nevertheless, several lines of evidence have indicated that LHP1 is a plant-specific PRC1 H3K27me3 reader subunit. The CHROMO domain of LHP1 specifically binds to H3K27me3 but not H3K9me in *Arabidopsis,* and the genome-wide distribution of LHP1 displays significant overlap with H3K27me3-enriched sites (Turck et al., 2007; Exner et al., 2009; Lu et al., 2011). While SHH1, CMT2, and CMT3 have the capability to bind to histones with H3K9me2 (Law et al., 2013; Stroud et al., 2014; **Figure 1**), their function is to maintain or initiate non-CG methylation but not the downstream H3K9me2 reader; therefore, the reader of H3K9me2 in plants had not been determined until two recent studies were conducted in *Arabidopsis*. Agenet domain (AGD)-containing p1 (AGDP1), also known as ADCP1, appears to be a plant-specific H3K9 reader and functions as an HP1 equivalent protein (Zhang C. et al., 2018; Zhao et al., 2019). The tandem AGDs of AGDP1 can specifically recognize H3K9me2 and unmethylated K4 on the H3 tail (H3K4me0) through two negatively charged surface pockets. In structural studies, AGD12 adopts a tandem Tudor-like conformation, which resembles the human UHRF1 tandem Tudor and *Arabidopsis* SHH1 SAWADEE domains, both of which function as H3K9me2 readers with similar recognition mechanisms (Arita et al., 2012; Cheng et al., 2013; Law et al., 2013). ADCP1 is responsible for H3K9me2-dependent silencing, and the *in vivo* binding site of ADCP1 largely overlaps with the regions enriched by H3K9me2, further supporting that ADCP1 is indeed an H3K9me2 reader (Zhao et al., 2019).

While ADCP1 has been successfully identified, how ADCP1 mediates H3K9me2-dependent transcriptional silencing still needs to be discovered. Given that ADCP1 is essential for heterochromatin formation and TE silencing, but ADCP1 itself is only a histone binding protein without any repressor domain (Zhao et al., 2019), other chromatin modeling proteins must be recruited by ADCP1 to heterochromatin. Recently, SMC4, a core subunit of condensins I and II, was identified to act in conjunction with CG methylation, CHG methylation, the chromatin remodeler DDM1 (DECREASE IN DNA METHYLATION 1), and histone modifications, including H3K9me2 and H3K27me1 (Wang et al., 2017). Considering the function of SMC4 in H3K9me2-mediated transcriptional silencing (Wang et al., 2017), it is worth knowing whether SMC4 works together with ADCP1 to mediate heterochromatic silencing. Another possibility is that ADCP1 mediates downstream silencing by driving nucleosome phase separation. It has been demonstrated that human HP1α and *Drosophila* HP1a may demix from aqueous solution to form phase-separated droplets (Larson et al., 2017; Strom et al., 2017), which rapidly induce compacted chromatin. Similarly, ADCP1 can mediate heterochromatin phase separation together

with reconstituted nucleosomes bearing H3K9me3 *in vitro* (Zhao et al., 2019). Thus, ADCP1 probably has a similar ability to mediate phase separation as the functional analog of mammalian HP1.

ROLE OF H3K9 METHYLATION IN *ARABIDOPSIS* DEVELOPMENT

The mutant with compromised KYP, SUVH5, and SUVH6 has no obvious abnormality in development; thus, H3K9 was considered to play minor roles in *Arabidopsis* development. Nevertheless, the role of H3K9me2 in *Arabidopsis* development has been identified with more careful observations and new approaches.

The main H3K9me2 methyltransferase, KYP, was proven to repress primary seed dormancy by suppressing the expression of dormancy and ABA pathway-related genes, such as *DOG1*, which is a master regulator in the control of seed dormancy (Bentsink et al., 2006), and *ABI3* and *ABI4,* which are components of ABA signaling (Koornneef et al., 2002; Zheng et al., 2012). However, evidence that H3K9me2 directly regulates the expression of these genes *via* H3K9me2 levels is not available. Until recently, SUVH5 was revealed to directly repress the expression of genes related to the ABA signaling pathway, *DOG*1, and its homologs *via* H3K9me2 in light-mediated seed germination (Gu et al., 2019). Thus, SUVH5-mediated H3K9me2 directly participates in controlling seed germination in *Arabidopsis*. After seed germination, plants enter the vegetative stage. While the role of H3K9me2 in the vegetative stage is not clear, H3K9me2 is crucial for the transition to flowering. Knockdown of *AHL16* leads to obvious late flowering, which results in increased expression of two flowering repressors, *FLOWERING LOCUS C* (*FLC*) and FWA. Consistent with the increased expression pattern, the H3K9me2 levels at the intron of *FLC* and *FWA* loci were reduced. Interestingly, the phenotype of late flowering in the *ahl16* mutant only occurs in Landsberg (Ler) accession but not in Columbia (Col) accession, indicating the ecotype-dependent regulation process (Xu et al., 2013).

During male meiosis, H3K9me2 is crucial for the distribution of meiotic recombination (Underwood et al., 2018). In plants, meiotic recombination is enriched in euchromatic regions, rather than pericentromeric heterochromatin, associated with H3K4me3 and histone variant H2A.Z but inversely correlated with DNA methylation. Suppression of meiotic recombination within the centromeric region is thought to be important for maintaining the fidelity of genome transmission during meiosis (Choi et al., 2018). Loss of DNA methylation in the *met1* mutant leads to epigenetic activation of meiotic double-strand breaks (DSBs) in proximity to centromeres (Choi et al., 2018). In addition, non-CG methylation and the H3K9me2 pathway are also responsible for suppressing pericentromeric recombination (Underwood et al., 2018). Epigenetic activation of recombination and crossovers (COs) can be induced *via* loss of H3K9me2 and non-CG methylation in the *kyp*, *suvh5*, *suvh6*, or *cmt3* mutant (Underwood et al., 2018), making it possible to induce COs near centromeres, which are otherwise very low-frequency CO regions in *Arabidopsis* and crops (Taagen et al., 2020).

In *Arabidopsis thaliana* and *Arabidopsis lyrata* seed development, H3K9me2 and CHG methylation are involved in the regulation of genomic imprinting that leads to differential expression of parent-of-origin alleles by maintaining or reinforcing the repression of maternal alleles of imprinted paternally expressed genes (PEGs) (Klosinska et al., 2016; Moreno-Romero et al., 2019). Moreover, the presence of the three repressive epigenetic marks H3K27me3, H3K9me2, and CHG methylation on the maternal alleles in endosperm can be considered a specific epigenetic signature of paternally expressed imprinted genes in the endosperm of *Arabidopsis* (Moreno-Romero et al., 2019). These marks are able to predict known PEGs at high accuracy and identify several new PEGs that were confirmed by INTACT-based endosperm transcriptomes (Moreno-Romero et al., 2019). In addition to maintaining genomic imprinting in the endosperm of diploid *Arabidopsis* seeds, H3K9me2 also functions in establishing a hybridization barrier from interploidy cross in the endosperm of triploid seeds (the triploid block) (Jiang et al., 2017). The triploid block acts as an instant reproductive barrier that prevents backcrossing of the newly formed polyploid plants with their progenitors (Schatlowski and Kohler, 2012). Multiple PEGs are enhanced in the endosperm of triploid seeds (Kradolfer et al., 2013; Wolff et al., 2015). Increased H3K9me2 levels in AT-rich TEs derived from overexpressed ADM and AHL10 contribute to enhancing the expression of PEGs, such as PEG2, which is a crucial component in establishing the triploid block. Moreover, H3K9me2 levels in AT-rich TEs are also associated with the different phenotypes of the triploid block in Col and Ler accessions.

CONCLUSION AND PERSPECTIVE

In plants, H3K9 methylation, mainly H3K9me2, functions importantly in suppressing TEs and repetitive sequences, protecting plant genomes from TE transposition and genome instability. To enable plants to correctly deposit H3K9me2 in the genome, multiple H3K9 methyltransferases are in charge of H3K9me2 deposition in different sequence contexts *via* DNA methylation-dependent and -independent activities. Apart from playing a role in genome stability, H3K9me2 also plays roles in plant development and environmental stimuli. Recent studies have enhanced our understanding of the structure and recruitment of H3K9 methyltransferases and the downstream effector of H3K9me2, but open questions remain.

Given that H3K9me2 plays important roles in plant development and environmental stress, how the H3K9 methylation pathway is in response to developmental cues or environmental stimuli will be highly interesting to explore. In addition, our mechanistic understanding of downstream effectors of H3K9 methylation is also limited, while the H3K9me reader has been identified in *Arabidopsis*. The mechanism by which ADCP1 mediates transcriptional silencing, the existence of other H3K9me downstream effectors, the role of phase separation

in chromatin condensation *in vivo*, and how H3K9me functions in response to developmental cues or environmental stimuli remains to be elucidated. Answering these questions will further broaden our understanding of H3K9 methylation-dependent transcriptional silencing.

AUTHOR CONTRIBUTIONS

Both authors listed have made a substantial, direct and intellectual contribution to the work, and approved it for publication.

REFERENCES

Arita, K., Isogai, S., Oda, T., Unoki, M., Sugita, K., Sekiyama, N., et al. (2012). Recognition of modification status on a histone H3 tail by linked histone reader modules of the epigenetic regulator UHRF1. *Proc. Natl. Acad. Sci. U.S.A.* 109, 12950–12955. doi: 10.1073/pnas.1203701109

Bannister, A. J., Zegerman, P., Partridge, J. F., Miska, E. A., Thomas, J. O., Allshire, R. C., et al. (2001). Selective recognition of methylated lysine 9 on histone H3 by the HP1 chromo domain. *Nature* 410, 120–124. doi: 10.1038/35065138

Baumbusch, L. O., Thorstensen, T., Krauss, V., Fischer, A., Naumann, K., Assalkhou, R., et al. (2001). The *Arabidopsis thaliana* genome contains at least 29 active genes encoding SET domain proteins that can be assigned to four evolutionarily conserved classes. *Nucleic Acids Res.* 29, 4319–4333. doi: 10.1093/nar/29.21.4319

Bentsink, L., Jowett, J., Hanhart, C. J., and Koornneef, M. (2006). Cloning of *DOG1*, a quantitative trait locus controlling seed dormancy in *Arabidopsis*. *Proc. Natl. Acad. Sci. U.S.A.* 103, 17042–17047. doi: 10.1073/pnas.0607877103

Bernatavichute, Y. V., Zhang, X., Cokus, S., Pellegrini, M., and Jacobsen, S. E. (2008). Genome-wide association of histone H3 lysine nine methylation with CHG DNA methylation in *Arabidopsis thaliana*. *PLoS One* 3:e3156. doi: 10.1371/journal.pone.0003156

Bian, C., Chen, Q., and Yu, X. (2015). The zinc finger proteins ZNF644 and WIZ regulate the G9a/GLP complex for gene repression. *eLife* 4:e05606. doi: 10.7554/eLife.08168

Cao, X., and Jacobsen, S. E. (2002). Role of the arabidopsis DRM methyltransferases in de novo DNA methylation and gene silencing. *Curr. Biol.* 12, 1138–1144. doi: 10.1016/s0960-9822(02)00925-9

Caro, E., Stroud, H., Greenberg, M. V., Bernatavichute, Y. V., Feng, S., Groth, M., et al. (2012). The SET-domain protein SUVR5 mediates H3K9me2 deposition and silencing at stimulus response genes in a DNA methylation-independent manner. *PLoS Genet.* 8:e1002995. doi: 10.1371/journal.pgen.1002995

Charron, J. B., He, H., Elling, A. A., and Deng, X. W. (2009). Dynamic landscapes of four histone modifications during deetiolation in *Arabidopsis*. *Plant Cell* 21, 3732–3748. doi: 10.1105/tpc.109.066845

Chen, X., El Gazzar, M., Yoza, B. K., and Mccall, C. E. (2009). The NF-kappaB factor RelB and histone H3 lysine methyltransferase G9a directly interact to generate epigenetic silencing in endotoxin tolerance. *J. Biol. Chem.* 284, 27857–27865. doi: 10.1074/jbc.M109.000950

Cheng, J., Yang, Y., Fang, J., Xiao, J., Zhu, T., Chen, F., et al. (2013). Structural insight into coordinated recognition of trimethylated histone H3 lysine 9 (H3K9me3) by the plant homeodomain (PHD) and tandem tudor domain (TTD) of UHRF1 (ubiquitin-like, containing PHD and RING finger domains, 1) protein. *J. Biol. Chem.* 288, 1329–1339. doi: 10.1074/jbc.M112.415398

Choi, K., Zhao, X., Tock, A. J., Lambing, C., Underwood, C. J., Hardcastle, T. J., et al. (2018). Nucleosomes and DNA methylation shape meiotic DSB frequency in *Arabidopsis thaliana* transposons and gene regulatory regions. *Genome Res.* 28, 532–546. doi: 10.1101/gr.225599.117

Ding, Y., Wang, X., Su, L., Zhai, J., Cao, S., Zhang, D., et al. (2007). SDG714, a histone H3K9 methyltransferase, is involved in Tos17 DNA methylation and transposition in rice. *Plant Cell* 19, 9–22. doi: 10.1105/tpc.106.048124

Dodge, J. E., Kang, Y. K., Beppu, H., Lei, H., and Li, E. (2004). Histone H3-K9 methyltransferase ESET is essential for early development. *Mol. Cell. Biol.* 24, 2478–2486. doi: 10.1128/mcb.24.6.2478-2486.2004

Du, J., Zhong, X., Bernatavichute, Y. V., Stroud, H., Feng, S., Caro, E., et al. (2012). Dual binding of chromomethylase domains to H3K9me2-containing nucleosomes directs DNA methylation in plants. *Cell* 151, 167–180. doi: 10.1016/j.cell.2012.07.034

Du, J. M., Johnson, L. M., Groth, M., Feng, S. H., Hale, C. J., Li, S. S., et al. (2014). Mechanism of DNA methylation-directed histone methylation by KRYPTONITE. *Mol. Cell* 55, 495–504. doi: 10.1016/j.molcel.2014.06.009

Du, J. M., Johnson, L. M., Jacobsen, S. E., and Patel, D. J. (2015). DNA methylation pathways and their crosstalk with histone methylation. *Nat. Rev. Mol. Cell Biol.* 16, 519–532. doi: 10.1038/nrm4043

Ebbs, M. L., and Bender, J. (2006). Locus-specific control of DNA methylation by the *Arabidopsis* SUVH5 histone methyltransferase. *Plant Cell* 18, 1166–1176. doi: 10.1105/tpc.106.041400

Espada, J., Ballestar, E., Fraga, M. F., Garea, A. V., Juarranz, A., Stockert, J. C., et al. (2004). Human DNA methyltransferase 1 is required for maintenance of the histone H3 modification pattern. *J. Biol. Chem.* 279, 37175–37184. doi: 10.1074/jbc.M404842200

Exner, V., Aichinger, E., Shu, H., Wildhaber, T., Alfarano, P., Caflisch, A., et al. (2009). The Chromodomain of LIKE HETEROCHROMATIN PROTEIN 1 is Essential for H3K27me3 binding and function during arabidopsis development. *PLoS One* 4:e5335. doi: 10.1371/journal.pone.0005335

Finnegan, E. J., Peacock, W. J., and Dennis, E. S. (1996). Reduced DNA methylation in *Arabidopsis thaliana* results in abnormal plant development. *Proc. Natl. Acad. Sci. U.S.A.* 93, 8449–8454. doi: 10.1073/pnas.93.16.8449

Fog, C. K., Galli, G. G., and Lund, A. H. (2012). PRDM proteins: important players in differentiation and disease. *Bioessays* 34, 50–60. doi: 10.1002/bies.201100107

Gehring, M., Missirian, V., and Henikoff, S. (2011). Genomic analysis of parent-of-origin allelic expression in *Arabidopsis thaliana* seeds. *PLoS One* 6:e23687. doi: 10.1371/journal.pone.0023687

Gu, D. C., Ji, R. J., He, C. M., Peng, T., Zhang, M. Y., Duan, J., et al. (2019). *Arabidopsis* histone methyltransferase SUVH5 is a positive regulator of light-mediated seed germination. *Front. Plant Sci.* 10:841. doi: 10.3389/fpls.2019.00841

Gu, X., Jiang, D., Yang, W., Jacob, Y., Michaels, S. D., and He, Y. (2011). *Arabidopsis* homologs of retinoblastoma-associated protein 46/48 associate with a histone deacetylase to act redundantly in chromatin silencing. *PLoS Genet.* 7:e1002366. doi: 10.1371/journal.pgen.1002366

Han, Y. F., Dou, K., Ma, Z. Y., Zhang, S. W., Huang, H. W., Li, L., et al. (2014). SUVR2 is involved in transcriptional gene silencing by associating with SNF2-related chromatin-remodeling proteins in *Arabidopsis*. *Cell Res.* 24, 1445–1465. doi: 10.1038/cr.2014.156

Harris, C. J., Scheibe, M., Wongpalee, S. P., Liu, W. L., Cornett, E. M., Vaughan, R. M., et al. (2018). A DNA methylation reader complex that enhances gene transcription. *Science* 362, 1182–1186. doi: 10.1126/science.aar7854

Honda, S., Bicocca, V. T., Gessaman, J. D., Rountree, M. R., Yokoyama, A., Yu, E. Y., et al. (2016). Dual chromatin recognition by the histone deacetylase complex HCHC is required for proper DNA methylation in Neurospora crassa. *Proc. Natl. Acad. Sci. U.S.A.* 113, E6135–E6144. doi: 10.1073/pnas.1621475114

Huo, X. R., Ji, L. Z., Zhang, Y. W., Lv, P., Cao, X., Wang, Q. F., et al. (2020). The nuclear matrix protein SAFB cooperates with major satellite RNAs to stabilize heterochromatin architecture partially through phase separation. *Mol. Cell* 77, 368–383.e7. doi: 10.1016/j.molcel.2019.10.001

Ikegami, K., Iwatani, M., Suzuki, M., Tachibana, M., Shinkai, Y., Tanaka, S., et al. (2007). Genome-wide and locus-specific DNA hypomethylation in G9a deficient mouse embryonic stem cells. *Genes Cells* 12, 1–11. doi: 10.1111/j.1365-2443.2006.01029.x

Jackson, J. P., Johnson, L., Jasencakova, Z., Zhang, X., Perezburgos, L., Singh, P. B., et al. (2004). Dimethylation of histone H3 lysine 9 is a critical mark for DNA methylation and gene silencing in *Arabidopsis thaliana*. *Chromosoma* 112, 308–315. doi: 10.1007/s00412-004-0275-7

Jackson, J. P., Lindroth, A. M., Cao, X., and Jacobsen, S. E. (2002). Control of CpNpG DNA methylation by the KRYPTONITE histone H3 methyltransferase. *Nature* 416, 556–560. doi: 10.1038/nature731

Jacobs, S. A., Taverna, S. D., Zhang, Y., Briggs, S. D., Li, J., Eissenberg, J. C., et al. (2001). Specificity of the HP1 chromo domain for the methylated N-terminus of histone H3. *EMBO J.* 20, 5232–5241. doi: 10.1093/emboj/20.18.5232

Jenuwein, T., and Allis, C. D. (2001). Translating the histone code. *Science* 293, 1074–1080.

Jenuwein, T., Laible, G., Dorn, R., and Reuter, G. (1998). SET domain proteins modulate chromatin domains in eu- and heterochromatin. *Cell. Mol. Life Sci.* 54, 80–93. doi: 10.1007/s000180050127

Jiang, H., Moreno-Romero, J., Santos-Gonzalez, J., De Jaeger, G., Gevaert, K., Van De Slijke, E., et al. (2017). Ectopic application of the repressive histone modification H3K9me2 establishes post-zygotic reproductive isolation in *Arabidopsis thaliana*. *Genes Dev.* 31, 1272–1287. doi: 10.1101/gad.299347.117

Jing, Y., Sun, H., Yuan, W., Wang, Y., Li, Q., Liu, Y., et al. (2016). SUVH2 and SUVH9 couple two essential steps for transcriptional gene silencing in *Arabidopsis*. *Mol. Plant* 9, 1156–1167. doi: 10.1016/j.molp.2016.05.006

Johnson, L. M., Bostick, M., Zhang, X., Kraft, E., Henderson, I., Callis, J., et al. (2007). The SRA methyl-cytosine-binding domain links DNA and histone methylation. *Curr. Biol.* 17, 379–384. doi: 10.1016/j.cub.2007.01.009

Johnson, L. M., Du, J., Hale, C. J., Bischof, S., Feng, S., Chodavarapu, R. K., et al. (2014). SRA- and SET-domain-containing proteins link RNA polymerase V occupancy to DNA methylation. *Nature* 507, 124–128. doi: 10.1038/nature12931

Johnson, L. M., Law, J. A., Khattar, A., Henderson, I. R., and Jacobsen, S. E. (2008). SRA-domain proteins required for DRM2-mediated de novo DNA methylation. *PLoS Genet.* 4:e1000280. doi: 10.1371/journal.pgen.1000280

Kim, K. C., and Huang, S. (2003). Histone methyltransferases in tumor suppression. *Cancer Biol. Ther.* 2, 491–499.

Klosinska, M., Picard, C. L., and Gehring, M. (2016). Conserved imprinting associated with unique epigenetic signatures in the Arabidopsis genus. *Nat. Plants* 2:16145. doi: 10.1038/nplants.2016.145

Koornneef, M., Bentsink, L., and Hilhorst, H. (2002). Seed dormancy and germination. *Curr. Opin. Plant Biol.* 5, 33–36.

Kradolfer, D., Wolff, P., Jiang, H., Siretskiy, A., and Kohler, C. (2013). An imprinted gene underlies postzygotic reproductive isolation in *Arabidopsis thaliana*. *Dev. Cell* 26, 525–535. doi: 10.1016/j.devcel.2013.08.006

Kramer, J. M. (2016). Regulation of cell differentiation and function by the euchromatin histone methyltranserfases G9a and GLP. *Biochem. Cell Biol.* 94, 26–32. doi: 10.1139/bcb-2015-0017

Larson, A. G., Elnatan, D., Keenen, M. M., Trnka, M. J., Johnston, J. B., Burlingame, A. L., et al. (2017). Liquid droplet formation by HP1alpha suggests a role for phase separation in heterochromatin. *Nature* 547, 236–240. doi: 10.1038/nature22822

Law, J. A., Du, J. M., Hale, C. J., Feng, S. H., Krajewski, K., Palanca, A. M. S., et al. (2013). Polymerase IV occupancy at RNA-directed DNA methylation sites requires SHH1. *Nature* 498, 385–389. doi: 10.1038/nature12178

Lei, L., Zhou, S. L., Ma, H., and Zhang, L. S. (2012). Expansion and diversification of the SET domain gene family following whole-genome duplications in *Populus trichocarpa*. *BMC Evol. Biol.* 12:51. doi: 10.1186/1471-2148-12-51

Leung, D. C., Dong, K. B., Maksakova, I. A., Goyal, P., Appanah, R., Lee, S., et al. (2011). Lysine methyltransferase G9a is required for de novo DNA methylation and the establishment, but not the maintenance, of proviral silencing. *Proc. Natl. Acad. Sci. U.S.A.* 108, 5718–5723. doi: 10.1073/pnas.1014660108

Li, G., Ji, T., Chen, J., Fu, Y., Hou, L., Feng, Y., et al. (2017). CRL4(DCAF8) ubiquitin ligase targets histone H3K79 and promotes H3K9 methylation in the liver. *Cell Rep.* 18, 1499–1511. doi: 10.1016/j.celrep.2017.01.039

Li, X., Harris, C. J., Zhong, Z., Chen, W., Liu, R., Jia, B., et al. (2018). Mechanistic insights into plant SUVH family H3K9 methyltransferases and their binding to context-biased non-CG DNA methylation. *Proc. Natl. Acad. Sci. U.S.A.* 115, E8793–E8802. doi: 10.1073/pnas.1809841115

Li, Y. H., Kirschmann, D. A., and Wallrath, L. L. (2002). Does heterochromatin protein 1 always follow code? *Proc. Natl. Acad. Sci. U.S.A.* 99, 16462–16469. doi: 10.1073/pnas.162371699

Lindroth, A. M., Cao, X., Jackson, J. P., Zilberman, D., Mccallum, C. M., Henikoff, S., et al. (2001). Requirement of CHROMOMETHYLASE3 for maintenance of CpXpG methylation. *Science* 292, 2077–2080. doi: 10.1126/science.1059745

Liu, C., Yu, Y., Liu, F., Wei, X., Wrobel, J. A., Gunawardena, H. P., et al. (2014). A chromatin activity-based chemoproteomic approach reveals a transcriptional repressome for gene-specific silencing. *Nat. Commun.* 5:5733. doi: 10.1038/ncomms6733

Liu, X., Yang, S., Zhao, M., Luo, M., Yu, C. W., Chen, C. Y., et al. (2014). Transcriptional repression by histone deacetylases in plants. *Mol. Plant* 7, 764–772. doi: 10.1093/mp/ssu033

Liu, Z. W., Shao, C. R., Zhang, C. J., Zhou, J. X., Zhang, S. W., Li, L., et al. (2014). The SET domain proteins SUVH2 and SUVH9 are required for Pol V Occupancy at RNA-Directed DNA methylation loci. *PLoS Genet.* 10:e1003948. doi: 10.1371/journal.pgen.1003948

Lu, F. L., Cui, X., Zhang, S. B., Jenuwein, T., and Cao, X. F. (2011). Arabidopsis REF6 is a histone H3 lysine 27 demethylase. *Nat. Genet.* 43, 715–719. doi: 10.1038/ng.854

Moreno-Romero, J., Del Toro-De Leon, G., Yadav, V. K., Santos-Gonzalez, J., and Kohler, C. (2019). Epigenetic signatures associated with imprinted paternally expressed genes in the Arabidopsis endosperm. *Genome Biol.* 20:41. doi: 10.1186/s13059-019-1652-0

Nakayama, J., Rice, J. C., Strahl, B. D., Allis, C. D., and Grewal, S. I. (2001). Role of histone H3 lysine 9 methylation in epigenetic control of heterochromatin assembly. *Science* 292, 110–113. doi: 10.1126/science.1060118

Naumann, K., Fischer, A., Hofmann, I., Krauss, V., Phalke, S., Irmler, K., et al. (2005). Pivotal role of AtSUVH2 in heterochromatic histone methylation and gene silencing in *Arabidopsis*. *EMBO J.* 24, 1418–1429. doi: 10.1038/sj.emboj.7600604

Peters, A. H., Kubicek, S., Mechtler, K., O'sullivan, R. J., Derijck, A. A., Perez-Burgos, L., et al. (2003). Partitioning and plasticity of repressive histone methylation states in mammalian chromatin. *Mol. Cell* 12, 1577–1589. doi: 10.1016/s1097-2765(03)00477-5

Rice, J. C., Briggs, S. D., Ueberheide, B., Barber, C. M., Shabanowitz, J., Hunt, D. F., et al. (2003). Histone methyltransferases direct different degrees of methylation to define distinct chromatin domains. *Mol. Cell* 12, 1591–1598. doi: 10.1016/s1097-2765(03)00479-9

Roudier, F., Teixeira, F. K., and Colot, V. (2009). Chromatin indexing in Arabidopsis: an epigenomic tale of tails and more. *Trends Genet.* 25, 511–517. doi: 10.1016/j.tig.2009.09.013

Saksouk, N., Simboeck, E., and Dejardin, J. (2015). Constitutive heterochromatin formation and transcription in mammals. *Epigenet. Chromatin* 8:3. doi: 10.1186/1756-8935-8-3

Schatlowski, N., and Kohler, C. (2012). Tearing down barriers: understanding the molecular mechanisms of interploidy hybridizations. *J. Exp. Bot.* 63, 6059–6067. doi: 10.1093/jxb/ers288

Scheer, S., and Zaph, C. (2017). The lysine methyltransferase G9a in immune cell differentiation and function. *Front. Immunol.* 8:429. doi: 10.3389/fimmu.2017.00429

Shin, J. H., Wang, H. L., Lee, J., Dinwiddie, B. L., Belostotsky, D. A., and Chekanova, J. A. (2013). The role of the Arabidopsis Exosome in siRNA-independent silencing of heterochromatic loci. *PLoS Genet.* 9:e1003411. doi: 10.1371/journal.pgen.1003411

Shinkai, Y., and Tachibana, M. (2011). H3K9 methyltransferase G9a and the related molecule GLP. *Genes Dev.* 25, 781–788. doi: 10.1101/gad.2027411

Sims, R. J. III, Nishioka, K., and Reinberg, D. (2003). Histone lysine methylation: a signature for chromatin function. *Trends Genet.* 19, 629–639. doi: 10.1016/j.tig.2003.09.007

Strom, A. R., Emelyanov, A. V., Mir, M., Fyodorov, D. V., Darzacq, X., and Karpen, G. H. (2017). Phase separation drives heterochromatin domain formation. *Nature* 547, 241–245. doi: 10.1038/nature22989

Stroud, H., Do, T., Du, J., Zhong, X., Feng, S., Johnson, L., et al. (2014). Non-CG methylation patterns shape the epigenetic landscape in Arabidopsis. *Nat. Struct. Mol. Biol.* 21, 64–72. doi: 10.1038/nsmb.2735

Taagen, E., Bogdanove, A. J., and Sorrells, M. E. (2020). Counting on crossovers: controlled recombination for plant breeding. *Trends Plant Sci.* doi: 10.1016/j.tplants.2019.12.017 [Epub ahead of print]

Tamaru, H., and Selker, E. U. (2003). Synthesis of signals for de novo DNA methylation in *Neurospora crassa*. *Mol. Cell Biol.* 23, 2379–2394. doi: 10.1128/mcb.23.7.2379-2394.2003

Tetko, I. V., Haberer, G., Rudd, S., Meyers, B., Mewes, H. W., and Mayer, K. F. (2006). Spatiotemporal expression control correlates with intragenic scaffold

matrix attachment regions (S/MARs) in *Arabidopsis thaliana*. *PLoS Comput. Biol.* 2:e21. doi: 10.1371/journal.pcbi.0020021

Thorstensen, T., Fischer, A., Sandvik, S. V., Johnsen, S. S., Grini, P. E., Reuter, G., et al. (2006). The Arabidopsis SUVR4 protein is a nucleolar histone methyltransferase with preference for monomethylated H3K9. *Nucleic Acids Res.* 34, 5461–5470. doi: 10.1093/nar/gkl687

Trojer, P., and Reinberg, D. (2007). Facultative heterochromatin: Is there a distinctive molecular signature? *Mol. Cell* 28, 1–13. doi: 10.1016/j.molcel.2007.09.011

Turck, F., Roudier, F., Farrona, S., Martin-Magniette, M. L., Guillaume, E., Buisine, N., et al. (2007). Arabidopsis TFL2/LHP1 specifically associates with genes marked by trimethylation of histone H3 lysine 27. *PLoS Genet.* 3:e86. doi: 10.1371/journal.pgen.0030086

Underwood, C. J., Choi, K., Lambing, C., Zhao, X., Serra, H., Borges, F., et al. (2018). Epigenetic activation of meiotic recombination near *Arabidopsis thaliana* centromeres via loss of H3K9me2 and non-CG DNA methylation. *Genome Res.* 28, 519–531. doi: 10.1101/gr.227116.117

Vaute, O., Nicolas, E., Vandel, L., and Trouche, D. (2002). Functional and physical interaction between the histone methyl transferase Suv39H1 and histone deacetylases. *Nucleic Acids Res.* 30, 475–481. doi: 10.1093/nar/30.2.475

Veiseth, S. V., Rahman, M. A., Yap, K. L., Fischer, A., Egge-Jacobsen, W., Reuter, G., et al. (2011). The SUVR4 histone lysine methyltransferase binds ubiquitin and converts H3K9me1 to H3K9me3 on transposon chromatin in Arabidopsis. *PLoS Genet.* 7:e1001325. doi: 10.1371/journal.pgen.1001325

Wang, J., Blevins, T., Podicheti, R., Haag, J. R., Tan, E. H., Wang, F., et al. (2017). Mutation of Arabidopsis SMC4 identifies condensin as a corepressor of pericentromeric transposons and conditionally expressed genes. *Genes Dev.* 31, 1601–1614. doi: 10.1101/gad.301499.117

Wierzbicki, A. T., Haag, J. R., and Pikaard, C. S. (2008). Noncoding transcription by RNA Polymerase Pol IVb/Pol V mediates transcriptional silencing of overlapping and adjacent genes. *Cell* 135, 635–648. doi: 10.1016/j.cell.2008.09.035

Wolff, P., Jiang, H., Wang, G., Santos-Gonzalez, J., and Kohler, C. (2015). Paternally expressed imprinted genes establish postzygotic hybridization barriers in *Arabidopsis thaliana*. *eLife* 4:e10074. doi: 10.7554/eLife.10074

Wolff, P., Weinhofer, I., Seguin, J., Roszak, P., Beisel, C., Donoghue, M. T., et al. (2011). High-resolution analysis of parent-of-origin allelic expression in the Arabidopsis Endosperm. *PLoS Genet.* 7:e1002126. doi: 10.1371/journal.pgen.1002126

Wu, H., Min, J., Lunin, V. V., Antoshenko, T., Dombrovski, L., Zeng, H., et al. (2010). Structural biology of human H3K9 methyltransferases. *PLoS One* 5:e8570. doi: 10.1371/journal.pone.0008570

Xiao, C., Chen, F., Yu, X., Lin, C., and Fu, Y. F. (2009). Over-expression of an AT-hook gene, AHL22, delays flowering and inhibits the elongation of the hypocotyl in *Arabidopsis thaliana*. *Plant Mol. Biol.* 71, 39–50. doi: 10.1007/s11103-009-9507-9

Xiao, X., Zhang, J., Li, T., Fu, X., Satheesh, V., Niu, Q., et al. (2019). A group of SUVH methyl-DNA binding proteins regulate expression of the DNA demethylase ROS1 in *Arabidopsis*. *J. Integr. Plant Biol.* 61, 110–119. doi: 10.1111/jipb.12768

Xu, Y. F., Wang, Y. Z., Stroud, H., Gu, X. F., Sun, B., Gan, E. S., et al. (2013). A matrix protein silences transposons and repeats through interaction with retinoblastoma-associated proteins. *Curr. Biol.* 23, 345–350. doi: 10.1016/j.cub.2013.01.030

Yoshida, K., Maekawa, T., Zhu, Y., Renard-Guillet, C., Chatton, B., Inoue, K., et al. (2015). The transcription factor ATF7 mediates lipopolysaccharide-induced epigenetic changes in macrophages involved in innate immunological memory. *Nat. Immunol.* 16, 1034–1043. doi: 10.1038/ni.3257

Yu, C. W., Tai, R., Wang, S. C., Yang, P., Luo, M., Yang, S., et al. (2017). HISTONE DEACETYLASE6 acts in concert with histone methyltransferases SUVH4, SUVH5, and SUVH6 to regulate transposon silencing. *Plant Cell* 29, 1970–1983. doi: 10.1105/tpc.16.00570

Yun, J., Kim, Y. S., Jung, J. H., Seo, P. J., and Park, C. M. (2012). The AT-hook motif-containing protein AHL22 regulates flowering initiation by modifying *FLOWERING LOCUS T* chromatin in *Arabidopsis*. *J. Biol. Chem.* 287, 15307–15316. doi: 10.1074/jbc.M111.318477

Zemach, A., Kim, M. Y., Hsieh, P. H., Coleman-Derr, D., Eshed-Williams, L., Thao, K., et al. (2013). The Arabidopsis nucleosome remodeler DDM1 allows DNA methyltransferases to access H1-containing heterochromatin. *Cell* 153, 193–205. doi: 10.1016/j.cell.2013.02.033

Zeng, W., Ball, A. R. Jr., and Yokomori, K. (2010). HP1: heterochromatin binding proteins working the genome. *Epigenetics* 5, 287–292. doi: 10.4161/epi.5.4.11683

Zhang, C., Du, X., Tang, K., Yang, Z., Pan, L., Zhu, P., et al. (2018). Arabidopsis AGDP1 links H3K9me2 to DNA methylation in heterochromatin. *Nat. Commun.* 9:4547. doi: 10.1038/s41467-018-06965-w

Zhang, L. S., and Ma, H. (2012). Complex evolutionary history and diverse domain organization of SET proteins suggest divergent regulatory interactions. *New Phytol.* 195, 248–263. doi: 10.1111/j.1469-8137.2012.04143.x

Zhang, Y., Harris, C. J., Liu, Q., Liu, W., Ausin, I., Long, Y., et al. (2018). Large-scale comparative epigenomics reveals hierarchical regulation of non-CG methylation in *Arabidopsis*. *Proc. Natl. Acad. Sci. U.S.A.* 115, E1069–E1074. doi: 10.1073/pnas.1716300115

Zhao, J. F., Favero, D. S., Qiu, J. W., Roalson, E. H., and Neff, M. M. (2014). Insights into the evolution and diversification of the AT-hook Motif Nuclear Localized gene family in land plants. *BMC Plant Biol.* 14:266. doi: 10.1186/s12870-014-0266-7

Zhao, S., Cheng, L., Gao, Y., Zhang, B., Zheng, X., Wang, L., et al. (2019). Plant HP1 protein ADCP1 links multivalent H3K9 methylation readout to heterochromatin formation. *Cell Res.* 29, 54–66. doi: 10.1038/s41422-018-0104-9

Zheng, B., Wang, Z., Li, S., Yu, B., Liu, J. Y., and Chen, X. (2009). Intergenic transcription by RNA polymerase II coordinates Pol IV and Pol V in siRNA-directed transcriptional gene silencing in *Arabidopsis*. *Genes Dev.* 23, 2850–2860. doi: 10.1101/gad.1868009

Zheng, J., Chen, F., Wang, Z., Cao, H., Li, X., Deng, X., et al. (2012). A novel role for histone methyltransferase KYP/SUVH4 in the control of Arabidopsis primary seed dormancy. *New Phytol.* 193, 605–616. doi: 10.1111/j.1469-8137.2011.03969.x

Zhou, J., Wang, X., He, K., Charron, J. B., Elling, A. A., and Deng, X. W. (2010). Genome-wide profiling of histone H3 lysine 9 acetylation and dimethylation in Arabidopsis reveals correlation between multiple histone marks and gene expression. *Plant Mol. Biol.* 72, 585–595. doi: 10.1007/s11103-009-9594-7

Conflict of Interest: The authors declare that the research was conducted in the absence of any commercial or financial relationships that could be construed as a potential conflict of interest.

frontiers in Plant Science

ORIGINAL RESEARCH
published: 20 August 2020
doi: 10.3389/fpls.2020.01254

Application of Aptamers Improves CRISPR-Based Live Imaging of Plant Telomeres

Solmaz Khosravi[1], *Patrick Schindele*[2], *Evgeny Gladilin*[1], *Frank Dunemann*[3], *Twan Rutten*[1], *Holger Puchta*[2]* *and Andreas Houben*[1]*

[1] Department for Breeding Research, Leibniz Institute of Plant Genetics and Crop Plant Research (IPK), Seeland, Germany, [2] Botanical Institute, Karlsruhe Institute of Technology, Karlsruhe, Germany, [3] Institute for Breeding Research on Horticultural Crops, Julius Kühn-Institut (JKI), Quedlinburg, Germany

Development of live imaging techniques for providing information how chromatin is organized in living cells is pivotal to decipher the regulation of biological processes. Here, we demonstrate the improvement of a live imaging technique based on CRISPR/Cas9. In this approach, the sgRNA scaffold is fused to RNA aptamers including MS2 and PP7. When the dead Cas9 (dCas9) is co-expressed with chimeric sgRNA, the fluorescent coat protein-tagged for MS2 and PP7 aptamers (tdMCP-FP and tdPCP-FP) are recruited to the targeted sequence. Compared to previous work with dCas9:GFP, we show that the quality of telomere labeling was improved in transiently transformed *Nicotiana benthamiana* using aptamer-based CRISPR-imaging constructs. Labeling is influenced by the copy number of aptamers and less by the promoter types. The same constructs were not applicable for labeling of repeats in stably transformed plants and roots. The constant interaction of the RNP complex with its target DNA might interfere with cellular processes.

Keywords: aptamer, CRISPR/dCas9, live imaging, *N. benthamiana*, R-loops, telomere

OPEN ACCESS

Edited by:
Iva Mozgova, Academy of Sciences of the Czech Republic (ASCR), Czechia

Reviewed by:
Martina Dvorackova, Central European Institute of Technology (CEITEC), Czechia
Sachihiro Matsunaga, The University of Tokyo, Japan

***Correspondence:**
Holger Puchta
holger.puchta@kit.edu
Andreas Houben
houben@ipk-gatersleben.de

Specialty section:
This article was submitted to Plant Cell Biology, a section of the journal Frontiers in Plant Science

Received: *03 June 2020*
Accepted: *30 July 2020*
Published: *20 August 2020*

Citation:
Khosravi S, Schindele P, Gladilin E, Dunemann F, Rutten T, Puchta H and Houben A (2020) Application of Aptamers Improves CRISPR-Based Live Imaging of Plant Telomeres. Front. Plant Sci. 11:1254. doi: 10.3389/fpls.2020.01254

INTRODUCTION

The 3D organization of the genome is involved in the regulation of various genomic functions including gene expression, transcription, DNA replication, and repair (Misteli, 2007). Different strategies have been developed to monitor the dynamics of defined genomic loci in living cells (Robinett et al., 1996; Lindhout et al., 2007; Chen et al., 2013; Saad et al., 2014; Fujimoto et al., 2016). Most recently, the clustered regularly interspaced short palindromic repeats (CRISPR)/CRISPR associated protein 9 (Cas9) based strategy has extensively been used mostly in non-plant species for live imaging. The first applications of CRISPR/Cas for live-cell imaging in plant (Dreissig et al., 2017; Fujimoto and Matsunaga, 2017) and non-plant cells (Chen et al., 2013) was based on fluorescent proteins directly fused to deactivated Cas9 (dCas9). Different dCas9 orthologues from *Streptococcus pyogenes* and *Staphylococcus aureus* successfully label telomeres in transiently transformed *Nicotiana benthamiana* leaves (Dreissig et al., 2017; Fujimoto and Matsunaga, 2017). Accordingly, it was shown that the locations of telomeres are in the periphery of the nucleus and dynamic positional changes of telomeres up to ± 2 μm were reported (Dreissig et al., 2017).

Indirect labeling of dCas9 with the SunTag method resulted in 19 fold brighter signals in mammalian cell cultures in comparison to GFP-fused dCas9 (Tanenbaum et al., 2014). However, this method like directly labeled dCas9 does not have the possibility of multi-targeting of genomic regions. For this purpose, different variants of dCas9 which have specific cognate gRNA were combined to label different genomic regions (Esvelt et al., 2013; Ma et al., 2015; Dreissig et al., 2017). To improve the efficiency of imaging and also the capacity of dCas9 for multi-targeting of different regions at the same time, other methods for indirect labeling of dCas9 were adapted including BIFC (Tanenbaum et al., 2014; Hong et al., 2018), Aio-Casilio (Zhang and Song, 2017) and RNA-aptamer-based methods (Fu et al., 2016; Ma et al., 2016; Shao et al., 2016; Wang et al., 2016; Qin et al., 2017). CRISPR-based live-cell imaging methods are reviewed in (Wu et al., 2019; Khosravi et al., 2020).

Among the improved indirect labeling methods, aptamer-based methods are used in mammalian cell cultures to target telomeric and other genomic regions. Aptamers are short RNA oligos which can be detected by specific RNA binding proteins (Urbanek et al., 2014). Aptamer-based imaging methods are based on three components including dCas9, sgRNA in which the aptamer sequence is integrated and the aptamer binding protein which is fused to the fluorescent protein (Fu et al., 2016; Ma et al., 2016; Shao et al., 2016). In plants, aptamers have been used for CRISPR/Cas9 targeted gene regulation with effector proteins like transcription activation domains, acetyltransferase or methyltransferase which were fused to the aptamer binding protein (Lee et al., 2019; Selma et al., 2019). The copy number of aptamers determines the number of effector proteins enriched in the targeted region. However, no application of CRISPR live-cell imaging based on aptamers is reported in plants yet.

In this research, we developed a CRISPR life imaging method based on the application of MS2 and PP7 aptamers for targeting telomeres in transiently transformed *N. benthamiana*. We investigate whether the copy number of aptamers, sgRNA scaffold changes and promoter type affect labeling efficiency of target sequences. However, the same method was not successful for constant labeling of chromosome regions in stably transformed plants (*N. benthamiana* and *A. thaliana*) and roots (*Daucus carota*), suggesting that a continuous interaction of the RNP complex with target sequences might interfere with the progression of the cell cycle and plant development.

MATERIALS AND METHODS

Plasmid Construction

Expression of dCas9 Driven by Different Promoters

To establish a three-component aptamer-based labeling method, dCas9 under the control of a ubiquitin parsley promoter was indirectly labeled with aptamer binding proteins (MS2 or PP7) fused to fluorescent proteins. The 35S promoter was amplified with *Eco*RI-35S-f1 and r1 primers flanking with an *Eco*RI recognition site from pCCNCEN using Q5 DNA polymerase under following conditions: 98°C for 2 min, 30x (98°C for 10 s, 58°C for 30 s, 72°C for 30 s) and 72°C for 2 min. (**Supplementary Table 1**). Then it was digested with *Eco*RI and cloned to linearized pDe-Sp-dCas9 GentR with *Eco*RI, which had another *Eco*RI site in the backbone and was removed in advance by site-directed mutation. The same method was used for substitution of the ubiquitin parsley promoter with a RPS5A promoter. The isolation of RPS5A was done by PRS5A-FWD and REV primers from the pGPTV-BAR using Q5 DNA polymerase under following conditions: 98°C for 2 min, 30x (98°C for 10 s, 59°C for 30 s, 72°C for 40 s) and 72°C for 2 min (**Supplementary Table 1**). The XVE inducible promoter was generated with primers (Cas9-XVE-F and XVE-Lexa-A-R; XVE-Lexa-A-F and LexA-Cas9-R (**Supplementary Table 1**) containing homologous flanks for further Gibson Assembly into the pDe-Sp-dCas9 GentR. Following PCR conditions was used for amplification with XVE-Lexa-A-F and LexA-Cas9-R primers: 98°C for 2 min, 30x (98°C for 10 s, 65°C for 30 s, 72°C for 20 s) and 72°C for 2 min. For amplification with Cas9-XVE-F and XVE-Lexa-A-R primers, the same conditions were used except the extension time which was increased to 2 min. The pER8-v3 plasmid was used for generation of the XVE inducible promoter (Zuo et al., 2000) (**Supplementary Table 1**). According to (Dreissig et al., 2017), a pChimera expression gRNA vector in combination with a dCas9-eGFP expression vector was used as a control vector to target telomeres.

Insertion of Aptamer Sequences Into the sgRNA Scaffold

For aptamer-mediated imaging, sgRNA expression vectors were created either harbouring one MS2 aptamer sequence each in the tetraloop and stem-loop 2 of the *S. pyogenes* sgRNA backbone (Konermann et al., 2015) or three PP7 aptamer sequences only in the tetraloop of the *S. pyogenes* sgRNA backbone additionally comprising an A-U pair flip and stem extension (Shechner et al., 2015). In case of MS2, the vector pDS2.0-MS2 was synthesized comprising the respective sgRNA under control of the AtU6-26 promoter together with the codon-optimized MS2 binding protein cds joined to a 3′ SV40 NLS by a 3x GGGGS linker under control of the ZmUbi-1 promoter. In case of PP7, the respective sgRNA and codon-optimized PP7 binding protein cds also harboring a 3′ SV40 NLS were synthesized and subcloned *via* restriction digestion and ligation into pDS2.0-MS2 creating pDS2.0-PP7. *Bsm*BI restriction sites downstream of the aptamer binding protein cds were used for in-frame cloning of a 3-fold fusion of either eGFP or mRuby2. For this purpose, the respective cds were amplified from pSIM24-eGFP and pcDNA3-mRuby2 (www.addgene.com) with primers (MS2(NLS)-GFP#1-f, GFP#1-linker1-r, linker1-GFP#2-f, GFP#2-linker2-r, linker2-GFP#3-f, GFP#3-nos_ter-r or MS2(NLS)-mRuby#1-f, mRuby#1-linker1-r, linker1-mRuby#2-f, mRuby#2-linker2-r, linker2-mRuby#3-f, mRuby#3-nos_ter-r) adding homologous flanks for subsequent Gibson Assembly into the linearized pDS2.0-MS2 or pDS2.0-PP7 similar as previously described (Dreissig et al., 2017) creating pDS2.0-MS2/PP7-3xeGFP/3xmRuby2 (**Supplementary Table 1**).

Changing the sgRNA Scaffold

An MS2 aptamer-harboring sgRNA additionally comprising an A-U flip and stem extension (Chen et al., 2013) was synthesized and subcloned into pDS2.0-MS2-eGFP/mRuby2. For this purpose, pDS2.0-MS2-eGFP/mRuby2 was amplified with primers (pDS2.0-ΔsgRNA-r, pDS2.0-ΔsgRNA-f) deleting the sgRNA and the synthesized sgRNA was amplified with primers (sgRNA2.0-MS2-flip/ext-f, sgRNA2.0-MS2-flip/ext-r) adding overhangs for subsequent Gibson Assembly into the linearized backbone (**Supplementary Table 1**).

Altering the Copy Number of Aptamers

To change the copy number of aptamers, pDS.2.0-MS2+3xeGFP gRNA expression vector was used. To delete one of MS2 copy numbers, pDS.2.0-MS2+3xeGFP was double digested with *Age*I and *Msc*I restriction enzymes and then was ligated to annealed primers Apta2-FWD and Apta2-Rev flanked by *Age*I overhang (**Supplementary Table 1**). Annealing of primers was done by mixing 2 µl of each primer (100 pM) in the total volume of 50 µl double distilled water and incubation at 95°C. Colony PCR was performed by SS42 and Apta2-Rev2 primers under following conditions: 95°C for 5 min, 30x (95°C for 30 s, 58°C for 30 s, 72°C for 30 s), 72°C 5 min. Positive clones were confirmed by sequencing with the SS42 primer (**Supplementary Table 1**). To increase the copy number of aptamer sequences, a pDS2.0-MS2-eGFP/mRuby2 sgRNA expression vector was used. First, according to Qin et al., 2017 a sgRNA scaffold harbouring 16 MS2 aptamers was synthesized and subcloned into pDS2.0-MS2-eGFP/mRuby2. For this purpose, pDS2.0-MS2-eGFP/mRuby2 was digested with *Bsm*BI and *Age*I for sgRNA deletion and the synthesized sgRNA was digested with *Bsa*I and *Age*I for subsequent ligation into the linearized pDS2.0-MS2-eGFP/mRuby2 creating pDS2.0-16xMS2-eGFP/mRuby2.

Designing Protospacers for Targeting Different Genomic Regions

The protospacer design was performed with the help of DeskGen (https://www.deskgen.com/). Each protospacer sequence was selected based on the PAM sequence of SpCas9 and synthesized as primer oligos with appropriate overhangs at 5' ends for cloning into the pDS2.0-MS2:3xeGFP/mRuby (**Supplementary Table 1**). Then, the pDS2.0-MS2:3xeGFP/mRuby was subcloned to dCas9 expression vector by Gateway cloning. The dCas9 expression vector carries a gentamycin resistant marker for selection of stably transformed plants. The telomere protospacer was designed based on *Arabidopsis*-type telomere repeat sequence 5′-(TTTAGGG)(n)-3′. *Arabidopsis*-type centromere-specific protospacers were designed based on centromeric satellite consensus sequences (**Supplementary Table 1**).

Plant Material and Transformation

All imaging constructs were separately transformed to *Agrobacterium tumefaciens* GV3101. For carrot transformation, *A. rhizogenes* 15843 was used. Agrobacteria were cultured overnight at 28°C in LB medium containing spectinomycin (100 mg/l^{-1}) and rifampicin (50 mg/l^{-1}) for transient transformation of *N. benthamiana* according to (Phan and Conrad, 2016). Additionally, a *N. benthamiana* line expressing CFP-histone H2B was used (Martin et al., 2009). For the telomeric repeat binding protein 1 fused to GFP (TRB1-GFP), Agrobacteria were cultured in LB medium containing kanamycin (100 mg/l^{-1}) and rifampicin (50 mg/l^{-1}) (Schrumpfová et al., 2014). For co-transformation experiments, bacterial cultures with the same OD_{600} (0.5) were mixed in a 1:1 ratio. Stable transformation of *N. benthamiana*, *D. carota* (cultivars Blanche, Yellowstone and Rotin) and *A. thaliana* (var. Columbia) with dCas9:2xMS2:GFP constructs were performed *via* leaf samples, *A. rhizogenes*-based hairy root transformation and floral dip method according to (Clemente, 2006), (Dunemann et al., 2019) and (Martin et al., 2009), respectively. PCR (95°C for 5 min, 30x (95°C for 30 s, 58°C for 30 s, 72°C for 30 s), 72°C for 5 min) and real-time PCR (95°C for 10 min, 40x(95°C for 10 s, 60°C for 1 min) and melt curve stage of 95°C for 30 s, 60°C for 15 s) were performed for putative transgenic plants using primers specific for dCas9 and GFP to confirm the presence and expression of T-DNA fragments (**Supplementary Table 1**).

Immunostaining and Fluorescence *In Situ* Hybridization (FISH)

Sampling for immunostaining was performed three days after infiltration of *N. benthamiana*. Briefly, a piece of leaf tissue with the size of ~1 cm^2 was excised and chopped in 0.5 ml chromosome isolation buffer (Doležel et al., 2007) and then filtrated through a 35 µm nylon mesh with subsequent centrifugation onto microscopic slides with a CytoSpin3 (Shandon) at 400 rpm for 5 min. To confirm the specificity of signals CRISPR imaging and FISH were combined. The intensity of CRISPR signals was increased by in direct immunostaining using a 1:2,500 diluted Dylight 488-labeled GFP mouse monoclonal antibody (cat. 200-341-215, Rockland) according to (Ishii et al., 2015). Detection of *Arabidopsis*-type telomeres *via* FISH was performed with a 5′Cy5-labeled probe (5′ GGGTTTAGGGTTTAGGGTTT). Immuno-FISH was performed as described by (Ishii et al., 2015). Immunostaining against dCas9, was performed with a DyLight 550-labeled SpCas9 mouse monoclonal antibody (cat. NBP2-52398R, Novus Biological).

Proteasome Inhibitor Test

The plants were kept on MS medium containing 50, 100, or 150 µM MG-132 (Serva) under dark condition at room temperature for 16 h.

Microscopy

Micrographs were captured using an epifluorescence microscope (Olympus BX61) equipped with a cooled charge coupled device (CCD) camera (Orca ER; Hamamatsu). Images were collected from at least 10 nuclei per experiment and then analyzed with ImageJ. For live-cell imaging, a confocal laser scanning microscope (LSM780, Carl Zeiss) was used. To detect fluorescence signals *in vivo*, a piece of infiltrated leaf was cut and with the use of 40x NA 1.2 water objective nuclei with clear signals were tracked for 20 min. 488-nm laser line was used for

excision of GFP and emission was detected over a range of 490–540 nm.

Statistics

For statistical analysis the program package SigmaStat 4.0 was used (Systat Software, Inc.; https://systatsoftware.com/). One-way ANOVA followed by pairwise comparison was used for more than two samples and two-tailed Student's t-test was used for comparison of two samples.

Analysis of Telomere Signals

To measure the labeling efficiency of telomeres, 20 nuclei were imaged for each construct by epifluorescent microscope. The number of telomere signals per nucleus was determined and the mean value was calculated. To evaluate the signal/background noise, the maximum signal intensity was divided by minimum signal intensity rising from the background using the ImageJ software. The mean value was calculated from three measurements in each nucleus.

To study the movement of telomeres, telomere tracking was performed for 5 nuclei and was based on time-laps z stacks from IMARIS 8.0 (Bitplane). The adjustments to calculate the coordinates (x, y, z) of each telomere and also measuring the inter-telomere distances was based on Dreissig et al. (2017). To assess true displacements of telomeres over time, global movements of nuclei have to be computationally eliminated. For this purpose, 3D point clouds of telomere mass centres for all subsequent time steps ($t>0$) were rigidly registered to the reference system of coordinates defined by the first time step ($t=0$) using absolute orientation quaternions (Horn, 1987). To quantify the intranuclear telomere motion, the mean square distance (MSD) of telomeres relatively to their initial position (t=0) was calculated as

$$MSD(t) = \frac{1}{N}\sum_{i=1}^{N}(R_i(t) - R_i(0))^2 \qquad \text{Eq. 1}$$

where $R_i(t)$ is the radius vector of the i-th registered telomere in the reference system of coordinates at the time point $t>0$.

RESULTS

Optimizing Live Imaging of Telomeres With Aptamer-Based CRISPR/dCas9 Imaging Vectors

The application of fluorescent proteins directly fused to dCas9 resulted in the labeling of ~27 telomeres of 72 expected signals in 2C nuclei of *N. benthamiana* (Dreissig et al., 2017). To improve the labeling efficiency, we established RNA aptamer-based CRISPR/dCas9 imaging constructs for plants. The three-component constructs (called dCas9:2xMS2:GFP and dCas9:3xPP7:GFP) encode dCas9 of *S. pyogenes*, an *Arabidopsis* telomere-specific sgRNA with integrated aptamer sequences (2x MS2 or 3x PP7) and aptamer coat proteins fused to three copies of fluorescent proteins (tdMCP : GFP or tdPCP : GFP binding to MS2 or PP7 aptamers, respectively) (**Figures 1A, B**). In addition, a dCas9:2xMS2 construct with a 3x mRuby-tagged coat protein (called dCas9:2xMS2:mRuby) was prepared (**Supplementary Figure S1**).

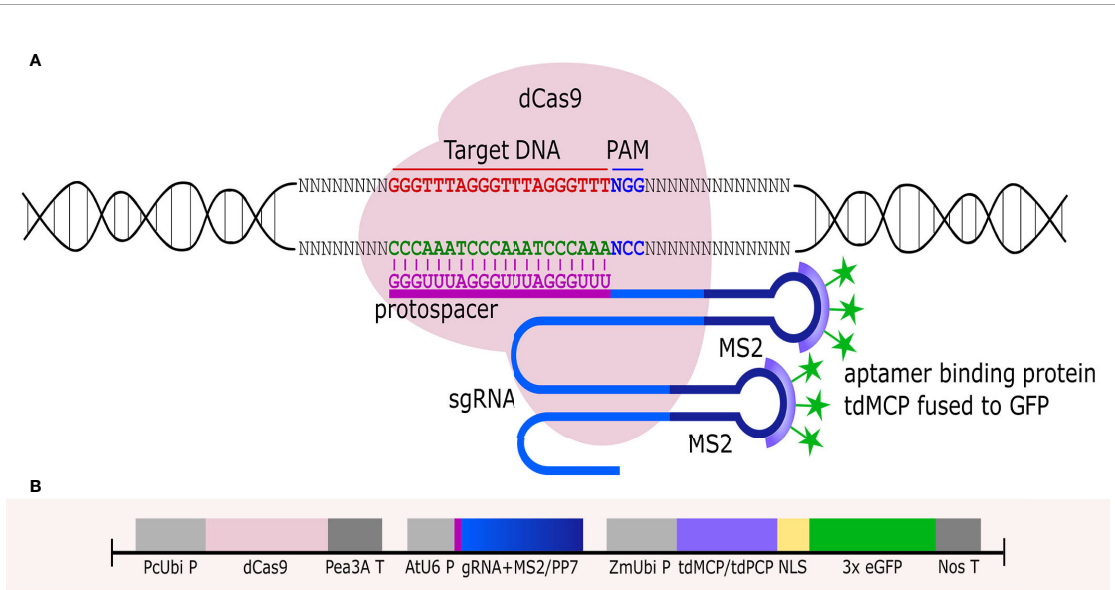

FIGURE 1 | RNA aptamer-based CRISPR/dCas9 imaging of telomere repeats. **(A)** Schemata depicting the components of the aptamer-based CRISPR labeling method: (1) dCas9 from *S. pyogenes*, (2) MS2 or PP7 aptamers (here only MS2 is shown) which are integrated into the sgRNA scaffold. (3) RNA binding protein (tdMCP or tdPCP) fused to fluorescent protein (3x eGFP) which recognizes aptamers. Protospacer designed to target *Arabidopsis*-type telomere DNA sequence. **(B)** Structure of the aptamer-based CRISPR imaging construct. dCas9 is driven by a ubiquitin promoter from parsley (PcUbi P), chimeric gRNA including aptamers (MS2/PP7) are driven by the AtU6 promoter (AtU6 P), aptamer binding proteins fused to a fluorescent protein (tdMCP/tdPCP) with the help of nuclear localization signal (NLS) are driven by a ubiquitin promoter from maize (ZmUbi P). Pea3A T and Nos T were used as terminators.

To compare the labeling efficiency of the newly designed constructs, *N. benthamiana* leaves were separately infiltered with both types of *Arabidopsis*-type telomere-specific dCas9-aptamer constructs (dCas9:2xMS2:GFP and dCas9:3xPP7:GFP) and the previously employed dCas9:GFP reporter (Dreissig et al., 2017). Both types of aptamer-based constructs successfully labeled telomeres in interphase nuclei (**Figures 2B, C**). In average, 48 and 37 signals were recognized by dCas9-2xMS2:GFP and dCas9-3xPP7:GFP, respectively (**Figure 2D**). In contrast, the application of dCas9:GFP resulted in ~28 CRISPR-based signals which is consistent with earlier research (Dreissig et al., 2017) (**Figures 2C, D**). The lower number of detected signals than the expected could be due to clustering of some telomeres or not all telomeres were detectable by the applied imaging constructs. Notably, the accumulation of GFP signals in the nucleolus, which was always observed by application of dCas9:GFP was not found in nuclei labeled with both types of dCas9-aptamer constructs (**Figures 2A–C**).

As a negative control, the transformation of *N. benthamiana* with partial constructs carrying dCas9:GFP without target-specific gRNA or pMS2:mRuby targeting telomeres without the dCas9 component was performed. For both, a nonspecific labeling of nuclei was found (**Figures 3A, B**). After co-transformation with both partial constructs, overlapping telomere-like signals of green and red fluorescence were found due to the presence of all components required for CRISPR imaging of telomeres (**Figure 3C**).

To confirm the target specificity of the observed telomere-like signals, FISH with a labeled telomere-specific probe was performed after CRISPR imaging. All dCas9:2xMS2:GFP signals co-localized with FISH signals, demonstrating the target specificity of the aptamer-based imaging approach (**Figure 4A**). However, the labeling efficiency of CRISPR was less than FISH as only 78% and 75% of FISH signals colocalized with dCas9:2xMS2:GFP and dCas9:3xPP7:GFP signals, respectively (**Figure 4B**). Co-expression of dCas9:2xMS2:mRuby with TRB1 and telomeric dCas9:2xMS2:GFP with CFP labeled histone H2B (Martin et al., 2009) showed that the aptamer-based CRISPR imaging method can also be successfully combined with fluorescence-labeled proteins to study DNA-protein interactions (**Supplementary Movies S1** and **S2**).

To test whether the copy number of aptamers affects the labeling efficiency, we compared dCas9:MS2:GFP carrying 1, 2, or 16 copies of the MS2 aptamer. By reducing the aptamer copy number to 1, the number of observed signals reduced (**Figure 5A**). 16 copies of MS2 did not result in enhanced telomere signals, instead strong background signals were produced (**Figure 5C**).

Because four sequential U nucleotides in the sgRNA stem-loop could be recognized as a transcription termination signal for the *A. thaliana* derived U6 pol-III promoter, a U to A substitution was performed and also the structure of sgRNA was changed by the insertion of an extension to improve the stability of sgRNA and its assembly with dCas9 according to (**Supplementary Figure S2**). The U/A flip along with increasing the length of the sgRNA stem size did not result in a significant increase of telomere signal intensity and did not improve the signal/background noise ratio of telomere signals in *N. benthamiana* (**Figures 6A–C**).

Comparing the Effect of Different Promoters to Express dCas9

Beside the ubiquitin promoter from parsley to drive the expression of dCas9 in *N. benthamiana*, we tested the cauliflower mosaic virus (CaMV) 35S (Tepfer et al., 2004), RPS5A (Weijers et al., 2001) and the β-estradiol inducible promoter XVE (Zuo et al., 2000). Changing the promoter in dCas9:2xMS2:GFP construct did not increase the number of

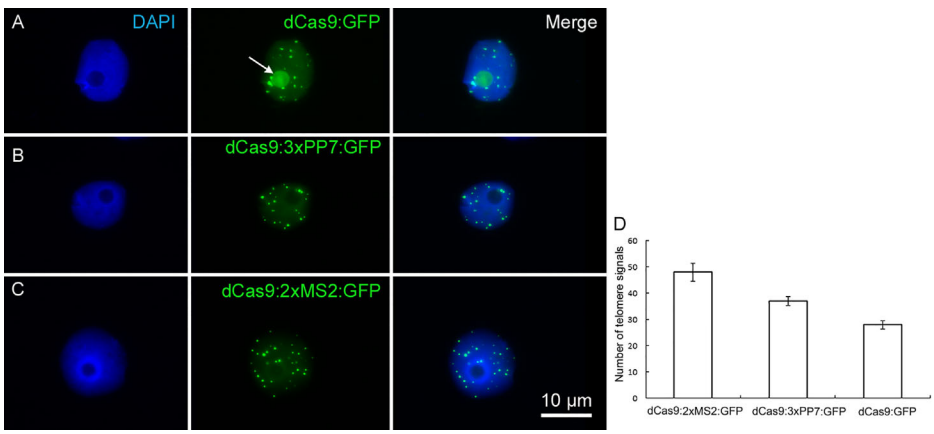

FIGURE 2 | Live imaging of telomeres in *N. benthamiana* leaf cells during interphase by CRISPR/dCas9. The distribution of telomeres recognized by **(A)** dCas9:GFP, **(B)** dCas9:3xPP7:GFP, and **(C)** dCas9:2xMS2:GFP. Note, aptamer-based imaging constructs (dCas9:3xPP7:GFP and dCas9:2xMS2:GFP) did not label nucleoli, while the application of dCas9:GFP does (nucleolus shown with white arrow). Nuclei are counterstained with DAPI (1.5 µg/ml) in VECTASHIELD. **(D)** Diagram showing the efficiency of indirectly and directly labeled dCas9 for targeting telomeric regions. The number of telomere signals was determined based on 20 nuclei per construct. dCas9 indirectly labeled either with MS2 or PP7 aptamers shows more telomeres ($p < 0.05$).

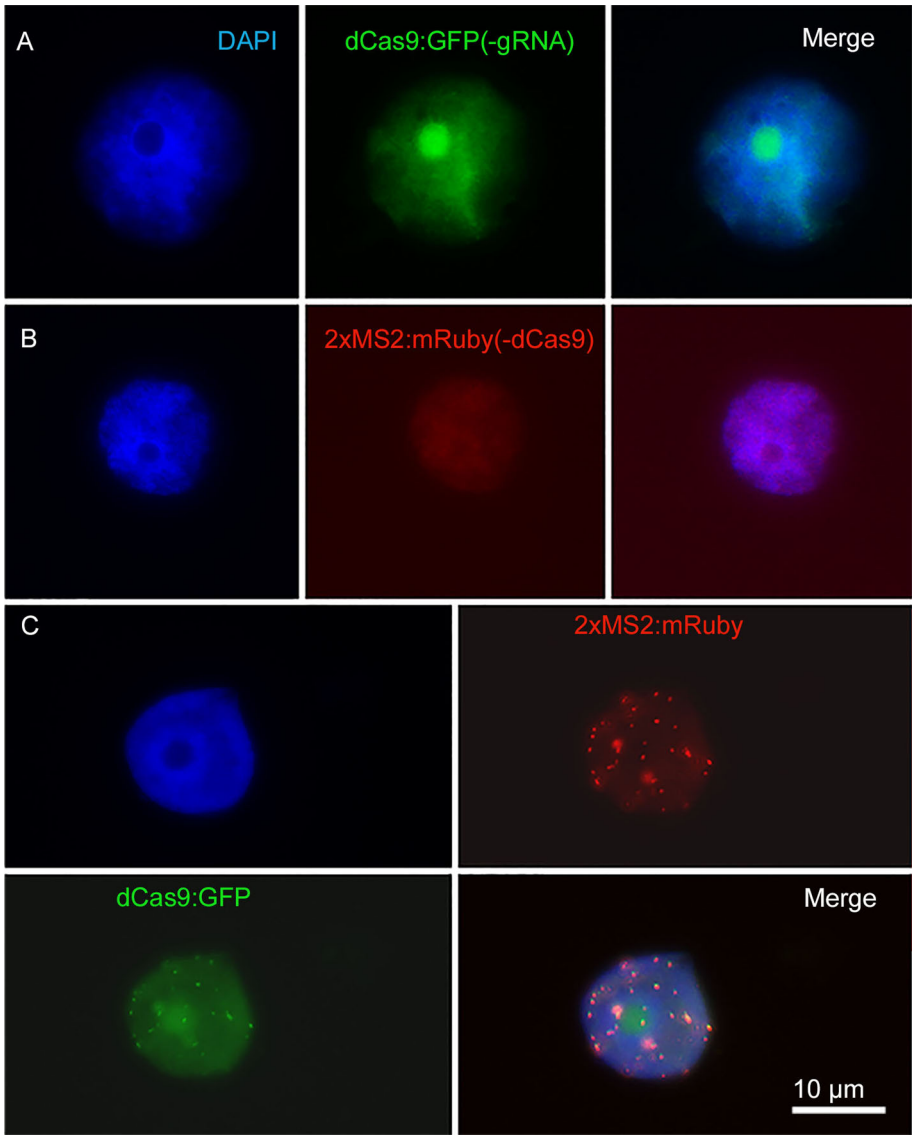

FIGURE 3 | Negative control with partial constructs carrying **(A)** dCas9:GFP without gRNA or **(B)** 2xMS2:3xmRuby targeting telomeres without dCas9. **(C)** Co-transformation of *N. benthamiana* leaves with both partial dCas9:GFP and 2xMS2:3xmRuby constructs resulted in labeling of telomeres, while no telomere-like signals were found after transformation with either partial construct **(A, B)**. Nuclei are counterstained with DAPI.

observed telomere signals in comparison to the ubiquitin promoter (**Figure 7A**). The 35S promoter led to a better signal/background noise ratio (**Figure 7B**). After induction of the β-estradiol inducible XVE promoter, the same number of telomere signals was observed which was recognized by the construct driven by the ubiquitin promoter (**Figure 7A**). Regardless of promoter type, dCas9 could label the telomeric regions in *N. benthamiana* (**Figures 7C–E**). The specificity of signals was approved by subsequent FISH with a telomere-specific probe (**Supplementary Figure S3A**). Without induction, no telomere-specific signal was observed (**Supplementary Figure S3B**).

Comparison of dCas9 transcription driven by the XVE or ubiquitin promoter revealed that even weak dCas9 expression by XVE is sufficient to produce telomere-specific CRISPR-based signals (**Supplementary Figure S4**). Regardless of the promoter type, telomeres showed similar dynamic and random movements (**Figure 8**). To quantify these movements the mean square displacement (MSD) of telomeres was measured over a period of time. Calculating the changes of intratelomeric distance showed the minimum ±1 µm to maximum ±4 µm of changes for each type of promoter (**Figure 9**). In summary, application of RNA-aptamers for CRISPR-based live-cell imaging increases the efficiency of telomere labeling in plant cells.

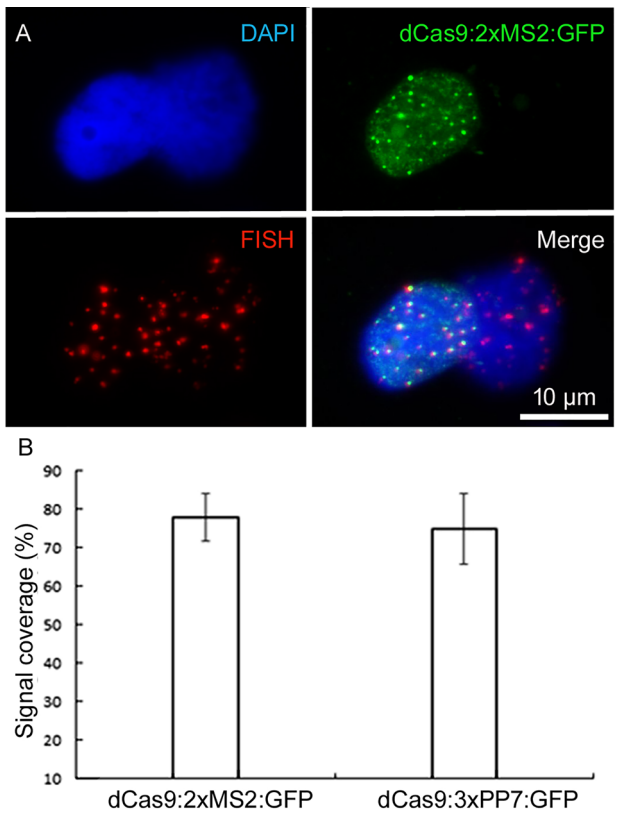

FIGURE 4 | Confirming the target specificity of aptamer-based CRISPR imaging. **(A)** Immunofluorescence staining against dCas9:2xMS2:GFP combined with telomere-specific FISH. Nuclei are counterstained with DAPI (in blue). **(B)** Comparing the efficiency of both types of aptamer-based CRISPR imaging with FISH. Telomeric signals based on 20 isolated nuclei per each construct after ImmunoFISH. dCas9:2xMs2:GFP and dCas9:3xPP7:GFP recognized 78% and 75% of telomere signals identified by FISH, respectively ($p < 0.05$).

Application of CRISPR-Imaging Is Limited in Stably Transformed Plants

Stable transformation of *N. benthamiana*, *A. thaliana* plants and *D. carota* roots with the telomere-specific dCas9:2xMS2:GFP construct did not result in transgenic plants exhibiting GFP-labeled telomeres in living leaf or root cells, although the presence and expression of dCas9 and GFP genes were confirmed by PCR and real-time RT-PCR (data not shown, **Supplement Table 2**). Only transformation of *A. thaliana* with dCas9:2xMS2:GFP targeting centromeric regions resulted in few plants that showed some dot-like signals, however, the number and pattern of signals were atypical for interphase centromeres (**Supplementary Figure S5**). In total, 141 selection marker resistant *A. thaliana* plants were screened for three different centromere imaging constructs by microscopy. Among them, 27 plants showed uniform labeling of nuclei and 9 plants showed dot-like signals. The dot-like signals were unstable and could not be detected in seedlings older than three weeks or subsequent generations (T3). Phenotype and seed setting of plants exhibiting dot-like signals were wild-type like. Among the three different protospacers used, only protospacer 1 and 2 produced signals. The same protospacer 1 was successfully used to label centromeres in fixed nuclei of *A. thaliana* with the help of CRISPR-FISH (Ishii et al., 2019).

Plants that were transformed with dCas9:2xMS2:GFP under the control of an inducible promoter with a centromere- or telomere-specific protospacer revealed no target sequence-specific signals after induction with β-estradiol (**Supplementary Table S2**).

To test whether the disappearance of dot-like signals is caused by degradation of the dCas9 protein, transgenic plants were treated with different concentrations of the proteasome inhibitor MG-132. However, no dot-like signals were recovered. Additionally, the presence of dCas9 protein was confirmed by dCas9 immunostaining (**Supplementary Figure S6**).

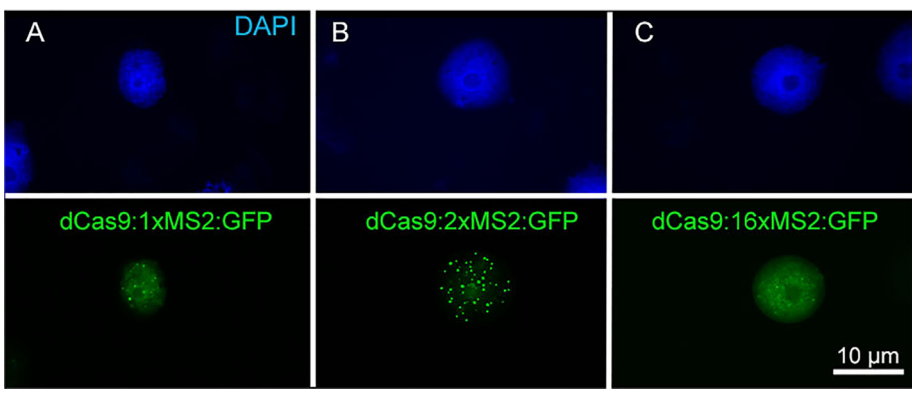

FIGURE 5 | Effect of MS2 aptamer copy number of aptamer-based CRISPR imaging constructs on signal intensity. **(A)** dCas9:1xMS2, **(B)** dCas9:2xMS2, and **(C)** dCas9:16xMS2. The construct with two copies of MS2 revealed the best labeling of telomeres. Nuclei are counterstained with DAPI.

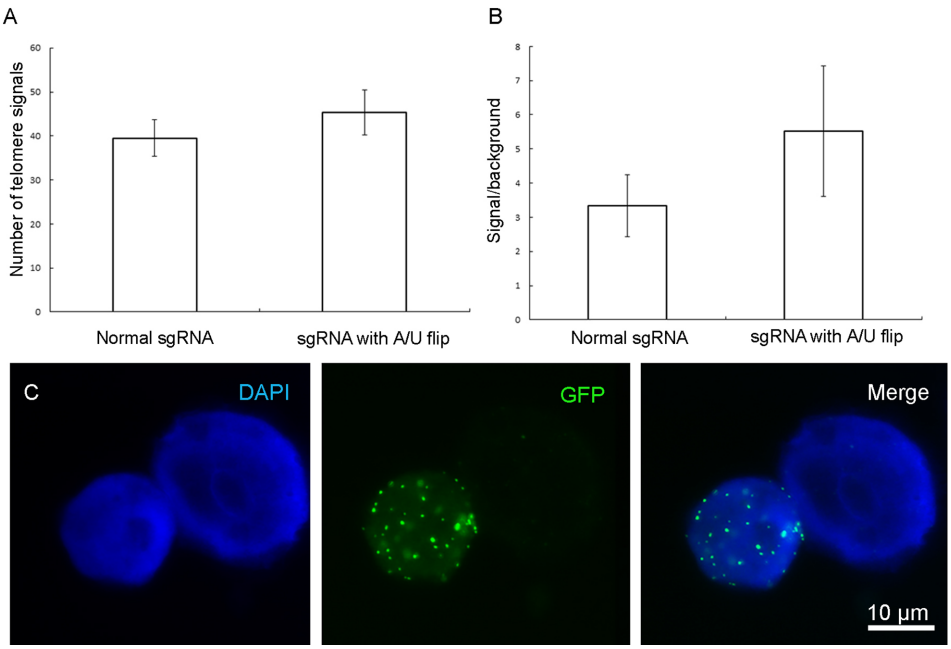

FIGURE 6 | Effect of changing the sgRNA scaffold with a U/A flip and extension on quantity and quality of observed telomere signals. No significant change was observed in the terms of **(A)** telomere number or **(B)** signal/background noise ratio ($p < 0.05$). **(C)** Labeled telomeres by the vector which has the change in sgRNA scaffold. Measurements were performed based on data from 10 isolated nuclei.

DISCUSSION

Optimization of Aptamer-Based CRISPR Imaging Constructs

The application of MS2 and PP7 aptamers resulted in improved CRISPR imaging constructs instrumental to trace telomeres in transiently transformed *N. benthamiana*. Labeling efficiency, based on the mean value of signal numbers per nucleus, was increased up to 1.7 fold in comparison to dCas9:GFP. The number of individual telomere signals per nucleus was lower than expected though, which may be due to clustering of individual telomeres. Clustering of telomeres has been also observed in other organisms like *A. thaliana* (Fransz et al., 2002), yeast and *Drosophila melanogaster* (Hozé et al., 2013; Wesolowska et al., 2013).

Despite the improved labeling of telomeres, the aptamer-based CRISPR imaging in *N. benthamiana* resulted in a labeling efficiency of 73%–75% compared with FISH. In contrast, in human cell cultures, the number of telomeric signals obtained by CRISPR imaging was almost equal to the number of FISH signals (Chen et al., 2013). The copy number difference of telomere repeats is unlikely the reason for this discrepancy because human telomeres are 5 to 15 kb (Moyzis et al., 1988) while the telomeres in *N. benthami*ana are 60 to 160 kb long (Fajkus et al., 1995). Since a temperature of 37°C is required for optimal Cas9 activity (Xiang et al., 2017), the temperature difference between plant (22°C) and mammalian cell cultures (37°C) might contribute to the observed labeling difference between mammalian and plant species.

While dCas9:GFP expressing cells showed background signals in nucleoli (Dreissig et al., 2017), such background was absent from leaves expressing aptamer-containing reporter constructs. Nucleolar accumulation of dCas9 has been noted in other samples like human cell cultures (Chen et al., 2013). Likely, unspecific labeling of nucleoli was reduced because fluorescent proteins were not directly fused to dCas9.

Substitution of the ubiquitin promoter with the inducible XVE promoter caused a 5-fold decrease in expression of dCas9. However, changing the expression of dCas9 gene by application of XVE promoter did not result in a significant change in the number of observed telomere signals. In contrast, it is demonstrated that the low applied dosage of sgRNA in mammalian cell cultures affects the quality of CRISPR imaging signals (Chen et al., 2013). The PRS5A promoter resulted in a lower number of telomere signals. This could be because PRS5A is more active in meristematic tissues rather than leaves, the tissue which was used for transient transformation (Winter et al., 2007). Regardless of the promoter type, telomeres showed random movement like reported for dCas9:GFP (Dreissig et al., 2017).

Increasing the number of MS2 aptamers to 16 copies did not enhance the efficiency of telomere labeling in *N. benthamiana*, although in human cell cultures increment of aptamer numbers up to 16 improved labeling (Qin et al., 2017). Additionally, changing the sgRNA scaffold did not increase the quantity and quality of observed signals. In human cell cultures though, similar modifications increased the number of CRISPR-labeled telomeres and improved the signal/background noise (Chen et al., 2013). Fujimoto and Matsunaga (2017) used sgRNA

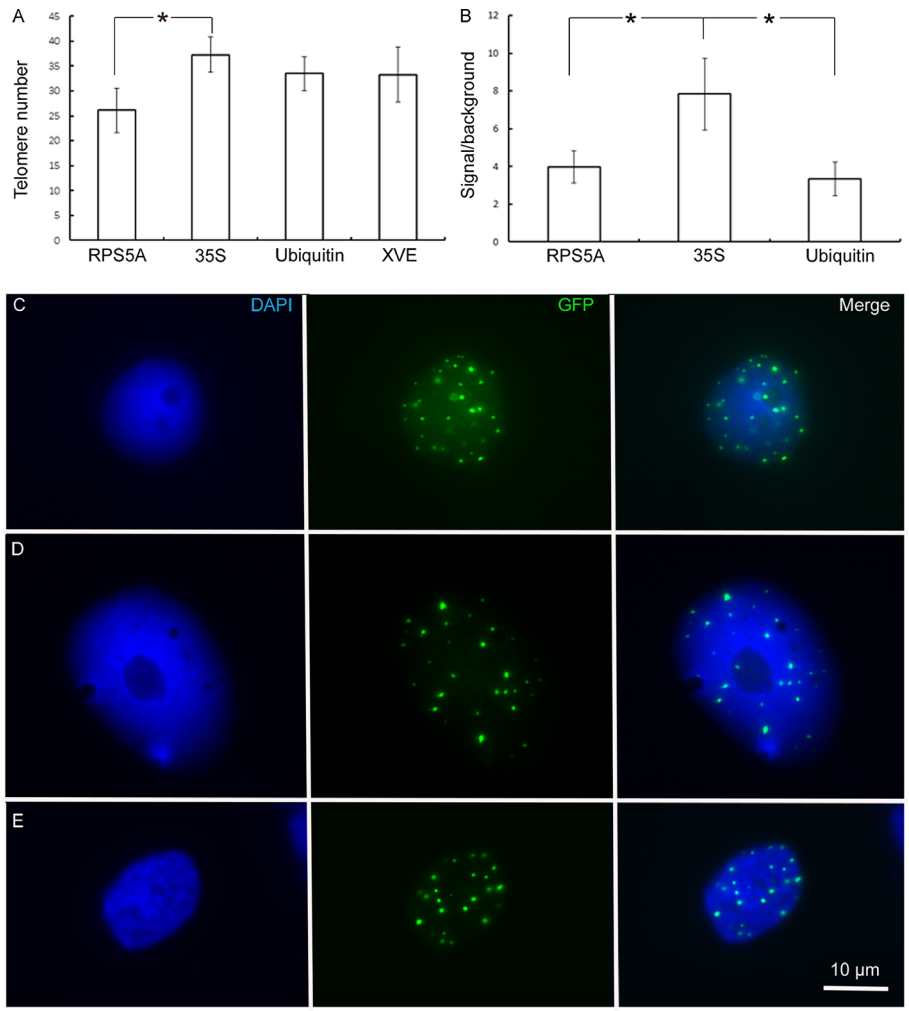

FIGURE 7 | Effect of different promotors used for expression of dCas9 on the efficiency of telomere labeling. **(A)** The expression of dCas9 by PRS5A promoter resulted in the recognition of a smaller number of telomeres compared to 35S and ubiquitin promoters. The XVE inducible promoter was as efficient as ubiquitin promoter regarding the number of labeled telomeres ($p < 0.05$). **(B)** 35S promoter caused the better signal to background noise ratio ($p < 0.05$). Data obtained from 10 isolated nuclei per construct. Regardless of promoter type, dCas9 driven by **(C)** RPS5A, **(D)** 35S, **(E)** XVE could label telomeric regions in *N. benthamiana*.

scaffold modifications (T to G change and A/U flip combined with UGCUG extension) within a CRISPR imaging construct to improve the signal to noise ratio of telomere labeling in transiently transformed *N. tabacum*. The different outcome reported here might be due to the different constructs used.

Why Does CRISPR Imaging Not Work in Stably Transformed Plants?

Our CRISPR imaging constructs which were successfully applied in transiently transformed *N. benthamiana* leaves could not be used to label defined sequences in stably transformed *N. benthamiana*, *A. thaliana* or *D. carota*. The same observation was made by (Fujimoto and Matsunaga, 2017) for GFP-fused dCas9 imaging constructs. Intriguingly, CRISPR-imaging of centromeric and telomeric repeats works-fine on fixed nuclei and chromosomes of different plant and animal species (Deng et al., 2015; Ishii et al., 2019; Nemeckova et al., 2019; Potlapalli et al., 2020). The *in situ* imaging method CRISPR-FISH (also called REGEN-ISL) is based on a fluorescence-labeled two-part guide RNA with a recombinant Cas9 endonuclease complex. For both imaging methods, we used telomere- and centromere-specific gRNA and *A. thaliana* and *N. benthamiana*, subsequently (Ishii et al., 2019), this work). Hence, our expectation was that the selected gRNA in combination with dCas9 should also work in stably transformed plants.

Why then did CRISPR imaging fail in stably transformed plants? In contrast to CRISPR-based editing, for CRISPR imaging a constant interaction of the RNP complex with the target DNA is a functional prerequisite. It is tempting to speculate that a permanent binding of the RNP complex with its target DNA interferes with processes required for plant development. The formation of R-loops, which is underlying

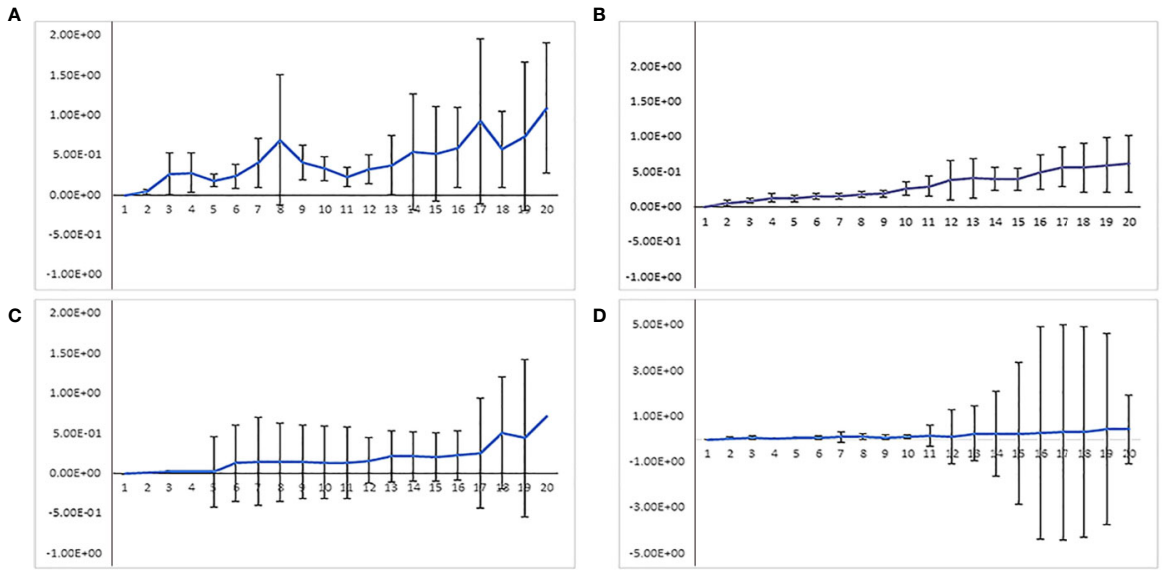

FIGURE 8 | Comparing mean square distance (MSD in μm) of telomeres labeled by indirectly labeled aptamer-dCas9 which were under the control of **(A)** 35S, **(B)** RPS5a, or **(C)** ubiquitin promoters. **(D)** Directly labeled dCas9, which was under the control of a ubiquitin promoter. Telomeres showed random movements regardless of promoter type and how dCas9 was labeled.

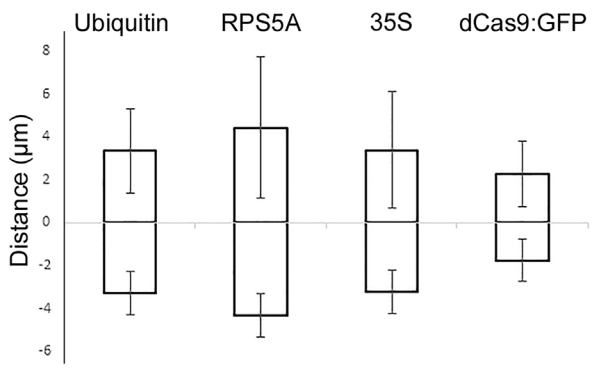

FIGURE 9 | Measurement of inter-telomeric distance changes in nuclei transformed with three different indirectly labeled aptamer-dCas9 which were under the control of ubiquitin, RPS5a or 35S promoters and directly labeled dCas9 which was under the control of the ubiquitin promoter. Intra-telomeric distance changes vary between minimum ±1 μm to maximum ±4 μm.

the CRISPR/Cas mechanism, might hamper cellular processes. R-loops are three-stranded nucleic acid structures composed of a DNA-RNA hybrid and a displaced single-stranded DNA. R-loops have a role in transcription, chromatin modification, DNA damage response. Once the R-loop homeostasis is perturbed, it can lead to genome instability (Crossley et al., 2019; Xu et al., 2020). The R-loop distribution atlas of *A. thaliana* has shown that R-loop distribution patterns are relatively preserved during different developmental and environmental conditions (Xu et al., 2020). Therefore, by imposing consistent formation of R-loops in targeted regions, CRISPR imaging constructs might change R-loop dynamics in defined genomic regions of stably transformed plants. Alternatively, the selected Cas9 variant of *S. pyogenes* is not suitable and further optimized Cas variants with higher efficiency could overcome this problem. A negative selection against CRISPR-imaging constructs in stably transformed plants at the transcript level is less likely because corresponding transcripts exist. In addition, uniform labeling of anti-Cas9 immunosignals was detected in transformed plants. Overcoming the discussed problem will also help to increase the efficiency of CRISPR-based editing in plants.

Taking advantage of the intrinsic stability of CRISPR guide RNA, (Wang et al., 2019) used fluorescent ribonucleoproteins consisting of chemically synthesized fluorescent gRNAs and recombinant dCas9 protein for imaging in transfected living human lymphocytes. Live-cell fluorescent *in situ* hybridization (LiveFISH) allowed tracking of multiple chromosomal loci in lymphocytes. Whether the transient transformation of cells with fluorescent RNP complexes could become another option to label defined sequences in living plant cells remains to be demonstrated.

CONCLUSIONS

A three-component labeling method using dCas9, PP7/MS2 aptamers and tdMCP : GFP/tdPCP : GFP binding to MS2/PP7 aptamers was successfully applied for labeling of telomeres in transiently transformed *N. benthamiana*. The labeling efficiency of telomeres was increased and the background labeling noise in the nucleolus was reduced compared to previous work (Dreissig

et al., 2017). The copy number of aptamers used in the aptamer-based imaging construct is critical. The level of *dCas9* gene expression does not affect CRISPR imaging. The application of CRISPR/Cas9 for live-cell imaging in stably transformed plants, however, was not successful.

DATA AVAILABILITY STATEMENT

All datasets presented in this study are included in the article/ **Supplementary Material**.

AUTHOR CONTRIBUTIONS

SK contributed in conducting lab work needed for stated experiments in the manuscript. PS contributed in conducting lab work needed for preparing required imaging vectors. EG participated in analysis of telomere signals. FD performed the Daucus carota transformation with live-imaging vectors. TR performed confocal microscopy. HP and AH initiated and supervised the project. All authors wrote the manuscript.

FUNDING

The work was funded by Deutsche Forschungsgemeinschaft (DFG) grant HO1779/28-1.

ACKNOWLEDGMENTS

We would like to thank Sabine Struckmeyer, Christine Helmold, Oda Weiß, Christin-Sophie Gäde, and Sylvia Swetik for technical support, Steven Dreissig for scientific discussion and Christian Hertig for preparing schemata for the manuscript and the statistical analysis with SigmaStat 4.0. We also thank Michael M. Goodin for providing *N. benthamiana* seeds expressing CFP-H2B, Bruno Müller for a plasmid containing the RPS5A promoter, Chua Nam Hai for the pER8 containing XVE promoter, Martina Dvořáčková and Jiri Fajkus for plasmid expressing TRB1-GFP. The work was funded by Deutsche Forschungsgemeinschaft (DFG) grant HO1779/28-1.

This manuscript has been released as a pre-print at BIORXIV (MS ID#: BIORXIV/2020/078246).

SUPPLEMENTARY MATERIAL

The Supplementary Material for this article can be found online at: https://www.frontiersin.org/articles/10.3389/fpls.2020.01254/full#supplementary-material

MOVIE SUPPLEMENT 1 | Co-expression of dCas9:2xMS2:mRuby (red) and TRB1 (green) in *N. benthamina*. Co-localization of telomeric dCas9:2xMS2:mRuby and TRB1 shows that aptamer-based imaging construct can be also used for DNA-protein interaction studies.

MOVIE SUPPLEMENT 2 | Dynamic of telomeres targeted by indirectly labeled dCas9 with MS2 aptamer in *N. benthamiana* leaf nuclei expressing CFP-H2B.

FIGURE SUPPLEMENT 1 | Different components of the aptamer-based labeling method: 1) dCas9 from *S. pyogenes*, 2) MS2 or PP7 aptamers (here only MS2 is shown) which are integrated into sgRNA scaffold. 3) RNA binding protein (tdMCP or tdPCP) fused to a fluorescent protein (mRuby) which recognizes aptamers.

FIGURE SUPPLEMENT 2 | Changing the sgRNA scaffold with A/U flip (in red) and insertion of an extension (in green).

FIGURE SUPPLEMENT 3 | Specificity control test by ImmunoFISH for the activity of the inducible XVE promoter. **(A)** Isolated nuclei after treatment of leaves with β-estradiol show telomeric signals. Co-localization of dCas9:2xMS2:GFP and FISH signals show that the observed signals are telomeric specific. **(B)** Nuclei isolated from β-estradiol-untreated leaves show a uniform labeling of nuclei.

FIGURE SUPPLEMENT 4 | Real time expression of dCas9 expressed by ubiquitin and XVE promoters. dCas9 expression is much lower when it is driven by inducible XVE promoter compared to ubiquitin from parsley. Error bars are standard deviation.

FIGURE SUPPLEMENT 5 | Selected nuclei of *A. thaliana* stably transformed with a centromere-specific dCas9:2xMS2:GFP construct exhibiting dot-like signals. **(A, B)** Application of the centromere-specific protospacer 1 and 2, respectively. The number of signals was higher than expected.

FIGURE SUPPLEMENT 6 | Immunostaining of dCas9 protein in isolated nuclei from leaf material of stably transformed *Arabidopsis* plants with dCas9:2xMS2:GFP targeting centromeric regions. **(A)** Immunostaining of dCas9 in stably transformed Arabidopsis plants showed the dCas9 is not degraded. **(B)** Immunostaining of isolated leaf nuclei from wild type *Arabidopsis* leaf nuclei did not result in signals which shows that the applied antibody against dCas9 is working specifically.

REFERENCES

Chen, B., Gilbert, L. A., Cimini, B. A., Schnitzbauer, J., Zhang, W., Li, G. W., et al. (2013). Dynamic imaging of genomic loci in living human cells by an optimized CRISPR/Cas system. *Cell* 155, 1479–1491. doi: 10.1016/j.cell.2013.12.001

Clemente, T. (2006). "Nicotiana (Nicotiana tobaccum, Nicotiana benthamiana)," in *Agrobacterium Protocols*. Ed. K. Wang (Totowa, NJ: Hummana Press), 153–154.

Crossley, M. P., Bocek, M., and Cimprich, K. A. (2019). R-Loops as cellular regulators and genomic threats. *Mol. Cell* 73, 398–411. doi: 10.1016/j.molcel.2019.01.024

Deng, W. L., Shi, X. H., Tjian, R., Lionnet, T., and Singer, R. H. (2015). CASFISH: CRISPR/Cas9-mediated *in situ* labeling of genomic loci in fixed cells. *Proc. Natl. Acad. Sci. U. S. A.* 112, 11870–11875. doi: 10.1073/pnas.1515692112

Doležel, J., Greilhuber, J., and Suda, J. (2007). Estimation of nuclear DNA content in plants using flow cytometry. *Nat. Protoc.* 2, 2233–2244. doi: 10.1038/nprot.2007.310

Dreissig, S., Schiml, S., Schindele, P., Weiss, O., Rutten, T., Schubert, V., et al. (2017). Live-cell CRISPR imaging in plants reveals dynamic telomere movements. *Plant J.* 91, 565–573. doi: 10.1111/tpj.13601

Dunemann, F., Unkel, K., and Sprink, T. (2019). "Using CRISPR/Cas9 to produce haploid inducers of carrot through targeted mutations of centromeric histone H3 (CENH3)," in *II International Symposium on Carrot and Other Apiaceae* Eds. D. Grzebelus and R. Barański (ISHS Acta Horticulturae), 211–219.

Esvelt, K. M., Mali, P., Braff, J. L., Moosburner, M., Yaung, S. J., and Church, G. M. (2013). Orthogonal Cas9 proteins for RNA-guided gene regulation and editing. *Nat. Methods* 10, 1116. doi: 10.1038/nmeth.2681

Fajkus, J., Kovařík, A., mKrálovics, R., and Bezděk, M. (1995). Organization of telomeric and subtelomeric chromatin in the higher plant Nicotiana tabacum. *Molec. Gen. Genet.* 247, 633–638.

Fransz, P., De Jong, J. H., Lysak, M., Castiglione, M. R., and Schubert, I. (2002). Interphase chromosomes in Arabidopsis are organized as well defined chromocenters from which euchromatin loops emanate. *Proc. Natl. Acad. Sci. U. S. A.* 99, 14584–14589. doi: 10.1073/pnas.212325299

Fu, Y., Rocha, P. P., Luo, V. M., Raviram, R., Deng, Y., Mazzoni, E. O., et al. (2016). CRISPR-dCas9 and sgRNA scaffolds enable dual-colour live imaging of satellite sequences and repeat-enriched individual loci. *Nat. Commun.* 7, 11707. doi: 10.1038/ncomms11707

Fujimoto, S., and Matsunaga, S. (2017). Visualization of Chromatin Loci with Transiently Expressed CRISPR/Cas9 in Plants. *Cytologia* 82, 559–562. doi: 10.1508/cytologia.82.559

Fujimoto, S., Sugano, S. S., Kuwata, K., Osakabe, K., and Matsunaga, S. (2016). Visualization of specific repetitive genomic sequences with fluorescent TALEs in Arabidopsis thaliana. *J. Exp. Bot.* 67, 6101–6110. doi: 10.1093/jxb/erw371

Hong, Y., Lu, G., Duan, J., Liu, W., and Zhang, Y. (2018). Comparison and optimization of CRISPR/dCas9/gRNA genome-labeling systems for live cell imaging. *Genome Biol.* 19, 39. doi: 10.1186/s13059-018-1413-5

Horn, B. K. P. (1987). Closed-form solution of absolute orientation using unit quaternions. *J. Optical Soc. Am. a-Optics Image Sci. Vision* 4, 629–642. doi: 10.1364/JOSAA.4.000629

Hozé, N., Ruault, M., Amoruso, C., Taddei, A., and Holcman, D. (2013). Spatial telomere organization and clustering in yeast Saccharomyces cerevisiae nucleus is generated by a random dynamics of aggregation–dissociation. *Mol. Biol. Cell* 24, 1791–1800. doi: 10.1091/mbc.e13-01-0031

Ishii, T., Sunamura, N., Matsumoto, A., Eltayeb, A. E., and Tsujimoto, H. (2015). Preferential recruitment of the maternal centromere-specific histone H3 (CENH3) in oat (Avena sativa L.) × pearl millet (Pennisetum glaucum L.) hybrid embryos. *Chromosome Res.* 23, 709–718. doi: 10.1007/s10577-015-9477-5

Ishii, T., Schubert, V., Khosravi, S., Dreissig, S., Metje-Sprink, J., Sprink, T., et al. (2019). RNA-guided endonuclease - *in situ* labelling (RGEN-ISL): a fast CRISPR/Cas9-based method to label genomic sequences in various species. *New Phytol.* 222, 1652–1661. doi: 10.1111/nph.15720

Khosravi, S., Ishii, T., Dreissig, S., and Houben, A. (2020). Application and prospects of CRISPR/Cas9-based methods to trace defined genomic sequences in living and fixed plant cells. *Chromosome Res.* 28, 7–17. doi: 10.1007/s10577-019-09622-0

Konermann, S., Brigham, M. D., Trevino, A. E., Joung, J., Abudayyeh, O. O., Barcena, C., et al. (2015). Genome-scale transcriptional activation by an engineered CRISPR-Cas9 complex. *Nature* 517, 583–588. doi: 10.1038/nature14136

Lee, J. E., Neumann, M., Iglesias Duro, D., and Schmid, M. (2019). CRISPR-based tools for targeted transcriptional and epigenetic regulation in plants. *PLoS One* 14, e0222778. doi: 10.1371/journal.pone.0222778

Lindhout, B. I., Fransz, P., Tessadori, F., Meckel, T., Hooykaas, P. J. J., and Zaal, B. J. (2007). Live cell imaging of repetitive DNA sequences *via* GFP-tagged polydactyl zinc finger proteins. *Nucleic Acids Res.* 35, e107. doi: 10.1093/nar/gkm618

Ma, H., Naserib, A., Reyes-Gutierreza, P., Wolfec, S. A., Zhangb, S., and Pedersona, T. (2015). Multicolor CRISPR labeling of chromosomal loci in human cells. *PNAS* 112, 3002–3007. doi: 10.1073/pnas.1420024112

Ma, H., Tu, L. C., Naseri, A., Huisman, M., Zhang, S., Grunwald, D., et al. (2016). Multiplexed labeling of genomic loci with dCas9 and engineered sgRNAs using CRISPRainbow. *Nat. Biotechnol.* 34, 528–530. doi: 10.1038/nbt.3526

Martin, K., Kopperud, K., Chakrabarty, R., Banerjee, R., Brooks, R., and Goodin, M. M. (2009). Transient expression in Nicotiana benthamiana fluorescent marker lines provides enhanced definition of protein localization, movement and interactions in planta. *Plant J.* 59, 150–162. doi: 10.1111/j.1365-313X.2009.03850.x

Misteli, T. (2007). Beyond the Sequence: Cellular Organization of Genome Function. *Cell* 128, 787–800. doi: 10.1016/j.cell.2007.01.028

Moyzis, R. K., Buckingham, J. M., Cram, L. S., Dani, M., Deaven, L. L., Jones, M. D., et al. (1988). A highly conserved repetitive DNA sequence, (TTAGGG) n, present at the telomeres of human chromosomes. *Proc. Natl. Acad. Sci. U. S. A.* 85, 6622–6626. doi: 10.1073/pnas.85.18.6622

Nemeckova, A., Wasch, C., Schubert, V., Ishii, T., Hribova, E., and Houben, A. (2019). CRISPR/Cas9-based RGEN-ISL allows the simultaneous and specific visualization of proteins, DNA repeats, and sites of DNA replication. *Cytogenet. Genome Res.* 159, 48–53. doi: 10.1159/000502600

Phan, H. T., and Conrad, U. (2016). "Plant-Based Vaccine Antigen Production," in *Vaccine Technologies for Veterinary Viral Diseases: Methods and Protocols*. Ed. A. Brun (New York, NY: Springer New York), 35–47.

Potlapalli, B. P., Schubert, V., Metje-Sprink, J., Liehr, T., and Houben, A. (2020). Application of Tris-HCl allows the specific labeling of regularly prepared chromosomes by CRISPR-FISH. *Cytogenet. Genome Res.* 160, 156–165. doi: 10.1159/000506720

Qin, P., Parlak, M., Kuscu, C., Bandaria, J., Mir, M., Szlachta, K., et al. (2017). Live cell imaging of low- and non-repetitive chromosome loci using CRISPR-Cas9. *Nat. Commun.* 8, 14725. doi: 10.1038/ncomms14725

Robinett, C. C., Straight, A. F., Li, G. W., Willhelm, C., Sudlow, G., Murray, A., et al. (1996). In vivo localization of DNA sequences and visualization of large-scale chromatin organization using lac operator/repressor recognition. *J. Cell Biol.* 135, 1685–1700. doi: 10.1083/jcb.135.6.1685

Saad, H., Gallardo, F., Dalvai, M., Tanguy-Le-Gac, N., Lane, D., and Bystricky, K. (2014). DNA dynamics during early double-strand break processing revealed by non-intrusive imaging of living cells. *PLoS Genet.* 10 (3), e1004187. doi: 10.1371/journal.pgen.1004187

Schrumpfová, P. P., Vychodilová, I., Dvořáčková, M., Majerská, J., Dokládal, L., Schořová, S., et al. (2014). Telomere repeat binding proteins are functional components of Arabidopsis telomeres and interact with telomerase. *Plant J.* 77, 770–781. doi: 10.1111/tpj.12428

Selma, S., Bernabé-Orts, J. M., Vazquez-Vilar, M., Diego-Martin, B., Ajenjo, M., Garcia-Carpintero, V., et al. (2019). Strong gene activation in plants with genome-wide specificity using a new orthogonal CRISPR/Cas9-based programmable transcriptional activator. *Plant Biotechnol. J.* 17, 1703–1705. doi: 10.1111/pbi.13138

Shao, S., Zhang, W., Hu, H., Xue, B., Qin, J., Sun, C., et al. (2016). Long-term dual-color tracking of genomic loci by modified sgRNAs of the CRISPR/Cas9 system. *Nucleic Acids Res.* 44, e86. doi: 10.1093/nar/gkw066

Shechner, D., Hacisuleyman, E., Younger, S., and Rinn, J. L. (2015). Multiplexable, locus-specific targeting of long RNAs with CRISPR-Display. *Nat. Methods* 12, 664–670. doi: 10.1038/nmeth.3433

Tanenbaum, M. E., Gilbert, L. A., Qi, L. S., Weissman, J. S., and Vale, R. D. (2014). A protein tagging system for signal amplification in gene expression and fluorescence imaging. *Cell* 159, 635. doi: 10.1016/j.cell.2014.09.039

Tepfer, M., Gaubert, S., Leroux-Coyau, M., Prince, S., and Houdebine, L. (2004). Transient expression in mammalian cells of transgenes transcribed from the Cauliflower mosaic virus 35S promoter. *Environ. Biosaf. Res.* 3, 91–97. doi: 10.1051/ebr:2004010

Urbanek, M. O., Galka-Marciniak, P., Olejniczak, M., and Krzyzosiak, W. J. (2014). RNA imaging in living cells – methods and applications. *RNA Biol.* 11, 1083–1095. doi: 10.4161/rna.35506

Wang, S., Su, J. H., Zhang, F., and Zhuang, X. (2016). An RNA-aptamer-based two-color CRISPR labeling system. *Sci. Rep.* 6, 26857. doi: 10.1038/srep26857

Wang, H., Nakamura, M., Zhao, D., Nguyen, C. M., Yu, C., Lo, A., et al. (2019). Temporal-Spatial Visualization of Endogenous Chromosome Rearrangements in Living Cells. *Science* 365 (6459), 1301–1305. doi: 10.1101/734483

Weijers, D., Franke-Van Dijk, M., Vencken, R. J., Quint, A., Hooykaas, P., and Offringa, R. (2001). An Arabidopsis Minute-like phenotype caused by a semi-dominant mutation in a RIBOSOMAL PROTEIN S5 gene. *Development* 128, 4289–4299.

Wesolowska, N., Amariei, F. L., and Rong, Y. S. (2013). Clustering and Protein Dynamics of Drosophila melanogaster Telomeres. *Genetics* 195, 381–391. doi: 10.1534/genetics.113.155408

Winter, D., Vinegar, B., Nahal, H., Ammar, R., Wilson, G. V., and Provart, N. J. (2007). An "Electronic Fluorescent Pictograph" browser for exploring and analyzing large-scale biological data sets. *PLoS One* 2, e718. doi: 10.1371/journal.pone.0000718

Wu, X., Mao, S., Ying, Y., Krueger, C. J., and Chen, A. K. (2019). Progress and Challenges for Live-cell Imaging of Genomic Loci Using CRISPR-based Platforms. *Genomics Proteomics Bioinf.* 17, 119–128. doi: 10.1016/j.gpb.2018.10.001

Xiang, G., Zhang, X., An, C., Cheng, C., and Wang, H. (2017). Temperature effect on CRISPR-Cas9 mediated genome editing. *J. Genet. Genomics* 44, 199–205. doi: 10.1016/j.jgg.2017.03.004

Xu, W., Li, K., Li, S., Hou, Q., Zhang, Y., Liu, K., et al. (2020). The R-loop Atlas of Arabidopsis Development and Responses to Environmental Stimuli. *Plant Cell.* 32, 888–903. doi: 10.1105/tpc.19.00802

Zhang, S., and Song, Z. (2017). Aio-Casilio: a robust CRISPR-Cas9-Pumilio system for chromosome labeling. *J. Mol. Histol.* 48, 293–299. doi: 10.1007/s10735-017-9727-2

Zuo, J., Niu, Q.-W., and Chua, N.-H. (2000). An estrogen receptor-based transactivator XVE mediates highly inducible gene expression in transgenic plants. *Plant J.* 24, 265–273. doi: 10.1046/j.1365-313x.2000.00868.x

Conflict of Interest: The authors declare that the research was conducted in the absence of any commercial or financial relationships that could be construed as a potential conflict of interest.

Advantages of publishing in Frontiers

OPEN ACCESS
Articles are free to read for greatest visibility and readership

FAST PUBLICATION
Around 90 days from submission to decision

HIGH QUALITY PEER-REVIEW
Rigorous, collaborative, and constructive peer-review

TRANSPARENT PEER-REVIEW
Editors and reviewers acknowledged by name on published articles

Frontiers
Avenue du Tribunal-Fédéral 34
1005 Lausanne | Switzerland

Visit us: www.frontiersin.org
Contact us: frontiersin.org/about/contact

REPRODUCIBILITY OF RESEARCH
Support open data and methods to enhance research reproducibility

DIGITAL PUBLISHING
Articles designed for optimal readership across devices

FOLLOW US
@frontiersin

IMPACT METRICS
Advanced article metrics track visibility across digital media

EXTENSIVE PROMOTION
Marketing and promotion of impactful research

LOOP RESEARCH NETWORK
Our network increases your article's readership